PROCEEDINGS OF SCIENCE

A journey to understand our Universe

Franco Giovannelli*
INAF - Istituto di Astrofisica e Planetologia Spaziali, Via del Fosso del Cavaliere, 100, 00133 Roma, Italy
E-mail: franco.giovannelli@iaps.inaf.it

In this review article I will deal, without claiming to be complete, the leading topics of astrophysics with the aim of making the current knowledge of our Universe easier for the reader. "Multifrequency Astrophysics" is a pillar of an interdisciplinary approach to the knowledge of the physics of our Universe. Indeed, as clearly demonstrated in the last decades, only with the multifrequency observations of cosmic sources is it possible to get nearly the whole behaviour of a source and then to approach the physics governing the phenomena that originate such a behaviour. I regard a multidisciplinary approach in the study of each kind of phenomenon occurring in each kind of cosmic source as even more powerful than a simple "astrophysical approach". A clear example of a multidisciplinary approach is that of "The Bridge between the Big Bang and Biology". This bridge can be described by using the competencies of astrophysicists, planetary physicists, atmospheric physicists, geophysicists, volcanologists, biophysicists, biochemists, and astrobiophysicists. The unification of such fields of expertise can provide the intellectual framework that will better enable an understanding of the physics governing the formation and structure of cosmic objects, seemingly uncorrelated with one another, but constitutive of the steps necessary for the origin of life (e.g. Giovannelli, 2001a). Indeed, a lot of the future research in astrophysics will be focussed on the discovery of exoplanets and on the possibility to detect signals for alien life somewhere in the Galaxy. An extension to a multidisciplinary approach comes from the use of historical news reported in "old chronicles" that are a fundamental source for the newborn "archaeoastronomy".
There are many problems in performing simultaneous nultifrequency, multisite, multiinstrument, multiplatform measurements due to: (i) objective technological difficulties; (ii) sharing common scientific objectives; (iii) problems of scheduling and budgets; and (iv) the political management of science. All these kinds of measurements converge in what is now called *Multimessenger Astrophysics*, this after the detection of gravitational wave events (GWEs) and the search for the electromagnetic counterparts of such events.
I will provide several examples that marked the continuous evolution on the knowledge of the physics of our Universe.

Multifrequency Behaviour of High Energy Cosmic Sources - XIV - (MULTIF2023)
12-17 June 2023, Palermo, Italy

*Speaker.

PoS(MULTIF2023)001

1. Content of the review

10. Conclusions and perspectives

2. Introduction

This paper follows the logic of an old review paper written long time ago by Giovannelli & Sabau-Graziati (2004: here after GSG2004) on "*The Impact of the Space Experiments on Our Knowledge of the Physics of the Universe*". The main idea is to discuss the salient topics of modern astrophysics in the light of the new era that has opened with the detection of numerous exoplanets and gravitational waves emitted by the merger of black holes and neutron stars. These topics have been dealt with in many international workshps, directed by me (Giovannelli & Sabau-Graziati, 2016a,b,c, 2017, 2019, 2020; Giovannelli, 2017, 2018, 2021). However I will discuss about the pillars that take the *Bridge Between the Big Bang and Biology* (Giovannelli, 2001a). This bridge undoubtedly exists because we are present here, regardless of the origin of our Universe. So we must understand how to cross this bridge and understand what are the tools that allow us to make out the structure of the pillars supporting the bridge.

An incisive example that shows the link between all the components of the Universe was reported by Sir Martin Rees (1988a) in his suggestive picture reported in Fig. 1.

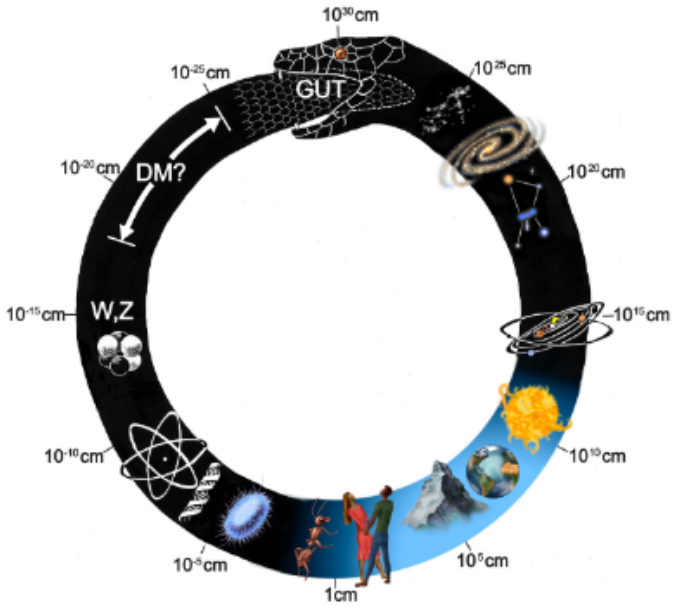

Figure 1: From the infinitely small to infinitely big (adopted from Rees, 1988a).

In a more extensive way, the link between different components of the Universe is reported: Fig. 2 (Upper left) a metabolic network of a "simple" bacterium where each point is connected to any other point through the complexity of the network (Luisi & Capra, 2014). Fig. 2 (Upper right) shows the cosmic network (Credit: Andrew Pontzen/Fabio Governato, 2014; see also in (https://it.wikipedia.org/wiki/Cosmologia del plasma). Shandarin, Habib & Heitmann (2010) quantitatively specified the underlying mechanisms that drive the formation of the cosmic network. Fig. 2 (Lower left and right) shows the human body network and the human society network, respectively (Luisi & Capra, 2014).

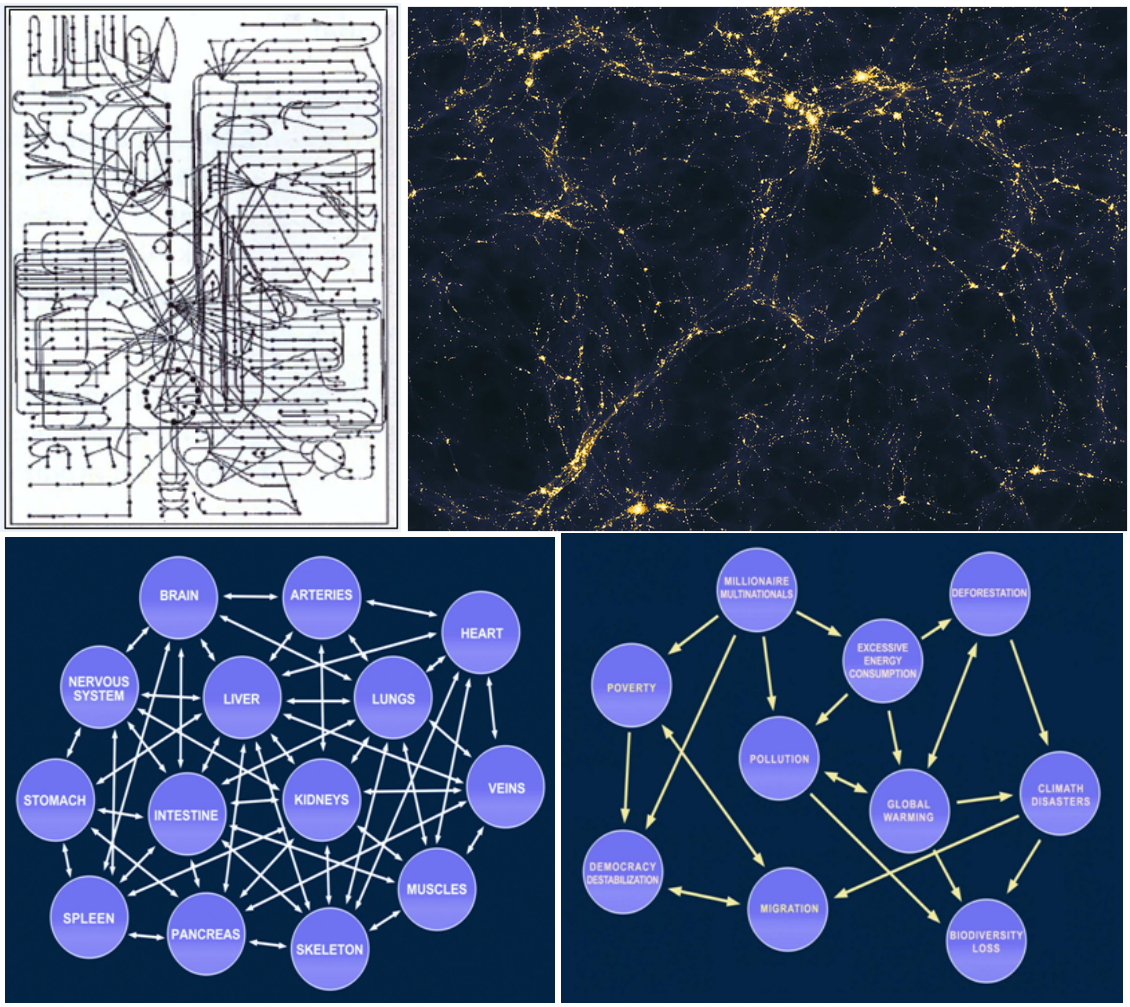

Figure 2: Upper left panel: Section of the metabolic network of a "simple" bacterium (Luisi & Capra, 2014). Upper right panel: the "cosmic network" (Credit: Andrew Pontzen/Fabio Governato, 2014) see also in (https://it.wikipedia.org/wiki/Cosmologia del plasma). Lower left panel: the human body network. Lower right panel: the human society network (Luisi & Capra, 2014).

Noting that all the components of the Universe are linked to each other in a more or less narrow, we try to find the glue that holds them together seamlessly. A key component of this glue is the accurate knowledge of the nuclear reactions that take place inside the stars. Without the experimental knowledge of these reactions every effort to thoroughly explain stellar evolution is, if not futile, certainly difficult.

2.1 Nuclear Reactions in Stars

The knowledge of the cross-sections of nuclear reactions occurring in the stars appears as one of the most crucial points of all astroparticle physics. Direct measurements of the cross sections of the ^{3}He(^{4}He,γ)^{7}Be and ^{7}Be(p,γ)^{8}Be reactions of the *pp* chain and ^{14}N(p,γ)^{15}O reaction of the *CNO-cycle* will allow a substantial improvement in our knowledge on stellar evolution.

Wolschin (2003) published a very interesting paper about the history of the "*Thermonuclear Processes in Stars and Stellar Neutrinos*".

An impressive review about nuclear reactions (*the pp chain and CNO cycles*) has been published by Adelberger et al. (2011).

It is in the nature of astrophysics that many of the processes and objects one tries to understand are physically inaccessible. Thus, it is important that those aspects that can be studied in the laboratory be rather well understood.

One such aspect are the nuclear fusion reactions, which are at the heart of nuclear astrophysics: they influence sensitively the nucleosynthesis of the elements in the earliest stages of the universe and in all the objects formed thereafter, and control the associated energy generation, neutrino luminosity, and evolution of stars.

At the moment the LUNA (Laboratory for Underground Nuclear Astrophysics) is a new experimental approach for the study of nuclear fusion reactions based on an underground accelerator laboratory.

It is devoted to measure nuclear cross sections relevant in astroparticle physics. It is the most valuable experiment running underground in the Gran Sasso Laboratory of the INFN. Reviews about LUNA experiment have been published by Broggini et al. (2010; 2018).

A discussion about the LUNA results has been reported in the paper by Giovannelli & Sabau-Graziati (2018) and the references therein.

A general data base for Experimental Nuclear Reaction Data (EXFOR) can be found in: https://www-nds.iaea.org/exfor/exfor.htm.

3. A journey within our galaxy

It is quite difficult to discuss everything that happens and has happened in our galaxy within relatively short space limits. The attempt is to try to give a reasonably exhaustive panorama taking into account the advances in knowledge made thanks to the countless experiments both from the ground and from space that have brought new light to the theoretical knowledge acquired thanks to the intellectual efforts of numerous groups of researchers. Most of these have made small but important contributions. Without these contributions, like the pieces of a puzzle, the work of putting the whole puzzle together would not have originated. And this thanks to the efforts of the few scientists with special synthesis skills.

3.1 Accretion processes in cosmic sources

Accretion is a universal phenomenon that takes place in the vast majority of astrophysical objects. The progress of ground-based and space-borne observational facilities has resulted in the great amount of information on various accreting astrophysical objects, collected within the last decades. The accretion is accompanied by the process of extensive energy release that takes place on the surface of an accreting object and in various gaseous envelopes, accretion disk, jets and other elements of the flow pattern. The results of observations inspired the intensive development of accretion theory, which, in turn, enabled us to study unique properties of accreting objects and physical conditions in the surrounding environment. One of the most interesting outcomes of this

intensive study is the fact that accretion processes are, in a sense, self-similar on various spatial scales from planetary systems to galaxies.

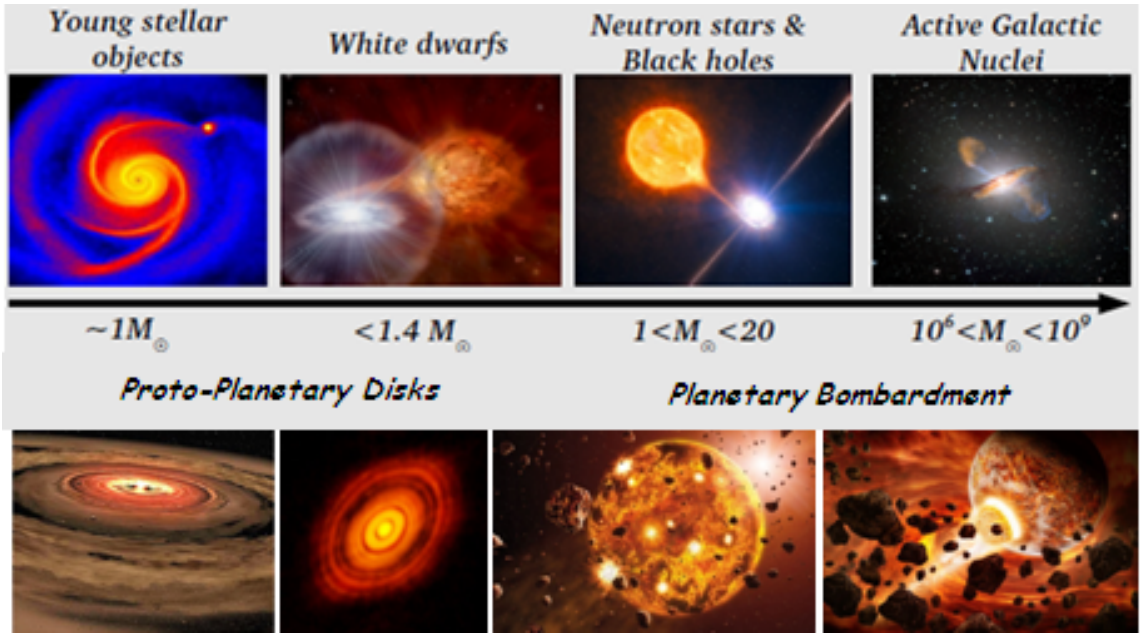

Figure 3: Accretion processes in different cosmic sources (adopted from Giovannelli & Sabau-Graziati, 2016a, after Scaringi, 2015).

This fact gives us new opportunities to investigate objects that, by various reasons, are not available for direct study.

Cataclysmic variable stars are unique natural laboratories where one can conduct the detailed observational study of accretion processes and accretion disks. Indeed, among the cosmic systems where accretion processes occur, undoubtedly, non-magnetic CVs, intermediate polars and polars constitute the most powerful probe to test our theories of the various modes of accretion. The reason is rather simple: CVs are enough close to us and their processes develop in time-scales relatively easy to be followed and enough energetic to be easily detected. The long term evolution of CV systems accreting at a prohibitive rate has become a hot topic both in terms of the fate of such systems (all sorts of supernovae) and the microphysics of Eddington and super Eddington mass accretion and mass loss flows. In particular we stress one of the hottest topics in present day astrophysics, namely the progenitors of SN-Ia. This problem is connected with fundamental issues in cosmology. Novae and recurrent novae are the most promising progenitor candidates but so far could not be nailed down.

Figure 3 shows a sketch of cosmic systems where accretion processes occur (Giovannelli & Sabau-Graziati, 2016a, after Scaringi, 2015).

It is important to remember the review paper by Girichidis et al. (2020) in which they deeply discuss the physical processes in star formation. Indeed star formation is a complex multi-scale phenomenon that is of significant importance for astrophysics in general. Stars and star formation are key pillars in observational astronomy from local star forming regions in the Milky Way up to high-redshift galaxies. From a theoretical perspective, star formation and feedback processes (ra-

diation, winds, and supernovae) play a pivotal role in advancing our understanding of the physical processes at work, both individually and of their interactions.

Stars impact their environment through a range of energetic processes including radiation, magnetically launched outflows, winds, and supernova explosions. This stellar feedback powers a variety of cosmic processes including heavy element production, evolution of galaxies, reionization of the Universe, formation of planetary systems and ultimately the prevalence of life. Stellar feedback acts over a broad range of physical scales, carrying mass, momentum and energy from stellar scales ($\sim$ au) up to galactic scales ($\sim$ kpc). Unlike the fundamental processes described above, feedback is not a single physical process but a heterogeneous set of effects that arise from the messy and energetic life cycle of stars.

Stars begin to shape their environment during formation. The process of accretion is surprisingly violent, producing significant radiation and flinging mass at velocities of 10s-100s of km/s out to $\sim$ 0.1-1 pc from the forming star in an outflow. Outflows form as a result of rotating gas that winds up the magnetic field lines. Mass coupled to the field is redirected outwards, carrying away angular momentum and thereby facilitating accretion of lower angular momentum material. The term outflow is referring to the phenomena of collimated mass-loss from young stars, while jet refers to a very narrowly collimated outflow.

Reviews about *Accretion Processes in Cosmic Sources: theories vs experiments* have been published by Giovannelli & Sabau-Graziati (2016a) and Giovannelli (2018) and the references therein.

3.2 Formation of planets

Following the very interesting review by Dullemond & Monnier (2010), to understand how planetary systems form in the dusty disks around pre-main-sequence stars, a detailed knowledge of the structure and evolution of these disks is required. Although this is reasonably well understood for the regions of the disk beyond about 1 AU, the structure of these disks inward of 1 AU remains a puzzle. This is partly because it is very difficult to spatially resolve these regions with current telescopes. But it is also because the physics of this region, where the disk becomes so hot that the dust starts to evaporate, is poorly understood.

Figure 4 shows the rich structure of protoplanetary disks, with very different physics playing a role in different regions of the disk.

One can see the strikingly large dynamic range that is involved: the outer radius of a protoplanetary disk can be anywhere from a few tens of astronomical units up to 1,000 AU or more, whereas the inner disk radius is typically just a few stellar radii, i.e., of the order of 0.02 AU. This spans a factor of 10^4–10^5 in spatial scale. For each orbit of the outer disk, we have up to ten million orbits of the inner edge of the disk. Equivalently, the dynamic timescale on which various processes in the disk take place is also a million times shorter (i.e., faster) in the very inner disk regions than in the outer disk regions. In addition, the temperatures differ vastly: from $T \gg 10^3$ K in the inner disk regions down to $T \sim$ 10–30 K in the outer regions.

This large dynamic range in spatial scale, density, and temperature means that very different observational techniques have to be applied to probe the various regions of these disks. Long wavelength telescopes [in the far-infrared (FIR) and millimeter regime] predominantly probe the outer $\sim$ 10 – few 100 AU of disks, whereas mid-IR observations probe intermediate radii about a few

AU, near-infrared (NIR) observations probe the inner AU, and finally optical and UV observations typically probe the regions very close to the stellar surface ($\sim$ 0.01–0.1 AU). Of course, due to dust scattering and sometimes due to quantum–heated grains, short wavelength radiation can also be used to probe the outer disk regions, but for thermally emitted radiation from the disk, this rule of thumb applies very well.

Beckwith et al. (1990) from a continuum observations at 1.3 mm of 86 pre-main-sequence stars in the Taurus-Auriga dark clouds showed that 42% have detectable emission from small particles. The detected fraction is only slightly smaller for the weak-line and "naked" T Tauri stars than for CTTSs, indicating that the former stars often have circumstellar material. The typical disk has an angular momentum comparable to that generally accepted for the early solar nebula, but very little stored energy, almost five orders of magnitude smaller than that of the central star. Their results demonstrate that disks more massive than the minimum mass of the proto-solar system commonly accompany the birth of solar-mass stars and suggest that planetary systems are common in the Galaxy.

This fact is supported also by the observations of submillimeter flux densities from the circumstellar disks around 29 pre-main-sequence stars (Beckwith & Sargent, 1991). The properties of these disks are of special interest, because they bear many similarities to those of the primitive solar nebula. Studies of such systems may therefore lead to a better understanding of the formation of planetary systems like our own.

Meyer et al. (2002) discussed the formation and evolution of planetary systems utilizing the sensitivity of SIRTF (the Space Infra-Red Telescope Facility) through the Legacy Science Program

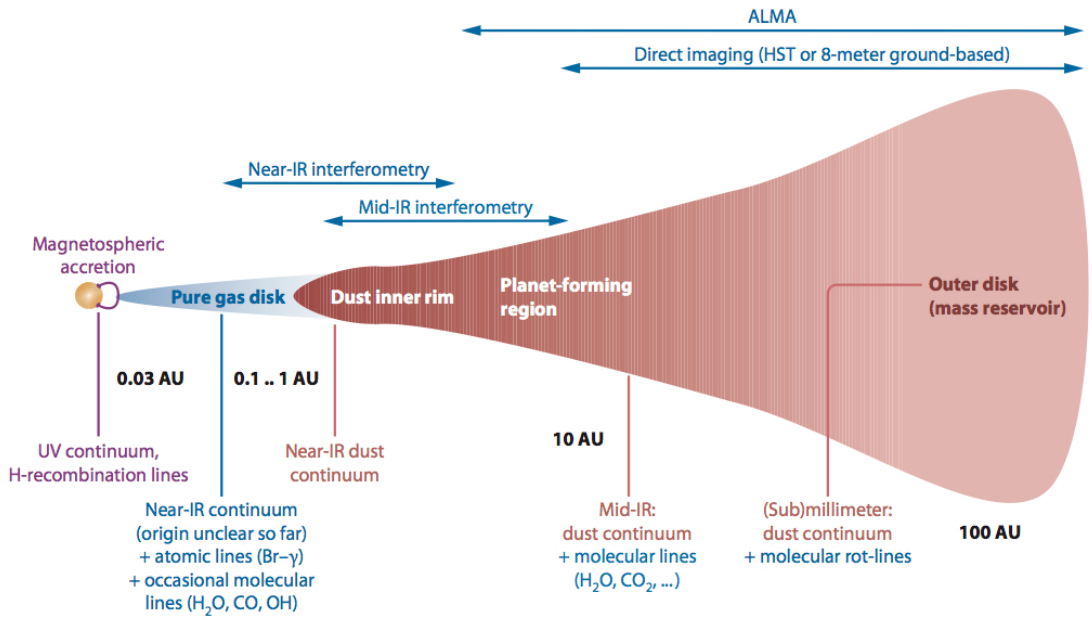

Figure 4: Pictogram of the structure and spatial scales of a protoplanetary disk. Note that the radial scale on the x-axis is not linear. Above the pictogram shows which techniques can spatially resolve which scales. Below shows which kind of emission arises from which parts of the disk (adopted from Dullemond & Monnier, 2010).

to carry out spectrophotometric observations of solar-type stars. They derived circumstellar dust properties around a representative sample of primordial disks (dominated by ISM grains in the process of agglomerating into planetesimals) and debris disks (dominated by collisionally generated dust) over the full range of dust disk optical-depths diagnostic of the major phases of planet system formation and evolution. Hillenbrand (2008) discussed disk-dispersal and planet-formation timescales starting that well before the existence of exo-solar systems was confirmed, it was accepted knowledge that most – if not all – stars possess circumstellar material during the first one-to-several million years of their pre-main sequence lives, and thus that these systems commonly have the potential to form planets.

Following the very interesting paper by Machida, Inutsuka & Matsumoto (2010) and references therein), we believe that stars are born with a circumstellar disk. The formation of the circumstellar disk is coupled with *the angular momentum problem* that is a serious problem in the star formation process, and the dynamics of disks may determine the mass accretion rate onto the protostar that determines the final stellar mass. In addition, planets are considered to form in the circumstellar (or protoplanetary) disk, and their formation process strongly depends on disk properties such as disk size and mass. Thus, the formation and evolution of the circumstellar disk can provide a significant clue to star and planet formation.

Stars form in molecular clouds that have an angular momentum (Arquilla & Goldsmith, 1986; Goodman, 1993; Caselli, 2002; 2003). Thus, the appearance of a circumstellar disk is a natural consequence of the star formation process when the angular momentum is conserved in the collapsing cloud core. In addition, observations have shown the existence of circumstellar disks around the protostar (e.g., Watson et al., 2007; Dutrey, 2007; Meyer et al., 2007). Numerous observations indicate that circumstellar disks around Class I and II protostars have a size of $\sim$ 10–1000 AU and a mass of $\sim 10^{-3}$ – 0.1 $M_{\odot}$ (e.g., Calvet, Hartmann & Strom, 2000; Natta, Grinin & Mannings, 2000). However, they correspond to phases long after their formation. Because the formation site of the circumstellar disk and protostar are embedded in a dense infalling envelope, we cannot directly observe newborn or very young circumstellar disks (and protostars). Thus, we only observe the circumstellar disks long after their formation, i.e., around the class I or II protostar phase.

Observations also indicate that a younger protostar has a massive circumstellar disk (Natta, Grinin & Mannings, 2000; Meyer et al., 2007). Enoch et al. (2009) observed a massive disk with $M_{\rm disk} \sim 1\ M_{\odot}$ around class 0 sources, indicating that this massive disk can be present early in the main accretion phase. However, unfortunately, observation cannot determine the real sizes of circumstellar disks, and how and when they form. Therefore, we cannot understand the formation process of the circumstellar disk by observations. The theoretical approach and numerical simulation are necessary to investigate the formation and evolution of the circumstellar disk.

For this reason Machida, Inutsuka & Matsumoto (2010) investigated the formation and evolution of the circumstellar disk in unmagnetized molecular clouds using three-dimensional hydrodynamic simulations from the prestellar core until the end of the main accretion phase. Their calculations indicate that the planet or brown-dwarf mass object may form in the circumstellar disk in the main accretion phase. In addition, the mass accretion rate onto the protostar shows strong time variability that is caused by the perturbation of proto-planets and/or the spiral arms in the circumstellar disk. Such variability provides a useful signature for detecting the planet-sized companion in the circumstellar disk around very young protostars.

Drouart et al. (1999) starting from the fact that each nebula disk is characterized by its initial mass M_D, its initial radius R_D, and the coefficient of turbulent viscosity α, they show that these parameters may be constrained by comparing temperature-density profiles to properly chosen physical and chemical Solar System data. They developed an analytical model that permits fruitful comparisons with available Solar System data and helpful constraints on the structure of the primitive solar nebula, as summarized below:

- Theories of the formation of giant planets provide relatively weak constraints on the main parameters which define the nebula, namely the initial mass M_D, the initial radius R_D, and the coefficient of turbulent diffusion α. However, they conclude that forming the cores of giant planets in a time compatible with the lifetime of the nebula requires a α value equal to at least a few 10^{-4}.

- The enrichment in fossil deuterium enrichment in water with respect to the protosolar abundance is by far more constraining. At t = 0, R_D must be between 8 and 28 AU, M_D between 0.03 and 0.3 $M_\odot$, and α must be between 0.003 and 1.

- The high viscosity disks they infer ($0.02 < \alpha < 1$) are characterized by a magnetohydrodynamic (MHD) turbulence while their low viscosity models ($0.003 < \alpha < 0.02$) are charaterized by hydrodynamical turbulence. Other mechanisms susceptible to generating a turbulent nebula compatible with observations seem to be ruled out.

- The strength of magnetic fields calculated from their selected models of nebula is consistent with the remanent magnetism found in carbonaceous chondrites. The lifetime of magnetic fields was short, no more than 10^5 years in the extreme case.

Now we can say that over the past 20 years abundant evidence has emerged that many (if not all) stars are born with circumstellar disks. Understanding the evolution of post-accretion disks can provide strong constraints on theories of planet formation and evolution.

Meyer et al. (2007) reviewed on developments in understanding: i) the evolution of the gas and dust content of circumstellar disks based on observational surveys, highlighting new results from the Spitzer Space Telescope; ii) the physical properties of specific systems as a means to interpret the survey results; iii) theoretical models used to explain the observations; iv) an evolutionary model of our own solar system for comparison to the observations of debris disks around other stars; and v) how these results impact our assessment of whether systems like our own are common or rare compared to the ensemble of normal stars in the disk of the Milky Way.

With a sample of $\sim$ 328 stars ranging in age from $\sim$ 3 Myr to $\sim$ 3 Gyr, Meyer et al. (2006) traced the evolution of circumstellar gas and dust from primordial planet-building stages in young circumstellar disks through to older collisionally generated debris disks. In addition to the observational program, they coordinated a concomitant theoretical effort aimed at understanding the dynamics of circumstellar dust with and without the effects of embedded planets, dust spectral energy distributions, and atomic and molecular gas line emission. Together with the observations, these efforts can provide an astronomical context for understanding whether our solar system – and its habitable planet – is a common or a rare circumstance.

The 2nd JEDI (JEts and Disks at INAF) meeting about *Jets, disks and the dawn of planets* has been very interesting. The proceedings contain papers about: i) Early Protostellar Phases; ii) Disk Accretion and YSOs; iii) Jets and Winds; iv) Physical and Chemical Properties of Disks (Alcalá et al., 2015).

Protoplanetary disks dissipate rapidly after the central star forms, on time-scales comparable to those inferred for planet formation. In order to allow the formation of planets, disks must survive the dispersive effects of UV and X-ray photoevaporation for at least a few Myr. Viscous accretion depletes significant amounts of the mass in gas and solids, while photoevaporative flows driven by internal and external irradiation remove most of the gas. A reasonably large fraction of the mass in solids and some gas get incorporated into planets. Gorti et al. (2016) review our current understanding of disk evolution and dispersal, and discuss how these might affect planet formation. They also discuss existing observational constraints on dispersal mechanisms and future directions. In the near future it is desirable to be able to connect disk evolution to planet formation and understand the close, and perhaps causal, correspondence between timescales for planet formation and disk dispersal.

Investigations about the possible correlation between the mass accretion rate onto the central young star and the mass of the surrounding protoplanetary disk – theoretically predicted – have been performed. For instance, Manara et al. (2016) have accurately and homogeneously determined the photospheric parameters, mass accretion rate, and disk mass for an essentially complete sample of young stars with disks in the Lupus clouds. They found a correlation between the mass accretion rate and the disk dust mass, with a ratio that is roughly consistent with the expected viscous timescale when assuming an interstellar medium gas-to-dust ratio. This confirms that mass accretion rates are related to the properties of the outer disk. We expect in the near future measurements in different clouds in order to better determine such a correlation.

Considering that star and planet formation are the complex outcomes of gravitational collapse and angular momentum transport mediated by protostellar and protoplanetary disks, Kratter & Lodato (2016) deeply discuss on the role of gravitational instability in this process. They highlight open questions related to the development of a turbulent cascade in thin disks and the role of mode-mode coupling in setting the maximum angular momentum transport rate in thick disks. Gravitational instability provides efficient angular momentum transport in relatively massive protostellar disks. Evidence of this phase observationally remains sparse but is likely to improve in the coming years with more ALMA data. For this purpose it is interesting to look at the paper "*The ALMA Development Road Map*" (Carpenter et al., 2018).

González-Casanova, Lazarian & Santos-Lima (2016) consider formation of accretion disks from a realistically turbulent molecular gas using 3D MHD simulations. In particular, they analyze the effect of the fast turbulent reconnection for the removal of magnetic flux from a disk. With their numerical simulations they demonstrate how the fast reconnection enables protostellar disk formation resolving the so-called "magnetic braking catastrophe".

What we can say about the step from disk to planet? Thanks to the unprecedented sensitivity and imaging capabilities offered by the Atacama Large Millimeter Array (ALMA) we have transformed our understanding of protoplanetary disks and, hence, of planet formation. Isella (2016) discuss the main results and caveats related to the measurement of the mass of solids in protoplanetary disks based on millimeter-wave observations. Then he present a recent analysis of the

ALMA observations of the HL Tau disk, which suggests that the observed circular rings might be due to the tidal interaction between Saturn mass planets and the circumstellar material. In the conclusion, Isella (2016) argues that the existing observations of protoplanetary disks suggest that planets might form very early on, perhaps at the same time as the formation of the disk itself.

MHD and photo-evaporative winds are thought to play an important role in the evolution and dispersal of planet-forming disks. Recently Fang et al. (2018) report the first high-resolution ($\Delta v \sim 6$ km s^{-1}) analysis of [SII] λ4068, [OI] λ5577, and [OI] λ6300 lines from a sample of 48 T Tauri stars. They decompose them into three kinematic components: a high-velocity component (HVC) associated with jets, and a low-velocity narrow (LVC-NC) and broad (LVC-BC) components. They estimate $\dot{M}_{wind}/\dot{M}_{acc}$ for the LVC and $\dot{M}_{jet}/\dot{M}_{acc}$ for the HVC. With the likely assumption that the NC wind height is larger than the BC, the LVC-BC $\dot{M}_{wind}/\dot{M}_{acc}$ is found to be higher than the LVC-NC. These results suggest that most of the mass loss occurs close to the central star, within a few AU, through an MHD driven wind. Depending on the wind height, MHD winds might play a major role in the evolution of the disk mass.

3.3 Gaia mission

While ESA's Gaia mission has been surveying more than one billion stars from space, scientific astronomical community have been regularly monitoring the satellite's position in the sky with telescopes across the world, including the European Southern Observatory in Chile, to further refine Gaia's orbit and ultimately improve the accuracy of its stellar census (e.g. Prusti et al., 2016).

Figure 5 shows a schematic comparison between the Gaia observatory potentiality with respect to those of the Hipparcos observatory.

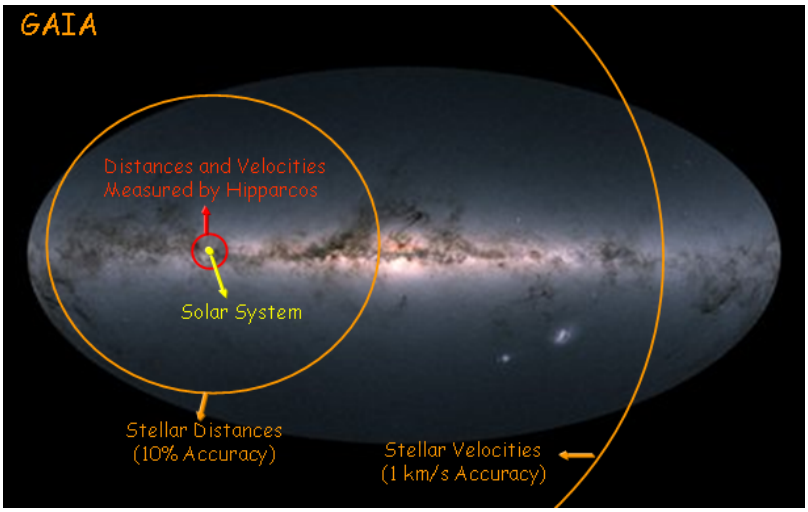

Figure 5: Comparison between Gaia and Hipparcos capabilities.

With its all-sky survey of the position, brightness and motion of over one billion stars in our Milky Way galaxy, Gaia provided a large dataset to search for exoplanets – planets orbiting stars other than the Sun. These will be uncovered by monitoring tiny changes in a star's position and motion caused by the gravitational pull of one or more planets around it, and by looking for dips in

the stellar light caused by a planet transiting in front of its parent star (https://sci.esa.int/web/gaia/-/58784-exoplanets).

The mass of the Milky Way has been one of the most fundamental measurements to be performed in modern astrophysics. However, despite decades of intense effort, even the best available estimates of the Milky Way's mass disagree wildly. Hubble & Gaia accurately weigh the Milky Way. In a striking example of multi-mission astronomy, measurements from the NASA/ESA Hubble Space Telescope and the ESA Gaia mission have been combined to improve the estimate of the mass of our home Galaxy: $\sim 1.12 \times 10^{12}$ $M_{\odot}$ within a radius of ~ 12 kpc from the galactic center. The mass attributed to the stars is $\sim 4.99 \times 10^{10}$ $M_{\odot}$ (Cautun et al., 2020).

Wang, W. et al. (2020) performed an extensive review of the numerous studies and methods used to determine the total mass of the Milky way.

Previous estimates of the mass of the Milky Way ranged from 5×10^{11} to 3×10^{12} $M_{\odot}$. This huge uncertainty arose primarily from the different methods used for measuring the distribution of dark matter – which makes up about 90% of the mass of the galaxy.

Important synergy between distances measured by Gaia and knowledge of cross sections of fundamental reactions occurring in the interior of stars (like results coming from the LUNA experiment) can provide a new vision of the real luminosity of stars, with strong implications on the stellar evolution theory.

3.4 Historical Introduction to HE Astrophysics

Important observations started early in the past century with the discovery of inexplicable effects - the supernovae. They had been observed in ancient times but it was only with the establishing of the stellar and galactic distance scales that their true enormity was realized, namely the release of $\geq 10^{50}$ erg within a matter of days.

The beginning of the Space Astrophysics Era is commonly located around the end of the fifties of the last century with the first space experiments, in the energy range 0.2–0.5 MeV, on board balloons. They were devoted to the detection of γ-rays generated in solar activity (Peterson & Winckler, 1958). But actually γ-ray astronomy was born in the last year of the XIXth century with the discoveries of penetrating gamma radiation (Villard, 1900), and the atmospheric ionization (Wilson, 1900). Wilson suggested that the extraterrestrial gamma radiation could be responsible for the atmospheric ionization. With balloon flights Hess (1912) demonstrated the extraterrestrial and extra-solar origin of the ionizing radiation, which was called *Cosmic Rays*.

Until 1927 it was thought that cosmic rays consisted of γ-rays. Thanks to the discovery of the dependence of the cosmic ray flux on the geomagnetic latitude during a trip from Java to Genoa made by Clay (1927), it was recognized that the composition of cosmic rays included charged particles. Later Hayakawa (1952) determined the contribution of γ-rays to the composition of cosmic rays as less than 1%. The experiments outside the atmosphere started in 1946, soon after the end of the second world war, when the Naval Research Laboratory (NRL) launched a V2 rocket with a payload which observed the Sun's UV spectrum.

Since that time many space experiments were prepared and several fundamental results were reached. In our opinion the actual beginning of the Space Era for studying the Universe is the year 1962. An X-ray experiment – prepared by Giacconi, Gursky, Paolini & Rossi – launched on board an Aerobee rocket discovered a strong X-ray emission from an extra-solar object, namely Sco X-1

(Giacconi et al., 1962). After this first historical experiment many others were launched on board rockets and later balloons and satellites. These experiments lead to our knowledge of an X-ray sky hitherto unknown which started to give experimental proofs of the first theories of Baade & Zwicky (1934) about the possible existence of neutron stars.

Indeed, Baade & Zwicky (1934) first suggested that the supernova was the result of the transition from a normal star to a neutron star. The essential point (Zwicky, 1939) being that the energy releases in such a process is comparable to the change in gravitational potential energy of a star, which collapses from its "normal" size of $\sim 10^6$ Km down to the size of a neutron star of ~ 10 Km.

In the 1950's, Burbidge et al. (1957) with their works on stellar nucleosynthesis suggested realistic models of stars prior to supernova explosion. The supernova process was seen as the result of catastrophic change of state occurring in the core of a highly evolved star, e.g. the transformation of an iron core into a helium core.

Contrary, Cameron (1958) suggested that this degenerate iron core would collapse to a neutron core through inverse beta decay.

The discovery (by chance) of the first X-ray source (Sco X-1) (Giacconi et al., 1962)[1] accelerated the studies on neutron stars, until that Zel'dovich & Guseinov (1965) suggested the presence of an unseen massive companion in a binary system.

Space orbiting observatories with larger and more sophisticated experiments – from Uhuru launched in 1970 (Giacconi et al., 1971) up to HEAO-1 launched in 1977 (Wood et al., 1984) – discovered the most luminous galactic and extragalactic X-ray sources, such as pulsars, X-ray binaries, supernova remnants (SNRs), bursters, and active galactic nuclei (AGNs). But the qualitative jump in the observational capabilities was obtained with the HEAO-2 satellite (Einstein) (Giacconi et al., 1979) in which the X-ray focussing optics of the instruments enhanced the sensitivity in the soft X-ray range by a factor of about 1000 with respect to the old generation of detectors. Also the angular resolution was improved up to ~ 2 arcsec.

This allowed a re-definition of the positions of the already known X-ray sources and the discovery of a large number of weaker ones, such as the normal galaxies and normal stars spread on the entire HR diagram (Vaiana et al., 1981). The detected X-ray fluxes from these stars are definitively larger than those expected from theories of formation and heating of stellar coronae.

This led to a revolution in the comprehension of the role of the star rotation and of the magnetic field in the turbulent transport of energy from the nucleus to the external parts of a star.

Figure 6 shows the evolution of the discovery of X-ray sources starting from UHURU catalog to HEAO A-1 catalog (left upper and lower panels) and γ-ray sources, starting from COS B catalog to 3rd EGRET catalog (right upper and lower panels).

After those experiments that opened the high-energy (HE) windows to the universe, many other satellites were successfully launched both in X-ray and γ-ray ranges, as well as ground-based experiments for the highest energies.

In the 1980-ies the VHE sky was empty and started to be populated only in the subsequent decade. Indeed, in the 1990-ies, high-energy γ-rays have come to play an important role especially in the study of AGNs. Before the launch of the CGRO in 1991, the only known extragalactic source of high-energy γ-rays was 3C 273, which had been detected with the COS B satellite (Swanenburg

[1]This was the first measurement that originated the Nobel Price of Riccardo Giacconi.

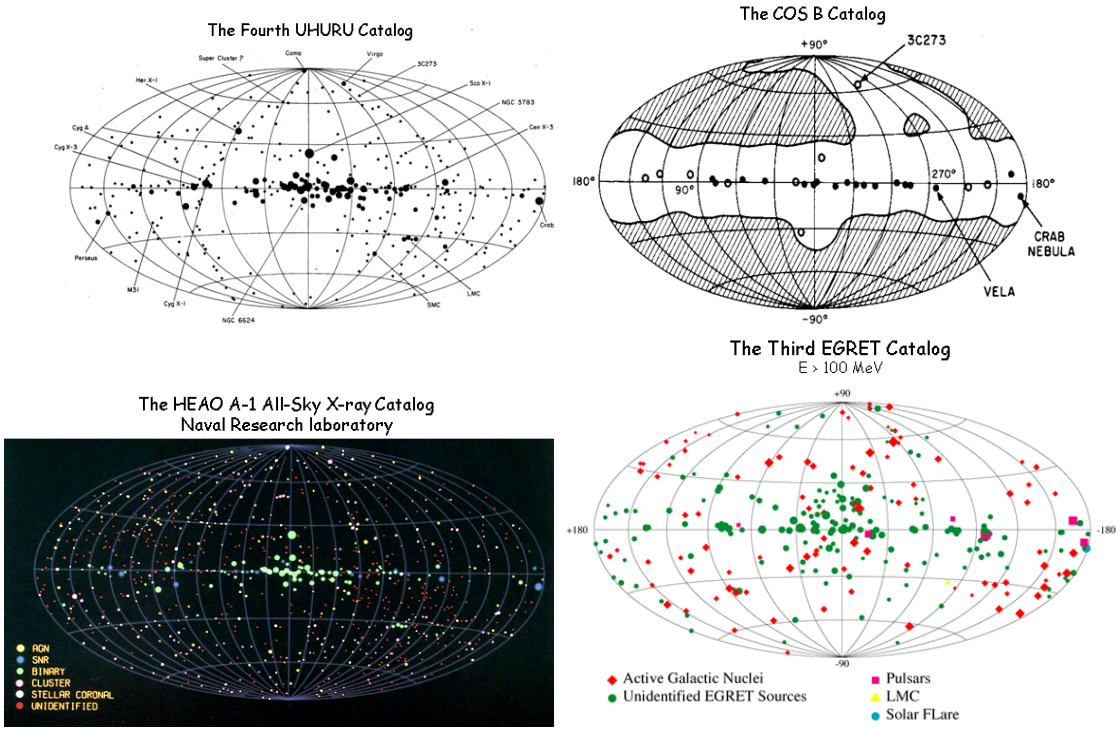

Figure 6: Clockwise from upper left panel: UHURU catalog (Forman et al., 1978), COS B catalog (Swanenburg, et al., 1981), 3rd EGRET catalog (Hartman et al., 1999), HEAO A-1 catalog (Wood et al., 1984).

et al. 1978). The EGRET detector on the CGRO has identified more than 65 AGNs which emit γ-rays at energies above 100 MeV (Hartman et al. 1999), and a substantial fraction of those sources which remain unidentified in the EGRET catalog are likely to be AGNs as well. In addition, the Whipple Observatory γ-ray telescope discovered three AGNs which emit at energies above 300 GeV (Mk 421: Punch et al., 1992; BL Lac object Mrk 501: Quinn et al., 1996; BL Lac object 1ES 2344+514: Catanese et al., 1998), and the detections of some other AGNs with Cerenkov telescopes (Blazar 3C 66A: Neshpor et al. 1998; 1ES 0323+022, PKS 0829+046, 1ES 1101-232, Cen A, PKS 1514-24, RX J10578-275, and 1ES 2316-423: Chadwick et al. 1999). During flaring episodes, the γ-ray emission can greatly exceed the energy output of the AGNs at all other wavelengths. Thus, any attempt to understand the physics of these objects must include consideration of the γ-ray emission.

Figure 7 shows the VHE sky as it was illustrated by Ong (2003) (upper panel) and how it is now: 208 sources (http://tevcat.uchicago.edu) (lower panel).

Following the review by Rieger, de Oña-Wilhelmi & Aharonian (2013), the discovery of more than 100 extraterrestrial sources of Very High Energy (VHE, $\geq$ 100 GeV) or TeV γ-radiation belongs to the most remarkable achievements of the last decade in astrophysics. The strong impact of these discoveries on several topical areas of modern astrophysics and cosmology are recognized and highly appreciated by different astronomical communities. The implications of the results obtained with ground-based TeV γ-ray detectors are vast; they extend from the origin of cosmic rays to the origin of Dark Matter, from processes of acceleration of particles by strong shock waves

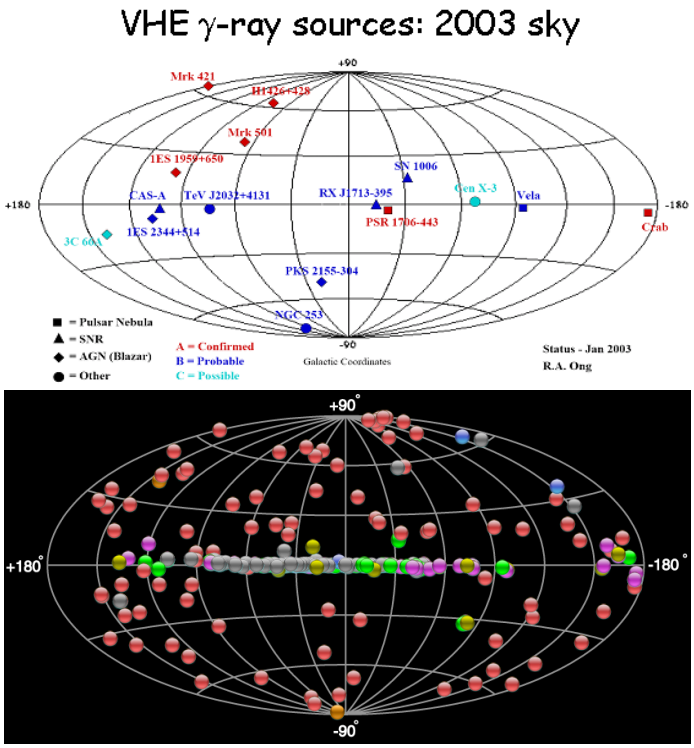

Figure 7: Upper panel: VHE sky as known in 2003 (Ong, 2003); lower panel: VHE sky updated to 2020 (http://tevcat.uchicago.edu).

to the magnetohydrodynamics of relativistic outflows, from distribution of atomic and molecular gas in the Interstellar Medium to the intergalactic radiation and magnetic fields. TeV γ-rays are copiously produced in environments where effective acceleration of particles (electrons, protons, and nuclei) is accompanied by their intensive interactions with the surrounding gas and radiation fields. These interactions contribute significantly to the bolometric luminosity of young Supernova Remnants (SNRs), Star Forming Regions (SFRs), Giant Molecular Clouds (GMCs), Pulsar Wind Nebulae (PWNe), compact Binary Systems, AGNs, and Radio Galaxies (RGs).

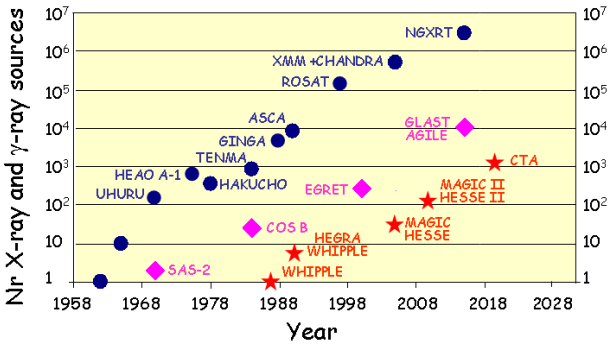

Figure 8: History of the number of X-ray and γ-ray sources detected (after Andrea Santangelo, 2006). Blue points: X-rays; fuchsia diamonds: HE γ-rays; red stars: VHE γ-rays.

Figure 8 shows the increasing number of X-ray and γ-ray sources, as seen by different experiments, since 1962, when the firs extra-solar X-ray source was detected.

Recent reviews on gamma-ray astronomy deeply discuss either the physics governing the energy emissions (e.g. De Angelis & Mallamaci, 2018) either the experiments designed for their detection (e.g. Park, 2017; Di Sciascio, 2019).

Indeed, photons are not deviated by galactic or extragalactic magnetic fields so their directions bring the information of the production sites and are easier to detect than neutrinos. Thus the search for γ primarily address in the framework of the search of cosmic ray sources and to the investigation of the phenomena in the acceleration sites.

Figure 9 shows the differential sensitivity (multiplied by E^2) to a Crab-like point γ-ray source of different experiments and projects (Di Sciascio, 2019).

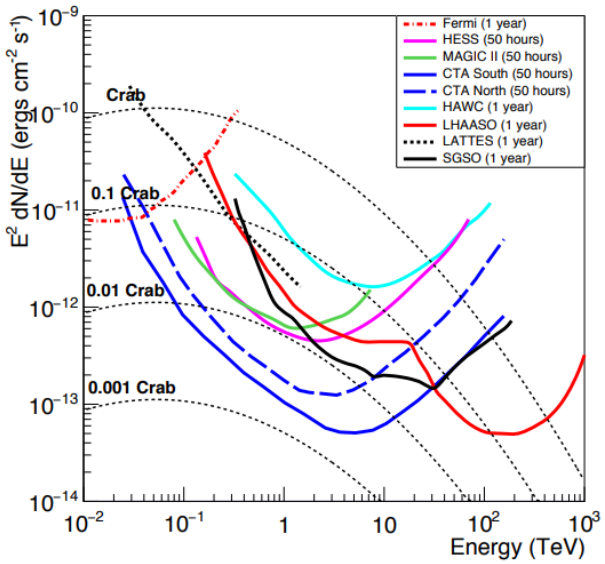

Figure 9: Differential sensitivity of LHAASO to a Crab-like point gamma ray sources compared to other experiments (multiplied by E^2). The Crab Nebula spectrum, extrapolated to 1 PeV, is reported as a reference together with the spectra corresponding to 10%, 1% and 0.1% of the Crab flux (adopted from Di Sciascio, 2019).

3.5 Stellar X-Ray Emission

As deeply discussed by Giovannelli & Sabau-Graziati (2004) (GSG2004), the Einstein satellite observed X-ray emission coming from stars distributed across the entire HR diagram (Vaiana et al., 1981).

If the Sun were the prototype of a late-type dwarf star we would have many fewer X-ray observations of the sky than actually observed. Indeed, the Sun is close to the extreme side of the range of luminosity of late-type stars observed by the Einstein satellite, which demonstrate that the coronal luminosity of the Sun is very small compared with those of other stars.

A large dispersion in the levels of X-ray emission has been observed for stars of any spectral type and luminosity class. Then the question is: Is it possible to determine the physical properties

of the stars in order to explain such an experimental fact? Since the total X-ray luminosity is weakly correlated with effective surface temperature of the late-type MS stars, it is necessary to find some stellar parameters — which are not those determining the position of the stars in the HR diagram — for determining the real level of the X-ray emission. Such 'new' parameters were suggested for the observations performed with the HEAO-1 satellite (Walter et al., 1980) and later for the Einstein observations (Walter & Bowyer, 1981) in RS CVn-type stars. In such stars the rotation is a fundamental parameter for the coronal luminosity. Such a relationship between the rotation velocity and chromospheric activity was already known by means of CaII (Kraft, 1967). The discovery of the luminosity–rotation relationship for individual late-type dwarf stars was obtained by analyzing the data coming from the stellar survey of the Einstein satellite (Pallavicini et al., 1981, 1982). However, since the first observations of X-ray emission from early-type stars, it was clear that the bolometric luminosity was the fundamental parameter responsible of the X-ray emission level (Long & White, 1980). Therefore for such stars their position in the HR diagram is a very good indicator of the X-ray emission levels.

Figure 10 shows the relationship between the soft X-ray coronal emission and the rotation of stars of F7-M5 spectral types and III, IV, and V luminosity class. For stars with spectral types from O to $\simeq$ B5, the X-ray emission level is proportional to the bolometric luminosity of the star. Such a constant is expressed by $L_{\rm x}/L_{\rm bol} \simeq 10^{-7}$ (Pallavicini et al., 1981).

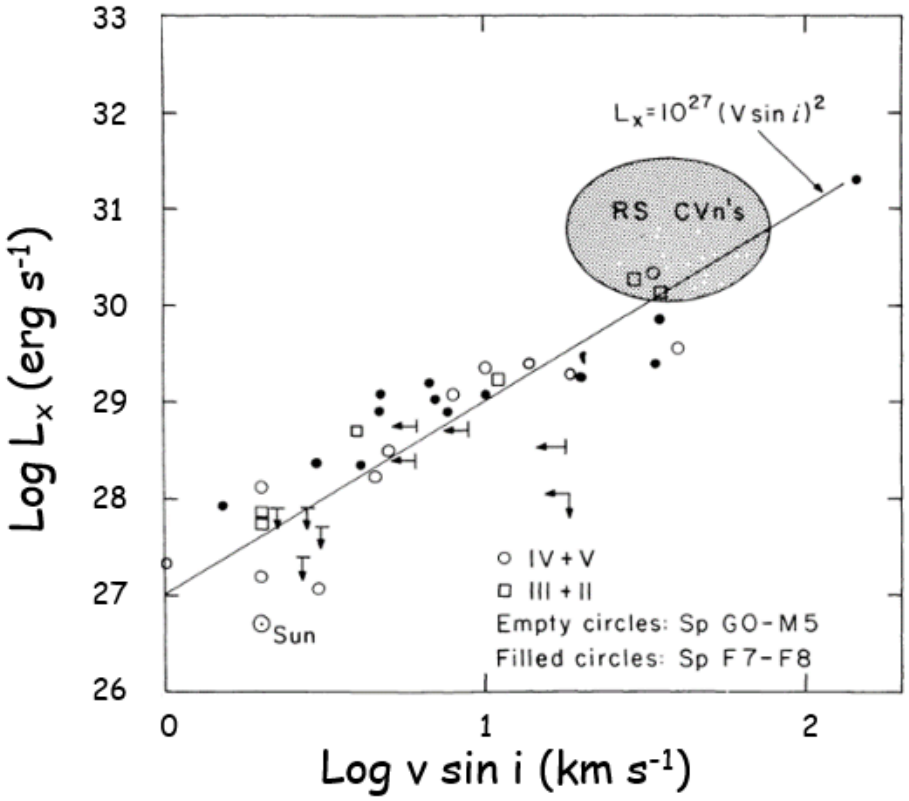

Figure 10: Relationship between the X-ray luminosity and rotational velocity of stars with different spectral types and luminosity class (adopted from Rosner, Golub & Vaiana, 1985, after Pallavicini et al., 1981).

The transition between the behaviour of early-type and late-type stars (whose emission de-

pends essentially on the rotation) occurs in the intermediate spectral range *A* (Topka et al., 1982). The coincidence between the localization of such a transition and the starting of the surface convection authorizes to think that the surface convection phenomenon is a necessary requirement for a solar-like stellar activity.

A particular aspect of the behaviour of the stars is that all of them, independently of the luminosity class, lie in the same regression line of the X-ray luminosity viz. the rotation (see Figure 10). This indicates that rotating stars, which possess external convection zones, emit X-rays independently of the effective gravity (with the exception of cold giant and supergiant stars). However, X-ray data from the first observations showed that the effective gravity plays an important role in young stars. This is because the effective gravity correlates with the bolometric luminosity (and bolometric and X-ray luminosity experimentally correlate). Therefore the effective gravity is correlated with the X-ray luminosity. However, since the theory predicts a relationship between the bolometric luminosity and the X-ray emission levels (at least for models considering instabilities in the radiation driven winds), the X-ray luminosity-effective gravity relationship for such stars is considered as secondary and without physical significance. The theoretical predictions become better if stars of colder spectral types are considered. The results from the Einstein Observatory revealed that giant and supergiant late-type stars are, probably, very weak X-ray sources (Rosner, Golub & Vaiana, 1985). It is possible to encounter a possible explanation invoking the analogy with the solar coronal holes: in such regions the coronal gas flows to the exterior parts in order to form the stellar wind, and therefore the X-ray emission level is strongly diminished.

3.6 X-ray binary systems

The trivial definition of X-ray binaries (XRBs) is that they are binary systems emitting X-rays. However it has been largely demonstrated that X-ray binary systems emit energy in IR, Optical, UV, X-ray, Gamma-ray and sometimes they show also valuable radio emission. They can be divided in different sub-classes (Giovannelli, 2016):

- High Mass X-ray Binaries (HMXB) in which the optical companion is an early type giant or supergiant star and the collapsed object is a neutron star or a black hole. They are concentrated around the galactic plane. The mass transfer is usually occurring via stellar wind; they show hard pulsed X-ray emission (from 0.069 to 1413 s) with KT $\geq$ 9 keV; typical X-ray luminosity is ranging from 10^{34} to 10^{39} erg s^{-1}, and the ratio of X-ray to optical luminosity is $\sim 10^{-3}$–10. The HMXBs can be divided in two sub-classes

  - Hard Transient X-ray Sources (HXTS) in which the neutron star is eccentrically (e $\sim$ 0.2–0.5) orbiting around a V-III luminosity-class Be star ($P_{orb} > 10$ days); they show strong variable pulsed hard X-ray emission ($L_{Xmax}/L_{Xmin} > 100$) with KT $\geq$ 17 keV, and P_{spin} ranging from 0.069 to 1413 s; $L_X = 10^{34} - 10^{39}$ erg s^{-1}.
  - Permanent X-ray Sources in which the neutron star or black hole is circularly orbiting (e $\sim$ 0) around a giant or supergiant OB star ($P_{orb} < 10$ days); they show an almost steady permanent pulsed hard X-ray emission ($L_{Xmax}/L_{Xmin} \ll 100$), and P_{spin} ranging from 0.069 to 1413 s; $L_X \sim 10^{37}$ erg s^{-1}.

    - Obscured Sources, which display huge amount of low energy absorption produced by the dense wind of the supergiant companion, surrounded by a weakly magnetized neutron star.
    - Supergiant Fast X-ray transients (SFXT), a new subclass of transients in which the formation of transient accretion discs could be partly responsible for the flaring activity in systems with narrow orbits. They show $L_{Xpeak} \approx 10^{36}$ erg s^{-1}, and $L_{Xquiecence} \approx 10^{32}$ erg s^{-1}.
  - Anomalous X-ray Pulsars (AXPs) in which the optical counterparts probably are not OB and Be stars. They show a soft-hard X-ray emission with KT $\sim$ 0.4–4 KeV, $L_{Xmax}/L_{Xmin} \approx 10$, and $L_X/L_{opt} \sim 0.001$–10, being $L_X = 10^{34} - 10^{36}$ erg s^{-1}. On the contrary to the former two classes the rotational period of the pulsar is limited in a very narrow range: $P_{spin} \sim$ 6–12 s.

- Low Mass X-ray Binaries (LMXB) in which the optical companion is a low-mass-late-type star and the collapsed object is a neutron star or a black hole (P_{orb} from 41 min to 11.2 days). They are concentrated around the galactic plane and especially in the galactic center. The mass transfer in these systems is usually occurring via Roche lobe overflow. Their emission in soft X-ray range is usually not pulsed with KT $\leq$ 9 keV. Their X-ray luminosity is ranging from 10^{36} to 10^{39} erg s^{-1} and $L_X/L_{opt} \sim 10^2$–10^4; many LMXBs show Quasi Periodic Oscillations (QPOs) between 0.02 and 1000 seconds and few of them also pulsed X-ray emission, such as Her X1, 4U 1626-27 and GX 1+4. Unlike HMXBs, LMXBs rarely harbour an X-ray pulsar. This is because the magnetic fields of the neutron stars in LMXBs are 10^{-1} – 10^{-4} times those in HMXBs, and so the accreted material is not funneled onto the polar caps.

- Cataclysmic Variables (CVs) in which the optical companion is a low-mass-late-type star and the compact object is a white dwarf. The detected CVs are spread roughly around the solar system at distance of 200-300 pc. Orbital periods are ranging from tens of minutes to about ten hours. The mass transfer is occurring either via Roche lobe overflow or via accretion columns or in an intermediate way depending on the value of the magnetic field. Typical X-ray luminosity is ranging from 10^{32} to 10^{34} erg s^{-1}. Updated reviews about CVs are those by Giovannelli (2008) and Giovannelli & Sabau-Graziati (2015a);

- RS Canum Venaticorum (RS CVn) type systems, in which no compact objects are present and the two components are a F or G hotter star and a K star. Typical X-ray luminosity is ranging from 10^{30} to 10^{31} erg s^{-1}. Usually in the current literature they are excluded from the class of X-ray binaries since historically they were discovered as X-ray emitters only with the second generation of X-ray experiments.

Relatively few binaries have been discovered at GeV and TeV energies (e.g. Rappoldi et al., 2016; Maier, 2015; Blanch Bigas et al., 2015). These objects are important test beds of our understanding of particle acceleration in astrophysical objects. The periodic occurrence of the same environmental conditions for the accelerator makes these objects one of the closest things a γ-ray astronomer can get to a physical "experiment" and can help to distinguish between external properties and the properties of the accelerator itself.

Thousand papers about these cosmic sources are available in the literature. We mention the last available exhaustive review by Postnov & Yungelson (2014) about "*The Evolution of Compact Binary Stars Systems*" in which they review the formation and evolution of compact binary stars consisting of WDs, NSs, and BHs. Merging of compact-star binaries are expected to be the most important sources for forthcoming gravitational-wave (GW) astronomy. Indeed, the Advanced LIGO observatory recently reported the first direct detection of gravitational waves (Abbott et al. 2016a) as a merger of two black holes with the mass of 36^{+5}_{-4} $M_{\odot}$ and 29 ± 4 $M_{\odot}$, and the final black hole mass is 62^{+4}_{-4} $M_{\odot}$ with $3.0^{+0.5}_{-0.5}$ $M_{\odot}c^2$ radiated in gravitational waves.

Several review papers have been published for discussing the different classes of galactic compact sources: i) Cataclysmic Variables (CVs) and related objects (e.g. Giovannelli, 2008; Giovannelli & Sabau-Graziati, 2012a; 2015a); ii) High Mass X-ray Binaries (HMXBs) (e.g. Giovannelli & Sabau-Graziati, 2001, 2004, 2014, and van den Heuvel, 2009 and references therein; iii) Obscured Sources and Supergiant Fast X-Ray Transients (e.g. Chaty, 2011); iv) Ultra–Compact Double–Degenerated Binaries (e.g. Wu, Ramsay & Willes, 2008; Wu, 2009); Magnetars (Kitamoto et al., 2014: White Paper for ASTRO-H Space X-ray observatory).

XRBs are the best laboratory for the study of accreting processes thanks to their relative high luminosity in a large part of the electromagnetic spectrum. For this reason, multifrequency observations are fundamental in understanding their morphology and the physics governing their behaviour.

Because of the strong interactions between the optical companion and collapsed object, low and high energy processes are strictly related.

Often, it is easier to perform observations of low energy processes (e.g. in radio, near-infrared (NIR) and optical bands) since the experiments are typically ground-based, on the contrary to observations of high energy processes, for which experiments are typically space-based.

The X-ray/Be binaries are the most abundant group of massive X-ray binaries in the galaxy, with a total inferred number of between 10^3 and 10^4. The ones which do occasionally flare-up as transient X-ray/Be systems are only the "tip" of this vast "iceberg" of systems (van den Heuvel and Rappaport, 1987). The mass loss processes are due to the rapid rotation of the Be star, the stellar wind and, sporadically, to the expulsion of casual quantity of matter essentially triggered by gravitational effects close to the periastron passage of the neutron star. The long orbital period (> 10 days) and a large eccentricity of the orbit (> 0.2) together with transient hard X-ray behavior are the main characteristics of these systems. Among the whole sample of galactic systems containing 114 X-ray pulsars (Liu, van Paradijs & van den Heuvel, 2006), only few of them have been extensively studied. Among these, the system A 0535+26/HDE 245770 – HDE 245770 was nicknamed Flavia' star by Giovannelli & Sabau-Graziati (1992) – is the best known thanks to concomitant favorable causes, which rendered possible forty six years of coordinated multifrequency observations, most of them discussed in the past by e.g. Giovannelli & Sabau-Graziati (1992), Burger et al. (1996), Piccioni et al. (1999), and by Giovannelli & Sabau-Graziati (2011) and Giovannelli et al. (2015a,b). Accretion powered X-ray pulsars usually capture material from the optical companion via stellar wind, since this primary star generally does not fill its Roche lobe. However, in some specific conditions (e.g. the passage at the periastron of the neutron star) and in particular systems (e.g. A 0535+26/HDE 245770), it is possible the formation of a temporary accretion disk around the neutron star behind the shock front of the stellar wind. This enhances the efficiency of the

process of mass transfer from the primary star onto the secondary collapsed star, as discussed by Giovannelli & Ziolkowski (1990) and by Giovannelli et al. (2007) in the case of A 0535+26.

Optical emission of HMXBs is dominated by that of the optical primary component, which is not, in general, strongly influenced by the presence of the X-ray source. The behavior of the primary stars can be understood in the classical (or almost) frame-work of the astrophysics of these objects, i.e. by the study of their spectra which will provide indications on mass, radius, and luminosity. Both groups of HMXBs (transient and permanent) differ because of the different origin of the mass loss process: in the first, the mass loss process occurs via a strong stellar wind and/or because of an incipient Roche lobe over-flow; in the second group, the mass transfer is probably partially due to the rapid rotation of the primary star and partially to stellar wind and sporadically to expulsions of a casual quantity of matter, essentially triggered by gravitational effects because of periastron passage where the effect of the secondary collapsed star is more marked. A relationship between orbital period of HMXBs and the spin period of the X-ray pulsars is shown in Fig. 11 (updated from Giovannelli & Sabau-Graziati, 2001 and from Corbet, 1984, 1986). It allows to recognize three kinds of systems, namely disk-fed, wind-fed [$P_{pulse} \propto (P_{orb})^{4/7}$], and X-ray/Be systems [$P_{pulse} \propto (P_{orb})^2$].

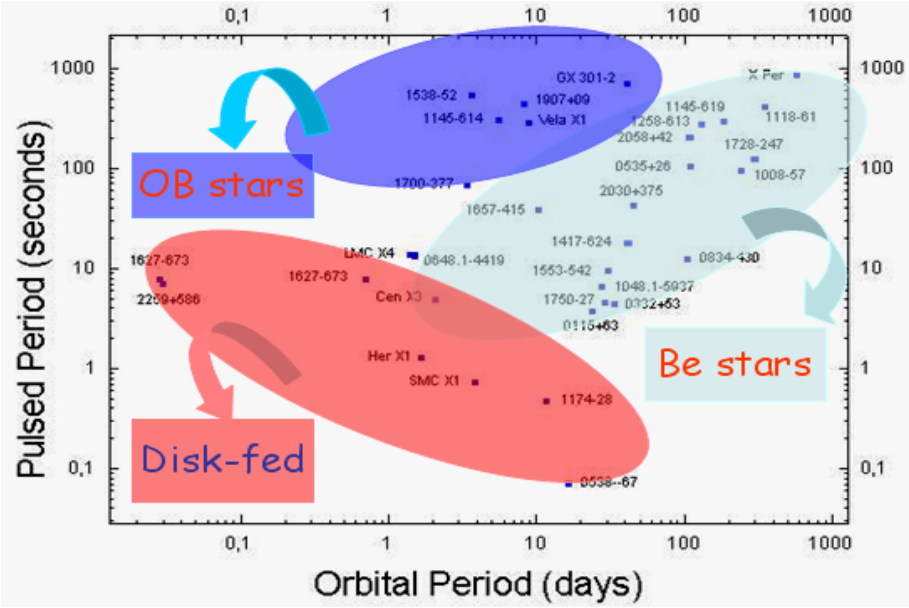

Figure 11: Spin period vs orbital period for X-ray pulsars. Disk–fed systems are clearly separated by systems having as optical counterparts either OB stars or Be stars (adopted from Giovannelli & Sabau-Graziati, 2001, after Corbet, 1984, 1986).

Most of the systems having a Be primary star are hard X-ray (KT $>$ 10 KeV) transient sources (HXTS). They are concentrated on the galactic plane within a band of $\sim 3.9°$. The orbits are quite elliptic and the orbital periods large (i.e. A 0538-66: e = 0.7, P_{orb} = 16.6 days (Skinner et al., 1982); A 0535+26: e = 0.47 (Finger, Wilson & Hagedon, 1994), P_{orb} = 111.0 days (Priedhorsky & Terrell, 1983). The X-ray flux during outburst phases is of order 10-1000 times greater than during quiescent phases. For this reason, on the contrary, the stars belonging to the class of permanent

X-ray sources, which do not present such strong variations in X-ray emission, can be also named "standard" high mass X-ray binaries. In X-ray/Be systems, the primary Be star is relatively not evolved and is contained within its Roche lobe. The strong outbursts occur almost periodically in time scales of the order of weeks-months. Their duration is shorter than the quiescent phases. During X-ray outbursts, spin-up phenomena in several systems have been observed (i.e. A 0535+26 and 4U 1118-61 (Rappaport & Joss, 1981). The observed spin-up rates during the outbursts are consistent with torsional accretion due to an accretion disk (e.g. Ghosh, 1994). So, the formation of a temporary accretion disk around the collapsed object should be possible during outburst phases (e.g. Giovannelli & Ziolkowski, 1990).

The number of X-ray pulsars slowly increases with time thanks to new detections performed with different new generation observatories. They were 95 in 2000 (Giovannelli & Sabau-Graziati, 2000) and the orbital periods were known only for about three dozens of them. They contain the group of the permanent HMXBs and that of transient HMXBs (X-ray/Be systems), whose components are an X-ray pulsing neutron star - the secondary - and a giant or supergiant OB or a Be star, respectively - the primary . Moreover, some low-mass X-ray Binaries (LMXBs) containing an X-ray pulsar and some pulsars belonging to Magellanic Clouds were contained too in the sample of 95 systems. In 2006 the known X-ray pulsars were 114 (Liu, van Paradijs & van den Heuvel, 2006). Coe et al. (2010) report $\sim$ 60 X-ray pulsars in the SMC. Later, Rajoelimanana & Charles (2012) listed 49 optical counterparts of SMC X-ray pulsars detected by MACHO and OGLE. Systems with known P_{spin} are 20 while the systems with known P_{orb} are 23, being 6 of them uncertain.

Another class of XRBSs is formed by the CVs, although usually the are not mentioned in literature as XRBSs, but as an apart class. The number of CVs is increasing very rapidly thanks to the many surveys, and in particular with the MASTER-Net Transient Detections program which detected 530 new CVs (Buckley, 2015). For reviews about CVs see the fundamental papers by Robinson (1976), Patterson (1984, 1994), Hack & la Dous (1993), and the books of Warner (1995) and Hellier (2001). The long review *The Impact of Space Experiments on our Knowledge of the Physics of the Universe* by Giovannelli & Sabau-Graziati (2004) contains also a part devoted to CVs. More recent reviews are those by Giovannelli (2008), and Giovannelli & Sabau-Graziati (2015a), de Martino (2016).

After the first historical Frascati 1984 Workshop about "*Multifrequency Behaviour of Galactic Accreting Sources*" (Giovannelli, 1985), it is important to remind the long biennial series of the Frascati Workshops about "*Multifrequency Behaviour of High Energy Cosmic Sources*" started in 1995, whose refereed proceedings can be found in Giovannelli & Sabau-Graziati (1996, 1999, 2002, 2010, 2012b).

3.7 A general model for compact accreting stars: The Scenario Machine

Starting from the trivial definition of XRBs: they are binary systems emitting X-rays, a natural question arises. Are these systems governed by few physical parameters independent of their nature? The answer is positive. Indeed, HMXRBs, LMXRBs, AXPs, and CVs can be considered as gravimagnetic rotators: a body with mass M, having a magnetic moment $\vec{\mu}$, rotating with rotational velocity $\vec{\omega}$, being the two axis not necessarily coincident, as sketched in Fig. 12. Introducing a physical parameter, $y = \dot{M}/\mu^2$, named *gravimagnetic parameter*, all the gravimagnetic rotators are contained in a plane Log P_{spin} vs Log y (Lipunov, 1987; Lipunov & Postnov, 1988).

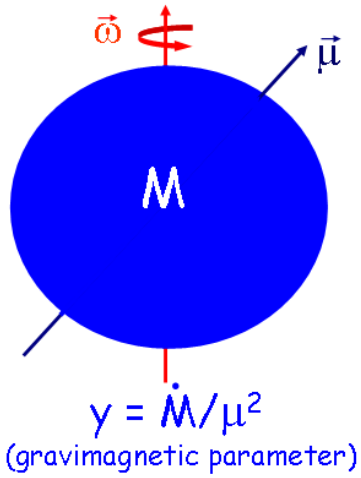

Figure 12: Gravimagnetic rotator: a body with mass M, having a magnetic moment $\vec{\mu}$, rotating with rotational velocity $\vec{\omega}$. The parameter $y = \dot{M}/\mu^2$ is called *gravimagnetic parameter* (Lipunov, 1987; Lipunov & Postnov, 1988).

The *Scenario Machine* (Monte Carlo simulations of binary evolution) permits to build up the complete picture of all possible evolutionary stages of binaries in the Galaxy. The basic evolution equation (1) used for 500,000 systems containing magnetized stars provided the results contained in the plane Log P_{spin}–Log y, reported in the upper panel of Fig. 13. P_{spin} is expressed in seconds and the gravimagnetic parameter is expressed in unit of 10^{-42} g s^{-1} G^{-2} cm^{-6}. The symbols used for the different types of binaries are explained in the lower panel of Fig. 13. The definition of the characteristic radii can be found in the paper by Lipunov (1987). Observational examples of various types of rotators are reported in Fig. 14 (Lipunov, 1987).

$$\frac{dI\omega}{dt} = \dot{M}K_{su} - \frac{\kappa_t \mu^2}{R_t^3} \tag{3.1}$$

where:

K_{su} = specific angular momentum applied by the accretion matter to the rotator;
$K_{su} = \sqrt{GM_x R_d}$ for Keplerian disk accretion;
$K_{su} = \eta_t \Omega R_g^2$ for wind accretion in a binary;
$K_{su} \sim 0$ for a single magnetic rotator;
R_d = radius of the inner disk edge;
Ω = rotational frequency of the binary system;
$\eta_t = 1/4$ (Illarionov & Sunyaev, 1975);
κ_t = dimensionless factor;
R_t = characteristic radius;
$\dot{M}$ = accretion rate in different regimes.

Using the "Scenario Machine" Raguzova & Lipunov (1999) obtained an evolutionary track that can lead to the formation of Be/BH systems. The modern evolutionary scenario predicts the

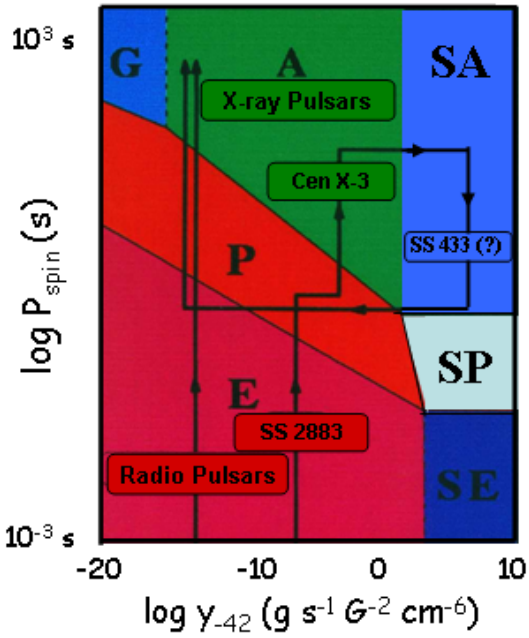

The rotator classification

Designation	Name	Physical sense
E	Ejector	$R_{st} > \max\{R_G, R_l\}$
P	Propeller	$R_c < R_{st} \leq \max\{R_G, R_l\}$
A	Accretor	$R_{st} \leq R_G$ and $R_{st} \leq R_c$ $\quad \dot{M}_c \leq \dot{M}_{cr}$
G	Georotator	$R_G < R_{st} \leq R_c$
M	Magnetor	$R_{st} > a$ and $R_c > a$
SE	Superejector	$R_{st} > R_l$
SP	Superpropeller	$R_c < R_{st} \leq R_l$ $\quad \dot{M}_c > \dot{M}_{cr}$
SA	Superaccretor	$R_{st} \leq R_c$ and $R_{st} \leq R_G$

Figure 13: Upper panel: distribution of magnetic rotators in the plane "Spin Period" – "Gavimagnetic Parameter" (adapted from Lipunov, 1995); lower panel: classification of rotators (Lipunov, 1987).

existence of binary black holes on eccentric orbits around Be stars and such systems may be discovered in the near future... Like happened!

Indeed, Raguzova & Lipunov (1999) calculations show that binary black holes with Be stars must have $0.2 < e < 0.8$. It is particularly difficult to detect such systems as most of their spectroscopic variations occur in a relatively small portion of the orbit, and could easily be missed if the systems are observed at widely separated epochs.

The critical initial mass of the supernova star that collapses to a BH is accepted to be equal to $55 < M_{cr} < 75\ M_{\odot}$, and the fraction of the presupernova mass ($M_{\star}$) collapsing to the BH, $k_{BH} = M_{BH}/M_{\star} = 0.5$. The kick velocity v_m = 0–200 km s^{-1}. The age of the system, according to their evolutionary scenario is 4×10^6 yr.

The expected number of Be/BH binaries – with orbital period 10 d $< P_{orb} <$ 1000 d, and eccentricity $0.2 < e < 0.8$ – is 1 Be/BH for 20-30 Be/NS.

Belczynski and Ziółkowski (2009) used binary population synthesis models to show that the expected ratio of Be/XRBs with neutron stars to black holes in the Galaxy is relatively high ($\sim$

Type of rotator	Designation	The clearly confirmed observational example	Model assumptions
Ejector	E	Radiopulsars	LSI + 61°303, Cyg X-3, BL Lac objects,
Propeller	P	–	Transient X-ray sources, γ-bursts, some cataclysmic variables (dwarf novae), magnetic Ap-stars
Accretor	A	X-ray pulsars, X-ray bursters, cataclysmic variables with white dwarfs, novae, intermediate polars	–
Superejector	SE	–	SS 433, AGN, QSO
Superpropeller	SP	–	–
Superaccretor	SA	–	SS 433
Georotator	G	–	–
Magnetor	M	Polars	–

Figure 14: Observational examples of rotators (Lipunov, 1987).

$30-50$), and so broadly in line with observations. Thus we can expect 1 Be/BH for 30–50 Be/NS.

Therefore, we can expect 1 Be/X-ray BH system for 20–50 Be/X-ray NS systems (Raguzova & Lipunov, 1999; Belczynski & Ziółkowski, 2009). We know 60 Be/X-ray NS systems (after INTEGRAL). Thus we expect 1–3 Be/X-ray BH systems. One of this systems – as I said – has been detected: MWC 656 (Casares et al., 2014).

New simulations – using the StarTrack binary population synthesis models have been conducted to understand the formation channel of MWC 656 – constrain the population of Be/BH systems and study the fate of MWC 656 as a possible NS–BH merger, and then possible gravitational wave emitter. In particular, it has been assumed that all donors beyond main sequence are allowed to survive the common envelope (CE) phase. Ten Gyr of evolution of the Galactic disk originates $\sim$ 8700 B/BH systems, and 1/3 of them would be Be/BH systems: namely $\sim$ 2900). However, only 13 of them had periods, eccentricities and masses similar to MWC 656 (Grudzinska et al., 2015).

3.8 Magnetic field intensity in gravimagnetic rotators

Magnetic fields are observed in main sequence stars and their white dwarf and neutron star progeny. The fields in these three groups of stars are likely to be linked via stellar evolution. Super-strong magnetic fields are observed in both white dwarfs and neutron stars. Therefore, the formation of strong magnetic fields in gravimagnetic rotators is a question of crucial importance (see e.g. Ferrario & Wickramasinghe, 2007). While there is strong evidence that the magnetic fields in late type stars are dynamo generated, it is likely that the magnetic fields of stars on the upper main sequence are of fossil origin, perhaps dating back to the time of star formation.

In the fossil scenario, the field strength B scales with the radius of the star ($R_\star$) as $B \propto R_\star^{-2}$. Therefore, if a star with initial magnetic field strength $B_i \sim 100$ G and typical radius $R_i \sim 10^6$ km collapses as a neutron star with a final radius $R_f \sim 10$ km, the final magnetic field strength will be $B_f \sim 10^{12}$ G, being valid the relationship $B_f = B_i \times (R_i/R_f)^2$.

The relationship between the spin period of a neutron star and a white dwarf is $P_{spin}^{NS} \approx P_{spin}^{WD} \times (R_{NS}/R_{WD})^2$. Therefore to a typical spin period of 1 ms of a NS corresponds a spin period of a WD of 1000 s.

The validity of the former relationships is clearly shown if Fig. 15 in which Log P_{spin} versus Log B are reported for WDs (left panel) and NSs (right panel) (Ferrario & Wickramasinghe, 2005) .

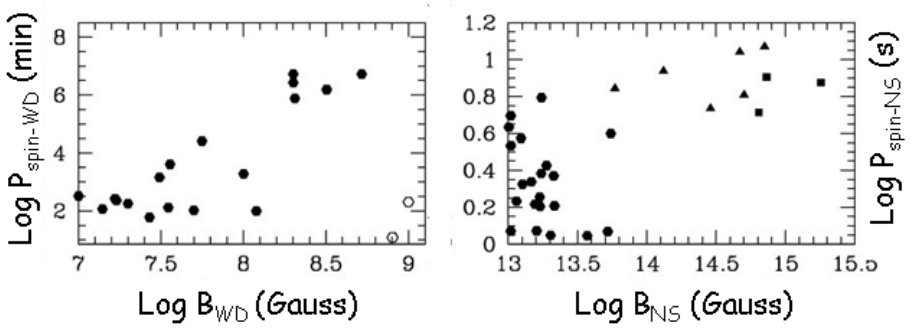

Figure 15: Relationships between spin period and magnetic field intensity for white dwarfs (left panel) and neutron stars (right panel) (adapted from Ferrario & Wickramasinghe, 2005).

Following the interesting review by Ferrario, de Martino & Gänsicke (2015), magnetic fields of isolated MWDs are observed to lie in the range 10^3 – 10^9 G. While the upper limit cutoff near 10^9 G appears to be real, the lower limit is more difficult to investigate. The incidence of magnetism below a few 10^3 G still needs to be established by sensitive spectropolarimetric surveys conducted on 8 m class telescopes. Highly magnetic WDs (HMWDs) tend to exhibit a complex and non-dipolar field structure with some objects showing the presence of higher order multipoles. There is no evidence that fields of HMWDs decay over time, which is consistent with the estimated Ohmic decay times scales of $\sim 10^{11}$ yr. The slow rotation periods ($\sim$ 100 yr) inferred for a large number of isolated MWDs in comparison to those of non-magnetic WDs (a few days) suggest that strong magnetic fields augment the braking of the stellar core. MWDs, as a class, also appear to be more massive (0.784 ± 0.047 $M_\odot$) than their weakly or non-magnetic counterparts (0.663 ± 0.136 $M_\odot$).

MWDs are also found in binary systems where they accrete matter from a low-mass donor star. These binaries, called magnetic Cataclysmic Variables (MCVs), comprise about 20–25 % of all known CVs. Zeeman and cyclotron spectroscopy of MCVs have revealed the presence of fields in the range $\sim$ 7–230 MG. Complex field geometries have been inferred in the high field MCVs (the

Table 1: Approximate correspondence of magnetic fields in stars of upper main sequence and compact objects. HFMWDs = High Field Magnetic White Dwarfs; NSs = Neutron Stars (adapted from Ferrario & Wickramasinghe, 2007).

	B (Gauss)			B (Gauss)
Spectral type stars B-F	300-3,000	$\Longrightarrow$	HFMWDs	10^6-10^9
Spectral type stars O-B	???-30,000	$\Longrightarrow$	NSs	10^{11}-10^{15}

polars) whilst magnetic field strength and structure in the lower field group (intermediate polars, IPs) are much harder to establish.

To date there are about $\sim$ 250 MWDs with well determined fields (as reported in the Table 1 of the review paper by Ferrario, de Martino & Gänsicke, 2015) and over $\sim$ 600 if we also count objects with no or uncertain field determination (see Kepler et al. 2013, 2015). The number of identified IPs has now increased to $\sim$ 60 systems (see Table 3 of the review paper by Ferrario, de Martino & Gänsicke, 2015 and updated results in Bernardini et al. (2015). The other $\sim$ 600 candidates still awaiting confirmation through X-ray follow-ups with sensitive facilities such as XMM-Newton and NuSTAR (see http://asd.gsfc.nasa.gov/Koji.Mukai/iphome/iphome.html).

Enormous progress has been made on observing stellar magnetism in stars from the main sequence through to compact objects. Recent data has brought stricter information on the origin of stellar magnetic fields. However, this theme is still one of the crucial points to be solved in astrophysics.

Ferrario, Melatos & Zrake (2015) review recent work in this area of research. In particular, they look at the fossil field hypothesis which links magnetism in compact stars to magnetism in main sequence and pre-main sequence stars and they consider why its feasibility has now been questioned particularly in the context of highly magnetic white dwarfs. They also review the fossil versus dynamo debate in the context of neutron stars and the roles played by key physical processes such as buoyancy, helicity, and superfluid turbulence, in the generation and stability of neutron star fields. Independent information on the internal magnetic field of neutron stars will come from future gravitational wave detections. the Laser Interferometer Gravitational Wave Observatory (LIGO) have already constrained the Crab pulsar gravitational wave luminosity to be $\lesssim 2\%$ of the observed spin-down luminosity, thus placing a limit of $\lesssim 10^{16}$ G on the internal field. Therefore we are witnessing the dawn of a new era of exciting discoveries in compact star magnetism driven by the opening of a new, non-electromagnetic observational window.

Beskin et al. (2016a) review about the role that strong magnetic fields play in the universe.

3.8.1 Magnetic field intensity measures

It is convenient to remind how the magnetic field intensity can be measured. A detailed discussion about the field determination in isolated magnetic WDs and in WDs in binary systems is reported in the review paper by Ferrario, de Martino & Gänsicke (2015). Direct measurements of the WD magnetic field strength in the high field magnetic CVs, the polars, can be obtained either (i) through Zeeman splitting of the photospheric hydrogen absorptions lines when these systems enter low accretion states or (ii) through the modeling of cyclotron emission features that characterizes the optical to IR spectra during intermediate and high accretion states (see Wickramasinghe & Ferrario, 2000) or (iii) via the study of Zeeman features arising from the halo of matter surrounding the accretion shock.

Figure 16 shows the distribution of B for MCVs and MWDs (adopted from Ferrario, de Martino & Gänsicke, 2015).

In MCVs there is an interesting relationship between the magnetic field strength and orbital period of the systems, as reported in Fig. 17 where the polars and IPs are separated by the blue line that marks the synchronization between orbital and spin periods of the cataclysmic systems.

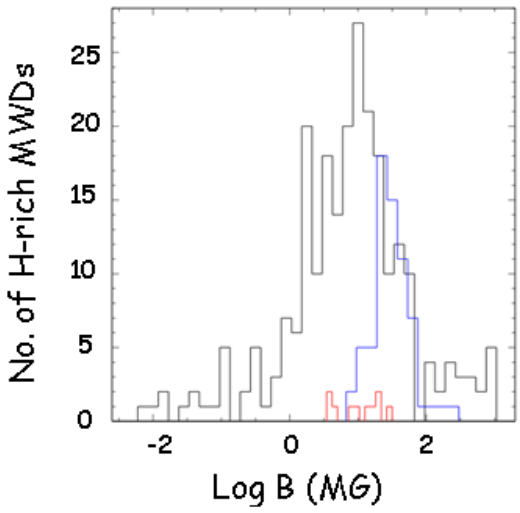

Figure 16: Distribution of magnetic field strength in polars (blue line), and IPs (red line) compared to that of single magnetic WDs (black line) (adapted from Ferrario, de Martino & Gänsicke, 2015).

Taking into account the average values of magnetic field intensity and orbital periods for polars and IPs, and the minimum and maximum value for both parameters (B and P_{orb}), it is possible to construct a very interesting plot (Fig. 18) that shows the evident continuity between the two classes of MCVs.

Also the system AM CVn ≡ HZ 29 with orbital period of 17.5 minutes, discovered by Smak (1967) was later recognized as a CV by Patterson (1992) and it constitutes the prototype of AM CVn stars – ultra-compact binaries – formed by a primary star WD, and a secondary degenerate or semi-degenerate star: e.g. white dwarf - white dwarf binaries ($P_{orb} < 80$ minutes). White dwarf primaries and main sequence secondaries have binary orbital periods greater than 80 minutes.

Levitan (2013) in his PhD thesis about "*AM CVn Systems with Palomar Transient Factory*" updates the number of AM CVn stars. Figure 19 shows the number of CVs versus orbital period. It is clearly evident that 50% of CVs lie over the "period gap", 39% of CVs lie below the "period gap", and 11% within the "period gap" (indicated with the light blue rectangle). The place where SW Sex systems lie (indicated with the light red rectangle) is partially in the "period gap". This demonstrates that the "period gap" does not exist. It appeared in the past like a gap because of lack of measurements and relatively low number of systems within the gap.

In my opinion is extremely important to remark once more that there is continuity among the "different classes" of CVs. This is coming from the pathway of evolution of CVs that is driven by angular momentum (J) loss. Orbital period (P_{orb}) decreases. All long P_{orb} CVs cross SW Sex regime before entering in the "period gap", where SW Sex systems lie. Thus, SW Sex phenomenon is an evolutionary stage in the life of CVs (Rodriguez-Gil, 2003; Schmidtobreick, 2013). Such a continuity has been noted also by Schmidtobreick & Tappert (2014, 2015).

An interesting indirect method for evaluating the magnetic field intensity in MCVs has been discussed by Giovannelli & Sabau-Graziati (2012a) in the case of SS Cyg whose nature (non magnetic

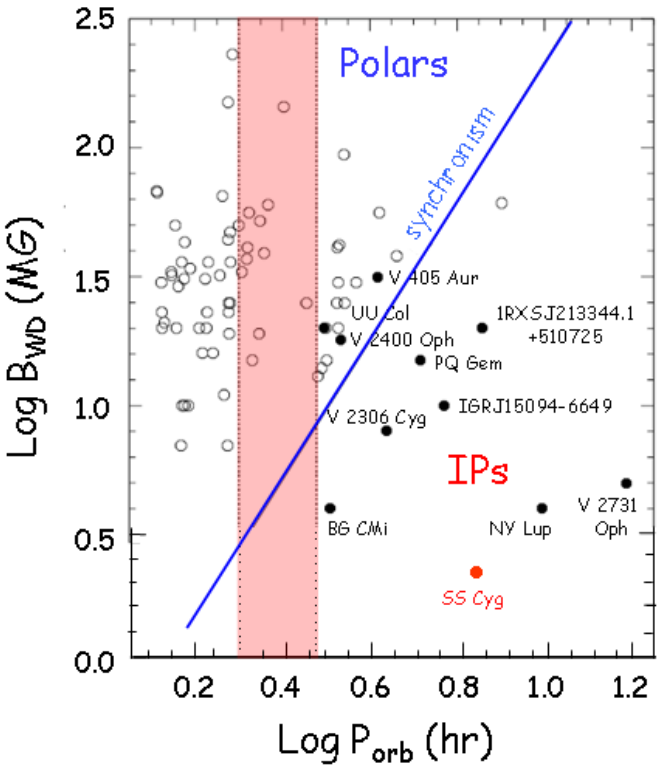

Figure 17: Magnetic field strength versus orbital period in MCVs. Polars and IPs are separated by the blue line that marks the border between systems with orbital period synchronized with the spin period (polars) and those without synchronization (IPs). Light red rectangle marks the so-called "period gap" (after Ferrario, de Martino & Gänsicke, 2015).

or IP) is largely disputed. From the fluxes of UV emission lines of SS Cyg, placed at distance d = 166.2 ± 12.7 pc (Harrison et al., 1999), Giovannelli & Sabau-Graziati (2012a) – by using the IUE measurements obtained by Gaudenzi et al. (1986) – derived the luminosity of C II and C IV: $L_{CII} \simeq 7.8 \times 10^{30}$ erg s^{-1} and $L_{CIV} \simeq 6.2 \times 10^{31}$ erg s^{-1}. Using these values of luminosity and the extrapolation of the line best fitting the emission line luminosity of C II and C IV versus B (Howell et al., 1999), the magnetic field intensity of SS Cyg is $B_{CII} = 2.0^{+0.5}_{-0.4}$ MG, and $B_{CIV} = 1.1^{+0.3}_{-0.6}$ MG, as shown in Fig. 20, left and right panels, respectively.

Then a reasonable value of the white dwarf magnetic field in SS Cyg is $B = 1.6 \pm 0.7$ MG This value is in complete agreement with the evaluation made by Fabbiano et al. (1981) ($B \leq 1.9$ MG) by using simultaneous X-ray, UV, and optical data.

Many other circumstantial proofs in favor of the IP nature of SS Cyg have been discussed by Giovannelli & Sabau-Graziati (2012a). One of the most important proof is coming from the paper by Körding et al. (2008). They detected a radio jet from SS Cyg. The hardness intensity diagram shows an analogy between the XRBs (the BH GX 339-4, and the NS Aql X-1) and SS Cyg. Moreover there is a radio flare simultaneous with the optical outburst of SS Cyg. During the 1.1-mJy "flare" they found upper limits for the linear polarization and circular polarization of $3.2 \pm 2.7\%$ and $-3.2 \pm 2.7\%$, respectively.

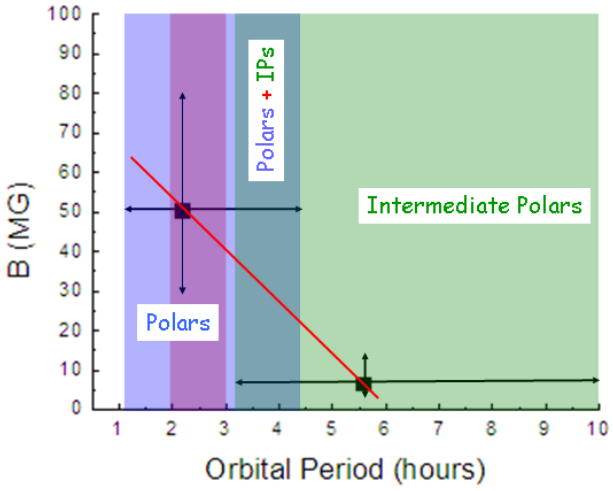

Figure 18: Magnetic field intensity versus orbital period for MCVs. Polars and IPs are contained in the light blue and light green rectangles, respectively. Violet rectangle indicates the so-called "period gap". Cyan-50 rectangle represents the intersection between the Polars and IPs (adopted from Giovannelli & Sabau-Graziati, 2015a).

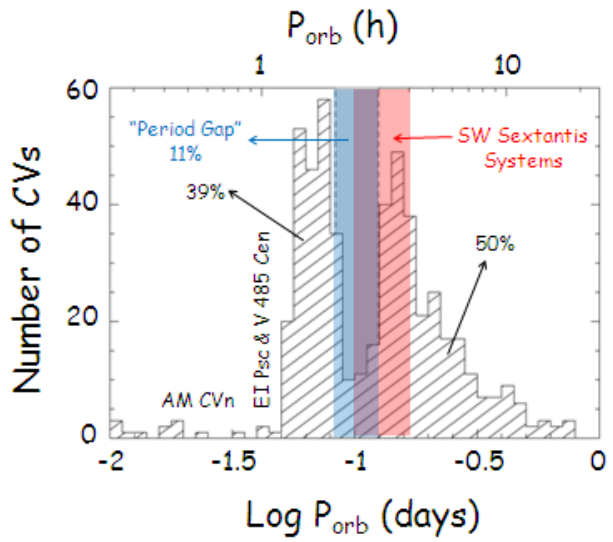

Figure 19: Number of CVs versus P_{orb}. Light blue and red rectangles mark the so-called "period gap" and the range in which SW Sex systems lie (adopted from Giovannelli & Sabau-Graziati, 2015a after Gänsicke, 2005, and Levitan, 2013).

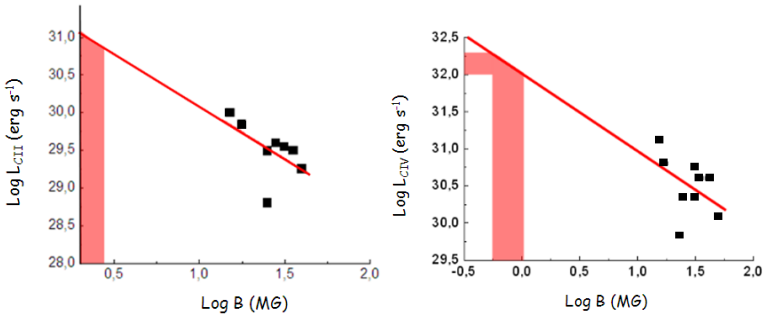

Figure 20: Observed emission fluxes converted to luminosity for magnetic CVs (after Howell et al., 1999) are indicated with black square. Left panel: C II luminosity versus B; right panel: C IV luminosity versus B. SS Cyg positions are indicated with red areas (adopted from Giovannelli & Sabau-Graziati, 2012a).

It is hard to explain these results without invoking the presence of a magnetic field (B $\approx$ 2 MG) in the white dwarf of SS Cyg system.

INTEGRAL/IBIS and SWIFT/XRT observations have shown that a conspicuous number of CVs have a strong hard X-ray emission (Landi et al., 2009; Scaringi et al., 2010). In their published sample of 23 CVs, 22 are classified as magnetic IPs and only one (SS Cyg) as NMCV, meanwhile all its characteristics are practically equal to those of the other 22 objects. This is a strong circumstantial proof in favor of the magnetic nature of SS Cyg. The experimental evidence that SS Cyg emits in the hard X-ray energy range is, in my opinion, the conclusive evidence about its magnetic nature.

Indeed, a simple question arises: "why all the CVs detected by the INTEGRAL observatory are magnetic (IPs) and SS Cyg non-magnetic? If so, why the same INTEGRAL observatory did not detect any other DN?".

The hard X-ray emission detected in those CVs is possible only if a sufficiently high magnetic field is present in those systems. Only accretion onto magnetic poles justify the hard X-ray emission in quiescence.

Probably, the "mistake" about the nature of SS Cyg born after the publication of a paper in Nature by Bath & van Paradijs (1983) where SS Cyg was classified as DN on the basis of optical behaviour, typical of DNe. This paper originated a bandwagon effect in the literature (see Michael Friedjung's comment in the first historical Frascati Workshop 1984: Giovannelli, 1985) that "obliged" almost all the subsequent authors to start the papers saying that SS Cyg is a DN (NMCVs), without paying attention to other possibilities well documented in the so-called second class literature.

Therefore, my suggestion is to reconsider the problem about the nature of SS Cyg without any a priori bias.

In the case of X-ray pulsars, B is expected to be of $\geq 10^{12}$ G. A method for measuring B was experimentally found with the first historical detection of a cyclotron line from Her X-1 at $\sim$ 58 keV (Trümper et al., 1978). This detection opened the road for searching such lines in X-ray binary systems. The relationship between the cyclotron line energy (E_c) and the magnetic field intensity B is:

$$E_c = 11.6 \times B/(10^{12}\ G) \times (1+z)^{-1}\ keV$$

The value of B in Her X-1 is then $\sim 5 \times 10^{12}$ Gauss. Coburn et al. (2002) published a list of cyclotron lines and relative B for 10 X-ray pulsars. An updated list of 27 X-ray pulsars with cyclotron lines detected is reported in the paper by Walter et al. (2015). Some of these pulsars show also absorption-like features, like for instance 4U 0115+63 in which the four measured features are close to the harmonic relation expected from cyclotron resonant scattering in a strong magnetic field when relativistic effects are taken into account. These results provided the first evidence for four harmonically spaced lines in the spectrum of an accreting X-ray pulsar, yielding the clearest confirmation of their magnetic origin (Santangelo et al., 1999). Table 2 shows the list of the 27 X-ray pulsars with the detected energy of the cyclotron lines and the correspondent magnetic field intensity. The table reports only the energy of the first harmonic of the cyclotron lines.

3.9 Anomalous X-ray Pulsars and Soft Gamma Repeaters: Magnetars

Since their discovery, neutron stars (NSs) have excited a broad range of interests not only in the astrophysical context, but also in terms of fundamental physics.

NSs are characterized by extreme conditions, such as dense matter, rapid rotation, and high magnetic field, they have proved to be ideal laboratories to test fundamental physics, which cannot be achieved by ground-based experiments.

Multi-wavelength observations from radio to the highest energy γ-rays have revealed a remarkable diversity of NSs (Kaspi, 2010).

In the last two decades a new class of X-ray binaries has been recognized. They are X-ray pulsars with properties clearly different from those of the common HMXBs. This new group of pulsars constitutes a subclass of the LMXBs, characterized by lower luminosities, higher magnetic fields and smaller ages than non-pulsating LMXBs. These objects have been called Anomalous X-ray Pulsars (AXPs) (e.g. GSG2004, and the references therein) and this is now the current accepted name. Soon after their discovery, this new class of objects, whose nature was recognized to be that of neutron stars, was characterized by a spin periods ranging between $5.5 - 11.8$ s – and $\dot{P}$, in the range $0.05 - 10 \times 10^{-11}$ s s^{-1} – contrary to the larger spread of those of HMXBs (0.069–few $\times 10^3$ s). Spin periods of AXPs are monotonically increasing on timescales of $\sim 10^4$–4×10^5 yr.

Sources we call now soft gamma-ray repeaters (SGRs) were initially confused with GRBs. The history of this misunderstanding is clearly and exhaustively reported in the paper by Hurley (2008). SGRs are transient very short (< 1 s) events, characterized by relatively soft bursts, peaked at $\sim$ 20–30 keV, with super-Eddington luminosity.

The durations and spectra of SGRs are very different from those of GRBs, like clearly shown in Figure 21 (Hurley, 2007).

Measurements of the spin down rates of SGRs and AXPs have been interpreted as evidence of very strong magnetic fields at the collapsed object poles, roughly two orders of magnitude greater than those of the 'normal' X-ray pulsars. For this reason they are now known as 'magnetars'. Their derived magnetic field intensity is $\sim 10^{14}$ - 10^{15} G.

The problem of the nature of magnetars is one of the hottest in modern astrophysics. Indeed, for instance, Dar (2003) argued that, instead, the observations support the hypothesis that SGRs and AXPs are neutron stars that have suffered a transition into a denser form of nuclear matter

Table 2: The list of the 27 X-ray pulsars with the detected energy of the cyclotron lines and the correspondent magnetic field intensity (after Walter et al., 2015).

Source Name	Cyclotron Energy (keV)	B (10^{12}) (Gauss)
4U 0115+63	11.6	1
V 0332+53	28	2.4
4U 0352+309 (X Per)	29	2.5
RX J0440.9+4431	32	2.76
RX J0520.5-6932	31.5	2.7
A 0535+26	50	4.3
MXB 0656-072	36	3.1
Vela X-1	27	2.3
GRO J1008-57	88	7.59
1A 1118-61	55	4.7
Cen X-3	28	2.4
GX 301-2	37	3.2
GX 304-1	50.8	4.4
4U 1538-52	20	1.7
Swift J1626.6-5156	10	0.87
4U 1626-67	37	3.2
Her X-1	42	3.6
OAO 1657-415	36	3.1
GRO J1744-28	4.7	0.4
IGR J18179-1621	21	1.8
GS 1843+00	20	1.7
4U 1907+09	19	1.6
4U 1909+07	44	3.8
XTE J1946+274	36	3.1
KS 1947+300	12.5	1.1
EXO 2030+375	11	0.95
Cep X-4	30	2.6

to become, presumably, strange stars or quark stars. Internal heat and slow gravitational contraction long after this transition can power both their quiescent X-ray emission and their star quakes, which produce 'soft' gamma ray bursts. Dar (2006) discussed once more this idea by using results from short–duration hard–spectrum GRBs, such as 050509B, 050709, 050724, and 050813, which could have been the narrowly beamed initial spike of hyperflares of SGRs in galaxies at cosmological distances. Such bursts are expected if SGRs are young hyperstars, i.e. neutron stars where a considerable fraction of their neutrons have converted to hyperons and/or strange quark matter.

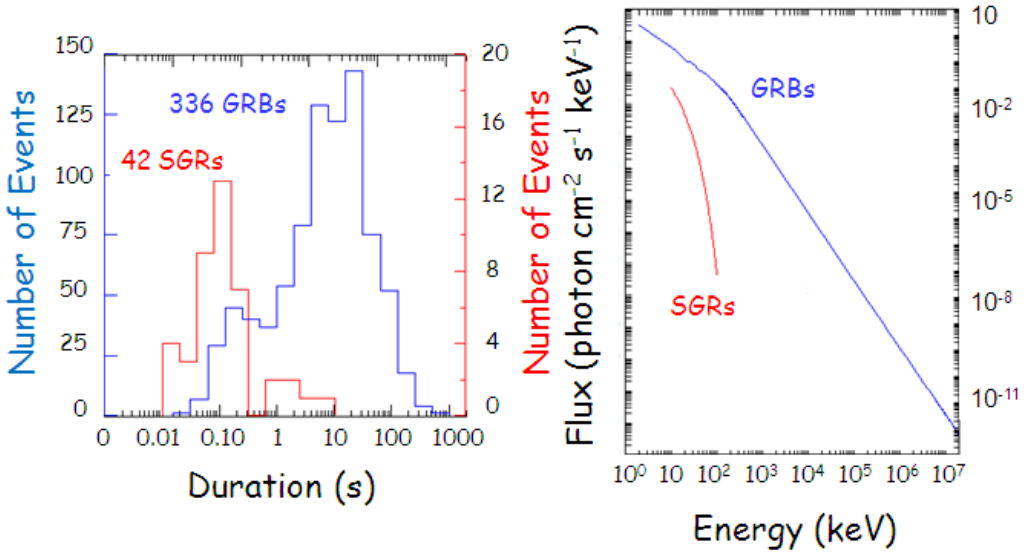

Figure 21: Comparison of the durations and spectra of SGRs and GRBs (adapted from Hurley, 2007).

Ghosh (2009) discussed some of the developments in the quark star physics along with the consequences of possible hadron to quark phase transition at high density scenario of neutron stars and their implications on the Astroparticle Physics.

Models based on strongly magnetized neutrons stars ($B \sim 10^{14}$–10^{15} G) have been developed in the last couple decades just in order to explain the behaviour of the SGRs (Duncan & Thompson, 1992; Thompson & Duncan, 1995, 1996). The possibility of having strong magnetic fields is well accepted. Indeed, a neutron star undergoes vigorous convection in the first $\sim$ 30 s after its formation. Coupled with rapid rotation ($\sim$ 1 ms period), this makes the neutron star a likely site for dynamo action. If the Rossby number (=rotation period/convective overturn time) < 1, the magnetic field amplification is not suppressed. In principle a magnetic field of B $\sim 3 \times 10^{17}$ G can be generated.

Thus, AXPs and SGRs are interpreted as magnetars, whose definition is a neutron star in which the magnetic field, rather than rotation, provides the main source of free energy; the decaying field powers the electromagnetic radiation (Hurley, 2008 and the references therein). Note that the definition does not specify any particular field strength, but rather, is based on an energy balance argument. Today we know of several possible manifestations of magnetars, and SGRs are one. With inferred magnetic field strengths B$\sim 10^{15}$ Gauss, magnetars indeed have the strongest cosmic magnetic fields that we know of in the Universe. But we also know of neutron stars with strong magnetic fields that are rotation-powered, and clearly do not fit the magnetar description (e.g. McLaughlin et al. 2003).

For long time the optical counterparts of AXPs were not known, with the possible exception of 4U 0142+61, for which Hulleman, van Kerkwijk & Kulkarni (2000) reported the discovery of a faint (R$\sim$ 25 mag) blue object in its error box. If such an association should be true, this faintness would rule out the presence of an accretion disk, thus favoring the magnetar interpretation. On the basis of the limits in the optical and IR wavelength regions, the presence of a massive early

type companion star, such as OB super giants or Be stars, can be excluded in AXPs. Moreover, no orbital motion signatures are present in their X-ray light curves.

Now we know 29 magnetars, 11 are reliably associated with supernova remnant shells, and an additional 2 have possible associations (Olausen & Kaspi, 2014a,b). The large number of remnant associations is fully consistent with the great youth implied both by magnetar spin-down ages and by their proximity to the Galactic Plane. The associated remnants lack unusual properties when compared with shell remnants that harbor neutron stars with lower magnetic fields (Vink & Kuiper 2006, Martin et al. 2014). This appears to be in conflict with the proposal of Duncan & Thompson (1992) that magnetars form from neutron stars rotating with period ~ 1 ms at birth, which assist a fast dynamo. The difficulty with this picture is that a neutron star with magnetic field $> 10^{14}$ G spinning at 1 ms quickly loses most of its rotational energy, releasing energy in excess of 10^{52} ergs, which is greater than the supernova explosion energy itself. It is therefore likely to be associated with either anomalously large shell remnants, or else no remnant at all, if it expanded sufficiently rapidly to dissipate on a timescale of a few hundred years. The normality of magnetar supernova remnants challenged the dynamo model and led to discussion of strong fossil fields from the progenitor star (Ferrario & Wickramasinghe 2006, and e.g. Kaspi & Beloborodov, 2017).

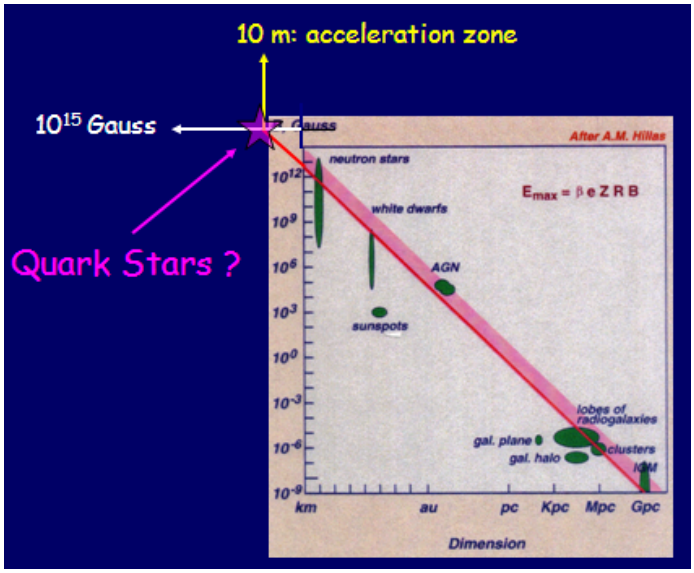

Figure 22: Magnetic field intensity vs dimensions of cosmic sources (adopted from Giovannelli & Sabau-Graziati, 2006; courtesy of Todor Stanev, 2002, after Hillas, 1984. The extrapolation to 10^{15} G provides a dimension of ~ 10 m: the acceleration zone in a supercompact star (quark star?)

.

However, the nature of magnetar is not yet definitively proved. Giovannelli & Sabau-Graziati (2006) speculated as follows: if magnetic fields of $\sim 10^{15}$ G can be expected in order to explain the behaviour of magnetars, an almost *'obvious'* consequence can be derived from the diagram magnetic field intensity versus the dimension of the relative cosmic source, like shown in Fig. 22. They extrapolated the value of B up to 10^{15} G; the correspondent dimension of the source is of ~ 10 m. This could be the dimension of the acceleration zone in a supercompact star, probably a quark star. *If you construct a trap, the rat falls into it!*

Table 3: Pulse timing properties of magnetars and magnetar candidates (after Olausen & Kaspi, 2014a and Kaspi & Beloborodov, 2017).

AXP & SGR (Magnetars) (name)	$P_{\rm pulse}$ (s)	$\dot{P}_{\rm pulse}$ 10^{-11} s s^{-1}	B (10^{14} G)	Spin-down Age (kyr)
CXOU J0110-721 (SMC)	8.02	1.88	3.9	6.8
4U 0142+614	8.69	0.20	1.3	68
SGR 0418+5729	9.08	0.0004	0.061	36000
SGR 0501+4516	5.76	0.582	1.9	16
SGR 0526-66 (N49)	8.05	3.8	5.6	3.4
1E 1048.1-5937	6.46	~ 2.25	3.9	4.5
PSR J1119-6127	0.41	-	4.1	1.6
1E 1547.0-5408	2.07	~ 4.77	3.2	0.69
PSR J1622-4950	4.33	1.7	2.7	4.0
SGR 1627-41 (G337.0-0.1)	2.59	1.9	2.2	2.2
CXOU J164710.2-455216	10.61	< 0.4	< 0.66	> 420
1RXS J170849.0-400910	11.00	1.91	4.6	9.1
CXOU J171405.7-381031	3.82	6.40	5.0	0.95
SGR J1745-2900	3.76	0.66	1.6	9.0
SGR 1806-20 (G10.0-0.3)	7.54	~ 49.5	20	0.24
XTE J1810-197	5.54	0.78	2.1	11
Swift J1822.3-1606	8.44	0.031	0.51	440
SGR 1833-0832	7.56	0.35	1.6	34
Swift J1834.9-0846	2.48	0.80	1,4	4.9
1E1841-045 (Kes 73)	11.78	3.93	6.9	4.7
PSR J1846-0258	0.33	-	0.49	0.73
3XMM J185246.6+003317	11.56	-	< 0.41	> 1300
SGR 1900+14(G42.8+0.6)	5.2	9.2	7.0	0.90
SGR 1935+2154	3.24	-	2.2	3.6
1E2259+586 (CTB 109)	6.98	0.048	0.59	230
Magnetar Candidates				
SGR 0755-2933	-	-	-	-
SGR 1801-23	-	-	-	-
SGR 1808-20	-	-	-	-
AX J 1818.8-1559	-	-	-	-
AX J1845-026(G29.6+586)	6.97	-	-	-
SGR 2013+34	-	-	-	-

Table 2 shows the pulse timing properties of magnetars, the derived magnetic field intensity, the age (after Olausen & Kaspi, 2014a and Kaspi & Beloborodov, 2017), and their association with SNRs (after Giovannelli & Sabau-Graziati, 2006).

The open questions about magnetars are numerous, namely: i) What are the distances of the Galactic magnetars? Then what is the Energetics? ii) What is the number-intensity relation for giant magnetar flares? iii) What are the SGR and AXP birth rate? What are their lifetimes? How many SGRs and AXPs are in the Milky Way? iv) What kind of supernova produces a SGR or an AXP? v) What is the relation between SGRs and AXPs? Does one evolve into the other, or are they separate manifestations of magnetars? vi) Are really the collapsed objects in SGRs and AXPs neutron stars? Alternatively, could they be quark stars? vii) How many other manifestations of

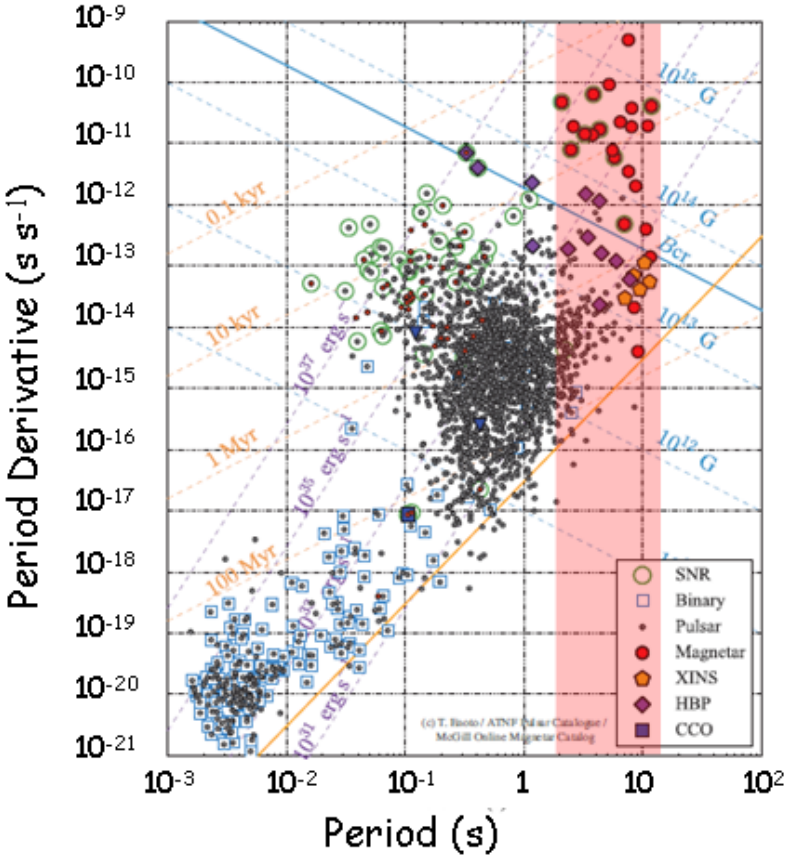

Figure 23: Magnetars and neutron stars on the P–$\dot{P}$ diagram. The light-red rectangle limits the range of magnetars periods (adapted from Enoto, 2018).

magnetars exist?

In order to answer to these open questions, more sensitive instruments, more detailed theories, and more data (probably in the next 30 years) are necessary.

In the extensive and excellent reviews by Kitamoto et al. (2014) and by Kaspi & Beloborodov (2017) most of the critical points about magnetars have been deeply discussed.

A large diversity of neutron stars has been discovered by multifrequency observations from the radio band to the X-ray and gamma-ray energy ranges. Among different manifestation of neutron stars – which include SGRs, AXPs, high-B pulsars (HBPs), high-E binaries (HEBs), rotating radio transients (RRATs), central compact objects (CCOs), rotation-powered radio pulsars (RPPs), and X-ray isolated neutron stars (XINSs) (Harding, 2013) – magnetars are the strongest magnetized objects.

These various manifestations of neutron stars show different characteristics of rotation period P and its derivative $\dot{P}$. The measurements of P and $\dot{P}$ provide to estimate the dipole magnetic field strength $B_d \propto \sqrt{P\dot{P}}$ and characteristic age $\tau_c = P/2\dot{P}$.

Figure 23 shows the P–$\dot{P}$ diagram (Enoto, 2018), where SGRs and AXPs are collectively called "**magnetars**" since their slow rotation (P $\sim$ 2–12 s) – with the exception of PSR J1119-6127 (P = 0.41 s) and PSR J1846-0258 (P = 0.33 s) – and high period derivatives ($\dot{P} \sim 10^{-13}$–10^{-9} s s^{-1})

indicate high magnetic fields B = 10^{14-15} G and young characteristic age $\tau_c \lesssim$ 10–100 kyr. To date, there are 29 known magnetars in the Milky Way and local universe (see Table 2).

It seems almost natural to think about a continuity among different classes of neutron star systems. However radio pulsations that have been observed from about 2000 neutron stars with weaker magnetic fields have never been detected from any of the known magnetars until the paper by Camilo et al. (2006) which showed that XTE J1810–197 — the first transient magnetar discovered (Ibrahim et al., 2004) — emits bright, narrow, highly linearly polarized radio pulses, observed at every rotation, thereby establishing that magnetars can be radio pulsars. Thus, these observations which link magnetars to ordinary radio pulsars, rule out alternative accretion models for AXPs, and provide a new window into the coronae of magnetars.

In the excellent review paper by Kaspi & Beloborodov (2017) most of the critical points about magnetars have been deeply discussed. They concluded that: "*The magnetar model has now been used to predict, naturally and uniquely, a wide variety of remarkable phenomena and behaviors in sources that once seemed highly anomalous. The now seamless chain of phenomenology from otherwise conventional radio pulsars through sources previously known for radically different behavior makes clear that* **these objects are one continuous family***, with activity correlated with spin-inferred magnetic field strength. Recent advances in the physics of these objects, from the core through the crust and to the outer magnetosphere, hold significant promise*.

The review by Bernardini (2015) discussed how the newly-born millisecond magnetars can compete with black holes as source of the GRB power, mainly with their rotational energy reservoir. They may be formed both in the core-collapse of massive stars, and in the merger of neutron star or white dwarf binaries, or in the accretion-induced collapse of a white dwarf, being thus a plausible progenitor for long and short GRBs, respectively. She reviewed the major observational evidences for the possible presence of a newly-born magnetar as the central engine for both long and short GRBs. She then discussed about the possibility that all GRBs are powered by magnetars, and she proposed a unification scheme that accommodates both magnetars and black holes, connected to the different properties and energetics of GRBs. Since the central engine remains hidden from direct electromagnetic observations, she reviewed the predictions for the GW emission from magnetars hosted from GRBs, and the observational perspectives with advanced interferometers.

3.10 Accretion onto compact objects

For a general deep tutorial lecture see "*Black Hole Accretion and Feedback*" by King (2019).

In the Galaxy there are different kinds of compact sources: white dwarfs (WDs), neutron stars (NSs) and black holes (BHs), both isolated and in binary systems. Thousand papers about these cosmic sources are available in the literature. We mention the last available exhaustive review by Postnov & Yungelson (2014) about "*The Evolution of Compact Binary Stars Systems* in which they review the formation and evolution of compact binary stars consisting of WDs, NSs, and BHs. Merging of compact-star binaries are expected to be the most important sources for forthcoming GW astronomy.

Several review papers have been published for discussing the different classes of galactic compact sources: i) Cataclysmic Variables (CVs) and related objects (e.g. Giovannelli & Sabau-Graziati, 2008, 2012a; 2015a,b); ii) High Mass X-ray Binaries (HMXBs) (e.g. Giovannelli & Sabau-Graziati, 2001, 2004, 2015c, and van den Heuvel, 2009 and references therein; iii) Obscured

Sources and Supergiant Fast X-Ray Transients (e.g. Chaty, 2011); iv) Ultra–Compact Double–Degenerated Binaries (e.g. Wu, Ramsay & Willes, 2008; Wu, 2009); Magnetars (Kitamoto et al., 2014: White Paper for ASTRO-H Space X-ray observatory).

A summary of these topics can be found in the review paper by Giovannelli & Sabau-Graziati (2014).

Among the cosmic systems where accretion processes occur, undoubtedly, non-magnetic CVs, intermediate polars and polars constitute the most powerful probe to test our theories of the various modes of accretion. The reason is rather simple: CVs are enough close to us and their processes develop in time-scales relatively easy to be followed and enough energetic to be easily detected.

The accretion structure depends on the magnetic field (B) of the white dwarf and on the transfer mass rate.

Upper panel of Fig. 24 shows from the left to the right the sketches of the so-called non-magnetic CVs (NMCVs), intermediate polars (IPs), and polars (Ps) (Giovanneli & Sabau-Graziati, 2015a); lower panel of Fig. 24 shows from the left to the right the 3D MHD simulations of the so-called non-magnetic CVs (NMCVs) (B $\sim 10^4 - 10^5$ G), intermediate polars (IPs) (B $\sim 10^6 - 10^7$ G), and polars (Ps) (B $\sim 10^7 - 10^8$ G) (Bisikalo & Zhilkin, 2015).

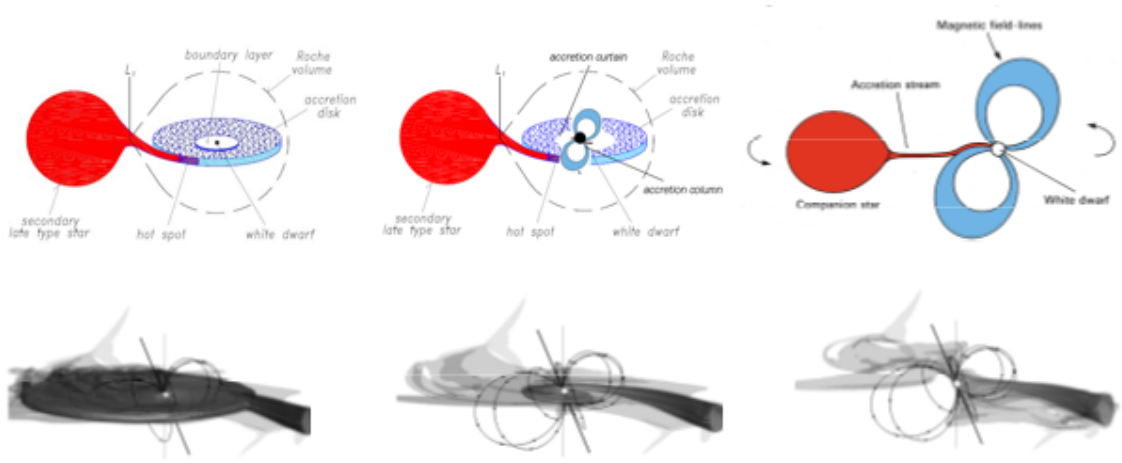

Figure 24: Upper panel from left to right shows sketches of: non-magnetic CV, intermediate polar, polar (Giovannelli & Sabau-Graziati, 2015a). Lower panel from left to right shows the 3D MHD simulations of NMCV, IP, and P obtained with B = 10^5, 10^6, and 10^7 G, respectively (Bisikalo & Zhilkin, 2015).

However we have a smooth continuity among the classes, as already shown in fig. 32 (Giovannelli & Sabau-Graziati, 2015a).

The long term evolution of CV systems accreting at a prohibitive rate has become a hot topic both in terms of the fate of such systems (all sorts of supernovae) and the microphysics of Eddington and super Eddington mass accretion and mass loss flows. In particular I stress one of the hottest topics in present day astrophysics, namely the progenitors of SN-Ia. This problem is connected with fundamental issues in cosmology. Novae and recurrent novae are the most promising progenitor candidates but so far could not be nailed down. One of the most important goals of our serial workshops about *The Golden Age of Cataclysmic Variables and Related Objects* is to discuss what is missing in our knowledge of CVs that will allow a unique determination and observational

confirmation (Giovannelli & Sabau-Graziati, 2012a, 2015a; Giovannelli, 2017).

3.10.1 Accretion driven X-ray sources

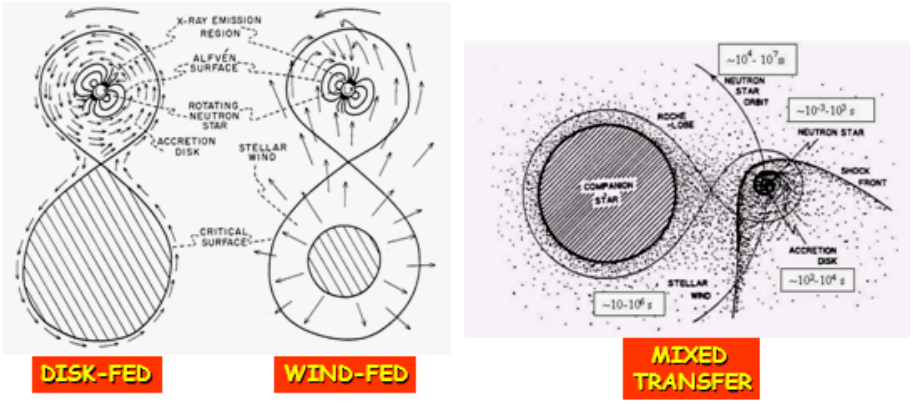

Figure 25: Left panel: accretion in X-ray binary systems disk-fed and wind-fed (Giovannelli & Sabau-Graziati, 2001, adapted from Blumenthal & Tucker, 1974). Right panel: mixed transfer (adopted from Giovannelli & Sabau-Graziati, 2001, after Nagase, 1989).

In binary systems there are essentially two ways for accreting matter from one star to the other: via accretion disk or via stellar wind (Giovannelli & Sabau-Graziati, 2001, adapted from Blumenthal & Tucker, 1974) (left panel of Fig 25). But in some cases there is a third way which is a mixture between the two, as for instance in eccentric binary systems close to the periastron passage where a temporary accretion disk can be formed around the neutron star (e.g. Giovannelli & Ziółkowski (1990), like shown in the right panel of Fig. 25 (Giovannelli & Sabau-Graziati, 2001, after Nagase, 1989).

3.10.2 Doppler tomography of accretion disks

The fast Fourier Transform (FFT) in one, two, or three dimensions is an efficient algorithm well known for decades (see Cooley & Tukey, 1965) as well as a traditional component of any serious numerical library. Three-dimensional (3D) FFT happens to be one of the most compute- and communication-intensive components in applications from a range of fields (for example, in turbulence, molecular dynamics, 3D tomography, and astrophysics), and for this reason there are many excellent parallel implementations in existence today. Pekurovsky (2012) introduced a popular software package called P3DFFT which implements FFT in three dimensions in a highly efficient and scalable way. This paper discussed P3DFFT implementation and performance in a way that helps guide the user in making optimal choices for parameters of their runs.

Horne (1985) and Marsh & Horne (1988) developed Doppler tomography as a technique aimed at constructing a two-dimensional velocity image (tomogram) of the accretion disks of CVs using an emission line in its spectra sampled at a number of orbital phases. Doppler tomography has revolutionized the interpretation of orbitally phase-resolved spectroscopic observations of interacting binary systems. It has become a valuable tool for resolving the distribution of line emission in CVs and other binary systems. For instance Marsh (2001) in his review discussed the results of Doppler

tomography applied to CVs. Outstanding successes to that date are the discovery of two-arm spiral shocks in cataclysmic variable accretion disks and the probing of the stream/magnetospheric interaction in magnetic cataclysmic variable stars. Doppler tomography has also told us much about the stream/disk interaction in non-magnetic systems and the irradiation of the secondary star in all systems.

Zhilkin & Bisikalo (2009) described a 3D numerical code designed for simulations of magnetohydrodynamical (MHD) flows in semidetached binary systems. They found that even in case of a moderate magnetic field (B = 10^5 G) the flow structure in the vicinity of the accretor of a CV was drastically changed and the funnel flows were formed in the system.

Bisikalo & Zhilkin (2012) discussed the Flow Structure in Magnetic CVs by studying the physical processes which go on in magnetic CVs with the mass transfer between the components. Using results of 3D MHD simulations, they investigated variations of the main characteristics of accretion disks depending on the value of the magnetic induction on the surface of the accreting star. Zhilkin, Bisikalo & Mason (2012) discussed on "Full 3D MHD calculations of accretion flow structure in magnetic cataclysmic variables with strong, complex magnetic fields".

Bisikalo et al. (2008) discussed Dopppler tomography of the CV SS Cygni in quiescence. Boneva et al. (2009) discussed the Doppler mapping in the case of SS Cygni in outburst and finally Kononov et al. (2012) used Doppler tomography for studying the pre-outburst accretion disk of SS Cygni.

Zhilkin & Bisikalo (2010, 2011) presented a 3D numerical model to simulate plasma flows in close binary systems with accretors having strong proper magnetic fields. The model is based on an assumption that plasma dynamics is determined by a slow average flow against a background of propagating MHD waves. Equations describing the slow plasma motion are obtained as a result of the corresponding averaging procedure. The model takes into account the magnetic diffusivity which is due to the current dissipation in turbulent vortexes, magnetic buoyancy and wave MHD turbulence. They presented results of the simulations for MHD flows in a polar-like binary system. Results of the simulations show that in semi-detached binary systems with strong magnetic fields (B = 10^7 G) the flow structure can differ sufficiently from that of systems with moderate magnetic fields (B = 10^5 G), Accretion disks in such magnetic systems systems (B = 10^7 G) are not formed and the flow is collimated into the accretion stream starting from the inner Lagrange point L_1 and finishing on the magnetic poles of the accretor. This flow structure corresponds to the case of polars.

Kotze, Potter & McBride (2015, 2016) explored inside-out Doppler tomography for non-magnetic and magnetic cataclysmic variables, respectively. The code they used is available at http://www.saao.ac.za/∼ejk/doptomog/main.html.

Doppler tomography has been applied also to fusion plasmas giving an image of the fast-ion velocity distribution function in the tokamak ASDEX Upgrade (Salewski et al., 2015). It is interesting to note that Bisikalo et al. (2016) presented a method that can be used to recover the spectrum of turbulence from observations of optically thin emission lines formed in astrophysical disks. Within this method, they analyze how line intensity fluctuations depend on the angular resolution of the instrument, used for the observations. The method allows us to restore the slope of the power spectrum of velocity turbulent pulsations and estimate the upper boundary of the turbulence scale.

Doppler tomography is very useful also for analyzing the asymmetric MHD outflows/jets from accreting T Tauri stars, and even in planetary science, as discussed by Giovannelli & Sabau-Graziati (2016a, and the references therein).

3.11 Accretion onto white dwarfs

Accretion of matter onto WD can take place through a disk, a ring-like structure or an accretion stream depending on the WD magnetic field strength, the binary orbital period and mass accretion rate. The physical conditions of the material impinging onto the WD and emitting X-rays are still to be investigated. In non-magnetic CVs the WD magnetic field strength is low enough, $B_{WD} \leq 10^5$ G, to allow the formation of an accretion disk and X-rays are emitted at the disk Boundary Layer (BL). In highly magnetized CVs, $B_{WD} \geq 10^7$ G, material is directly accreted onto the WD poles flowing along the magnetic field lines. A partial accretion disk (a sort of ring) can be formed at intermediate field strengths ($10^5 \leq B_{WD} \leq 10^7$ G (see Fig. 24, where the 3D MHD simulations of the three cases are reported).

At the WD poles a stand-off shock is formed. The post-shock accretion column is thought to cool via bremstrahlung (hard X-rays), recombination processes and cyclotron radiation. The relative proportion of these cooling mechanisms strongly depends on the WD magnetic field (Fischer & Beuermann 2001). An interesting discussion about *Dissecting accretion and outflows in accreting white dwarf binaries* is reported by de Martino et al. (2015).

Therefore, the magnetic field intensity plays a fundamental role in the process of accretion of matter onto the compact star. Thus Lipunov's diagram (log P_{spin} vs log y) appears as the best way for localizing the position of MWDs, both polars and IPs, as shown in Fig. 26. In this figure, also the positions of other gravimagnetic rotators are shown.

The extraordinary discovery of the first white dwarf pulsar, AR Sco ($P_{orb} = 3.57$ h ; $P_{spin} = 1.97$ m; 0.81 $M_\odot < M_1 \leq 1.29 M_\odot$; 0.28 $M_\odot < M_2 \leq 0.45 M_\odot$) (Marsh et al., 2016), and the strong linear polarization ($\leq 40\%$) variable with P_{orb} and P_{spin} and beat period detected by Buckley et al. (2017) suggested to Lipunov (2018) and to Lipunov, Grinshpun & Vlasenko (2021) to update Lipunov's diagram Log P_{spin} vs Log μ. Indeed, the pulsed luminosity of AR Sco is powered by the spin-down of the rapidly-rotating WD which is highly magnetised ≤ 500 MG. In the updated diagram of Fig. 26 the position of AR Sco is also reported. It lies just in the ejector zone together with the pulsars.

Sion (http://astronomy.villanova.edu/faculty/sion/CV/index.html) states
that in the Galaxy we could expect $\approx 10^6$ CVs. One of the big questions that arises is: "can all of the observed CVs and the phenomena associated with them be understood in terms of a single unified picture?" Other questions relate to the relative probabilities that CVs will be observed at particular stages in their evolution, and how the observations of CVs at the current epoch can be used to determine their ultimate fate.

To address these questions Nelson (2012) and Goliasch & Nelson (2015) have undertaken a massive computational effort to theoretically simulate the evolution of most of the possible CVs that could be produced by nature. The temporal evolution of 56,000 nascent CVs was followed over an age of 10 billion years using the MESA stellar evolution code. According to Nelson, "*This is the most ambitious analysis of the properties of an entire CV population that has ever been undertaken. The whole project required several core-years of CPU time*."

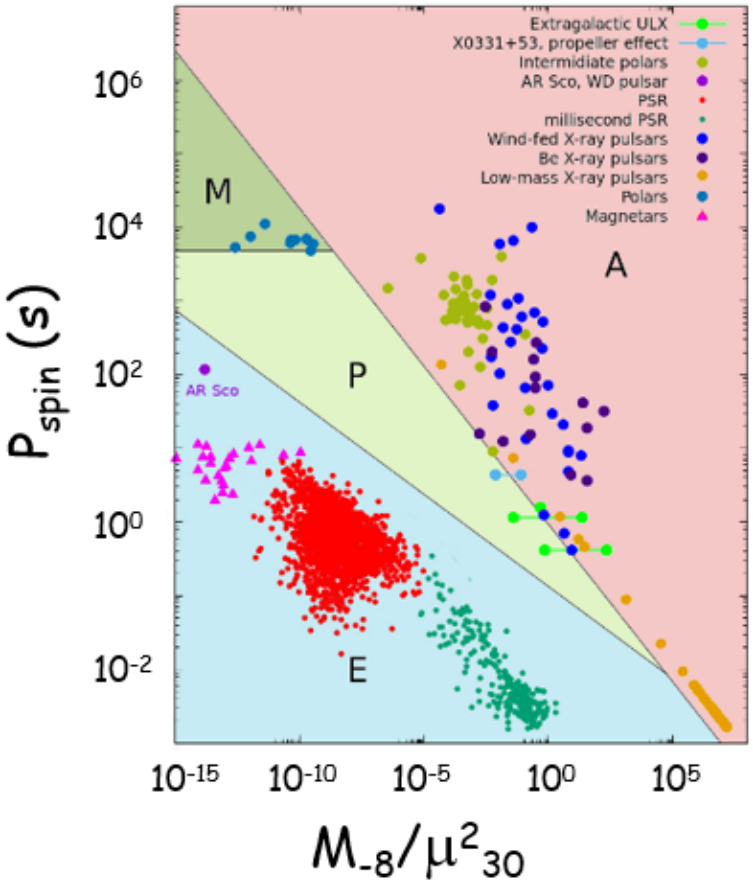

Figure 26: Lipunov's diagram: the position of different kind of gravimagnetic rotators are shown as well as those of several polars and IPs (Adopted from Lipunov, Grinshpun & Vlasenko, 2021).

While many of the results confirmed what had already been inferred about the properties of CVs, there were a number of surprises including the identification of a number of previously unexplored evolutionary pathways. But, as expected, a sharp bifurcation was found between nascent CVs that evolved to produce double white-dwarf binaries (including ones containing helium and hybrid white dwarfs), and ones that continuously transferred mass over the lifetime of the universe. In addition, the predictions of the theoretical simulations were in good general agreement with the observations of CVs with reasonably well-measured properties.

What was surprising was the large number of short-period "ultracompact" binaries (AM CVn stars) that were produced and, especially, the enormous depletion of carbon relative to nitrogen and oxygen that is predicted at certain epochs for evolved systems. As Nelson points out, "*It seems that nature has provided us with a unique way to identify CVs that descended from a highly evolved state based on their carbon abundances. There is already some observational evidence to suggest that there is a significant depletion of carbon in certain CVs. This could be a really critical test that will allow us to infer the lineage of some CVs and predict what their fate will be*".

3.12 Classical and Recurrent Novae

Classical novae are expected to recur on timescales from 100,000 years to just a few decades. The most important physical parameters controlling this recurrence timescale are the WD mass, and the mass accretion rate from the secondary (e.g. Yaron et al. 2005). Once classical nova (CN) is recorded more than once, it can be designated as "recurrent" (RN). Since the WD and the binary system remain intact after an outburst, it is possible that classical novae may actually be the same as recurrent novae if observed over a long enough time period. While the interval between outbursts of recurrent novae range from 10 to 100 years, it has been estimated that the time interval for classical novae would range from about 30,000 years for a 1.3 $M_{\odot}$ WD to 100,000 years for a 0.6 $M_{\odot}$ WD. Given long enough - it is expected that all classical novae will be observed as recurrent novae.

The long term behaviour of classical old novae, and the optical behaviour of CNe in outburst were discussed by Bianchini (1990), and Seitter (1990), respectively. The books by Cassatella & Viotti (1990) and by Bode & Evans (2008) are very useful for studying the physics of classical novae.

Recurrent novae are a rare sub-class of CVs; WDs accreting material from a binary companion in which more than one classical nova-type outburst has been observed (see the book of Hellier, 2001 for a comprehensive review of CVs). Nova outbursts are suspected to be due to a thermonuclear runaway on the surface of the WD, which releases huge amounts of thermal energy once a critical pressure is reached at the base of the shell of accreted material.

One of the most interesting RNe is RS Ophiuchi (RS Oph). It is an amazingly prolific recurrent nova, with recorded outbursts in 1898, 1907, 1933, 1945, 1958, 1967, 1985 and 2006 (Schaefer 2010). The short time between outbursts ($\sim$ 20 yrs) suggests that RS Oph hosts a massive WD accreting material at a significantly high rate.

In the latter paper Schaefer discussed not only RS Oph, but also the photometric histories of all known galactic RNe.

Classical and recurrent nova outbursts have been discussed by Bode (2011a,b) and Evans (2011). The proceedings of a conference about RS Oph and recurrent phenomenon can be very useful for details (Evans et al., 2008). General properties of quiescent novae have been discussed by Warner (2002). The very useful book of Bode & Evans (2008) about classical novae examines thermonuclear processes, the evolution of nova systems, nova atmospheres and winds, the evolution of dust and molecules in novae, nova remnants, and observations of novae in other galaxies. It includes observations across the electromagnetic spectrum, from radio to gamma rays, and discusses some of the most important outstanding problems in classical nova research.

Of the $\sim$ 400 known Galactic classical novae, only 10 of them are recurrent. Eight of them harbour evolved secondary stars, contrary to classical novae that contain main sequence stars (Darnley et al., 2012). They propose a new nova classification based on the evolutionary state of the secondary star, contrary the current schemes based on the properties of outbursts. Such classification contains three groups of novae: i) Main Sequence Nova (MS–Nova); ii) Sub–Giant Nova (SG–Nova); and iii) Red Giant branch Nova (RG–Nova).

An important not yet resolved problem is connected with the evolution and fate of Classical Novae. Patterson (2014) discussed this crucial problem. Classical novae rise from obscurity to shine among the brightest stars in the Galaxy. The story of how they return to quiescence is still

only dimly known. Vast amounts of energy are loosed upon the WD and its companion, and the light curves of post-novae suggest that they take not a few years, but a few thousand years, to return to quiescence. In the meantime, the secondary may experience a lot of heating from the WD's radiation - enough to overwhelm its intrinsic nuclear luminosity. For this purpose he mentioned the case of BK Lyncis – the oldest old nova and a bell-wether for CVs evolution (Patterson et al., 2013). They discussed stellar physics behind this suggestion and proposed how it might be tested by time-series photometry in the months and years (and if possible, centuries) after outburst.

RNe play an important role in the studies of SN Ia progenitors (Surina, Bode & Darnley, 2011). RNe are likely progenitors of Type–Ia supernovae.

On the contrary, Shafter et al. (2015) estimated that $\sim 4\%$ of the nova eruptions seen in M31 over the past century are associated with RNe. A Monte Carlo analysis shows that the discovery efficiency for RNe may be as low as 10% that for novae in general, suggesting that as many as one in three nova eruptions observed in M31 arise from progenitor systems having recurrence times $\lesssim 100$ yr. For plausible system parameters, it appears unlikely that RNe can provide a significant channel for the production of Type–Ia supernovae.

Important works have been developed about extragalactic nova populations (Shafter et al., 2014). Nova rates have been measured for more than a dozen galaxies spanning a wide range of Hubble types. They found that the recurrent nova population in the LMC appears to be higher than that seen in M31 and the Galaxy.

In order to brave this important problem the use of archival data is the only way to answer the big question. Now, huge and comprehensive set of archival RN data go back to 1890.

Excellent work about the archival data has been promoted by René Hudec, who scanned thousands plates belong to numerous astronomical observatories spread in the whole world (e.g. Hudec, R. & Hudec, L., 2013). Indeed, the astronomical plate archives represent the only method how to study the behavior of the CVs (and other astrophysical objects in general) over very long (100 years or even more) time intervals, and the only method to go back in time. In addition, huge monitoring times (up to 30,000 hrs of continuous monitoring) are available allowing to detect and to study rare events such as outbursts. The databases allow to study prominent spectra and/or spectral changes as well (Hudec, R. Hudec, L. & Klíma, M., 2012).

A review about galactic and extragalactic novae has been published by Poggiani (2017a), in which she discusses the multifrequency observations that are contributing to understanding the process of explosions and of the long term evolution. She discusses the observations of novae over the electromagnetic spectrum, focusing on the morphology of the decline light curves, the spectroscopic investigations, the long term evolution, the recurrent novae, the gamma ray emission in novae, extragalactic novae, and the gravitational emission of novae.

3.13 Progenitors of SN Ia

It is well accepted by the community that Type–Ia SNe are the result of the explosion of a carbon–oxygen WD that grows to near Chandrasekhar's limit in a close binary system (Hoyle & Fowler, 1960). But the debate is focussed around the different kinds of progenitors. Indeed, in the past, two families of progenitor models have been proposed. They differ in the mode of WD mass increase. The first family is the so–called *single degenerate* (SD) model (Whelan & Iben, 1973), in which the WD accretes and burns hydrogen–rich material from the companion. The second family

is the so–called *double degenerate* (DD) model, in which the merging of two WDs in a close binary triggers the explosion (Webbing, 1984; Iben & Tutukov, 1984). The two scenarios produce different delay times for the birth of the binary system to explosion. Thus it is hopefully possible to discover the progenitors of Type–Ia SNe by studying their delay time distribution (DDT). The DDT can be determined empirically from the lag between the cosmic star formation rate and Type–Ia SN birthrate.

The energy released through runaway thermonuclear process ejects the majority of the unburnt hydrogen from the surface of the star in a shell of material moving at speeds of up to 1.5×10^3 km s^{-1}. This produces a bright but short-lived burst of light - the nova.

Although Type–Ia supernovae appear to have similar origin to classical novae, there are key differences. The most important is that in a classical nova, the thermonuclear runaway occurs only on the surface of the star, allowing the WD and the binary system to remain intact (e.g. Townsley & Bildsten, 2005). In a Type–Ia supernova, the thermonuclear runaway occurs within WD itself, completely disrupting the progenitor. This is reflected in the amount of energy released in the explosions, with classical novae releasing $\sim 10^{44}$ erg, and Type–Ia supernovae $\sim 10^{51}$ erg.

The possible progenitors of SN Ia are: i) Recurrent Novae; ii) Symbiotic stars; iii) Super-soft sources; iv) Double WD Binaries; and v) WDs accreting material from red–giant companions.

i) Recurrent Novae are just a subset of ordinary novae that happen to go off more than once per century.

As such, they are binary systems with matter flowing off a companion star onto a WD, accumulating on its surface until the pressure gets high enough to trigger a thermonuclear runaway that is the nova.

Only 10 RNe are known in our Milky Way galaxy, including: U Sco (1863, 1907, 1917, 1936, 1945, 1969, 1979, 1987, 1999); T Pyx (1890, 1902, 1920, 1944, 1967); T CrB (1866, 1946); RS Oph (1898, 1907, 1933, 1945, 1958, 1967, 1985, 2006).

To recur with $\tau_{rec} < 100$ years, RNe must have: high WD mass ($1.2M_\odot < M_{WD} < M_{Chandra}$), and high accretion rate ($\dot{M} \sim 10^{-7}$ $M_\odot$ yr^{-1}). SN Ia occurs if: i) the mass ejected for each eruption is less than the mass accreted onto the WD ($M_{ejected} < \dot{M}\ \tau_{rec}$); ii) the rate of death RNe must be enough to produce the SN Ia rate ($R_{RNdeath} = R_{SNIa}$), being $R_{RNdeath} = N_{RN} \times (0.2M_\odot \dot{M})$.

In order to solve the problems we need to know τ_{rec} (recurrence time scale) from archive plates, N_{RN} (number of RNe in the Milky Way) from archive plates and AAVSO, $\dot{M}$ (mass accretion rate onto WD) from the average in the last century, $M_{ejected}$ (mass ejected in eruption) from pre–eruption eclipse timing.

Some results have been obtained for becoming optimists in solving the problem of SN Ia production. Indeed Schaefer (2011) obtained for CI Aql and U Sco $M_{ejected} << \dot{M}\ \tau_{rec}$).

Thus, WDs are gaining mass and the latter RNe will collapse as SN Ia. Moreover, for the Milky Way, M31, and LMC $R_{RNdeath} \sim N_{RN}$. Then there are enough RNe to supply the Type–Ia SN events.

ii) Symbiotic Stars contain WDs efficiently accreting material from the secondary star. In most cases they steadily burn H–rich material allowing them to grow in mass. Some of these systems can produce high mass WDs. In symbiotic RNe (SyRNe) the WD mass is already very close to Chandrasekhar's limit. For instance in V 407 Cyg a very massive WD is accreting material

at a rate of $\sim 10^{-7}$ $M_{\odot}$ yr^{-1} from a Mira–type companion (Miszalski, Mikołajewska & Udalski, 2013).

iii) Super–soft Sources are probably WDs that accrete material and burn hydrogen. Voss & Nelemans (2008) discovered an object at the position of the Type–Ia SN2007on in the elliptical galaxy NGC1404 on pre–supernova archival X–ray images. This result favours the accretion model (SD) for this supernova, although the host galaxy is older than the age at which the explosions are predicted in SD models. However, the DD model cannot be ruled out by this event because a hot accretion disc is probably the intermediate configuration of the system, between first WD–WD Roche–lobe contact and explosion (Yoon, Podsiadlowski & Rosswog, 2007).

Greggio, Renzini & Daddi (2008) starting from the fact that Type–Ia SN events occur over an extended period of time, following a distribution of delay times (DDT), discussed theoretical DDT functions that accommodate both 'prompt' and 'tardy' SN events derived by empirically–based DDT functions. Moreover such theoretical DDT functions can account for all available observational constraints. The result is that SD/DD mix of SNIa's is predicted to vary in a systematic fashion as function of cosmic time (redshift).

iv) Double WDs Binaries are systems containing two WDs that can merge and giving rise to SN explosion. Yoon, Podsiadlowski & Rosswog (2007) explored the evolution of the merger of two carbon–oxygen (CO) WDs. Their results imply that at least some products of double CO WDs merger may be considered good candidates for the progenitors of Type–Ia SNe. Brown et al. (2011) and Kilic et al. (2011) studied a complete colour–selected sample of double–degenerate binary systems containing extremely low mass (ELM) (≤ 0.25 $M_{\odot}$) WDs. Milky Way disc ELM WDs have a merger rate of $\approx 4 \times 10^{-5}$ yr^{-1} due to gravitational wave radiation. The ELM WD systems that undergo stable mass transfer can account for about 3% of AM CVn stars. The most important fact is that the ELM WD systems that may detonate merge at a rate comparable to the estimate rate of underluminous SNe. These SNe are rare explosions estimated to produce only ~ 0.2 $M_{\odot}$ worth of ejecta. At least 25% of ELM WD sample belong to the old tick disc and halo components of our Galaxy. Thus, if merging ELM WD systems are the progenitors of underluminous SNe, transient surveys must find them in both elliptical and spiral galaxies.

v) WDs accreting material from red–giant companions. Observations carried out by Patat et al. (2008) with VLT–UVES allowed to detect circumstellar material in a normal Type–Ia SN. The expansion velocities, densities and dimensions of the circumstellar envelope indicate that this material was ejected from the system prior to the explosion. The relatively low expansion velocities favour a progenitor system where a WD accretes material from a companion star, which is in the red–giant phase at the time of explosion.

Bianco et al. (2011) searched for a signature of a non–degenerate companion in three years of Supernova Legacy Survey data. They found that a contribution from WD/red–giant binary system to Type–Ia SN explosions greater than 10% at 2σ, and than 20% at 3σ level is ruled out.

Type–Ia SNe are used as primary distance indicators in cosmology (e.g. Phillips, 2005). Phillips (2011) reviewed the near–infrared (NIR) of Type–Ia SNe concluding that such SNe are essentially perfect standard candles in the NIR, displaying only a slight dependence of peak luminosity on decline rate and colour. Lira (1995) first noted that B–V evolution during the period from 30 to 90 days after V maximum is remarkably similar for all SN Ia events, regardless of light–curve

shape. This fact was used by Phillips et al. (1999) to calibrate the dependence of the B_{max}–V_{max} and V_{max}–I_{max} colours on the light curve parameter Δm_{15} (B) which can, in turn, be used to separately evaluate the host galaxy extinction. Using these methods for eliminating the effect of the reddening, they reanalyzed the functional form of the decline rate versus luminosity relationship and gave a value of the Hubble constant of $H_0 = 63.3 \pm 2.2 \pm 3.3$ km s^{-1} Mpc^{-1}.

The use of Type–Ia SNe is also fundamental for determining some cosmological constraints, such as Ω_M and Ω_Λ that fit a ΛCDM models with values of 0.211 ± 0.034 (stat) ± 0.069 (sys) using a set of 252 high–redshift SNe (Guy et al., 2010) and $0.713^{+0.027}_{-0.029}$ (stat) $^{+0.036}_{-0.039}$ (sys) using a set of low–redshift nearby–Hubble–flow SNe (Kowalski et al., 2008), respectively.

In order to explore the difficult topic of the expansion of the Universe it is necessary to know the evolution of metallicity in old Universe that changes the Hubble Diagram shape. The proposed space observatory Super Nova Acceleration Probe (SNAP) is designed to measure the expansion of the Universe and to determine the nature of the mysterious Dark Energy that is accelerating this expansion (Aldering, 2005). SNAP is being proposed as part of the Joint Dark Energy Mission (JDEM) (Stril, Cahn & Linder, 2010), which is a cooperative venture between NASA and the U.S. Department of Energy. SNAP haS been superseded by WFIRST (Wide Field InfraRed Survey Telescope) (Gehrels et al., 2015).

WFIRST is a space telescope that will conduct unprecedented large surveys of the infrared universe to explore everything from our solar system to the edge of the observable universe, including planets throughout our galaxy and the nature of dark energy. The telescope was initially developed as the WFIRST0, and renamed in 2020 to honor Nancy Grace Roman, NASA's first Chief of Astronomy. Roman has been called the "mother" of NASA's Hubble Space Telescope. The Roman Space Telescope (RST) is currently planned for launch in the mid-2020s, and no later than 2027.

However, RST cannot achieve its main goal without progenitor/evolution solution.

The research about the progenotors of SN Ia is of course one of the most important problems, since it is strictly connected with the evolution of CVs. For instance, Maguire et al. (2012) present an analysis of the maximum light, near-ultraviolet (NUV; $2900 < \lambda < 5500$) spectra of 32 low-redshift ($0.001 < z < 0.08$) SNe Ia, obtained with the Hubble Space Telescope (HST) using the Space Telescope Imaging Spectrograph. They combine this spectroscopic sample with high-quality *gri* light curves obtained with robotic telescopes to measure SN Ia photometric parameters, such as stretch (light-curve width), optical colour and brightness. They confirm and strengthen earlier conclusions regarding the complex behaviour of SNe Ia in the NUV spectral region, but suggest that the correlations found are more useful in putting tighter constraints on the progenitor systems of SNe Ia and how their progenitor channels may vary with host galaxy properties (e.g. metallicity: Kistler et al., 2013) rather than improving the use of SNe Ia as cosmological probes.

Darnley et al. (2014) discussed on the galactic nova progenitor population. They presented a selection of the work and rationale that led to the proposal of a new nova classification scheme based not on the outburst properties but on the nature of the quiescent system. They also outlined the results of a photometric survey of a sample of quiescent Galactic novae, showing that the evolutionary state of the secondary can be easily determined and leading to a number of predictions, including their relevance to extragalactic work and the proposed link to type–Ia SNe.

In order to solve the problem of determining the SN Ia progenitors, it is also important to look

at the RNe that show many similarities to CNe, but have had more than one recorded outburst. RNe play an important role as one of the suspected progenitor systems of Type–Ia SNe, which are used as primary distance indicators in cosmology. Thus, it is important to investigate the nature of their central binary systems to determine the relation between the parameters of the central system and the outburst type, and finally ascertain the population of novae that might be available to give rise to the progenitors of Type–Ia SNe. Surina, Bode & Darnley (2015) adopted a low outburst amplitude as a criterion that may help distinguish RNe from CNe and was therefore used to select targets for observations from ground-based observatories including the Liverpool Telescope and the Southern African Large Telescope as well as the full-sky space-based archive of the Solar Mass Ejection Imager (SMEI). They found that at least four objects currently classified as CNe are possibly RNe candidates based on their quiescent spectra. They also searched the SMEI archive for additional outbursts of bright CNe that might otherwise have been missed but did not find a conclusive example.

Another possible channel for triggering the explosion of SN Ia is that discussed by Chiosi et al. (2015). They explore the possibility that isolated CO–WDs with mass smaller than the Chandrasekhar limit may undergo nuclear runaway and SN explosion. If this channel could be confirmed it should be possible (i) to explain the star formation rate dependence of the SN Ia rate (e.g. Mannucci, Della Valle & Panagia, 2006); (ii) to provide some clues to interpreting the observational data on the ejected mass distribution of type–Ia SNe showing a significant rate of non-Chandrasekhar-mass progenitors of mass as low as 0.8 $M_{\odot}$ (Scalzo, Ruiter & Sim, 2014); and (iii) to account for the SNe exploding inside Planetary Nebulae in alternative to the core-degenerate scenario in which a WD merges with the hot core of an AGB star on a time interval $\leq 10^8$ yr since the WD formation (see Tsebrenko & Soker, 2015, for more details). With the models of Chiosi et al. (2015), a single CO–WD may reach the explosion stage soon after the formation if sufficiently massive ($> 1.0\,M_{\odot}$) and sufficiently rich in residual hydrogen ($X_H \simeq 10^{-19} - 10^{-20}$). The expected time delay after formation can be as low as about a few ten of thousand years.

Williams et al. (2014, 2016) report the results of a survey of M31 novae in quiescence. The derived catalog contains data for 38 spectroscopically confirmed novae from 2006 to 2012. They used Liverpool Telescope images of each nova during eruption to define an accurate position for each system. These positions were then matched to archival Hubble Space Telescope (HST) images and they performed photometry on any resolved objects that were coincident with the eruption positions. This in order to facilitate a search for their progenitor systems within archival Hubble Space Telescope (HST) data, with the aim of detecting systems with red giant secondaries (RG-novae) or luminous accretion disks. They found an elevated proportion of nova systems with evolved secondaries that may imply the presence of a much larger population of recurrent novae than previously thought. This would have considerable impact, particularly with regards to their potential as Type–Ia SN progenitors. Their results also imply that RG-novae in M31 are more likely to be associated with the M31 disk population than the bulge, indeed the results are consistent with all RG-novae residing in the disk. If this result is confirmed in other galaxies, it suggests any Type–Ia SNe that originate from RG-nova systems are more likely to be associated with younger populations, and may be rare in old stellar populations, such as early-type galaxies.

An important paper by Churazov et al. (2014) reports the first ever detection of ^{56}Co lines at 847 and 1237 keV and a continuum in the 200-400 keV band from the Type–Ia SN2014J in M82

with INTEGRAL observatory. The data were taken between 50th and 100th day since the SN2014J outburst. The line fluxes suggest that 0.62 ± 0.13 $M_\odot$ of radioactive ^{56}Ni were synthesized during the explosion. Line broadening gives a characteristic ejecta expansion velocity $V_e \sim 2100 \pm 500$ km s^{-1}. The flux at lower energies (200-400 keV) is consistent with the three-photon positronium annihilation, Compton downscattering and absorption in the ~ 1.4 $M_\odot$ ejecta composed from equal fractions of iron-group and intermediate-mass elements and a kinetic energy $E_k \sim 1.4 \times 10^{51}$ erg. All these parameters are in broad agreement with a "canonical" model of an explosion of a Chandrasekhar-mass WD, providing an unambiguous proof of the nature of Type–Ia SNe as a thermonuclear explosion of a solar mass compact object. Late optical spectra (day 136 after the explosion) show rather symmetric Co and Fe line profiles, suggesting that, unless the viewing angle is special, the distribution of radioactive elements is symmetric in the ejecta (Churazov et al., 2015).

For comments and prospects about Type–Ia SN science in the decade 2010–2020 see the paper by Howell et al. (2009).

3.14 Some Open Questions

Several fundamental questions concerning CVs still remain waiting for a proper answer. Here we will present briefly only some of them.

One of them is the lack of a coherent classification, especially for NLs. On the other hand, in gross features and in most respects, DN and NLs, as well as quiescent novae, are almost indistinguishable, although, in addition to their different outbursts' behaviour, there appear to be some further minor differences which are not yet understood (see Hack & la Dous 1993). The question arises of whether the outburst behaviour, the current basis of almost all classification is really a suitable criterion for sorting CVs in physically related groups. There are also too many exceptions, either systems that do not fit in any particular group or that can be included in several of them, to be able to render the observational behaviour, at least as it is used at the present, suitable.

Could CVs be considered simply gravimagnetic rotators? This should be the most suitable approach for studying them from a physical point of view.

Studies of rotational equilibria of MCVs predict that IPCVs will evolve either into PCVs or into low field strength polars – presumably unobservable, and possibly EUV emitters – depending on their magnetic moments and orbital periods. Indeed, there are systems, like EX Hya-type, having magnetic moment similar to IPCVs above the 'period gap' and comparable to the weakest field AM Her-like systems.

Moreover, the detection of several SW Sex systems having orbital periods inside the so-called 'period gap' opens a new interesting problem about the continuity in the evolution of CVs.

The rare AM CVn stars have extremely short orbital periods, between 10 and 65 minutes, and their spectra show no evidence for hydrogen. They appear to be helium-rich versions of CVs. They are still waiting for a general model. They are probably binary systems of two white dwarfs, but even this is still controversial.

Despite all the work developed during the last decades, the problem of modeling accretion disks in CVs is by no means closed, especially in quiescence. Closely related is the problem of the cause of outbursts. We really do not know which of the present two families of models (Disk Instability Models or Secondary Instability Models) is responsible for the CVs outburst phenomenon,

or in which system is each model valid, although Martinez-Pais et al. (1996) gave a contribution in solving this problem at least in the case of SS Cygni; they found some evidence for an increase of the mass transfer rate from the secondary star as the mechanism responsible for symmetric outbursts. Something similar can be said about the super-outburst phenomenon in SU UMa systems.

Gaudenzi et al. (1990), analyzing IUE spectra of SS Cygni, discussed about the outburst production as due to the destruction of the accretion disk. The matter slowly accretes onto the WD. Long and short outbursts correspond to total or partial destruction of the disk, respectively.

Alternatively, could nuclear burning be responsible of the production of outbursts in CVs? Indeed, nuclear burning onto white dwarf' surface was proposed by Mitrofanov (1978, 1980) as a mechanism suitable to generate X-rays in CVs. In spite of this shrewd suggestion, the community of theoreticians did not consider such a mechanism – certainly possible – worthy of taking up a part of their time. However, we believe that this alternative solution in explaining the generation of outbursts in CVs would deserve theoretician community's care. For instance, the white dwarf surface interested in the accretion in the system SS Cygni has been evaluated as 24% of the total (Gaudenzi et al., 2002). There, nuclear burning could occur.

Accretional heating by periodic DN events increases substantially the surface temperature of the WD in CVs (Godon & Sion, 2002). Then, the envelope thermal structure resulting from compression and irradiation should be a crucial component in understanding the envelope structure of a pre–nova WD.

Another problem still open is connected with the classification of CVs in three kinds, namely NMCVs, PCVs and IPCVs. This is, in our opinion, another convenient classification, although artificial, probably not necessary if CVs are studied as gravimagnetic rotators. In this way a smooth evolution of the systems could be responsible of the variations of the gravimagnetic parameters.

Are the IPCVs and PCVs smoothly connected via the SW Sex-like systems placed just in between? SW Sex systems have indeed orbital periods belong to the so-called 'period gap', and then their presence there sure cancel that gap.

Could some systems behave in different ways depending on their instantaneous physical conditions? For this reason they could apparently behave sometimes as PCVs and sometimes as NPCVs.

An example very clear is that of SS Cygni, usually classified as a non-magnetic dwarf nova. It has been detected by the INTEGRAL observatory in a region of the spectrum (up to ~ 100 keV). This emission is very hard to be explained without the presence of polar caps in the WD of the system. Several proofs have been shown and discussed many times by Giovannelli's group in order to demonstrate the Intermediate Polar nature of it (e.g., Giovannelli, 1996, and references therein; Giovannelli & Sabau-Graziati, 1998; 2012a); indeed, SS Cygni shows characteristics of a NMCV, as well as those of IP and sometimes even those of polars, although its position in the $\log P_{spin}$–$\log P_{orb}$ plane is very close to the line where IPs lie.

Important results are coming from the SPITZER space telescope with the detection of an excess (3-8) μm emission from MCVs, due to dust (Howell et al., 2006; Brinkworth et al., 2007). Gaudenzi et al. (2011) discussed about the reasons of the variable reddening in SS Cyg and demonstrated that this reddening is formed by two components: the first is interstellar in origin, and the second (intrinsic to the system itself) is variable and changes during the evolution of a quiescent phase. Moreover, an orbital modulation also exists. The physical and chemical parameters of the system are consistent with the possibility of formation of fullerenes.

The SPITZER space telescope detected the presence of fullerenes in a young planetary nebula (Cami et al., 2010). Fullerenes are the first bricks for the emergence of the life. Therefore, the possible presence of fullerenes in CVs opens a new line of investigation, foreboding of new interesting surprises.

Further information can be considered in order to better synthetize the open problems in the knowledge of CVs and related objects.

Sion (http://astronomy.villanova.edu/faculty/sion/CV/index.html) states that in the Galaxy we could expect $\approx 10^6$ CVs. One of the big questions that arises is: "can all of the observed CVs and the phenomena associated with them be understood in terms of a single unified picture?" Other questions relate to the relative probabilities that CVs will be observed at particular stages in their evolution, and how the observations of CVs at the current epoch can be used to determine their ultimate fate.

To address these questions Nelson (2012) and Goliasch & Nelson (2015) have undertaken a massive computational effort to theoretically simulate the evolution of most of the possible CVs that could be produced by nature. The temporal evolution of 56,000 nascent CVs was followed over an age of 10 billion years using the MESA stellar evolution code. According to Nelson, "*This is the most ambitious analysis of the properties of an entire CV population that has ever been undertaken. The whole project required several core-years of CPU time*."

While many of the results confirmed what had already been inferred about the properties of CVs, there were a number of surprises including the identification of a number of previously unexplored evolutionary pathways. But, as expected, a sharp bifurcation was found between nascent CVs that evolved to produce double white-dwarf binaries (including ones containing helium and hybrid white dwarfs), and ones that continuously transferred mass over the lifetime of the universe. In addition, the predictions of the theoretical simulations were in good general agreement with the observations of CVs with reasonably well-measured properties.

What was surprising was the large number of short-period "ultracompact" binaries (AM CVn stars) that were produced and, especially, the enormous depletion of carbon relative to nitrogen and oxygen that is predicted at certain epochs for evolved systems. As Nelson points out, "*It seems that nature has provided us with a unique way to identify CVs that descended from a highly evolved state based on their carbon abundances. There is already some observational evidence to suggest that there is a significant depletion of carbon in certain CVs. This could be a really critical test that will allow us to infer the lineage of some CVs and predict what their fate will be*".

The paper by Otulakowska-Hypka, Olech & Patterson (2016) present a statistical study of all measurable photometric features of a large sample of dwarf novae during their outbursts and superoutbursts. They used all accessible photometric data for all their objects to make the study as complete and up to date as possible. Their aim was to check correlations between these photometric features in order to constrain theoretical models which try to explain the nature of dwarf novae outbursts. They managed to confirm a few of the known correlations, that is the Stolz and Schoembs relation, the Bailey relation for long outbursts above the period gap, the relations between the cycle and supercycle lengths, amplitudes of normal and superoutbursts, amplitude and duration of superoutbursts, outburst duration and orbital period, outburst duration and mass ratio for short and normal outbursts, as well as the relation between the rise and decline rates of superoutbursts. However, they question the existence of the Kukarkin-Parenago relation but they found

an analogous relation for superoutbursts. They also failed to find one presumed relation between outburst duration and mass ratio for superoutbursts. This study should help to direct theoretical work dedicated to dwarf novae.

Szkody & Gänsicke (2012) provided a list of unanswered problems and questions and references for seeking additional information. Indeed, while the general evolutionary picture and the characteristics of the types of CVs are known at some level, there are major unsolved questions which remain. These include:

1. What is the actual number density and distribution of CVs in the Galaxy?
2. What happens to CVs once they reach the period minimum?
3. What are the detailed physics occurring in the common envelope?
4. What is the correct physics to describe viscosity in accretion disks?
5. What is the correct angular momentum prescription below the gap (besides gravitational radiation) that can account for the observed period minimum spike and the exact period distribution?
6. What causes the period gap?
7. How do Polars form and why are no magnetic white dwarfs in wide binaries observed? Are LARPS (Low Accretion Rate Polars) the progenitors of polars? Is there a difference in the emergence of systems containing magnetic white dwarfs versus non-magnetic?
8. What causes Polars, as well as the novalike disk systems with orbital periods between 3 and 4 hours, to cease mass transfer and enter low states? Are the associated mass transfer variations of the companion stars a general phenomenon among all CVs?
9. Can the white dwarfs in CVs grow in mass?
10. Do CVs contain exoplanets?

    I can add one point more:

11. Do CVs emit gravitational waves?

    A possible answer to this point has been discussed by Poggiani (2017b), who reports that the most probable sources of GWs are AM CVn systems.

In order to answer to these not yet solved problems, a series of biennial Palermo Workshops about "*The Golden Age of Cataclysmic Variables and Related Objects*" has been organized since 2011. The refereed proceedings can be found in Giovannelli & Sabau-Graziati (2012c, 2015d).

3.15 Accretion onto Neutron Stars and Black Holes

In LMXBs (Low-Mass X-ray Binaries) the compact object can be either a neutron star or a black hole and the optical companion is a low mass star. The exchange of matter occurs via Roche lobe overflow, like shown in the left panel of Fig. 25. In HMXBs (High-Mass X-ray Binaries) the

compact object can be either a neutron star or a black hole and the optical companion is a high mass star: giant or super-giant. The exchange of matter occurs mainly via stellar wind since usually the optical star does not fill its Roche lobe (Fig. 25, left panel). However, sometimes, the exchange of matter can occur in a mixed way because of the formation of an accretion disk around the compact object around the periatron passage (e.g. Giovannelli & Ziółkowski, 1990) (Fig. 25, right panel).

McClintock, Narayan & Rybicki (2004) found a very interesting relationship between the minimum X-ray luminosity in the range 0.5–10 keV and the orbital periods of BH LMXBs and NS LMXBs. BH LMXBs are on average a factor of ~ 100 fainter than NS LMXBs with similar orbital periods (Fig. 27).

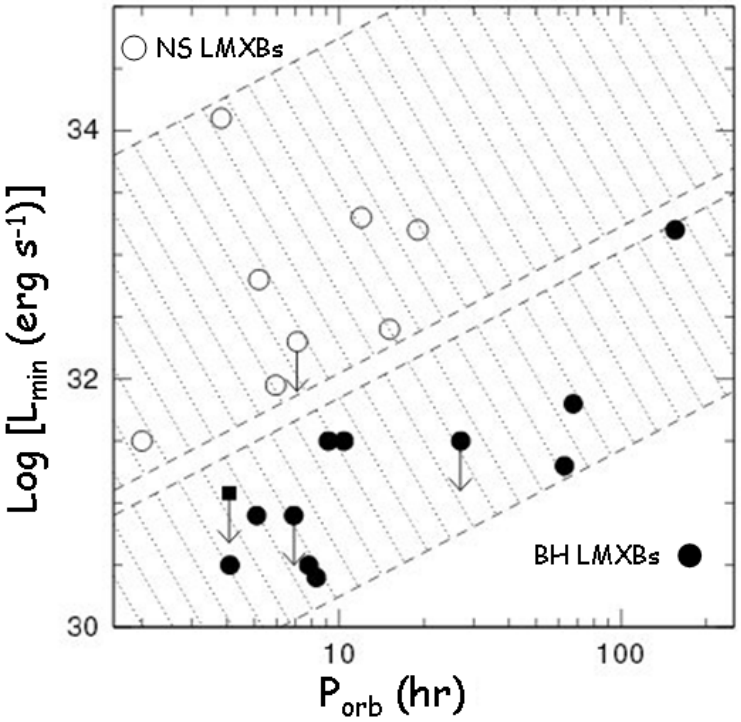

Figure 27: Minimum X-ray luminosity (0.5-10 keV) versus orbital period for BH LMXBs and NS LMXBs. The diagonal hatched areas delineate the regions occupied by the two classes of sources and indicate the dependence of luminosity on orbital period (adapted from McClintock, Narayan & Rybicki, 2004).

As well known, X-ray/Be systems are formed by a compact star and an optical star. Obviously there is a mutual influence between the two stars. Low-energy (LE) processes influence high-energy (HE) processes and vice versa. Never confuse the effect with the cause. There is a general law in the Universe: **Cause and Effect**. The *Cause* generates an *Effect* and NOT vice versa!

Time-lag between HE events and LE events in disk-fed accreting X-ray binaries (XRBs) has been noted in many systems, but the trigger of the work resulted in a model for explaining in general such a phenomenon (Bisnovatyi-Kogan & Giovannelli, 2017) was given by Giovannelli & Sabau-Graziati (2011) who noted a systematic delay between the relative enhancement in luminosity of the optical Be star – occurring at the periastron passage of the neutron star – and the subsequent X-ray flare in the system HDE 245770/A 0535+26. The model for such a system was developed

and corroborated by many events (Giovannelli, Bisnovatyi-Kogan & Klepnev, 2013: GBK13), and later by events reported in Giovannelli et al. (2015) where also a relationship between ΔV_{mag} of the optical star at the periastron and X-ray intensity (I_X) of the 8-day delayed flare was produced.

It is right to remind that the mechanism proposed by GBK13 for explaining the X-ray-optical delay in A 0535+26/HDE 245770 is based on an enhanced mass flux propagation through the viscous accretion disk. This mechanism, known as UV-optical delay (the delay of the EUV flash with respect to the optical flash) was observed and modeled for cataclysmic variables (e.g. Smak, 1984; Lasota, 2001). Time delays have been detected also in several other X-ray transient binaries. This is the reason that urged Bisnovatyi-Kogan & Giovannelli (2017) to generalize the aforementioned model, developed for the particular case of A 0535+26/HDE 245770 (Flavia' star). This general model provides the formula (3.2) of the time delay between the optical and X-ray flashes appearance in transient cosmic accreting sources:

$$\tau = 6.9 \frac{m^{2/3} \dot{m}^{1/15}}{\alpha^{4/5} (T_4)^{28/15}} \tag{3.2}$$

where:

$m = M/M_\odot$; $\dot{m} = \dot{M}/(10^{-8}\ M_\odot/yr)$; $T_4 = T_0/10^4$ K ;
α = viscosity , and T_0 = maximum temperature in optics.

By using this formula it is possible to obtain an excellent agreement between the experimental and theoretical delays found in:

- X-ray/Be system A0535+26/HDE245770: $\tau_{exp} \simeq 8$ days (GBK13); $\tau_{th} \simeq 8$ days;
- Cataclysmic variable SS Cygni; τ_{exp} = 0.9–1.4 days (Wheatley, Mauche & Mattei, 2003); $\tau_{th} \simeq 1.35$ days;
- Low-mass X-ray binary Aql X-1/V1333 Aql: $\tau_{exp} \sim 3$ days (Shahbaz et al., 1998); $\tau_{th} \simeq$ 3.2days
- Black hole X-ray transient GRO J1655-40: $\tau_{exp} \sim 6$ days (Orosz et al., 1997); $\tau_{th} \simeq 6.5$ days.

In this general formula the α-viscosity parameter plays an important role, and usually it is hard to be determined. However, if the other parameters are known, because experimentally determined, the formula (3.2) can be used for determining α, taking into account the experimental delay measured in a certain source.

Over the last couple of decades we have witnessed the discovery of a multitude of highly ionized absorbers in high-resolution X-ray spectra from both BH and NS XRBs. The first detections were obtained thanks to ASCA on the BH binaries GROJ1655-40 and GRS 1915+105. Narrow absorption lines in the spectra of these systems identified as Fe XXV and Fe XXVI indicated the first of many discoveries of photo-ionized plasmas in LMXBs (Chandra, XMM-Newton and Suzaku). Black hole hot accretion flows occur in the regime of relatively low accretion rates and are operating in the nuclei of most of the galaxies in the universe. One of the most important progress in recent years in this field is about the wind or outflow. This progress is mainly attributed

Table 4: Comparison of numbers of different classes of X-ray Binary Systems in the Milky Way and in the Magellanic Clouds (Ziółkowski, 2013; Ferrario, de Martino & Gänsicke, 2015; Buckley, 2015).

Name of the Class	Milky Way	LMC	SMC
Total mass of the galaxy (in M_{SMC} units)	100	10	1
High Mass X-ray Binaries	118	26	83
in this Be/X-ray	72	19	79
Low Mass X-ray Binaries	197	2	-
Black Hole Candidates	62	2	-
Cataclysmic Variables	≈ 2000	-	-
in this MCVs	≈ 250	-	-
IPs	~ 60	-	-
B not yet determined	≈ 600	-	-

to the rapid development of numerical simulations of accretion flows, combined with observations on, e.g., Sgr A*, the SMBH in the Galactic center. The mass loss from a BH via wind is related to the mass accretion rate onto the BH and can be described as (Yuan, 2016):

$$\dot{M}_{wind}(r) = \dot{M}_{BH}(r/20r_s)^s \tag{3.3}$$

where $s \approx 1$, and $\dot{M}_{BH}$ is the mass accretion rate at the black hole horizon and $r_s = 2GM/c^2$ is the Schwarzschild radius.

At this point it is useful to make a sort of summary about the number of XRBSs, including CVs. Liu, van Paradijs & van den Heuvel (2006, 2007) and Ziółkowski (2013) report 315 galactic XRBs: 197 LMXBs (63%) and 118 HMXBs (37%), 72 of which are Be/X-ray systems; moreover there are 62 BH candidates. Coleiro & Chaty (2013) report that in the Milky way there are ≥ 200 HMXBs. Ritter & Kolb (2003) catalogue, in the 7.20 (Dec. 2013) version, reports 1166 CVs. Buckley (2015) reports about the discoveries of 530 new CVs from MASTER-Network and 855 CVs from Catalina Real Time Susrvey (CRTS) (http://nesssi.cacr.caltech.edu/DataRelease/). Ferrario, de Martino & Gänsicke (2015) report the number of MCVs as ≈ 250, and ~ 60 of which IPs, and considering those systems for which the magnetic field intensity has not yet been determined, their number is of ≈ 600. Table 1 shows the content of XRBSs, including CVs, in the Galaxy, and in the LMC and SMC (Ziółkowski, 2013; Ferrario, de Martino & Gänsicke, 2015; Buckley, 2015). The mass are expressed in unit of SMC.

Grimm (2003) published: (i) a list of the 17 most luminous LMXBs contributing $\approx 90\%$ to the integrated luminosity of LMXBs in the 2-10 keV band in the whole Galaxy, averaged over 1996-2000. The 12 most luminous sources (Cir X-1, GRS 1915+105, Sco X-1, Cyg X-2, GX 349+2, GX 17+2, GX 5-1, GX 340+0, GX 9+1, NGC 6624, Ser X-1, GX 13+1) contribute $\approx 80\%$ of the

integrated luminosity of the Galaxy; (ii) a list of the 10 most luminous HMXBs (Cyg X-3, Cen X-3, Cyg X-1, X 1657-415, V 4641 Sgr, GX 301-2, XTE J1855-024, X 1538-522, GS 1843+009, X 1908+075) that contribute $\approx 40\%$ to the integrated luminosity of HMXBs in the 2-10 keV band in the whole Galaxy, averaged over 1996-2000.

As already mentioned in the Section (2.11) "Scenario Machine", Raguzova & Lipunov (1999) obtained an evolutionary track that can lead to the formation of Be/BH systems. This result has been confirmed fifteen years later by Casares et al. (2014) who discovered MWC 656, the first Be/BH binary.

Indeed, Raguzova & Lipunov (1999) calculations show that binary black holes with Be stars must have $0.2 < e < 0.8$. It is particularly difficult to detect such systems as most of their spectroscopic variations occur in a relatively small portion of the orbit, and could easily be missed if the systems are observed at widely separated epochs.

The critical initial mass of the supernova star that collapses to a BH is accepted to be equal to $55 < M_{cr} < 75\ M_{\odot}$, and the fraction of the presupernova mass ($M_{\star}$) collapsing to the BH, $k_{BH} = M_{BH}/M_{\star} = 0.5$. The kick velocity v_m = 0–200 km s^{-1}. The age of the system, according to their evolutionary scenario is 4×10^6 yr.

The expected number of Be/BH binaries – with orbital period 10 d $< P_{orb} <$ 1000 d, and eccentricity $0.2 < e < 0.8$ – is 1 Be/BH for 20-30 Be/NS.

Belczynski and Ziółkowski (2009) used binary population synthesis models to show that the expected ratio of Be/XRBs with neutron stars to black holes in the Galaxy is relatively high ($\sim 30 - 50$), and so broadly in line with observations. Thus we can expect 1 Be/BH for 30–50 Be/NS.

Therefore, we can expect 1 Be/X-ray BH system for 20–50 Be/X-ray NS systems (Raguzova & Lipunov, 1999; Belczynski & Ziółkowski, 2009). We know 60 Be/X-ray NS systems (after INTEGRAL). Thus we expect 1–3 Be/X-ray BH systems. One of this systems has been detected: MWC 656 (Casares et al., 2014).

New simulations – using the StarTrack binary population synthesis models have been conducted to understand the formation channel of MWC 656 – constrain the population of Be/BH systems and study the fate of MWC 656 as a possible NS–BH merger, and then possible gravitational wave emitter. In particular, it has been assumed that all donors beyond main sequence are allowed to survive the common envelope (CE) phase. Ten Gyr of evolution of the Galactic disk originates $\sim$ 8700 B/BH systems, and 1/3 of them would be Be/BH systems: namely $\sim$ 2900). However, only 13 of them had periods, eccentricities and masses similar to MWC 656 (Grudzinska et al., 2015).

There are so many black holes in the Universe that it is impossible to count them.

Stellar-mass black holes (SBHs) form from the most massive stars when their lives end in supernova explosions. The Milky Way galaxy contains some 10^{11} stars. Roughly one out of every thousand stars that form is massive enough to become a black hole. Therefore, our galaxy must harbor some 10^8 stellar-mass black holes. Most of these are invisible to us, and only nineteen have been identified (Wiktorowicz, Belczynski & Maccarone, 2014) with masses up to $\sim 15\ M_{\odot}$. Theoretically the mass of a SBH depends on the initial mass of the progenitor, how much mass is lost during the progenitor's evolution and on the supernova explosion mechanism (Belczynski et al., 2010; Fryer et al., 2012). Mass is lost through stellar winds, and the amount of mass lost strongly depends on the metallicity of the star. For a low metallicity star (~ 0.01 of the solar metallicity)

it is possible to leave a black hole of ≤ 100 $M_\odot$ (Belczynski et al., 2010). In the region of the Universe visible from Earth, there are perhaps 10^{11} galaxies. Each one has about 10^8 stellar-mass black holes. And somewhere out there, a new stellar-mass black hole is born in a supernova every second.

However, some attempts of evaluation of the number of SBHs in the Galaxy have been done. For instance, taking into account the γ-ray emissivity of the Galaxy (between ~ 1 and 1.3×10^{42} s^{-1} for $E > 100$ MeV) measured by the SAS II satellite (Bignami et al., 1975; Strong, Wolfendale & Worral, 1976) and the processes of disk-fed accretion onto black holes, Giovannelli, Karakuła & Tkaczyk (1981, 1982) found a possible upper limits to the number of black holes ($M \sim 10$ $M_\odot$ and $\dot{M} \approx 10^{-8}$ $M_\odot$ yr^{-1}) of 10^{-5} or 10^{-4} of the total star population of the Galaxy, for Mach's number 1 and 2, respectively. (*)

(*) The Mach number is given by the ratio of the velocity of the gas to the local sound speed. In order to evaluate the temperature, concentration and velocity of the plasma near the black hole it is necessary to solve the system of equations describing the plasma motion (Michel, 1972) taking into account the distance from the black hole in units of gravitational radius and the u = R-component of four velocity. Mach's number 1 and 2 correspond to different values of u_0^2 (1.0266 and 2.1213, respectively) at a distance r_0 from the black hole (Giovannelli, Karakuła & Tkaczyk, 1981, 1982).

There is a class of intermediate-mass black holes (IMBHs), with masses > 100 $M_\odot$ up to $\approx 10^5$ $M_\odot$. It contains a dozen systems, as listed in Johnstone (2004). However, black holes with masses of several hundred to a few thousand solar masses remain elusive, as reported in a review by Casares & Jonker (2014) where a deeply discussion about the mass measurements of SBHs and IMBHs is contained.

Supermassive black holes (SMBHs) are 10^6–10^9 times more massive than our Sun and are found in the centers of galaxies (see the exhaustive review by Kormendy & Ho, 2013). Most galaxies, and maybe all of them, harbor such a black hole. So in our region of the Universe, there are some 10^{11} SMBHs. The nearest one resides in the center of our Milky Way galaxy. The most distant one we know of resides in a quasar galaxy billions of lightyears away. SMBHs grow in size as they gorge on surrounding matter.
Figure 28 show the relative masses of super-dense cosmic objects versus the mass of the bulge (Kormendy & Ho, 2013).

A list of BH candidates, compiled by Wm, has been reported by Johnston (2004) and provides the input for constructing the map of sky locations of BH candidates, as shown in Fig. 29. Stellar-mass black holes in red, intermediate-mass black holes in purple, supermassive black holes in blue. The base image is from Tycho sky map from JPL's Solar System Simulator.

In the case of galactic compact sources, by using the softness and hardness ratios, coming for the measurements of the many X-ray satellites, it is possible to construct a diagram in which BHs in high state are separated by those in low state, and by other kind of objects, such as X-ray pulsars and other systems, as shown in Fig. 30 (Giovannelli, 2016, after Tanaka, 2001).

There are several relationships in which the mass of black holes correlates with stellar dispersion velocity σ, and the bulge luminosity L_V, like shown in Fig. 31 (left and right panel) (McConnell et al., 2011), and the size of the disk, as shown in Fig. 32 (Mudd et al., 2018).

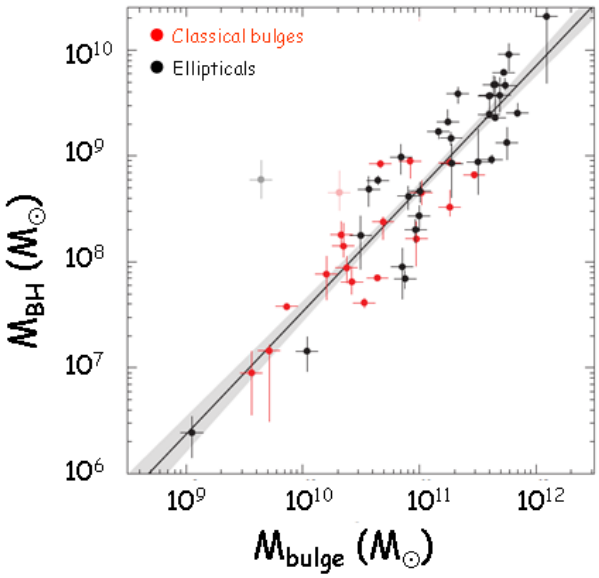

Figure 28: The correlation of the black hole mass (M_{BH}) versus the bulge mass (M_{bulge}) (adopted from Kormendy & Ho, 2013).

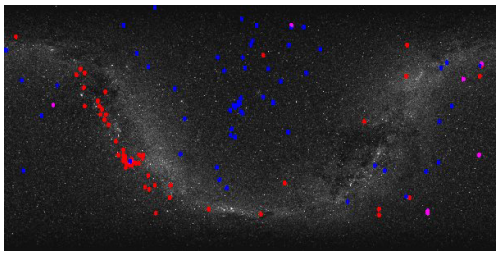

Figure 29: The map of sky locations of BH candidates. Red (stellar mass BHs), Purple (IMBHs), Blue (SMBHs). The base image is from Tycho sky map from JPL's Solar System Simulator (adopted from Johnstone, 2004).

It is important to mention the paper by Casares (2015) in which he found that the FWHM of the Hα line in (soft X-ray transient (SXTs) is tightly correlated with the velocity semi-amplitude of the donor star K_2 = 0.233(13) FWHM. This new correlation, when combined with P_{orb} (i.e., through photometric light curves), allows for the possibility of estimating compact object mass functions from single integration, low resolution spectroscopy. The correlation is the following:

$$\mathrm{FWHM} \simeq \mathrm{A}(\mathrm{M}_1/\mathrm{P}_{orb})^{1/3} \sin \mathrm{i}$$

with A = 876 $\pm$ 48 km s^{-1}; M_1 = Mass of the accreting star ($M_\odot$); P_{orb} (days)

Figure 33 (Casares, 2015) shows the Hα-FWHM vs K_2 correlation for SXTs with the best linear fit. Blue solid circles indicate BHs while Ns are marked by open circles (upper panel), and the Hα-FWHM vs K_2 correlation for CVs (lower panel). Filled triangles indicate CVs above the period

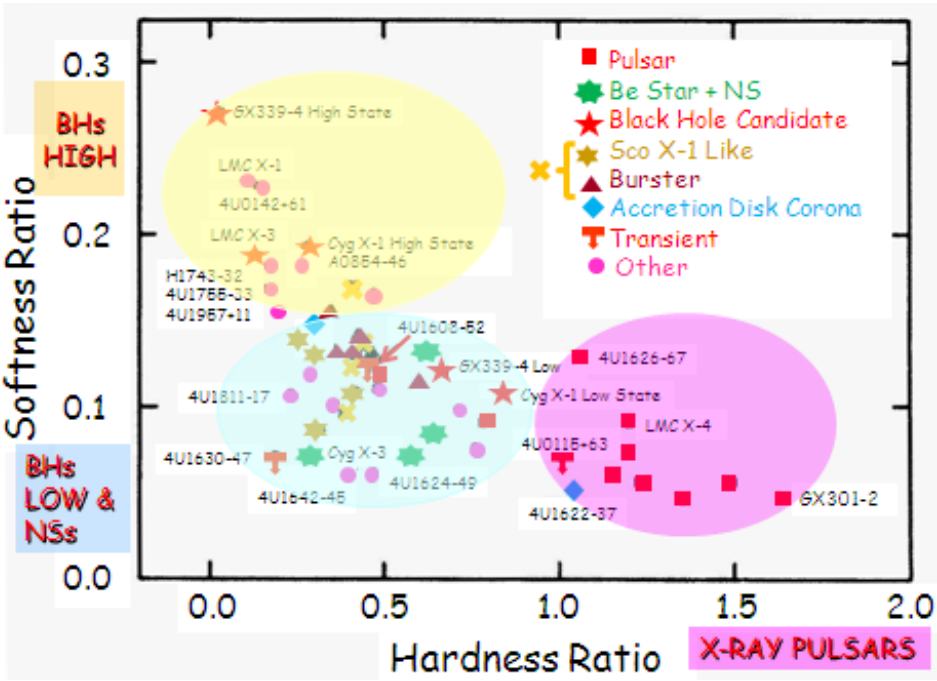

Figure 30: Softness ratio versus hardness ratio for galactic compact systems. Light yellow ellipse marks the zone where BHs in high state lie, light turquoise ellipse marks the zone of the BHs in low state and NSs, and light fuchsia ellipse marks the zone of the X-ray pulsars (adopted from Giovannelli, 2016, after Tanaka, 2001).

gap while open triangles indicate those below/within the gap. Like in the case of SXTs, long period CVs display a tight Hα-FWHM vs K_2 correlation, though with a flatter slope. Dotted lines mark theoretical correlations derived by Casares's formulae.

Another important paper by Wu et al. (2016) reproduces the X-ray light curve of the hyperluminous X-ray source (HLX-1, whose peak X-ray luminosity $\sim 10^{42}$ erg s^{-1}) near the spiral galaxy ESO 243-49, which underwent recurrent outbursts within a period of $\sim$ 400 days (Fig. 34 left panel). This source is possibly the best candidate for an intermediate mass black hole (IMBH). The physical reason for this quasiperiodic variability is still unclear. Wu et al. (2016) explore the possibility of radiation-pressure instability in the accretion disk by modeling the light curve of HLX-1, and find that it can roughly reproduce the duration, period, and amplitude of the recurrent outbursts in HLX-1 with an IMBH of $\sim 10^5$ $M_\odot$. Their result provides a possible mechanism to explain the recurrent outbursts in HLX-1. They further find a universal correlation between the outburst duration and the bolometric luminosity for the black hole sources with a very broad mass range (e.g., X-ray binaries, HLX-1, and active galactic nuclei), which is roughly consistent with the prediction of radiation-pressure instability of the accretion disk (Fig. 34 right panel). These results imply that "heartbeat" oscillations triggered by radiation-pressure instability may appear in different-scale BH systems.

As already noted black hole accretion is a fundamental physical process in the universe. It is the standard model for the central engine of active galactic nuclei (AGNs), and also plays a central

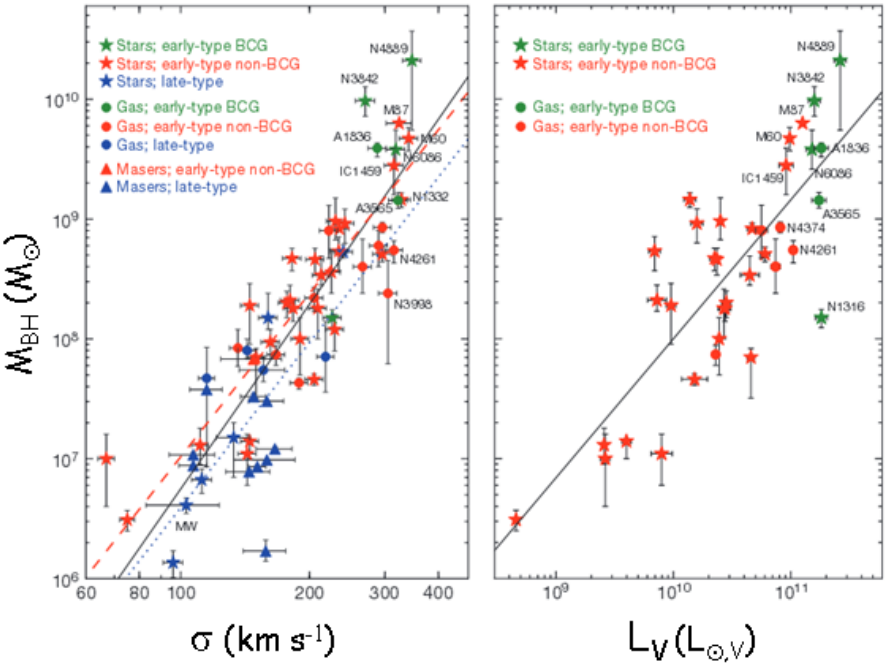

Figure 31: Correlations of dynamically measured black hole masses and bulk properties of host galaxies (adopted from McConnell et al., 2011).

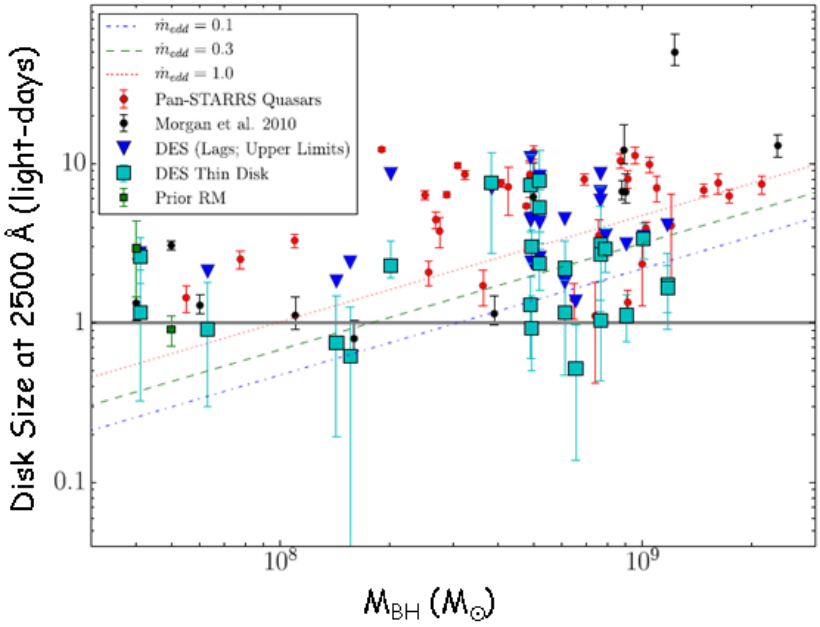

Figure 32: Disk size as a function of black hole mass (adopted from Mudd et al., 2018).

role in the study of black hole X-ray binaries, Gamma-ray bursts, and tidal disruption events. According to the temperature of the accretion flow, the accretion models can be divided into two

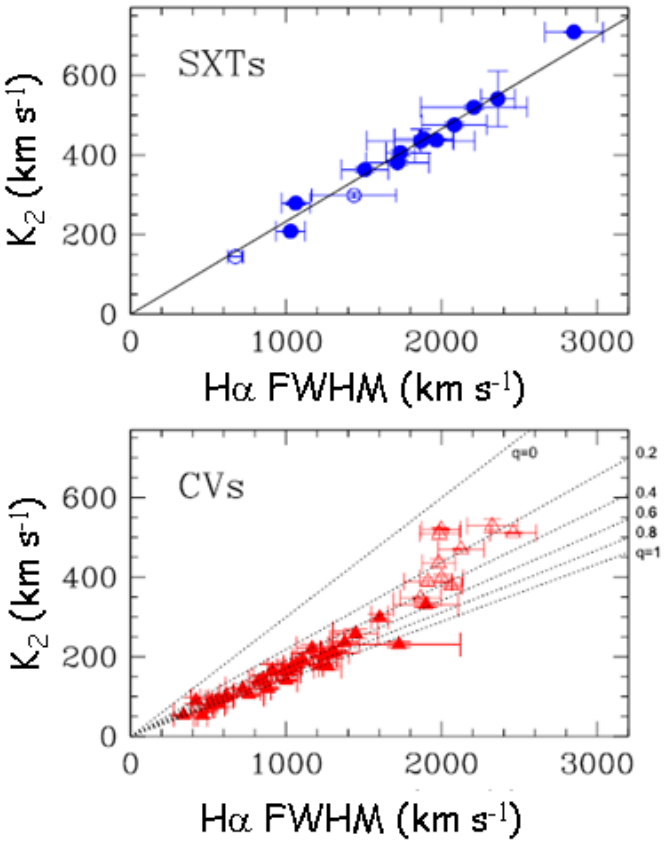

Figure 33: Hα-FWHM vs K_2 correlation for SXTs and CVs (adopted from Casares, 2015).

classes, namely cold and hot. The standard thin disk model belongs to the cold disk, since the temperature of the gas is far below the virial value (Shakura & Sunyaev, 1973) (see reviews by Pringle, 1981; Frank, King & Rayne, 2002; Abramowicz & Fragile, 2013; Blaes, 2014). The disk is geometrically thin but optically thick and radiates multi-temperature black body spectrum. The radiative efficiency is high, ~ 0.1, independent of the accretion rate. The model has been successfully applied to luminous sources such as luminous AGNs and black hole X-ray binaries in the thermal state. The most recent review about the accretion onto black holes was published by Lasota (2016).

The tidal disruption of stars by massive BHs has been discussed since many years by Rees (1988b), and e.g. Magorrian & Tremaine (1999). Rees (1988b) argued that stars in galactic nuclei can be captured or tidally disrupted by a central black hole. Some debris would be ejected at high speed, the remainder would be swallowed by the hole, causing a bright flare lasting at most a few years. Such phenomena are compatible with the presence of 10^6–10^8 $M_\odot$ holes in the nuclei of many nearby galaxies. Stellar disruption may have interesting consequences in our own Galactic Centre if a $\approx 10^6$ $M_\odot$ hole lurks there.

In a recent paper, Bisnovatyi-Kogan & Giovannelli (2017) developed models of time lags between optical and X-ray flashes for close-binary galactic sources with accretion disks and for

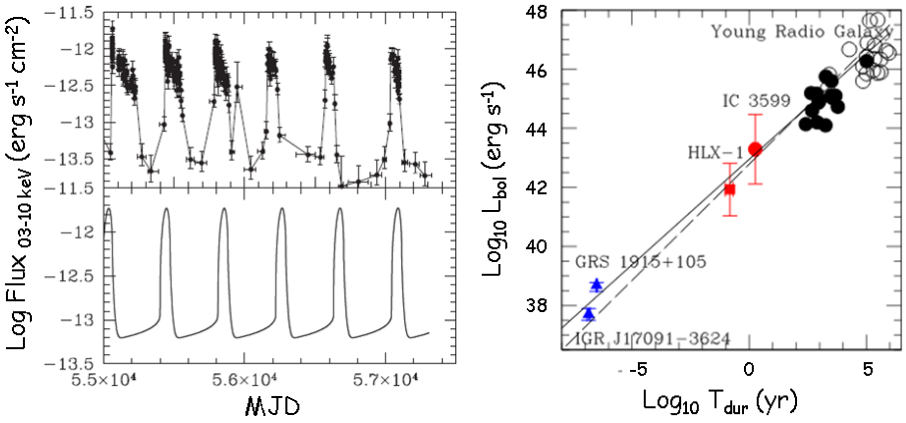

Figure 34: Left panel shows the observational light curve of HLX-1 (top panel) and modeled light curve of accretion disk (bottom). Right panel shows Correlation between the bolometric luminosity and the outburst duration for different-scale BHs. The black filled and empty circles represent the Gigahertz-peaked spectrum (GPS) and compact steep-spectrum (CSS) sources, respectively. The solid line represents the best fit and the dashed line shows the prediction of the disk model under radiation-pressure instability (α = 0.02) (adopted from Wu et al., 2016).

an AGN with an SMBH that is embedded in a quasi-spherical bulge. The flashes in an AGN are considered in the model when a disruption of a star that is in the evolution phase of a giant enters the radius of strong tidal forces. The matter with a low angular momentum that is released by the star falls into the SMBH in the form of a quasi-spherical flow with a velocity that is close to the free-fall velocity. An X-ray flash occurs when the falling matter reaches the hot inner regions. The time lag observed in these sources is identified with the time of the matter falling from the tidal radius onto the central region. The values of the tidal radius that they calculated in this model were compared with the theoretical radii of a tidal disruption that depends on the masses of the SMBH and of the star, and on the radius of the star. Knowing the SMBH masses from observations, and making a reasonable suggestion for the stellar mass that is on the order of one solar mass, they obtained that the radii of the disrupted star are between a few tens and a few hundreds of $R_{\odot}$. These radii are characteristic of stars of moderate mass on the giant phase of evolution (e.g. Bisnovatyi-Kogan, 2011).

Recently several books about black holes appeared in the literature:

- *The Physics of Accretion onto Black Holes* (Falanga et al., 2015). It provides a comprehensive summary on the physical models and current theory of black hole accretion, growth and mergers, in both the supermassive and stellar-mass cases.

- *The Strongest Magnetic Fields in the Universe* (Beskin et al. 2015). The topic of this volume contains reviews of completely new aspects of magnetic fields in the astrophysical Universe. The strength of the magnetic fields of the compact objects reviewed in this volume is up to 8 to 10 orders of magnitude higher than that of typical sunspots which are the strongest fields in the solar system. Large-scale astrophysical magnetic fields, such as interstellar and galactic fields are weaker still than the fields experienced in the solar system.

- *The Formation and Disruption of Black Hole Jets* (Contopoulos, Gabuzda & Kylafis, 2015). The main aim of this book is to present reviews of the varied phenomenology regarding the radio to X-ray spectra of stellar binaries and the properties of AGN jets on the wide range of scales through which they propagate, as well as recent theoretical efforts to understand the physical mechanisms that contribute to the origin of black hole jets on all scales. Particular emphasis is given to the role and the origin of the black hole magnetosphere and the magnetic fields that drive, collimate, and accelerate the jets. The final goal is a tentative of giving a consistent, unified physical picture of the formation and disruption of jets in accreting black hole systems. New observational and theoretical results are piling up every day, so the contents of this volume only represent our current best ideas. Time will tell how close our present understanding is to reality.

- *Astrophysics of Black Holes* (Bambi, 2016). This book contains the most relevant papers discussed during the Fudan Winter School on Astrophysical Black Holes (held at Fudan University, in Shanghai, from February 10 to 15, 2014): *Black Hole Accretion Discs*, *Transient Black Hole Binaries*, *Black Hole Spin: Theory and Observation*, *Winds from Black Hole Accretion Flows: Formation and Their Interaction with ISM*, *A Brief Review of Relativistic Gravitational Collapse*, and *General Relativity in a Nutshell*.

- *Black Holes: A Laboratory for Testing Strong Gravity* (Bambi, 2017). The main aim of this book is to discuss the electromagnetic techniques to study the strong gravity region around astrophysical black holes. For completeness, gravitational wave methods will be also reviewed, but only very briefly and without the necessary details to start working on the corresponding line of research. This book has not the ambition to be a complete manual on this research field. Hopefully, it may be a good starting point.

Important news were reported over the last couple of decades. We have witnessed the discovery of a multitude of highly ionized absorbers in high-resolution X-ray spectra from both BH and NS XRBs. The first detections were obtained thanks to ASCA on the BH binaries GROJ1655-40 and GRS 1915+105. Narrow absorption lines in the spectra of these systems identified as Fe XXV and Fe XXVI indicated the first of many discoveries of photo-ionized plasmas in LMXBs (Chandra, XMM-Newton and Suzaku).

3.16 Accretion processes onto oceans

A huge, swirling pile of trash in the Pacific Ocean is growing faster than expected and is now about three times the size of France (https://www.theoceancleanup.
com/great-pacific-garbage-patch/). An astonishing partial image of this disaster is shown in Fig. 35 (left panel) (http://www.eioba.pl/a/4f00/zabije-nas-plastik). The right panel of Fig. 35 shows a sea turtle entangled in a ghost net (Photo credits: Francis Perez).

Our trash harms the deepest fish in the ocean. Humans have produced 8.3×10^{12} kg of plastic since the '50s (Geyer, Jambeck & Law, 2017). That is equal in weight to $\approx 1.6 \times 10^{9}$ elephants, considering the average weight of an elephant of ≈ 5000 kg (https://www.livescience.com/27320-elephants.html).

Figure 35: Left panel: partial image of the swirling pile of trash in the Pacific Ocean. Right panel: A sea turtle entangled in a ghost net (Photo credits: Francis Perez).

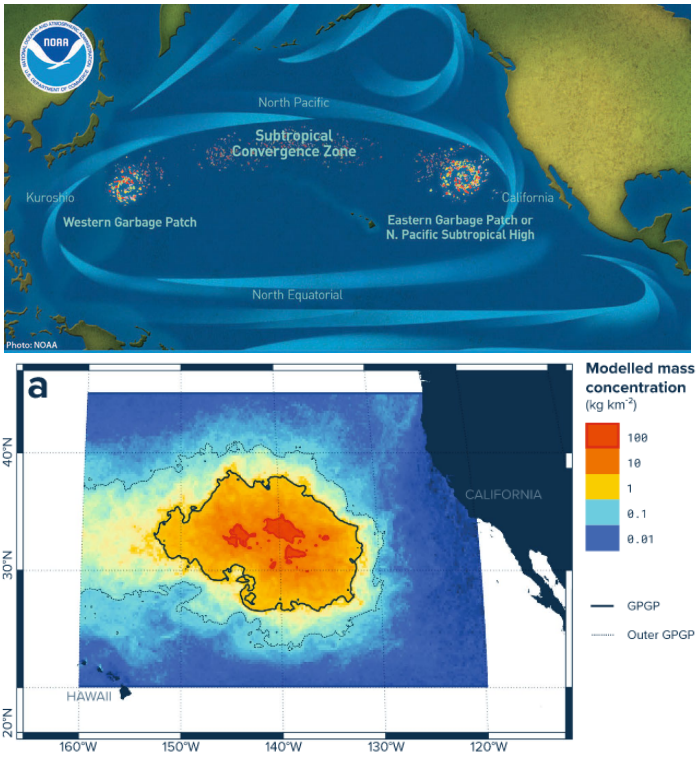

Figure 36: The great pacific garbage patch: upper panel - the extension (Map by NOAA); lower panel - the model (adopted from Lebreton et al., 2018).

Garbage patches are large areas of the ocean where litter, fishing gear, and other debris – known as marine debris – collects. They are formed by rotating ocean currents called "gyres". There are five gyres in the oceans. One in the Indian Ocean, two in the Atlantic Ocean, and two in the Pacific Ocean. Garbage patches of varying sizes are located in each gyre. The most famous of these patches is often called the "Great Pacific Garbage Patch". It is located in the North Pacific Gyre (between Hawaii and California). "Patch" is a misleading nickname, causing many to believe that these are islands of trash. Instead, the debris is spread across the surface of the water and from the surface all the way to the ocean floor. The debris ranges in size, from large abandoned fishing nets to tiny microplastics, which are plastic pieces smaller than 5 mm in size. This makes

it possible to sail through some areas of the Great Pacific Garbage Patch and see very little to no debris (https://marinedebris.noaa.gov/info/patch.html).

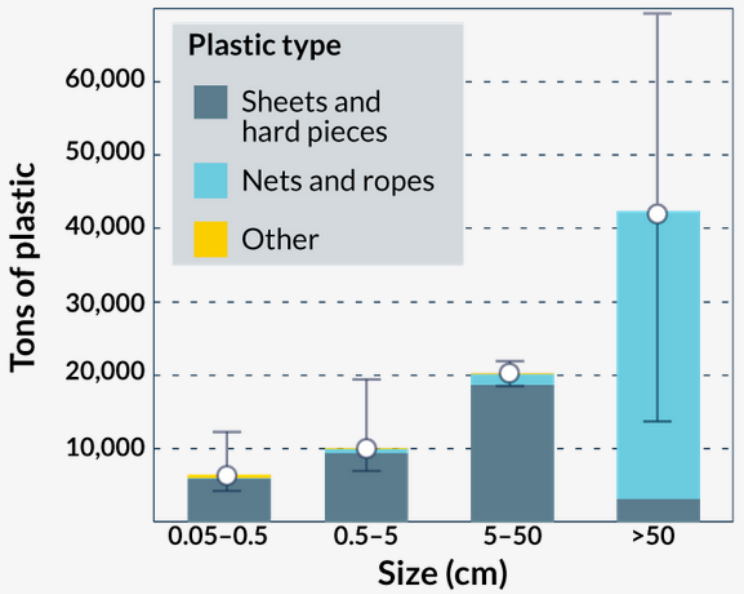

Figure 37: Inventory of plastic in the great pacific garbage patch (GPGP) (adopted from Lebreton et al., 2018).

Figure 36 (upper panel) shows the dramatic extension of the great pacific garbage patch (NOAA, Marine Debris Program, 2012 - https://marinedebris.no
aa.gov/info/patch.html. However, a paper describing the dramatic situation of the garbage has been published by Lebreton et al. (2018). They state that ocean plastic can persist in sea surface waters, eventually accumulating in remote areas of the world's oceans. They characterize and quantify a major ocean plastic accumulation zone formed in subtropical waters between California and Hawaii: The Great Pacific Garbage Patch (GPGP). Their model, calibrated with data from multi-vessel and aircraft surveys, predicted at least 79^{+50}_{-34} thousand tonnes of ocean plastic are floating inside an area of 1.6×10^6 km^2; a figure four to sixteen times higher than previously reported (Fig. 36, lower panel). They explain this difference through the use of more robust methods to quantify larger debris. Over three-quarters of the GPGP mass was carried by debris larger than 5 cm and at least 46% was comprised of fishing nets. Microplastics accounted for 8% of the total mass but 94% of the estimated $1.8^{+1.8}_{-0.7} \times 10^9$ pieces floating in the area. Plastic collected during their study has specific characteristics such as small surface-to-volume ratio, indicating that only certain types of debris have the capacity to persist and accumulate at the surface of the GPGP. Finally, their results suggest that ocean plastic pollution within the GPGP is increasing exponentially and at a faster rate than in surrounding waters.

Figure 37 shows an inventory of plastic in the GPGP (Lebreton et al., 2018).

3.17 Accretion processes in the space around the Earth

The Soviet Union launched the first space vehicle Sputnik I on October 4, 1957 (Stoiko, 1970). Since then, the exploration and use of space have proliferated dramatically. Activities in space have

generated millions of pounds of debris, most of it remaining in Earth orbit. This debris poses a threat to individuals and equipment moving in space. On rare occasions, the debris also threatens the Earth's biosphere (Roberts, 1992). This author discusses the global legal regime that currently regulates outer space comprises four international agreements. This regime consists of the Treaty on Principles Governing the Activities of States in the Exploration and Use of Outer Space, Including the Moon and Other Celestial Bodies (Outer Space Treaty), the Convention on International Liability for Damage Caused by Space Objects (Liability Convention), the Convention on Registration of Objects Launched into Outer Space (Registration Convention), and the Agreement Governing the Activities of States on the Moon and Other Celestial Bodies (Moon Treaty). Although covering a wide range of issues relating to outer space, these agreements (collectively, Outer Space Agreements or Agreements) have not effectively managed the problem of space debris. Moreover, the Agreements are partly responsible for creating the problem.

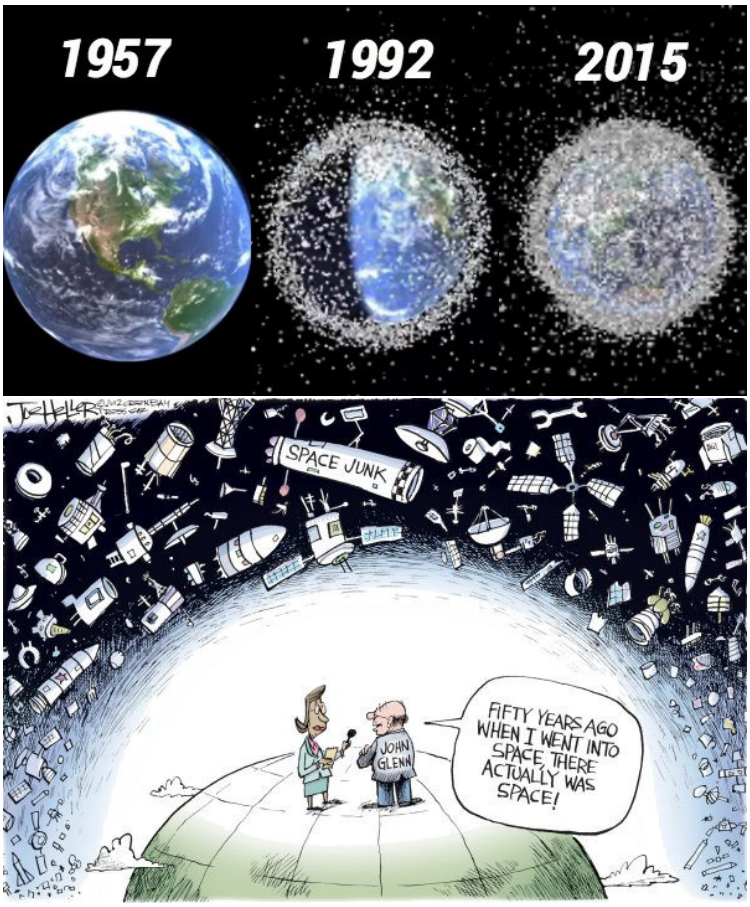

Figure 38: Upper panel: the amount of space junk in our atmosphere has skyrocketed, with dangerous consequences (Fisher-Quann, 2017). Lower panel: John Glenn's disconsolate statement (Credit: Joe Heller).

The Outer Space Agreements were intended primarily to facilitate access to and use of the space environment, although they also included elements of environmental regulation. The Agreements typically raised environmental concerns only in the context of efficient use of space resources or research opportunities. They did not attempt to provide broader protection of the space environ-

ment. These factors, as well as the complexities of the space environment, make it difficult for the Agreements to provide a solution to the continuing degradation of the space environment.

This degradation, as well as the pollution of the entire planet, has reached alarming levels, as shown schematically in Figure 38 (upper panel) (Rayne Fisher-Quann, 2017 at https://quarkmag.com/is-space-junk-a-problem-67e865f
702a9). Lower panel of Fig. 38 shows John Glenn's disconsolate statement in a cartoon (Credit: Joe Heller).

More than 500,000 pieces of debris, or "space junk", are tracked as they orbit the Earth. They all travel at speeds up to 28,000 km h^{-1}, fast enough for a relatively small piece of orbital debris to damage a satellite or a spacecraft.

The rising population of space debris increases the potential danger to all space vehicles, but especially to the International Space Station, space shuttles and other spacecraft with humans aboard.

Indeed, currently there is about six metric tons of space debris in earth orbit and about 45% of that is in low-earth orbit and polar orbits where the threat of collisions continues to increase. This process can lead to an escalating cascade of more and more debris. Today we are very much at risk of such a cascading build-up that is known as the "Kessler Syndrome". Two events in recent years have particularly contributed to orbital space debris build-up. One event was the collision of the defunct Russian Kosmos 2251 weather satellite with the Iridium 33 low earth orbit mobile communications satellite. The other was the shooting down of an old and defunct Chinese Fen Yun weather satellite by the Chinese military. Each of these events led to the creation of nearly 3,000 new tracked debris elements. Currently 22,000 of these space debris elements are being actively tracked by U.S. surveillance networks. Each of these debris elements are capable of creating major new debris, especially if they collided with another satellite or upper stage rocket. In short, without further remedial action to remove space debris from Earth orbit, the problem will continue to get worse [NASA Office of Orbital Debris] (Pelton, 2015a). Pelton in his interesting book "*New Solutions for the Space Debris Problem*" discusses with extreme clarity the serious problem of why space services are now of vital importance to our global society. He writes: "*Space systems have become so very vital, that if we were suddenly denied access to our space-based infrastructure for weather forecasting and warning, for space-based navigation and timing, for civil and military communications, and for remote sensing and surveillance from space we would be in danger. We would suffer almost immediately-economically, militarily, and socially. Many of our transportation and our communications systems would go down along with our weather and rescue services and defense systems. Internet would lost its synchronization, credit card validation would no longer work, we would not be alerted to major storm systems, air traffic control, shipping navigation, and trucking routing services would be lost.*

Unfortunately as our space-based systems have become more and more common, other factors have served to make our satellites more at risk. One risk is that of extreme solar flares and coronal mass ejections."

Then, as mentioned in the introduction, we have a further demonstration of the interconnection of all human activities closely related to each other (Luisi & Capra, 2014).

In conclusion I can affirm that Humans are so intelligent that manage to contaminate even the space, which is the only escape from the planet!

The risk is that someone in the future will look at our species as we look at that of the dinosaurs!

Then, if we look for "Intelligent Lives" in the Universe .... Why we should look for those like ours? (Giovannelli, 2001b).

However, positive messages can be taken into account: many people are involved in the tentative of protection of the planet from different points of view.

Since the problem of space debris is now urgent, many attempts of removing it are in progress. This imply also legal problems as clearly discussed by Joyeeta Chatterjee (2013) in her thesis on *Legal Aspects of Space Debris Remediation: Active Removal of Debris and On-Orbit satellite Servicing*, for obtaining the Master Degree in Law.

In this regard it is important to mention the fundamental *Handbook of Cosmic Hazards and Planetary Defense* (Pelton & Allahdadi, 2015) that analyzes all the cosmic hazards, including also the pollution produced by humanity in the close space surrounding the Earth, and possible defense. It has been presented in a wonderful way by Lord Martin Rees – Royal Astronomer of the United Kingdom – in his foreword: .... *This Handbook is hugely impressive and deserves wide readership: it offers us a broad and well-informed perspective on our cosmic environment. More important, I hope it will stimulate appropriate efforts to understand and counter these threats – an enterprise valuable in its own right, but one which offers an opportunity for international partnership, both governmental and private, in a common cause. We are all members of the crew of "Spaceship Earth" – a precious and fragile "pale blue dot" in the wider cosmos. The recipes and insights in this Handbook will help to protect and safeguard it for future generations* (Rees, 2015).

Part XV of this handbook deals with *Mounting Hazards of Man-Made Threats in Space* (Klinkrad, 2015; Jonas, 2015; Pelton, 2015b; Jonas & Allahdadi, 2015; Botts, 2015).

Part XVI of this handbook deals with *Future of Planetary Defense* (Chatterjee, Pelton & Allahdadi, 2015; Lubin & Hughes, 2015; Hertzfeld & Schieb, 2015; Pelton, 2015c; Tronchetti, 2015; Potter, 2015; Simpson, 2015; Jakhu, 2015; Ross, 2015).

4. A journey outside our galaxy

And now it is the time to go outside our galaxy. Thanks to many important experiments, such as for instance Hubble Space Telescope (HST), our vision of the Universe became very wide. However the future (i.e. James Webb Space Telescope - JWST) will show us even more details for constructing a model of the whole Universe. This together with the detection of gravitational waves and the experiments for detecting the Cosmic Microwave Background with possible polarization will provide fundamental pieces of the puzzle that will show the most reliable model of the Universe.

In the following, without any pretension of completeness, I will try to discuss the most important results obtained in the recent past.

4.1 Gamma Ray Bursts

Long discussions about Gamma-ray bursts (GRBs) can be found in numerous publications. A list of these can be found in GSG2004 and in Giovannelli & Sabau-Graziati (2016c).

Although big progress has been obtained in the last few years, GRBs theory needs further investigation in the light of the experimental data coming from old and new satellites, often coordinated, such as BeppoSAX or BATSE/RXTE or ASM/RXTE or IPN or HETE or INTEGRAL or SWIFT or AGILE or FERMI or MAXI. Indeed, in spite of thousands papers appeared in the literature since the discovery of GRBs, the problem of their energy emission is still elusive: i) what is jet's composition? (kinetic or magnetic?); ii) where is dissipation occurring? (photosphere? deceleration radius?); iii) how is radiation generated? (synchrotron, Inverse Compton, hadronic?) (Zhang, 2013a,b).

Kumar & Zhang (2015) in a review paper *The Physics of Gamma-Ray Bursts & Relativistic Jets* discussed what we have learned about relativistic collisionless shocks and particle acceleration from GRB afterglow studies, and the current understanding of radiation mechanism during the prompt emission phase. They pointed out how these explosions may be used to study cosmology, e.g. star formation, metal enrichment, reionization history, as well as the formation of first stars and galaxies in the Universe.

The idea that GRBs could be associated to gravitational waves (GWs) emission is now popular. Indeed, short GRBs are believed to be produced by the mergers of either double NSs or NS-BH binaries (Nakar, 2007) and the observation of a kilonova associated with GRB130603B (Tanvir et al., 2013; Berger, Fong & Chornock, 2013) lends support to this hypothesis. In a recent review, D'Avanzo (2015) discussed the observational properties of short GRBs and showed how the study of these properties can be used as a tool to unveil their elusive progenitors and provide information on the nature of the central engine powering the observed emission. The increasing evidence for compact object binary progenitors makes short GRBs one of the most promising sources of gravitational waves for the Advanced LIGO/Virgo experiments. This idea obtained recently its experimental verification with the detection of GW 170817 event associated with the GRB 170817A (Abbott et al,, 2017a,b).

Thanks to the NASA's Swift satellite we assisted to ten years of amazing discoveries in time domain astronomy. Its primary mission is to chase GRBs. The list of major discoveries in GRBs and other transients includes the long-lived X-ray afterglows and flares from GRBs, the first accurate localization of short GRBs, the discovery of GRBs at high redshift ($z > 8$) (Gehrels & Cannizzo, 2015). And essentially thanks to these discoveries we are now closer to understand the real nature of GRBs.

The review by Bernardini (2015) discussed how the newly-born millisecond magnetars can compete with black holes as source of the GRB power, mainly with their rotational energy reservoir. They may be formed both in the core-collapse of massive stars, and in the merger of neutron star or white dwarf binaries, or in the accretion-induced collapse of a white dwarf, being thus a plausible progenitor for long and short GRBs, respectively.

Ghirlanda et al. (2015) discussed about the apparent separation of short and long GRBs in the hardness ratio vs duration plot. This separation has been considered as a direct evidence of the difference between these two populations. The origin of this diversity, however, has been only confirmed with larger GRB samples but not fully understood. They concluded that short and long GRBs have similar luminosities and different energetics (i.e. proportional to the ratio of their average durations). Then, it seems that the results are pointing toward the possibility that short and long GRBs could be produced by different progenitors but the emission mechanism responsible for

their prompt emission might be similar.

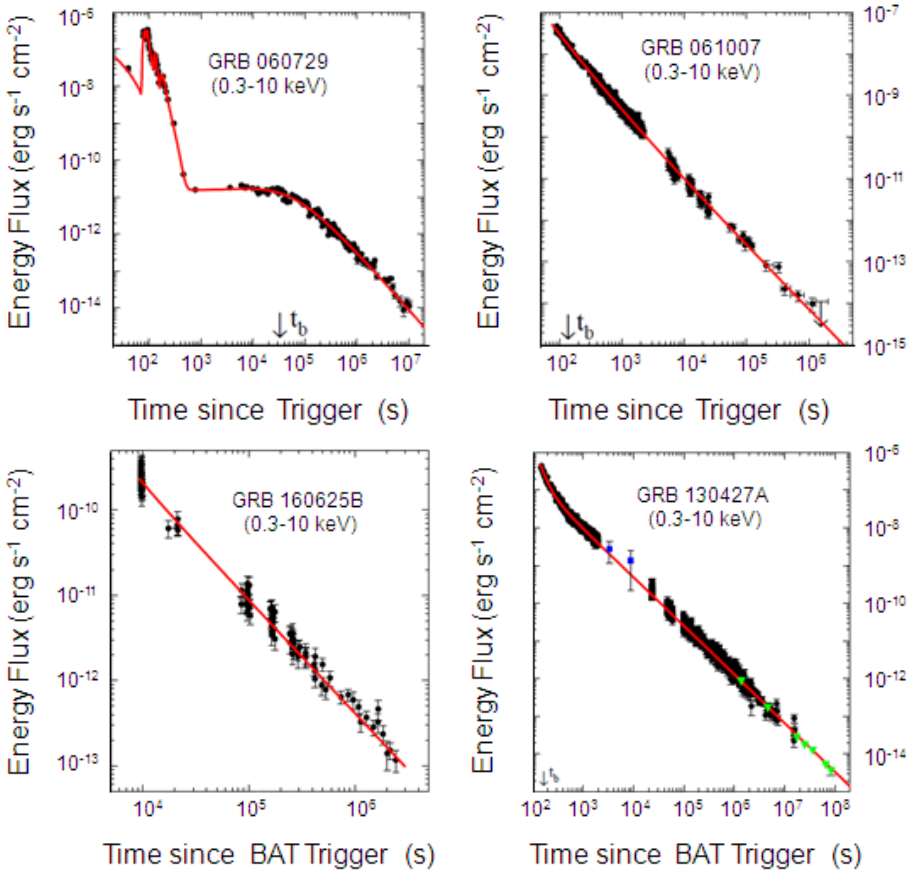

Figure 39: The 0.3-10keV X-ray light-curve measured with the Swift XRT (Evans et al., 2009), and the comparison between Swift observations and their CB-model description (adapted from Dado & Dar, 2016) for: top left GRB 060729, top right GRB 061007, bottom left GRB 160625B, bottom right GRB 130427A. This latter figure reports data from different experiments: Swift XRT (black circles), XMM Newton and Chandra (green triangles) (De Pasquale et al., 2016), and the two MAXI data points (blue squares) (Maselli et al., 2014) at t = 3257 s and t = 8821 s. The BAT trigger time is marked with t_b.

Piron (2016) in his review discussed the updated knowledge of GRBs at very high energies. Their huge luminosities involve the presence of a newborn stellar-mass black hole emitting a relativistic collimated outflow, which accelerates particles and produces non-thermal emissions from the radio domain to the highest energies. He reviewed recent progresses in the understanding of GRB jet physics above 100 MeV, based on Fermi observations of bright GRBs, and discussed the physical implications of these observations and their impact on GRB modeling.

Recently Arnon Dar (2017) proposed again to the attention of the international community his Cannonball (CB) model for explaining the physics of GRBs. In the CB model, GRBs and their afterglows are produced by the interaction of bipolar jets of highly relativistic plasmoids (CBs) of ordinary matter with the radiation and matter along their trajectory. Such jetted CBs are presumably ejected in accretion episodes of fall-back material on the newly formed compact stellar object in core-collapse supernovae (SNe) of Type Ic, in merger of compact stellar objects in close binary

systems, and in phase transitions in compact stars (Shaviv & Dar, 1995; Dar, 1997; Dar & De Rujula, 2000; Dado & Dar, 2013a). Dado, Dar & De Rújula (2009) discussed a long series of different SWIFT GRBs, showing that the CB model fits all their broadband light curves. Dado & Dar (2013b) discussed the jet break in the X-ray afterglow of GRBs that appears to be correlated to other properties of the X-ray afterglow and the prompt gamma ray emission, but the correlations are at odds with those predicted by the conical fireball (FB) model of GRBs (Piran, 1999). On the contrary they are in good agreement, however, with those predicted by the CB model of GRBs.

Finally, Dado & Dar (2016) discussed on the *critical test of gamma-ray bursts theories* and demonstrated definitively the validity of the CB model against the popular FB model (Piran, 1999).

Figure 39 shows, as example, the fits of light curves of GRB 060729, GRB 061007, GRB 160625B, and GRB 130427A by using the CB model.

In our opinion the problem of the models for explaining the behaviour of GRBs can be considered closed. The CB model is the best in absolute for the description of the physics governing the GRBs.

However, recent papers have been published about statistical studies of GRBs.

Zhao et al. (2019) performed an analysis for the shallow decay component of GRBs X-ray afterglow, in order to explore its physical origin with an updated sample of GRBs – data from Swift/XRT GRBs between February 2004 and July 2017 – with respect to that used by Liang et al. (2007) based on the early-year observations from Neil Gehrels Swift Observatory.

Overall, their results are generally consistent with Liang, Zhang & Zhang (2007), confirming their suggestion that the shallow decay segment in most bursts is consistent with an external forward shock origin, probably due to a continuous energy injection from a long-lived central engine.

Tang et al. (2019) considering that a plateau phase in the X-ray afterglow is observed in a significant fraction of GRBs performed a statistical study of this class. Previously, it has been found that there exists a correlation among three key parameters concerning the plateau phase, i.e., the end time of the plateau phase in the GRB rest frame (T_a), the corresponding X-ray luminosity at the end time (L_X) and the isotropic energy of the prompt GRB ($E_{\gamma,iso}$). They systematically searched through all the Swift GRBs with a plateau phase that occurred between 2005 May and 2018 August. They collected 174 GRBs, with redshifts available for all of them. They confirmed that a correlation exist and the best fit gives $L_X \propto T_a^{-1.01} E_{\gamma,iso}^{0.84}$. Such an updated three-parameter correlation still supports that the central leftover after GRBs is probably a millisecond magnetar. It is interesting to note that short GRBs with duration less than 2 s in their sample also follow the same correlation, which hints that the merger production of two neutron stars could be a high mass magnetar, but not necessarily a black hole. Moreover, GRBs having an "internal" plateau (i.e., with a following decay index being generally smaller than -3) also obey this correlation. It further strengthens the idea that the internal plateau is due to the delayed collapse of a high mass neutron star into a black hole. The updated three-parameter correlation indicates that GRBs with a plateau phase may act as a standard candle for cosmology study.

Wang et al. (2019b) performed a comprehensive statistical study using 6289 GRBs. They arrived to the conclusion that in order to reveal more physical principles one should try to classify the GRBs into more precise subgroups based on their physical origin, and the classification itself is a process to reveal the intrinsic properties of GRBs. With the detailed classifications, the correlations inside each group may be more tighter and more physical. The correlations are then can be used

to study the radiation mechanism as well as the high energy radiation, to be indicators as standard candle or pseudo redshift, and to study the gravitational waves of compact binary mergers.

Thus also after this interesting paper, the answer to the real processes occurring in GRBs is still open.

4.2 Confirmation of the Theory of General Relativity

In the last few years two further experimental results confirmed the validity of the theory of General Relativity (GR theory).

4.2.1 Gravitational lenses

Renn, Sauer & Stachel (1997) published a historical reconstruction of some of Einstein's research notes dating back to 1912. These notes reveal that he explored the possibility of gravitational lensing 3 years before completing his general theory of relativity. On the basis of preliminary insights into this theory, Einstein had already derived the basic features of the lensing effect. When he finally published the very same results 24 years later, it was only in response to prodding by an amateur scientist.

Kochanek (2003) discussed "The whys and hows of finding 10,000 lenses", mentioning the first radio lens survey – the MIT - Green Bank survey (MG) – that found lenses by obtaining Very Large Array (VLA) snapshot images of flux-limited samples of 5 GHz radio sources. The Hubble Space Telescope (HST), and Chandra observations (e.g. Dai & Kochanek, 2005) showed without any doubt that the gravitational lensing is operating.

Gravitational lensing is widely and successfully used to study a range of astronomical phenomena, from individual objects, like galaxies and clusters, to the mass distribution on various scales, to the overall geometry of the Universe (Williams & Schechter, 1997). They describe and assess the use of gravitational lensing as "gold standards" in addressing one of the fundamental problems in astronomy, the determination of the absolute distance scale to extragalactic objects, namely the Hubble constant.

Several papers have been published about the strong gravitational lensing (e.g. Tyson, Kochanski & Dell'Antonio, 1998; Tyson, 2000 and references therein), and the weak gravitational lensing (Wittman et al., 2000). A review on "Gravitational Lenses" have been published by Blandford & Kochanek (2004). A book on "Gravitational Lensing: Strong, Weak and Micro" was published by Meylan et al. (2006). Winn, Rusin & Kochanek (2004) reported the most secure identification of a central image, based on radio observations of PMN J1632-0033.

Therefore, a further dowel supports the GR theory.

It is important to mention the paper *Resource Letter GL-1: Gravitational Lensing* by Treu, Marshall & Clowe (2012). This Resource Letter provides a guide to a selection of the literature on gravitational lensing and its applications. Journal articles, books, popular articles, and websites are cited for the following topics: foundations of gravitational lensing, foundations of cosmology, history of gravitational lensing, strong lensing, weak lensing, and microlensing.

Indeed, each Resource Letter focuses on a particular topic and intends to help teachers to improve course content in a specific field of physics or to introduce nonspecialists to this field.

4.2.2 Gravitational waves

The Universe that contains by definition all the matter or all the energy available showed one important event that was possible to be detected on the Earth. This event was a further direct experimental demonstration of the validity of the GR theory. Indeed, on September 14, 2015 at 09:50:45 UTC the two detectors of the Laser Interferometer Gravitational-Wave Observatory (LIGO) simultaneously observed a transient gravitational-wave signal. It matches the waveform predicted by GR theory for the inspiral and merger of a pair of black holes and the ringdown of the resulting single black hole. The signal was observed with a significance $\geq 5.1\sigma$ (Fig. 40). The source lies at a luminosity distance of 410^{+160}_{-180} Mpc corresponding to a redshift z = $0.090^{+0.03}_{-0.04}$. In the source frame, the initial black hole masses are 36^{+5}_{-4} $M_\odot$ and 29 ± 4 $M_\odot$, and the final black hole mass is 62 ± 4 $M_\odot$ with 3.0 ± 0.5 $M_\odot$ c^2 radiated in gravitational waves. All uncertainties define 90% credible intervals. These observations demonstrate the existence of binary stellar-mass black hole systems. This is the first direct detection of gravitational waves and the first observation of a binary black hole merger (Abbott et al., 2016a).

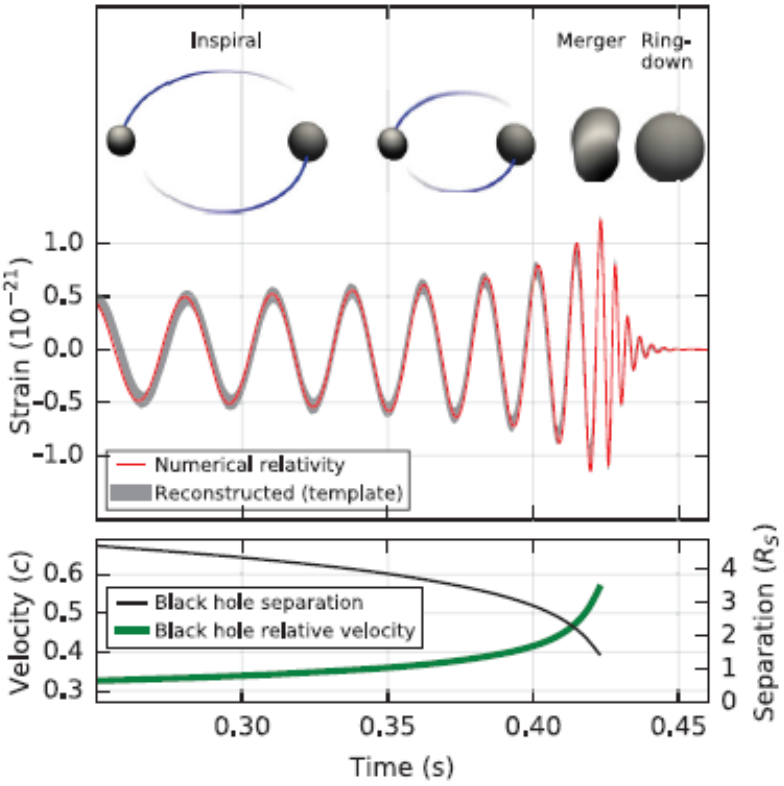

Figure 40: The GW150914 event. Top: estimated gravitational-wave strain amplitude. Bottom: the Keplerian effective black hole separation in units of Schwarzschild radii (adopted from Abbott et al., 2016a).

Abbott et al. (2016b) reported the second observation of a gravitational-wave signal produced by the coalescence of two stellar-mass black holes. The signal, GW151226, was observed by the twin detectors of the LIGO on December 26, 2015 at 03:38:53 UTC. The signal was detected at significance $\geq 5\sigma$. The inferred source-frame initial black hole masses are $14.2^{+8.3}_{-3.7}$ $M_\odot$ and 7.5 ± 2.3 $M_\odot$, and the final black hole mass is $20.8^{+6.1}_{-1.7}$ $M_\odot$. One finds that at least one of the component

black holes has spin greater than 0.2. This source is located at a luminosity distance of 440^{+180}_{-190} Mpc corresponding to a redshift z = $0.09^{+0.03}_{-0.04}$. All uncertainties define a 90% credible interval. This second gravitational-wave observation provides improved constraints on stellar populations and on deviations from the GR theory.

For these detections of gravitational waves – first predicted by Einstein 100 years ago – Rainer Weiss, Barry Barish & Kip Thorne have been awarded the 2017 Nobel prize in physics.

Abbott et al. (2016c) present a possible observing scenario for the Advanced LIGO (aLIGO) and Advanced Virgo gravitational-wave detectors over the next decade, with the intention of providing information to the astronomy community to facilitate planning for multimessenger astronomy with gravitational waves.

Gravitational waves provide a revolutionary tool to investigate yet unobserved astrophysical objects. Especially the first stars, which are believed to be more massive than present-day stars, might be indirectly observable via the merger of their compact remnants. An interesting paper by Hartwig et al. (2016) developed a self-consistent, cosmologically representative, semi-analytical model to simulate the formation of the first stars. They estimated the contribution of primordial stars to the merger rate density and to the detection rate of the aLIGO. Owing to their higher masses, the remnants of primordial stars produce strong GW signals, even if their contribution in number is relatively small. They found a probability of $\geq 1\%$ that the current detection GW150914 is of primordial origin. The higher masses of the first stars boost their GW signal, and therefore their detection rate. Up to five detections per year with aLIGO at final design sensitivity originate from Pop III BH-BH mergers. Approximately once per decade, we should detect a BH-BH merger that can unambiguously be identified as a Pop III remnant.

On 2017 August 17 the merger of two compact objects with masses consistent with two neutron stars was discovered through gravitational-wave (GW170817), gamma-ray (GRB 170817A), and optical (SSS17a/AT2017gfo) observations. The optical source was associated with the early-type galaxy NGC 4993 at a distance of just $\sim$ 40 Mpc, consistent with the gravitational-wave measurement, and the merger was localized to be at a projected distance of $\sim$ 2 kpc away from the galaxy's center (Abbott et al., 2017a,b).

Lipunov et al. (1995) predicted the NS-NS merger at a distance of $\leq$ 50 Mpc and the possibility of detecting GWs!

This prediction was born by the "Scenario Machine" that describes the evolution of gravimagnetic rotators (Lipunov, 1987; Lipunov, & Postnov, 1988), and commented by Giovannelli (2016).

On August 17, 2017 Multimessenger Astrophysics born! As pioneer of the Multifrequency Astrophysics, I am particularly happy!

Poggiani (2018) published an extensive review about the GW170817 event, in which she discussed also the related multimessenger observations.

The LIGO and Virgo interferometers have now confidently detected gravitational waves from a total of 10 stellar-mass binary black hole mergers and one merger of neutron stars, which are the dense, spherical remains of stellar explosions. Table 5 shows the eleven events (adapted from Abbott et al., 2019).

Figure 41 shows the Gravitational-Wave Transient Catalog-1 where the plots (frequency vs time) of the 11 events listed in Table 5 are reported together with the Einstein's theory predictions

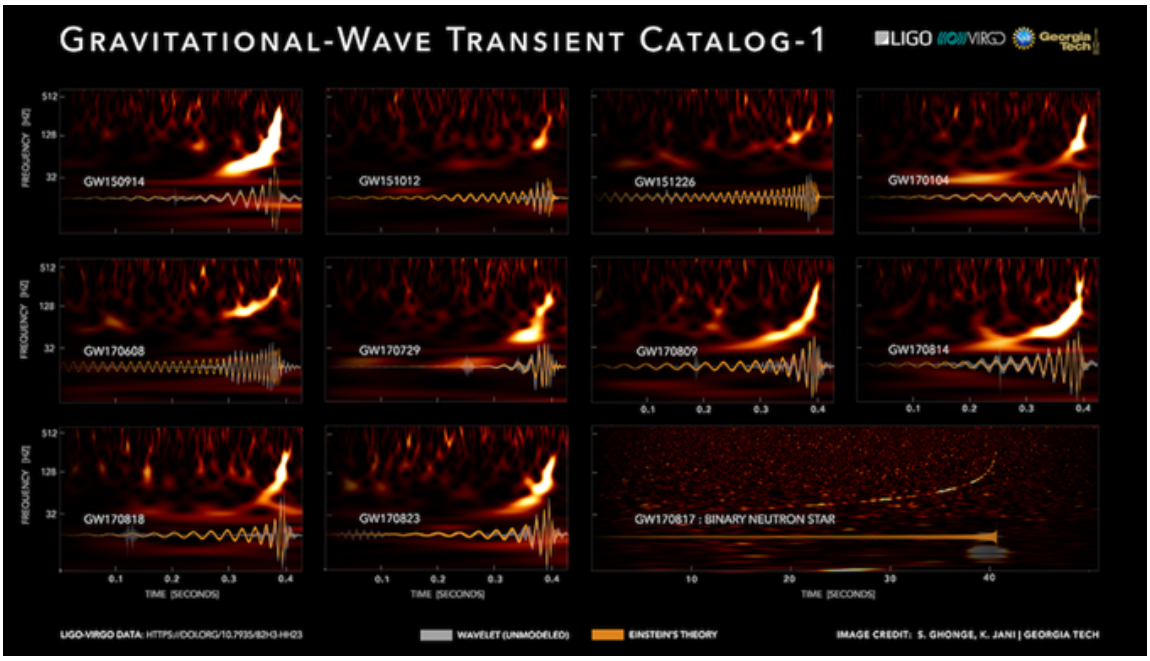

Figure 41: Gravitational Wave Transient Catalog-1. Credit: LIGO Scientific Collaboration and Virgo Collaboration/Georgia Tech/; Image Credit: S. Ghonge & K. Jani.

(Credit: LIGO Scientific Collaboration and Virgo Collaboration/Georgia Tech/S. Ghonge & K. Jani).

Figure 42 shows the localizations of the eleven gravitational-wave detections in the sky – listed in Table 5 (http://www.virgo-gw.eu/ (2018)).

The Advanced LIGO and Advanced Virgo detector network observed 90 binary-system mergers from 2015 to 2020. This is an updated version of the Gravitational-Wave Transient Catalog (https://www.ligo.org/detections/O3bca
talog.php).

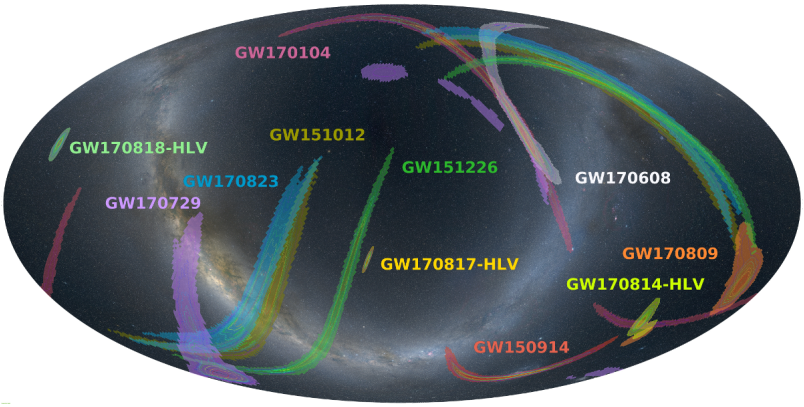

Figure 42: The localizations of the eleven gravitational-wave detections in the sky (http://www.virgo-gw.eu/ (2018)).

Barone et al. (1992) analyzed the class of CVs as sources of Gravitational Radiation, basing

Table 5: Selected source parameters of the 11 confident detections. The columns show source-frame component masses m_1 and m_2, the chirp mass M, final source-frame mass M_f, luminosity distance d_L, and redshift z (adapted from Abbott et al., 2019).

GW Event (name)	m_1 ($M_\odot$)	m_2 ($M_\odot$)	M ($M_\odot$)	M_f ($M_\odot$)	d_L (Mpc)	z (redshift)
GW 150914	$35.6^{+4.7}_{-3.1}$	$30.6^{+3.0}_{-4.4}$	$28.6^{+1.7}_{-1.5}$	$63.1^{+3.4}_{-3.0}$	440^{+150}_{-170}	$0.09^{+0.03}_{-0.03}$
GW 151012	$23.2^{+14.9}_{-5.5}$	$13.6^{+4.1}_{-4.8}$	$15.2^{+2.1}_{-1.2}$	$35.6^{+10.8}_{-3.8}$	1080^{+550}_{-490}	$0.21^{+0.09}_{-0.09}$
GW 151226	$13.7^{+8.8}_{-3.2}$	$7.7^{+2.2}_{-2.5}$	$8.9^{+0.3}_{-0.3}$	$20.5^{+6.4}_{-1.5}$	450^{+180}_{-190}	$0.09^{+0.04}_{-0.04}$
GW 170104	$30.8^{+7.3}_{-5.6}$	$20.0^{+4.9}_{-4.6}$	$21.4^{+2.2}_{-1.8}$	$48.9^{+5.1}_{-4.0}$	990^{+440}_{-430}	$0.20^{+0.08}_{-0.08}$
GW 170608	$11.0^{+5.5}_{-1.7}$	$7.6^{+1.4}_{-2.2}$	$7.9^{+0.2}_{-0.2}$	$17.8^{+3.4}_{-0.7}$	320^{+120}_{-110}	$0.07^{+0.02}_{-0.02}$
GW 170729	$50.2^{+16.2}_{-10.2}$	$34.0^{+9.1}_{-10.1}$	$35.4^{+6.5}_{-4.8}$	$79.5^{+14.7}_{-10.2}$	2840^{+1400}_{-1360}	$0.49^{+0.19}_{-0.21}$
GW 170809	$35.0^{+8.3}_{-5.9}$	$23.8^{+5.1}_{-5.2}$	$24.9^{+2.1}_{-2.7}$	$56.3^{+5.2}_{-3.8}$	1030^{+320}_{-390}	$0.20^{+0.05}_{-0.07}$
GW 170814	$30.6^{+5.6}_{-3.0}$	$25.2^{+2,8}_{-4,0}$	$24.1^{+1.4}_{-1.1}$	$53.2^{+3.2}_{-2.4}$	600^{+150}_{-220}	$0.12^{+0.03}_{-0.04}$
GW 170817	$1.46^{+0.12}_{-0.10}$	$1.27^{+0.09}_{-0.09}$	$1.186^{+0.001}_{-0.001}$	≤ 2.8	40^{+7}_{-15}	$0.01^{+0.00}_{-0.00}$
GW 170818	$35.4^{+7.5}_{-4.7}$	$26.7^{+4.3}_{-5.2}$	$26.5^{+2.1}_{-1.7}$	$59.4^{+4.9}_{-3.8}$	1060^{+420}_{-380}	$0.21^{+0.07}_{-0.07}$
GW 170823	$39.5^{+11.2}_{-6.7}$	$29.0^{+6.7}_{-7.8}$	$29.2^{+4.6}_{-3.6}$	$65.4^{+10.1}_{-7.4}$	1940^{+970}_{-900}	$0.35^{+0.15}_{-0.16}$

their analysis only on known objects at that time (168 CVs) taken from the Catalog of Ritter (1990).

From the analysis of GW emission from CVs, they derived that the emission frequencies are in the range 10^{-3} - 10^{-5} Hz and that the GW flux at Earth is in the range 10^{-10} - 10^{-13} erg s^{-1} cm^{-2} while the dimensionless amplitude is in the range 10^{-21} - 10^{-23}. These results constituted a solid basis for planning the construction of GW detectors (especially space-borne GW antennas). Moreover, these results provided the possibility of experimentally proving the effectiveness of the mechanism of Gravitational Radiation on CV evolution.

This important work was not sufficiently taken into account by the international community. However, now, after the detection of GWs coming from the fusion of black holes and neutron stars, the interest for that work has been rekindled in order to test the possibility of detecting GWs from CVs. Poggiani (2017b), and the references therein) discussed this possibility, reaching the conclusion that AM CVn systems and generally short-period systems are candidates for GW emission.

Amaro-Seoane et al. (2017) in response to the ESA call for L3 mission concepts, presented the Laser Interferometer Space Antenna (LISA) that since 2030 will allow to observe Gravitational Waves from cosmic sources, then to explore a Universe inaccessible otherwise, a Universe where

gravity takes on new and extreme manifestations. They concluded as follows: *The groundbreaking discovery of Gravitational Waves by ground-based laser interferometric detectors in 2015 has changed astronomy, by giving us access to the high-frequency regime of Gravitational Wave astronomy. By 2030 our understanding of the Universe will have been dramatically improved by new observations of cosmic sources through the detection of electromagnetic radiation and high-frequency Gravitational Waves. But in the low-frequency Gravitational Wave window, below one Hertz, we expect to observe the heaviest and most distant objects. Using our new sense to 'hear' the Universe with LISA, we will complement our astrophysical knowledge, providing access to a part of the Universe that will forever remain invisible with light. LISA will be the first ever mission to survey the entire Universe with Gravitational Waves. It will allow us to investigate the formation of binary systems in the Milky Way, detect the guaranteed signals from the verification binaries, study the history of the Universe out to redshifts beyond 20, when the Universe was less than 200 million years old, test gravity in the dynamical sector and strong-field regime with unprecedented precision, and probe the early Universe at TeV energy scales. LISA will play a unique and prominent role in the scientific landscape of the 2030s*.

4.3 The accelerating Universe

The discovery of the accelerating expansion of the Universe is a milestone for cosmology. A very interesting paper about this argument has been published in 2011 by the "Class for Physics of the Royal Swedish Academy of Sciences" as Scientific Background on the Nobel Prize in Physics 2011. In this paper a historical journey about the last century development of cosmology is brilliantly presented.

The discovery in 1998 that the universe is speeding up and not slowing down (Riess et al. 1998; Perlmutter et al. 1999) opened a question about the possibility of having different phases of acceleration and deceleration of the Universe along its life. Turner & Riess (2002) from observations of SN 1997ff at $z \sim 1.7$ favor the accelerating universe interpretation and provide some direct evidence that the universe was once decelerating. They show that the strength of this conclusion depends upon the nature of the dark energy causing the present acceleration. Only for a cosmological constant is the SNe evidence definitive. Using a new test which is independent of the contents of the universe, they show that the SN data favor recent acceleration ($z < 0.5$) and past deceleration ($z > 0.5$).

Nielsen, Guffanti & Sarkar (2016) found marginal evidence for cosmic acceleration from type Ia Supernovae. On the contrary, Haridasu et al. (2017) found that the SN data alone indicate an accelerating Universe at more than 4.56σ confidence level.

Considering that some divergent conclusions about cosmic acceleration were obtained using Type Ia supernovae (SNe Ia), with opposite assumptions on the intrinsic luminosity evolution, Tu, Hu & Wang (2019) use strong gravitational lensing systems to probe the cosmic acceleration. They found that the flat ΛCDM is strongly supported by the combination of the data sets from 152 strong gravitational lensing systems.

4.4 The Big Bang Nucleosynthesis theory has been proved

The Big Bang Nucleosynthesis (BBN) theory predits the presence of a fixed content of light

elements, the temperature of the Universe inversely proportional to the typical distance between galaxy clusters: T = T(0) (1+z), and the CMB radiation temperature of $\sim$ 2.7 K.

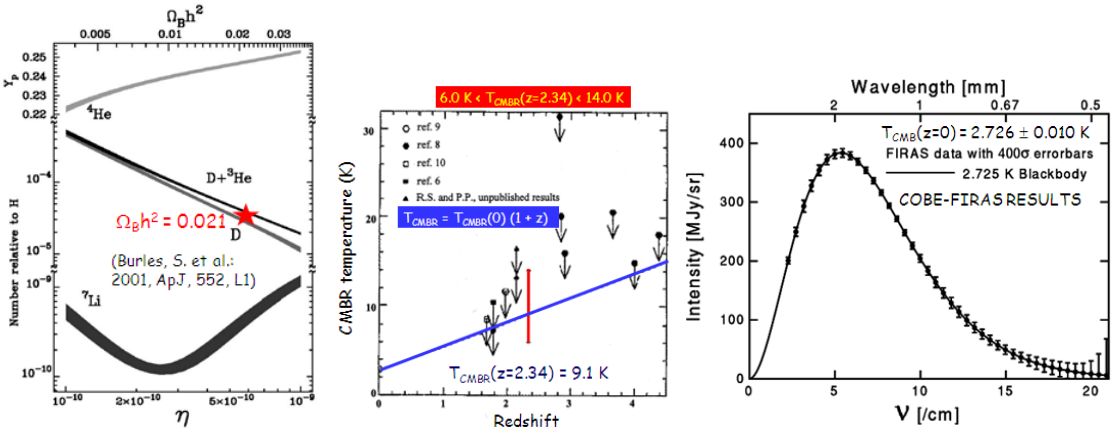

Figure 43: Three experimental results in favor of the BBN (see text for explanation).

In the last decade several experiments provided results confirming the validity of the BBN. In Fig. 43 one can see: i) (left panel): red star - the experimental confirmation of the content of the primordial light elements (de Bernardis et al., 2000) superimposed to the theoretical curves (Burles et al., 2001); ii) (middle panel): red line - the temperature of the Cosmic Microwave Background Radiation (T_{CMBR}) at redshift z = 2.34, ranging between 6 and 14 K (Srianand, Petitjean & Ledoux, 2000), in agreement with the theoretical temperature law T_{CMBR}= $T_{CMBR}(0)(1+z)$, which gives at z = 2.34 a temperature of 9 K; iii) (right panel): the CMB radiation temperature (2.726 ± 0.010 K) (Bartelmann, 2008, after Mather et al., 1990).

However, the Big Bang model can be tested further, thanks to the WMAP (Wilkinson Microwave Anisotropy Probe). Given a precise measurement of the abundance of ordinary matter, the predicted abundances of the other light elements becomes highly constrained. The WMAP satellite is able to directly measure the ordinary matter density and finds a value of 4.6% ($\pm$ 0.2%), indicated by the vertical red line in the Fig. 44 (https://map.gsfc.nasa.gov/universe/). This leads to predicted abundances shown by the circles in the graph, which are in good agreement with observed abundances. This is an important and detailed test of nucleosynthesis and is further evidence in support of the Big Bang theory.

4.5 Is the Universe Flat?

One of the most critical points about our Universe is the problem of its flatness. The present state of the cosmological tests is illustrated in Fig. 45.

The left panel of Fig. 45 shows the results obtained with the BOOMERanG (Balloon Observations Of Millimetric Extragalactic Radiation and Geomagnetics) experiment (de Bernardis et al., 2000). They are fully consistent with a spatially flat Universe. The right panel of Fig. 45 shows the combination of the likelihood contours obtained with three different observational approaches: i) type-Ia SNe (Tonry et al., 2003; Riess et al. 2004); ii) CMB (Spergel et al. 2003; Bennett et al. 2013); iii) galaxy clusters (Schuecker et al. 2003; Schuecker, 2005). One can see that the cosmic matter density is close to Ω_m = 0.3, and that the normalized cosmological constant is around Ω_Λ =

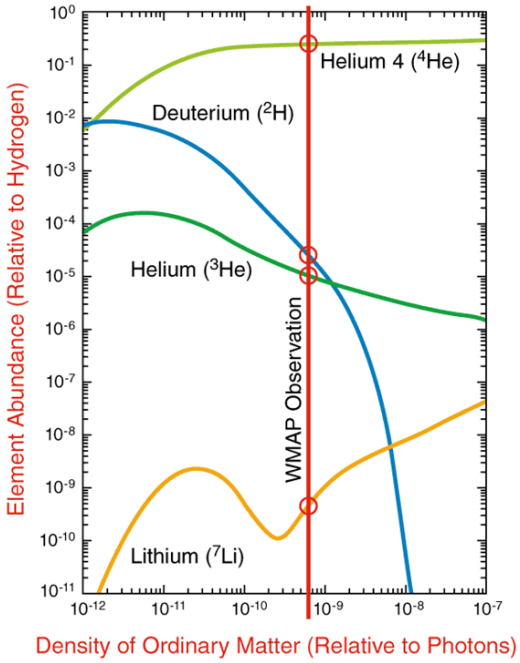

Figure 44: The experimental confirmation of the content of the primordial light elements from WMAP (https://map.gsfc.nasa.gov/universe/).

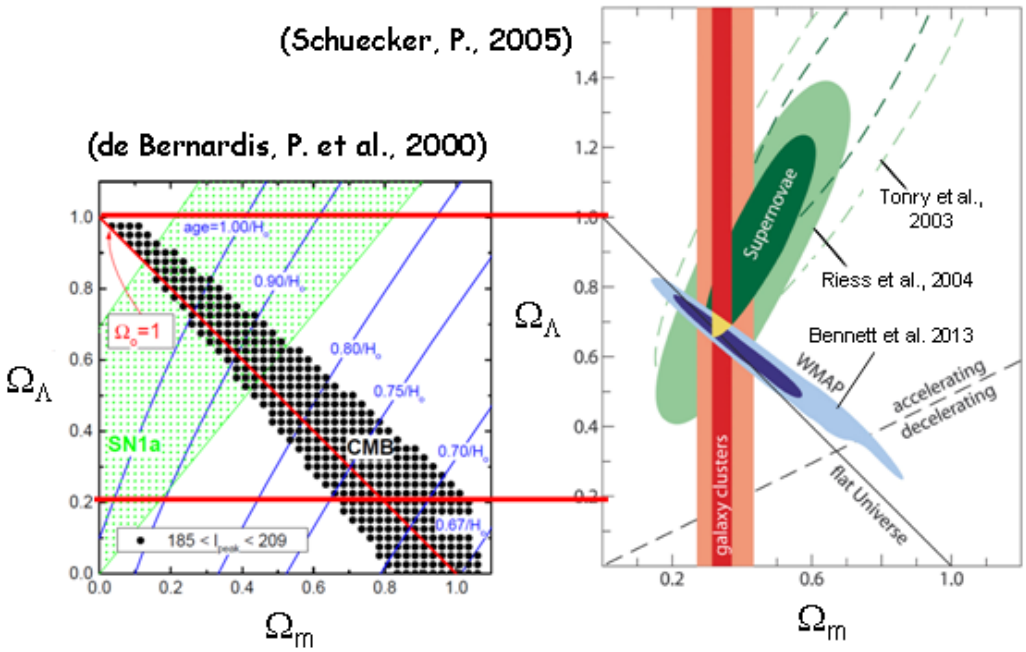

Figure 45: Constraints of cosmological parameters (after de Bernardis et al., 2000; Schuecker, 2005, Bennett et al., 2013).

0.7. This sums up to unit total cosmic energy density and suggests a spatially flat universe. However, the density of cosmic matter growths with redshift like $(1 + z)^3$ whereas the density ρ_Λ related

to the cosmological constant Λ is independent of z. The final results from WMAP (Bennett et al., 2013) show a little misalignment with the line of "flat Universe". Thus it is necessary to be careful in the conclusions.

4.6 Hubble Constant

The Hubble constant (H_0) is one of the most important numbers in cosmology because it is needed to estimate the size and age of the universe. The important problem of determination of H_0 value is one of the most exciting. Indeed, in the literature it is possible to find many determinations coming from different experiments using different methods. However, it is very complicated to obtain a true value for H_0. It is necessary to have two measurements: i) spectroscopic observations that reveal the galaxy's redshift, indicating its radial velocity; ii) the galaxy's precise distance from Earth (and this is the most difficult value to determine).

A large summary about the methods used for H_0 determination, and its derived values can be found in the Proceedings of the Fall 2004 Astronomy 233 Symposium on "*Measurements of the Hubble constant*" (Damon et al., 2004). In this book, Teymourian (2004), after a comparison of many constraints on the Hubble constant determinations, reports a value $H_0 = 68 \pm 6$ km s^{-1} Mpc^{-1}.

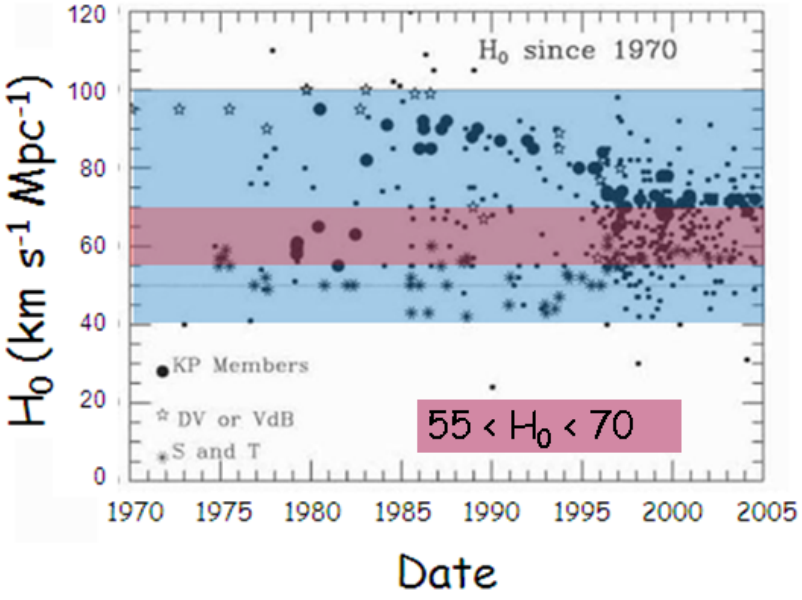

Figure 46: The Hubble constant determinations since 1970. The light-blue rectangle limits all the H_0 determinations. The light-red rectangle shows the narrow limits to to which the values of H_0 are converging (Giovannelli & Sabau-Graziati (2016c) after John Huchra, 2008).

Freedman & Madore (2010) published a review about *The Hubble Constant* in which they discuss the considerable progress made in determining the Hubble constant over the past two decades. They discuss the cosmological context and importance of an accurate measurement of the Hubble constant, focusing on six high-precision distance-determination methods: Cepheids, tip of the red giant branch, maser galaxies, surface brightness fluctuations, the Tully-Fisher relation, and Type

Ia supernovae. Their best current estimate of the Hubble constant is H_0 = 73 $\pm$2 (random) $\pm$4 (systematic) km s^{-1} Mpc^{-1}.

A discussion about the Hubble constant has been published by Giovannelli & Sabau-Graziati (2014), where it is possible to find also a large number of references, reporting the many controversial evaluations of H_0.

Figure 46 shows the determinations of H_0 since 1970 (adapted from John Huchra, 2008). Practically all the determinations lie in the range 40-100 km s^{-1} Mpc^{-1} (marked with light-blue rectangle), and most of them are converging in the range 55-70 km s^{-1} Mpc^{-1} (marked with light-red rectangle).

John Huchra (2010) listed the last updated collection of data on October 7, 2010, just one day before his sudden death (https://www.cfa.harvard.edu/∼dfab
ricant/huchra/hubble.plot.dat). (*)

However, Riess et al. (2011) with the HST determined a value of H_0 = 73.8 $\pm$ 2.4 km s^{-1} Mpc^{-1}. This value agrees with the WMAP results: H_0 = 71.0 $\pm$ 2.5 km s^{-1} Mpc^{-1} (Komatsu et al., 2011). Bennett et al. (2014) discussed the progress occurred in recent years for determining the Hubble constant: results coming from the cosmic distance ladder measurements at low redshift and CMB measurements at high redshift.

(*) Professor John Huchra, died unexpectedly October 8th, 2010.

The CMB is used to predict the current expansion rate of the universe by best-fitting cosmological model. At low redshift baryon acoustic oscillation (BAO) measurements have been used – although they cannot independently determine H_0 – for constraining possible solutions and checks on cosmic consistency. Comparing these measurements they found H_0 = 69.6 $\pm$ 0.7 km s^{-1} Mpc^{-1}.
Does this determination, finally, close the history about the search of the "true" value of H_0?

However, an important pioneer of science paper (Schutz, 1986) reported how gravitational wave observations can be used to determine the Hubble constant. The nearly monochromatic gravitational waves emitted by the decaying orbit of an ultra-compact, two-neutron-star binary system just before the stars coalesce are very likely to be detected by the kilometer-sized interferometric gravitational wave antennas – at that time being designed. The signal is easily identified and contains enough information to determine the absolute distance to the binary, independently of any assumptions about the masses of the stars. Ten events out to 100 Mpc may suffice to measure the Hubble constant to 3% accuracy.

Fishbach et al. (2019) performed a statistical standard siren analysis of GW170817. Their analysis did not utilize knowledge of NGC 4993 as the unique host galaxy of the optical counterpart to GW170817. Instead, they consider each galaxy within the GW170817 localization region as a potential host; combining the redshifts from all of the galaxies with the distance estimate from GW170817 provides an estimate of the Hubble constant as $H_0 = 77^{+37}_{-18}$ km s^{-1} Mpc^{-1}.

Soares-Santos et al. (2019) presented a multimessenger measurement of the Hubble constant using the binary-black-hole merger GW170814 as a standard siren, combined with a photometric redshift catalog from the Dark Energy Survey (DES). Their analysis results in $H_0 = 75^{+40}_{-32}$ km s^{-1} Mpc^{-1}, which is consistent with both SN Ia and CMB measurements of the Hubble constant.

Independent estimation of the Hubble constant from the luminosity distance of GW signal (GW 170817) and the event association with NGC 4993 (Abbott et al., 2017c) gives a value $H_0 = 70.0^{+12.0}_{-8.0}$ km s^{-1} Mpc^{-1}.

However, due to large errors, these values of Hubble constant do not add any significative information, but being obtained with independent methods provide a good support for the value of $H_0 = 69.6 \pm 0.7$ km s^{-1} Mpc^{-1}, determined by Bennett et al. (2014).

4.7 Reionization Epoch

Ground-based observations of the CMB on subdegree angular scales suggest that the gas content of the universe was mostly neutral since recombination at z$\sim$ 1000 until about z$\sim$ 100 (Gnedin, 2000) and the references therein) because earlier reionization would have brought the last scattering surface to lower redshift, smoothing the intrinsic CMB anisotropy. At the same time, we know that the universe is highly ionized, since z$\approx$ 5, from observations of the spectra of quasars with the highest redshifts (e.g. Giallongo et al. 1994). This change of the ionization state of the universe from neutral to highly ionized is called "*reionization*". How large is the redshift to which the reionization started and stopped is object of strong debate.

The formation of the first stars and quasars marks the transformation of the universe from its smooth initial state to its clumpy current state. In current cosmological models, the first sources of light began to form at a redshift z $\sim$ 30 and reionized most of the hydrogen in the universe by z $\sim$ 7 (see review by Loeb & Barkana, 2001).

Recently Matsuoka et al. (2016) reported the discovery of 15 QSOs and bright galaxies at $5.7 < z < 6.9$ from the Subaru High-z Exploration of Low-Luminosity Quasars (SHELLQs) project.

The argument for an extended period of reionization is now proved by measurements. Indeed, the WMAP has detected the correlation between temperature and polarization on large angular scales (Kogut et al., 2003) that has an amplitude proportional to the total optical depth of CMB photons to Thomson scattering, τ (Kaplinghat et al., 2003; Sunyaev & Zeldovich, 1980; Zaldarriaga, Spergel & Seljak, 1997).

Modeling reionization with a single sharp transition at z_{ri}, a multi–parameter fit to the WMAP data gives $z_{ri} = 17 \pm 5$ (Spergel et al., 2003). On the other hand, the evolution of quasar spectra from z$\approx$ 7 and z$\approx$ 6 shows a rapid decrease in the amount of neutral hydrogen, indicating the end of reionization (Fan et al., 2003). A simple interpretation to explain these two very different datasets is that reionization started early, $z_{ri} \sim 20$, but did not conclude until much later (z$\sim$ 6) (Knox, 2003).

This was also confirmed by the results from Subaru Deep Field (SDF) (Kashikawa et al., 2006; Kashikawa, 2007): the reionization of the universe has not been completed at z = 6.5. Also Ota et al. (2008) in performing narrowband imaging of the SDF found two Lyα emitters (LAEs) at z = 7. This established a new redshift record, showing that galaxy formation was in progress just 750 Myr after the Big Bang. They found that the attenuation of the Lyα photons from LAEs by the neutral hydrogen possibly left at the last stage of cosmic reionization at $z \sim 6-7$.

Ouchi et al. (2009a) suggested an existence of a well-developed ionized bubble at z = 7. Ouchi et al. (2009b) reported the discovery of a giant LAE with a Spitzer/Infrared Array Camera (IRAC) counterpart near the reionization epoch at z = 6.595. Although the nature of this object is not yet clearly understood, this could be an important object for studying cooling clouds accreting

onto a massive halo, or forming-massive galaxies with significant outflows contributing to cosmic reionization and metal enrichment of intergalactic medium.

Ouchi et al. (2010) presented the Lyα luminosity function (LF), clustering measurements, and Lyα line profiles based on the largest sample to date of 207 LAEs at z = 6.6. The combination of various reionization models and their observational results about the LF, clustering, and line profile indicates that there would exist a small decrease of the intergalactic medium's (IGM's) Lyα transmission owing to reionization, but that the hydrogen IGM is not highly neutral at z = 6.6. Their neutral-hydrogen fraction constraint implies that the major reionization process took place at $z \geq 7$.

Jiang et al. (2011) presented Keck spectroscopic observations of $z > 6$ Lyman-break galaxy (LBG) candidates in the Subaru Deep Field (SDF). Their Lyα LF is also generally in agreement with the results of LAEs surveys at $z \sim 5.7$ and 6.6. This study shows that deep spectroscopic observations of LBGs can provide unique constraints on both the UV and Lyα LFs at $z > 6$.

Ono et al. (2012) presented the results of their ultra-deep Keck/DEIMOS spectroscopy of z-dropout galaxies in the SDF and Great Observatories Origins Deep Survey's northern field. The fractions of Lyα-emitting galaxies drop from $z \sim 6$ to 7 and the amplitude of the drop is larger for faint galaxies than for bright galaxies. These two pieces of evidence would indicate that the neutral hydrogen fraction of the IGM increases from $z \sim 6$ to 7 and that the reionization proceeds from high- to low-density environments, as suggested by an inside-out reionization model.

The WMAP detection of reionization (Kogut et al. 2003) implies the existence of an early generation of stars able to reionize the universe at $z \sim 20$. Panagia et al. (2005) in deep HST/VLT/Spitzer images found that the source UDF 033238.7-274839.8 – a post–starburst galaxy with a mass $\sim 6 \times 10^{11}$ $M_{\odot}$ placed at $z \geq 6.5$ – may be capable of reionizing its surrounding region of the universe, starting the process at a redshift as high as $z = 15 \pm 5$.

The question about the end of the reionization is strongly disputed. However, in our opinion probably it is possible to put a reasonable limit to the epoch of the reionization end ($z \sim 6$), looking at the paper by Toshikawa et al. (2012). They reported the discovery of a protocluster at $z \sim 6$ containing at least eight cluster member galaxies with spectroscopic confirmations in the wide-field image of the SDF. They found no significant difference in the observed properties, such as Lyα luminosities and UV continuum magnitudes, between the eight protocluster members and the seven non-members. The velocity dispersion of the eight protocluster members is 647 ± 124 km s^{-1}, which is about three times higher than that predicted by the standard cold dark matter model. This discrepancy could be attributed to the distinguishing three-dimensional distribution of the eight protocluster members. They discussed two possible explanations for this discrepancy: either the protocluster is already mature, with old galaxies at the center, or it is still immature and composed of three subgroups merging to become a larger cluster. In either case, this concentration of z = 6.01 galaxies in the SDF may be one of the first sites of formation of a galaxy cluster in the universe.

Figure 47 shows schematically the updated experimental situation about cosmic sources (galaxies, GRBs, QSOs, SNe) detected at high redshifts. The light–red rectangle marks the possible range of z during which the reionization occurred.

However, although there is rather good agreement about the epoch of reionization, how really reionization occurs is still object of debate. Indeed, Dopita et al. (2011), considering that observa-

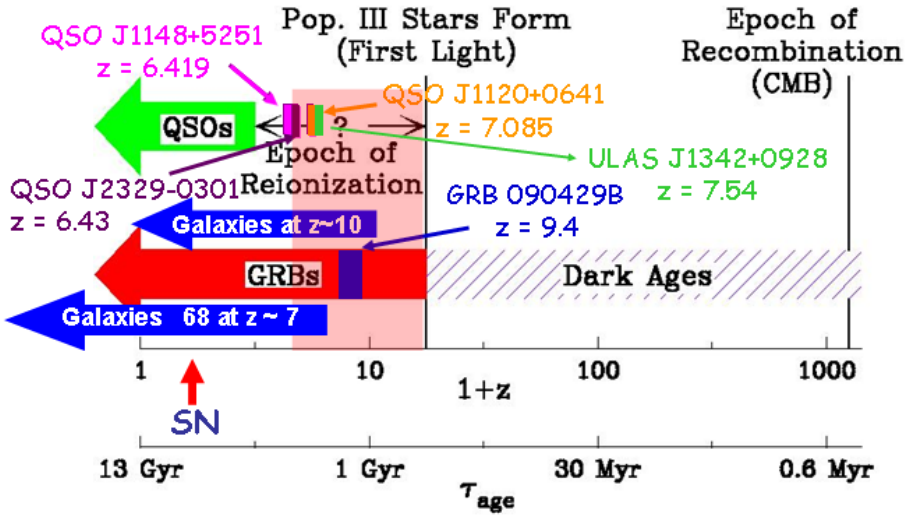

Figure 47: A sketch of reionization epoch (after Xiangping Wu's Talk at the Summer School on "Cosmic Reionization" at the KIAA-PKU , Beijing, China, July 1-11, 2008).

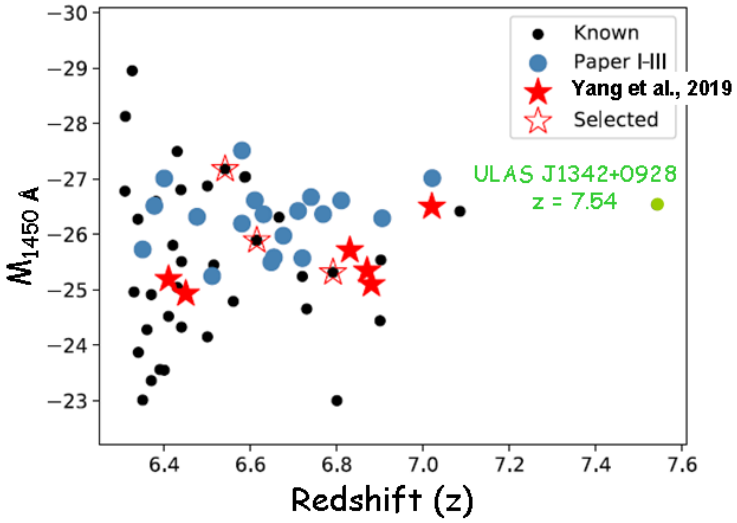

Figure 48: Redshift and M_{1450} distribution of quasars at $z \gtrsim 6.3$ (adapted from Yang et al., 2019). The black filled circles are the previously known quasars. The blue filled circles denote quasars from surveys in the northern sky (Wang et al. 2017, 2018, 2019a). The red filled stars represent the six new quasars from Yang et al (2019) survey and the red open stars are the three known quasars in the Dark Energy Survey (DES) area that meet their selection criteria. The green dot represents the z = 7.54 quasar ULAS J1342+0928 (Bañados et al., 2019).

tions show that the measured rates of star formation in the early universe are insufficient to produce reionization, suggest the presence of another source of ionizing photons. This source could be the fast accretion shocks formed around the cores of the most massive haloes.

An interesting review about *The epoch of reionization* was published by Zaroubi (2013). Recently *An Introductory Review on Cosmic Reionization* have been published by Wise (2019).

Recently, Yang et al. (2019) announced the discovery of six new $z \geq 6.5$ quasars. They plotted the positions of these new quasars in a diagram magnitude at 1450 Å versus redshift where also the known quasars at $z \geq 6.3$ have been reported in Fig. 48. The meaning of the symbols are reported in the caption of Fig. 48. Note that the z = 7.54 quasar ULAS J1342+0928, hosted by a galaxy merger is also reported (green dot) (Bañados et al., 2019).

A recent paper by Yan et al. (2023) by using data coming from JWST suggests the possibility of having detected objects at $z \approx$ 11-20 in the supercluster SMACS 0723-73. They very probably are galaxies.

These works open a glimmer of light on the possibility of revealing in the future, with the advent of JWST, the presence of quasars immediately after the formation of the first Pop. III stars at $z \approx 25$, as well as the possibility of detecting GRBs up to that redshift (Lamb & Reichart, 2000; Ciardi & Loeb, 2000; Bromm & Loeb, 2002). Indeed, the detection of the GRB 090429B at $z \simeq 9.4$ (Cucchiara et al., 2011) is a good omen to think that future experiments can reveal GRBs up to the fateful threshold of $z \approx 25$.

4.8 Star Formation

In his splendid review, Robert C. Kennicutt, Jr. (1998) discussed the observations of star formation rates (SFRs) in galaxies that provide vital clues to the physical nature of the Hubble sequence and showing that these observations are key probes of the evolutionary histories of galaxies.

About the evolutionary history of galaxies, interesting results were discussed in the review paper "*Star-Formation Histories, Abundances, and Kinematics of Dwarf Galaxies in the Local Group*" by Tolstoy, Hill & Tosi (2009). They discussed the results of quantitative studies in nearby dwarf galaxies, since within the Local Universe, galaxies can be studied in great detail star by star. The color-magnitude diagram synthesis method is well established as the most accurate way to determine star-formation histories of galaxies back to the earliest times. These studies have shown how the properties of stellar populations can vary spatially and temporally. This leads to important constraints to theories of galaxy formation and evolution. The continuity of structural properties from dwarf galaxies to larger spheroidal and late-type systems is most likely dominated by physical processes that scale with mass, for example, the efficiency with which gas and/or metals can be lost from a system during its evolution through supernova winds and/or interactions.

Zinnecker & Yorke (2007) discussed in their review a basic description of the collapse of a massive molecular core and a critical discussion of the three competing concepts of massive star formation:

- monolithic collapse in isolated cores;
- competitive accretion in a protocluster environment;
- stellar collisions and mergers in very dense systems.

They concluded that high-mass star formation is not merely a scaled-up version of low-mass star formation with higher accretion rates, but partly a mechanism of its own, primarily owing to the role of stellar mass and radiation pressure in controlling the dynamics.

Kennicutt, Jr & Evans II (2012) reviewed the progress over the previous decade in observations of large-scale star formation, with a focus on the interface between extragalactic and galactic studies. Methods of measuring gas contents and star-formation rates have been discussed, and updated prescriptions for calculating star-formation rates were provided. They reviewed relations between star formation and gas on scales ranging from entire galaxies to individual molecular clouds.

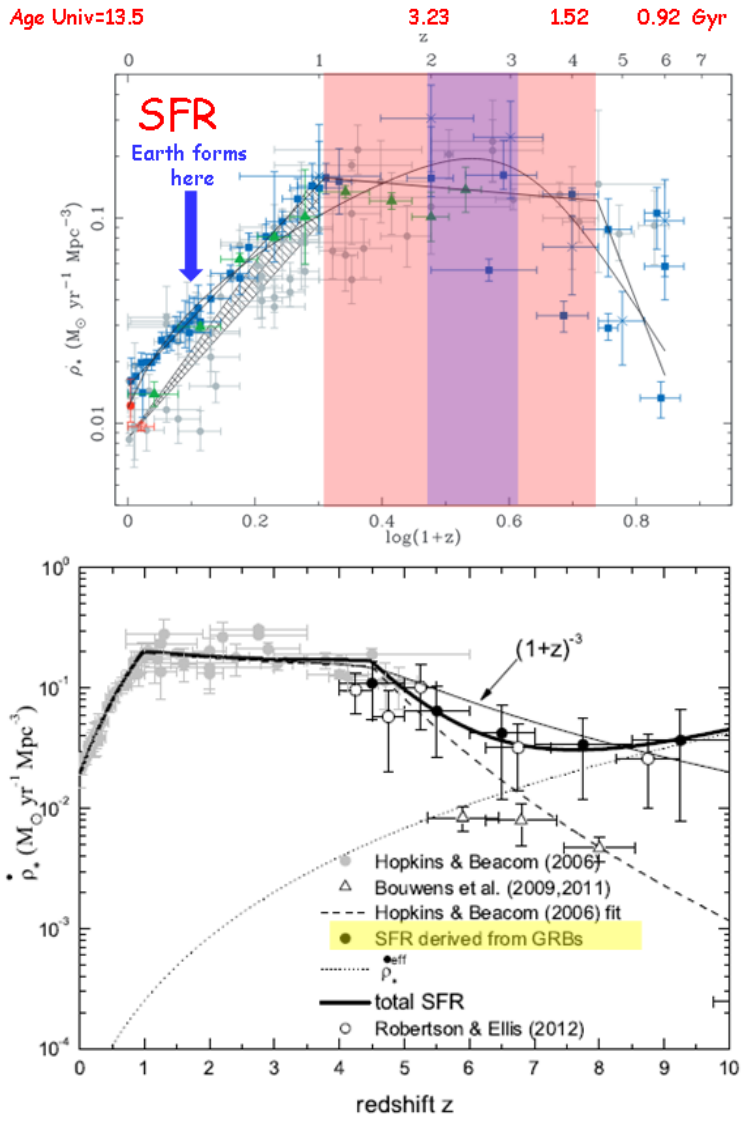

Figure 49: Upper panel: Evolution of SFR density with redshift (after Madau & Dickinson, 2014). Lower panel: Evolution of SFR density with redshift; black dots for $z \gtrsim 4.5$ mark the values of SFR density derived from GRBs (Wang, Dai & Liang, 2015).

The key dynamical processes involved in star formation – turbulence, magnetic fields, and self-gravity – are highly nonlinear and multidimensional. Therefore, it is extremely difficult a

complete quantitative description of the physics involved in the process of star formation. McKee & Ostriker (2007) attempted to review the theory of star formation. For this reason they divided star formation into large-scale and small-scale regimes and reviewed each in turn. Large scales range from galaxies to giant molecular clouds (GMCs) and their substructures. Important problems include how GMCs form and evolve, what determines the star formation rate (SFR), and what determines the initial mass function (IMF) have been discussed. Small scales range from dense cores to the protostellar systems they beget. They discussed formation of both low– and high–mass stars, including ongoing accretion. The development of winds and outflows is increasingly well understood, as are the mechanisms governing angular momentum transport in disks. However, they concluded that a comprehensive theory of star formation will be tested by the next generation of telescopes.

Fumagalli et al. (2012) investigated the evolution of the H_α equivalent width, EW(H_α), with redshift and its dependence on stellar mass, using the first data from the 3D-HST survey, a large spectroscopic Treasury program with the HST-WFC3. Combining these data with those from ground-based telescopes, they found that at all masses the characteristic EW(H_α) is decreasing towards the present epoch, and that at each redshift the EW(H_α) is lower for high-mass galaxies.

The cosmic history of star formation, heavy element production, and reionization of the Universe from the cosmic "dark ages" to the present epoch has been discussed in the review paper by Madau & Dickinson (2014). A consistent picture is emerging, whereby the star-formation rate density peaked approximately 3.5 Gyr after the Big Bang, at $z \approx 1.9$, and declined exponentially at later times, with an e-folding timescale of 3.9 Gyr. Half of the stellar mass observed today was formed before a redshift z = 1.3. About 25% formed before the peak of the cosmic star-formation rate density, and another 25% formed after z = 0.7. Less than $\sim 1\%$ of today's stars formed during the epoch of reionization.

However, these results were already largely discussed and presented by Hopkins & Beacom (2006), and later by Madau & Dickinson (2014) and summarized in the Fig. 49 (upper panel). The light–red rectangle marks the range of redshift where the star formation density had the maximum ($1 \leq z \leq 4.5$) whose peak is between z = 2 and z = 3 and marked with the light violet rectangle. This will be better understood when the supernova rate density evolution, the ranges of stellar masses leading to core-collapse and type Ia supernovae, and the antineutrino and neutrino backgrounds from core-collapse supernovae will be known thanks to the next generation experiments both ground– and space–based. Figure 49 (lower panel) clearly show the values of SFR (black dots) derived from GRBs by Wang, Dai, & Liang (2015) at redshifts $z \geq 4.5$.

A recent book about "*Star Formation in Galaxy Evolution: Connecting Numerical Models to Reality*" (Gnedin et al., 2015) reports an inventory of the physical processes related to the star formation involved at different scales and also to provide an overview of the major computational techniques used to solve the equations governing self-gravitating fluids, essential to galactic modeling. Together this provides a unique framework essential to developing and improving the simulation techniques used to understand the formation and evolution of galaxies.

4.9 Background Radiation in the Universe

Tiny inhomogeneities in the early Universe left their imprint on the microwave background in the form of small anisotropies in its temperature. These anisotropies contain information about

basic cosmological parameters, particularly the total energy density and curvature of the universe.

On April 23, 1992, the COBE team announced the historical discovery of the anisotropies of cosmic microwave background radiation with characteristic anisotropy $\Delta T/T \approx 10^{-5}$ or $\Delta T \sim 30$ μK on angular scales larger than $\sim 7^{\circ}$ at the annual meeting of American Physical Society in Washington, D.C. (Smoot et al., 1992).

Observations of the cosmic microwave background temperature anisotropies have revolutionized and continue to revolutionize our understanding of the universe. The observation of the CMB anisotropies angular power spectrum with its plateau, acoustic peaks, and high frequency damping tail have established a standard cosmological model consisting of a flat – critical density – geometry, with contents being mainly dark energy and dark matter and a small amount of ordinary matter. In this successful model the dark and ordinary matter formed its structure through gravitational instability acting on the quantum fluctuations generated during the very early inflationary epoch. Current and future observations will test this model and determine its key cosmological parameters with spectacular precision and confidence (see the Nobel Lecture of George F. Smoot (2007) for an exhaustive review about the Cosmic Background Radiation Anisotropies).

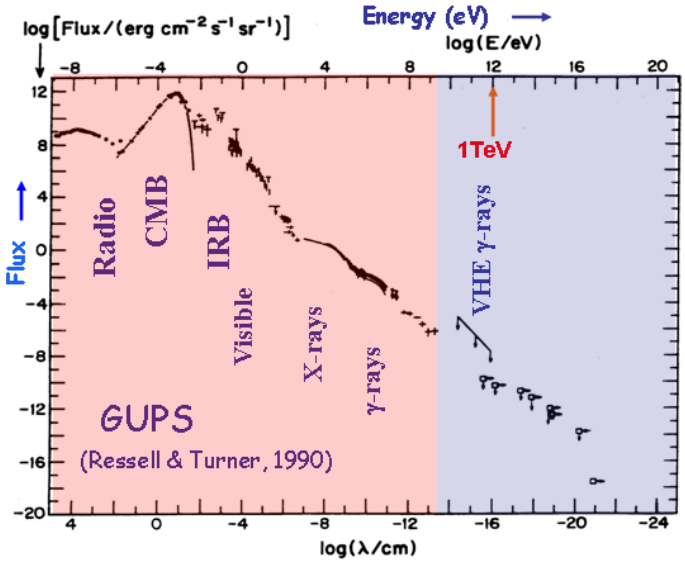

Figure 50: The Grand Unified Photon Spectrum of the Diffuse Extragalactic Background Radiation (after Ressell & Turner, 1990).

But the cosmic background radiation, although is peaked in the microwave region, permeates through the whole electromagnetic spectrum and is known as the Diffuse Extragalactic Background RAdiation (DEBRA). It is possible to consider the DEBRA as a radiation produced by a cosmic source: the whole Universe. Such a background radiation from radio to HE γ-ray energy bands has been deeply discussed by Ressell & Turner (1990), and in GSG2004 and the references therein. The analysis of the different components of DEBRA leads to the Grand Unified Photon Spectrum (GUPS), covering 29 orders of magnitude of the electromagnetic spectrum, from 10^{-9} to 10^{20} eV, as shown in Fig. 50 (after Ressell & Turner, 1990). The light–red and the light–indico rectangles indicate the domains with energies less or greater than ≈ 10 GeV, respectively. The domain at higher energies is now explored by numerous experiments space–based, like Fermi LAT obser-

vatory (up to 300 GeV) and ground–based, like Whipple, Veritas, HESS, Magic, and the coming CTA (Cherenkov Telescopes Array). All these experiments will provide to fill the zone of the GUPS diagram prepared by Ressell & Turner (1990) where only upper limits were reported.

Henry (1999, 2002) thoroughly discussed the experimental situation of the cosmic background till 2000.

4.10 Extragalactic Background Light

The intergalactic space is filled with the light produced by all the stars and accreting compact objects that populated the observable Universe throughout the whole cosmic history. This relic cosmic background from IR to UV is called the diffuse Extragalactic Background Light (EBL), long before known as DEBRA (Ressel & Turner, 1990).

Direct measurements of the EBL are difficult due to bright local foregrounds. A powerful approach for probing these diffuse radiation fields in the UV to far-IR bands is through γ–γ absorption of high-energy photons. Actually pair production (e^+ e^-) against EBL photons with wavelengths from ultraviolet to infrared is effective at attenuating γ–rays with energy above $\sim$ 10 GeV. This process introduces an attenuation in the spectra of γ–ray sources above a critical energy (e.g. Costamante, 2012; Buson, 2014).

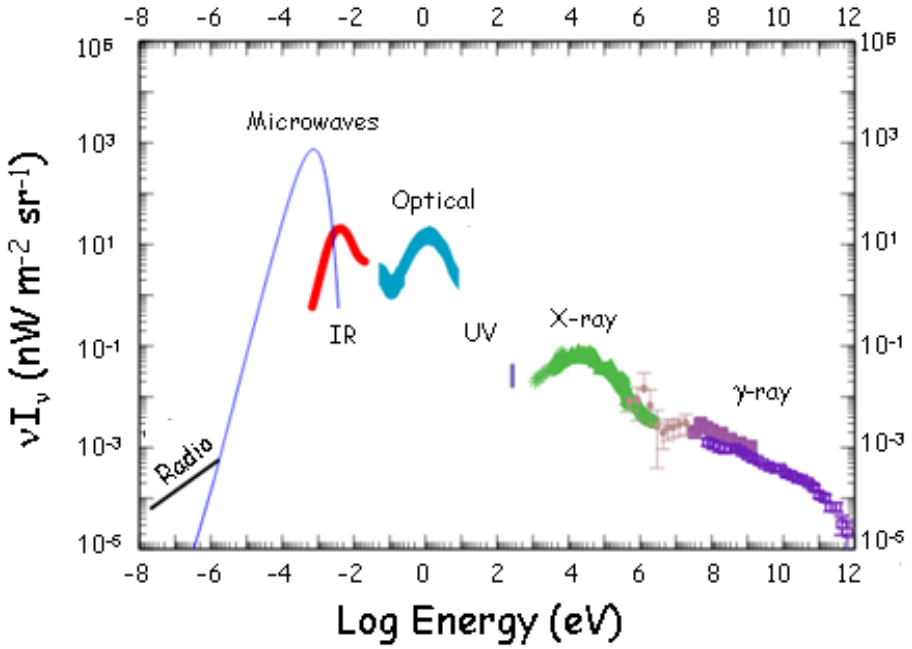

Figure 51: Intensity of the extragalactic background (νI_ν in units of nW m^{-2} sr^{-1}) as a function of the energy (adopted from Giovannelli & Sabau-Graziati, 2019, after Cooray, 2016).

The last decade has been foreboding of a full coverage of the HE-VHE γ-ray energy band, thanks to the many ground– and space–based high sensitivity experiments. Thus it has been possible to collect a large amount of data from many extragalactic emitters at high redshift (e.g. Costamante, 2012). Thanks to measurements of the quasar 3C 279 ($z \simeq 0.54$) obtained with the MAGIC experiment (Albert et al., 2008), and with the many sources at high redshift, including Gamma

Ray Bursts (GRBs) measured with the FERMI observatory (Abdo et al., 2010), it has been demonstrated that the Universe is more transparent to γ–rays than before believed (Coppi & Aharonian, 1997).

Cooray (2016) reviews the Extragalactic Background Light Measurements and Applications. This review covers the measurements related to the extragalactic background light intensity from γ-rays to radio in the electromagnetic spectrum over 20 decades in wavelength. Figure 51 shows such EBL measurements that updated those reported by Ressel & Turner (1990). It is important to remark that the numerous measurements in the range of the VHE γ-rays (Log E $\approx 9-13$ eV) have filled the zone where no measurements or only upper limits were available in the 1990-ies.

The CMB remains the best measured spectrum with an accuracy better than 1%. Durrer (2015) in her interesting review describes the discovery of the cosmic microwave background radiation in 1965 and its impact on cosmology in the 50 years that followed.

Henry et al. (2015) discussed the diffuse cosmic background radiation in the Galaxy Evolution Explorer far-ultraviolet (FUV, 1300-1700 Å. They deduced that the UV diffuse cosmic background radiation originates only partially in the dust-scattered radiation of FUV-emitting stars: the source of a substantial fraction of the FUV background radiation remains a mystery. They also discussed about our limited knowledge of the cosmic diffuse background at ultraviolet wavelengths shortward of Lyα - it could be that a "second component" of the diffuse FUV background persists shortward of the Lyman limit and is the cause of the reionization of the universe.

4.11 Unified Model for Compact Sources

The argument of the possibility of describing all the collapsed objects with a unique scheme have been discussed since long time by many authors. In their review paper, Begelman, Blandford & Rees (1984) discussed the theory of extragalactic radio sources and in particular the unified model of active galactic nuclei (AGNs).

From the evidence that the shapes of SEDs (Spectral Energy Distributions) of different kind of AGNs (Cen A, NGC 4151, and 3C 273) are practically the same (e.g. Ramaty & Lingenfelter, 1982), Giovannelli & Polcaro (1986) (GP86), by using experimental data coming from the EINSTEIN observatory, constructed the maximum luminosity diagram for extragalactic objects, independent of the current classification of those objects. Indeed, those extragalactic objects have the same engine producing energy (supermassive black hole with accretion disk and jet) and they are classified as blazars, or radio-loud QSOs, or radio galaxies depending on the angle between the line of sight and the jet axis. The attenuation in the emission of a cosmic source containing a black hole in function of such an angle and the beam Lorentz's factor of the particles have been calculated by Bednarek et al. (1990), as shown in Fig. 52.

The emission of the extragalactic X-ray sources can be expressed as $L_{TOT} = L_{NUC} + L_{HG}$, where, L_{NUC} is the nuclear luminosity and L_{HG} is the host galaxy luminosity, formed by the integrated emission of its discrete sources. Such components can be derived by using the GP86 diagram. In the long review paper by Giovannelli & Sabau-Graziati (2004: GSG2004) there is a discussion about the GP86 diagram.

GP86 found a general relationship between log z and the logarithm of the 2 keV equivalent monochromatic luminosity of the brightest object in a given redshift interval (regardless of the class of the object). This function is almost constant for $z < 0.001$; it has a continuous inflection of about

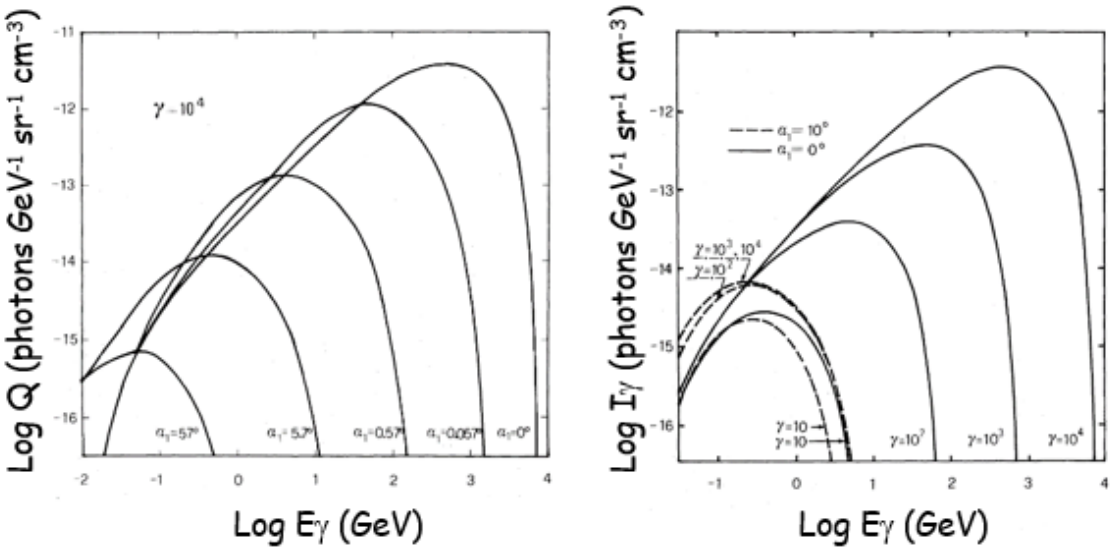

Figure 52: Left panel: the photon spectra from π^0-decay for the proton beam Lorentz's factor $\gamma = 10^4$ and selected angles α_1 calculated for unit densities ($n_b = n_h = 1$ cm^{-3}). Right panel: the photon spectra from π^0-decay from the proton beam Lorentz's factor $\gamma = 10$, 10^2, 10^3 and 10^4 and two values of the angles between the direction of the emitted photons and the beam axis $\alpha_1 = 0°$ (solid line) and 10° (dashed line, for unit densities ($n_b = n_h = 1$ cm^{-3}) (adopted from Bednarek et al., 1990).

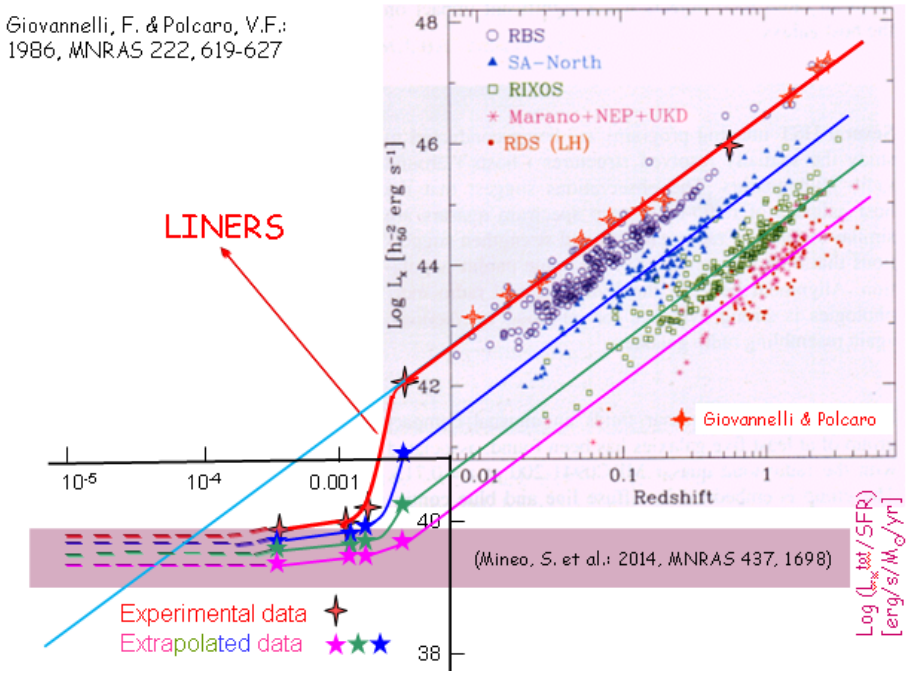

Figure 53: $L_{\rm xmax}$ versus z for extragalactic X-ray emitters. Red crosses and red line represent GP86 diagram. The deeper surveys (Hasinger, Miyaji & Schmidt, 2000) shown in the diagram are indicated with different colors. The light plum-colored band indicates the range of Mineo et al. (2014) results.

two orders of magnitude between z = 0.001 and z = 0.01, and at z $>$ 0.01, where only AGNs are present, it matches with a straight line, with slope equal to 1.6. They suggested that such a smooth function implies a physical continuity of these objects.

Later, with the advent of higher sensitivity X-ray experiments, different samples of extragalactic X-ray emitters were discovered (Hasinger, Miyaji & Schmidt, 2000, and the references therein). Figure 53 shows all these samples with the maximum X-ray luminosity function found by GP86 (red line). For the weaker sources, the luminosity functions are parallel to the GP86 function (blue, green, and fuchsia lines). For z $<$ 0.001, there is a substantial constancy of the functions. In other words this means that the contribution to the luminosity is mostly coming from the discrete sources of the host galaxies. This is in complete agreement with the results obtained by Mineo et al. (2014) (light plum-colored band). The light blue line in continuation of the red line indicates the contribution of the nucleus (L_{NUC}) to the total luminosity of galaxies with z $\leq$ 0.002.

4.12 Jets in Astrophysics

Every object rotating with adequate energy produces a jet. Relativistic jets have been found in numerous galactic and extragalactic cosmic sources at different energy bands. They can be formed by electrons and protons – accelerated up to relativistic energies – which through interactions with the matter and/or photons generate high energy radiation. The spectra of such a radiation are strongly dependent on the angle formed by the beam axis and the line of sight, and obviously by the Lorentz factor of the particles (e.g. Bednarek et al., 1990 and the references therein; Beall, Guillory & Rose, 1999; Beall, 2002, 2003; Beall et al., 2006, 2007).

Jets are thought to be produced by the powerful electromagnetic forces created by magnetized gas swirling toward a collapsed object (i.e. black hole). Although most of the material falls into the collapsed object, some can be ejected at extremely high speeds. Magnetic fields spun out by these forces can extend over vast distances and may help explain the narrowness of the jet (e.g. Clarke et al., 2008).

However, highly collimated supersonic jets and less collimated outflows are observed to emerge from a wide variety of astrophysical objects. They are seen in young stellar objects (YSOs), protoplanetary nebulae, compact objects (like galactic black holes or microquasars, and X-ray binary stars), and in the nuclei of active galaxies (AGNs). Despite their different physical scales (in size, velocity, and amount of energy transported), they have strong morphological similarities. What physics do they share? These systems are either hydrodynamic or magnetohydrodynamic (MHD) in nature and are, as such, governed by non-linear equations. An important review on this topic was published by de Gouveia dal Pino (2005). Very interesting discussion has been published about the role of magnetic reconnection on jet/accretion disk systems, valid in different kind of cosmic sources, like from microquasars to low luminous AGNs, till YSOs (de Gouveia Dal Pino, Piovezan & Kadowaki, 2010).

Astrophysical jets are a remarkable laboratory for a number of important physical processes. They provide a confirmation of special relativity in terms of relativistic Doppler boosting, superluminal motion, and time dilation effects. When coupled with their black-hole/neutron-star origins, jets have implications for testing general relativity. Over the course of two decades of astrophysical research, we have become aware that jets are ubiquitous phenomena in astrophysics. Extended linear structures now associated with jets can be found in star–forming regions, galactic binaries,

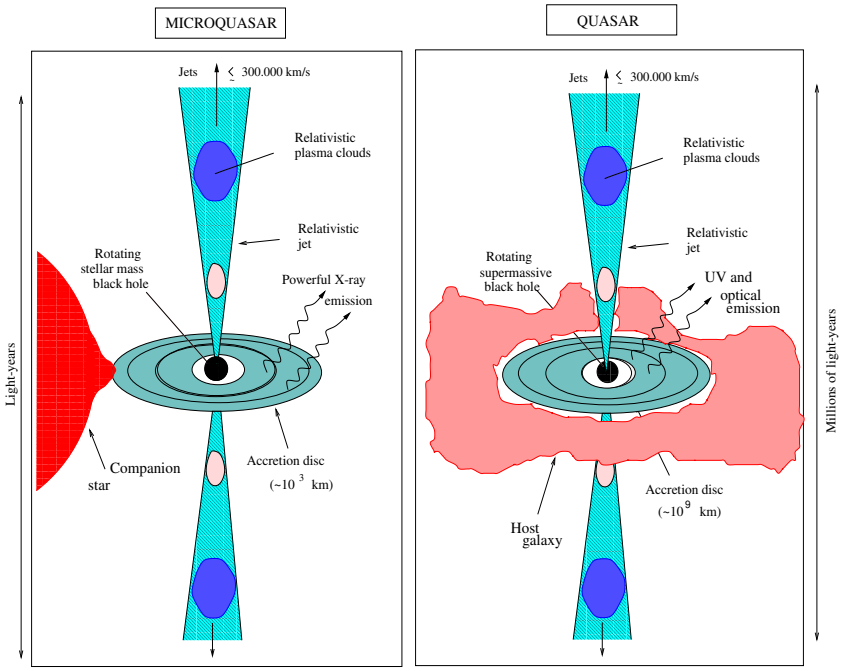

Figure 54: Sketch showing analogies between quasars and microquasars. Note the different mass and length scales between both types of objects (Chaty, 1998).

microquasars, active galaxies and quasars, clusters of galaxies, and γ-ray bursts. The presence and evolution of these jet–like structures is of course a testament to the principle of conservation of angular momentum.

The association of jets with accretion disks strengthens the case for similar physical processes in all these phenomena (e.g., Beall, 2003; Marscher, 2005), and it has become plausible that essentially the same physics is working over a broad range of temporal, spatial, and luminosity scales. Jets have, therefore, become a 'laboratory' or perhaps an anvil, that we can use to help us forge our understanding of the physical processes in the sky.

In 1992 the first so-called microquasar, *annihilateur*, was identified (Mirabel et al., 1992). This source was exhibiting bipolar radio jets spread over several light-years. This was the first such observation in our Galaxy, however jets had been already observed emanating from distant galaxies. Therefore this observation made clear the existence of a morphological analogy between quasars and microquasars. Indeed, Mirabel & Rodríguez (1994) detected from the black hole candidate GRS 1915+105 – discovered by Castro Tirado et al. (1994) – apparent superluminal motions, while frame velocity was v$\sim$ 0.92c. It became then rapidly clear that the advantages of microquasars compared to quasars were that i) they are closer, ii) it is possible to observe both (approaching and receding) jets, and iii) the accretion/ejection timescale is much shorter. After this observation of superluminal motions, the morphological analogy with quasars became stronger, and the question was then: is this morphological analogy really subtended by physics? If the answer is yes, then microquasars really are "micro"–quasars. For instance, there should exist microblazars (microquasar whose jet points towards the observer), in order to complete the analogy with quasars.

A schematic view of a microquasar, compared with quasars, is given in Fig. 54 (Chaty, 1998).

Microquasars are among the best laboratories for high energy phenomena and astroparticle physics. They are good candidates to be emitters of astroparticles: very high energy photons, cosmic rays and neutrinos. For these reasons the study of microquasars is one of the main goal of current space missions. Since each component of the system emits at different wavelengths, it is necessary to undertake multifrequency observations in order to understand phenomena taking place in these objects.

Theoretical and observational works show that jets from AGN can trigger star formation. However, in the Milky Way the first – and so far – only clear case of relativistic jets inducing star formation has been found in the surroundings of the microquasar GRS 1915+105. Mirabel et al. (2015) discussed jet-induced star formation by a microquasar. Although star formation induced by microquasar jets may not be statistically significant in the Milky Way, jets from stellar black holes may have been important to trigger star formation during the re-ionization epoch of the universe (Mirabel et al. 2011).

A review about jets in astrophysics has been published by Beall (2014).

4.13 The tidal disruption of stars by massive Black Holes

As already noted black hole accretion is a fundamental physical process in the universe. It is the standard model for the central engine of active galactic nuclei (AGNs), and also plays a central role in the study of black hole X-ray binaries, Gamma-ray bursts, and tidal disruption events. According to the temperature of the accretion flow, the accretion models can be divided into two classes, namely cold and hot. The standard thin disk model belongs to the cold disk, since the temperature of the gas is far below the virial value (Shakura & Sunyaev, 1973) (see reviews by Pringle, 1981; Frank, King & Rayne, 2002; Abramowicz & Fragile, 2013; Blaes, 2014). The disk is geometrically thin but optically thick and radiates multi-temperature black body spectrum. The radiative efficiency is high, ~ 0.1, independent of the accretion rate. The model has been successfully applied to luminous sources such as luminous AGNs and black hole X-ray binaries in the thermal state. The most recent review about the accretion onto black holes was published by Lasota (2016).

The tidal disruption of stars by massive BHs has been discussed since many years by Rees (1988b), and e.g. Magorrian & Tremaine (1999). Rees (1988b) argued that stars in galactic nuclei can be captured or tidally disrupted by a central black hole. Some debris would be ejected at high speed, the remainder would be swallowed by the hole, causing a bright flare lasting at most a few years. Such phenomena are compatible with the presence of 10^6–10^8 $M_\odot$ holes in the nuclei of many nearby galaxies. Stellar disruption may have interesting consequences in our own Galactic Center if a $\approx 10^6$ $M_\odot$ hole lurks there.

The sources of radiation during tidal disruption event are given in Figure 55.

Recently, Bisnovatyi-Kogan & Giovannelli (2017) developed models of time lags between optical and X-ray flashes for close-binary galactic sources with accretion disks and for an AGN with an SMBH that is embedded in a quasi-spherical bulge. The flashes in an AGN are considered in the model when a disruption of a star that is in the evolution phase of a giant enters the radius of strong tidal forces. The matter with a low angular momentum that is released by the star falls into the SMBH in the form of a quasi-spherical flow with a velocity that is close to the free-fall velocity. An X-ray flash occurs when the falling matter reaches the hot inner regions. The time lag

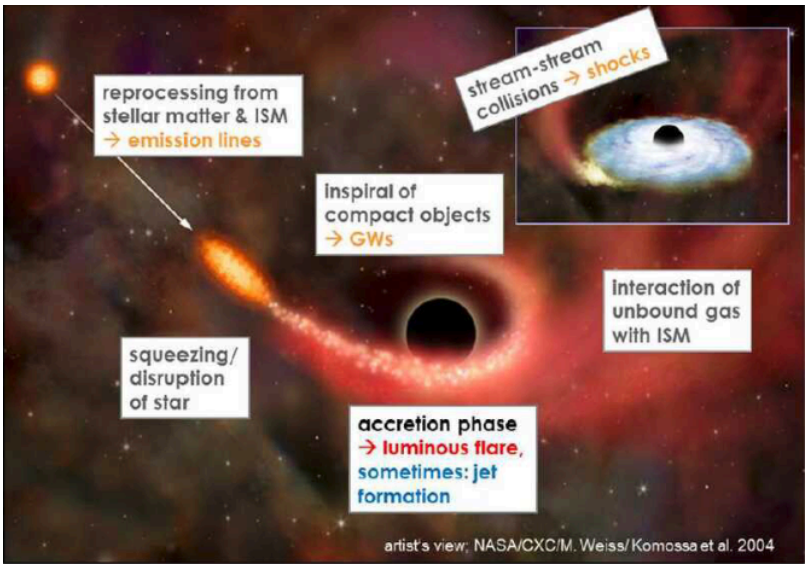

Figure 55: Sites and sources of radiation during the evolution of Tidal Disruption Event (TDE), after Komossa (2015).

observed in these sources is identified with the time of the matter falling from the tidal radius onto the central region. The values of the tidal radius that they calculated in this model were compared with the theoretical radii of a tidal disruption that depends on the masses of the SMBH and of the star, and on the radius of the star.

Table 6: Properties of stars tidally disrupted by SMBH in AGNs (adopted from Bisnovatyi-Kogan & Giovannelli, 2017).

Source name	τ_{obs} (days)	$r_{opt} = r_t$ (cm)	R_s (cm)
Mrk 509	15	5.2×10^{15}	$114 \times r_s^{1/3} R_\odot$
NGC 7469	4	8.95×10^{14}	$47 \times r_s^{1/3} R_\odot$
3C 120	3.9-6.2? (10)	3.3×10^{15}	$100 \times r_s^{1/3} R_\odot$
NGC 3516	100	1.1×10^{16}	$409 \times r_s^{1/3} R_\odot$
NGC 4051	2.4	2.5×10^{14}	$36 \times r_s^{1/3} R_\odot$
ASASSN-14li	5	1.1×10^{15}	$98 \times r_s^{1/3} R_\odot$

Knowing the SMBH masses from observations, and making a reasonable suggestion for the stellar mass that is on the order of one solar mass, they obtained that the radii of the disrupted star are between a few tens and a few hundreds of $R_\odot$ (see Table 6). These radii are characteristic of stars of moderate mass on the giant phase of evolution (e.g. Bisnovatyi-Kogan, 2011).

The time delay between the optical and X-ray flashes is experimentally determined. The radius at which the optical flash occurs is calculated for the motion with free-fall velocity V_{ff} as:

$V_{ff} = (2GM/r)^{1/2}$; $dr/dt = V_{ff}$; $\tau_{ff} = 2/3\ [r^{3/2}/(GM)^{1/2}]$

Taking $\tau_{ff} = \tau_{obs}$, we obtain a radius of the optical flash r_{opt} as:

$r_{opt} = 1.65 \times 10^{12}\ \tau_{obs}\ m^{1/3}$ cm

where: τ_{obs} expressed in days, and SMBH mass: m expressed in $M_{\odot}$.

4.14 Neutrinos

One of the most important questions of fundamental physics, that is still unanswered today, is the reason for our existence, namely why the Universe is made up mostly of matter. To put it in more microscopic terms, the important unanswered question relates to a theoretical understanding of the magnitude of the observed Baryon Asymmetry in the Universe (BAU). According to the Big Bang theory, matter and antimatter have been created at equal amounts in the early Universe. The observed charge-parity (CP) violation in particle physics (Christenson, et al., 1964), prompted Sakharov (1991a,b) to conjecture that non-equilibrium physics in the early Universe produces Baryon number (B), charge (C) and charge-parity (CP) violating, but CPT conserving, interactions/decays of anti-particles in the early Universe, resulting in the observed baryon-anti-baryon asymmetry. In fact there are two types of non-equilibrium processes in the early Universe that could produce this asymmetry: the first type concerns processes generating asymmetries between leptons and anti-leptons (*Leptogenesis*), while the second produces asymmetries between baryons and anti-baryons (*Baryogenesis*) (Abazajian et al., 2012).

The knowledge of the neutrino physics is the key for answering to this fundamental question. However, we cannot enter in a deep discussion about the physics of neutrinos. This argument deserves particular attention and space for discussion. A deep and exhaustive discussion about neutrinos can be found in the *Light Sterile Neutrinos: A White Paper* (Abazajian et al., 2012), *Neutrino Oscillation Physics Potential of the T2K Experiment* (Abe et al., 2015), and in *Neutrino Physics with JUNO* (An et al., 2015). However, we want to spend a few words about an important result obtained few years ago.

We know that neutrino oscillations are consistently described by three families ν_1, ν_2, ν_3 with mass values m_1, m_2 and m_3 that are connected to the flavor eigenstates ν_e, ν_μ and ν_τ by a mixing matrix U. The neutrino oscillation probability depends on: i) three mixing angles, Θ_{12}, Θ_{23}, Θ_{13}; ii) two mass differences, $\Delta m^2_{12} = m_{22} - m_{21}$, $\Delta m^2_{23} = m_{23} - m_{22}$; iii) and a Charge-Parity (CP) phase δ_{CP}. The mixing angle Θ_{13} is the key parameter of three-neutrino oscillations and regulates at the first order all the oscillation processes that could contribute to the measurement of mass hierarchy and leptonic CP violation (Mezzetto, 2011). Indeed, the neutrino mixing angle Θ_{13} is at the focus of current neutrino research. Fogli et al. (2008) reported hints in favor of $\Theta_{13} > 0$ at 90% C.L.. Such hints are consistent with the recent indications of $\nu_\mu \rightarrow \nu_e$ appearance in the T2K (Abe et al., 2011) and MINOS long-baseline accelerator experiments as reported by Fogli et al. (2011). They found $\sin^2\Theta_{13} = 0.021 \pm 0.007$ or $\sin^2\Theta_{13} = 0.025 \pm 0.007$, depending on reactor neutrino flux systematics.

The evidence for $\sin^2\Theta_{13} > 0$ opens the door to CP violation searches in the neutrino sector, with profound implications for our understanding of the matter-antimatter asymmetry in the uni-

verse. Fogli et al. (2012) found interesting indications for $\Theta_{23} < \pi/4$ and possible hints for $\delta \sim \pi$, with no significant difference between normal and inverted mass hierarchy.

Recent results coming from the OPERA experiment – designed to perform the most straightforward test of the phenomenon of neutrino oscillations (Acquafredda et al., 2009) – allowed to affirm that $\nu_\mu \rightarrow \nu_\tau$ oscillations really appeared in the CERN to Gran Sasso Neutrino beam (CNGS) with 6.1σ significance obtained with the complete data sample, corresponding to 5603 ν interactions fully reconstructed.

The values obtained are $|\Delta m^2_{32}| = (2.7^{+0.7}_{-0.6}) \times 10^{-3}$ eV^2, assuming $\sin^2 2\Theta_{23} = 1$ (Agafonova et al., OPERA Collaboration, 2018).

5. The challenge to know the Universe

Without a doubt, this challenge can only be met experimentally. At the present time we can say that we know only a small part of the Universe.

The Universe manifests not only through Electromagnetic Radiation but also through Astroparticles, including Neutrinos and Gravitational Waves (GVs).

Since each cosmic source is variable at different levels both in time and intensity, Multifrequency Observations (possibly Simultaneous) are Fundamental in Photonic Astrophysics and Particle Astrophysics. There are many problems in performing Simultaneous Multifrequency, Multisite, Multiinstrument, Multiplatform Measurements due to: (i) objective technological difficulties; (ii) sharing common scientific objectives; (iii) problems of scheduling and budgets; (iv) politic management of science. All these kind of measurements converge in what is now called *Multimessenger Astrophysics*, after the detection of gravitational wave events (GWEs) and the search for the electromagnetic counterparts of such events.

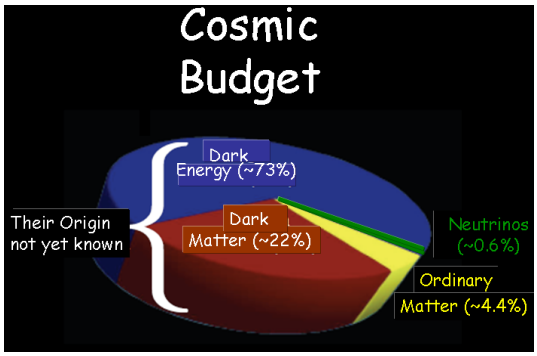

Figure 56: A Sketch of the Cosmic Budget.

The composition of the Universe is poorly known, as shown in Fig. 56. Only $\sim$ 4.4% of ordinary matter, $\sim$ 0.6% of neutrinos, $\sim$ 22% of Dark Matter (DM), and $\sim$ 73% of dark Energy (DE). With the detection of GWEs a new window to the Universe has been opened.

As we can see looking at the Fig. 56, we know – and not very well – only $\sim$ 5% of our Universe. The one million dollars question is how to improve our knowledge, The answer can be obtained by using *Big Experiments* (space- and ground-based), and *Small Experiments* (space- and ground-based).

5.1 Big experiments

Several examples of big experiments are:

- GAIA (distances of billions stars: already discussed in Section 2.7);
- The Large Hadron Collider (LHC) (the world's largest and most powerful particle accelerator);
- Cherenkov Telescope Array (CTA);
- European–Extreme Large Telescope: E-ELT (the next generation ground telescope);
- Canadian Hydrogen Intensity Mapping Experiment (CHIME) (Fast Radio Bursts);
- eASTROGAM ($\sim$ 200 keV–2 GeV, High Sensitivity);
- James Webb Space Telescope: JWST (the next generation space telescope);
- The GAMMA-400 gamma-ray telescope (high angular and energy resolutions);
- The BICEP (Background Imaging of Cosmic Extragalactic Polarization) and the Keck Array.
- The Large Scale Polarization Explorer (LSPE)
- The QUBIC Experiment
- Square Kilometre Array
- HAWC (High-Altitude Water Cherenkov Gamma-ray Observatory)
- LHAASO (Large High Altitude Air Shower Observatory)
- TAIGA (Tunka Advanced Instrument for cosmic ray physics and Gamma Astronomy)

We will discuss later in the sections 4.3, 4.4 and 4.5 the main characteristic of these experiments.

5.2 Small experiments

In this short excursion about the tools necessary for an advance of our knowledge of the physics of the Universe, we cannot omit the extreme importance of small experiments, like those Space–based: small–, mini–, micro–, nano–, and cube–satellites, and those Ground–based: small–telescope, and Robotic–telescopes.

Castro-Tirado (2010a) in his review "*Robotic Autonomous Observatories: A Historical Perspective*" presented a historical introduction to the field of Robotic Astronomy, discussing the basic definitions, the differing telescope control operating systems, observatory managers, as well as a few current scientific applications in that time.

The number of automatic astronomical facilities worldwide continues to grow, and the level of robotisation, autonomy, and networking is increasing as well. This has a strong impact in many astrophysical fields, like the search for extrasolar planets, the monitoring of variable stars in our

Galaxy, the study of active galactic nuclei, the detection and monitoring of supernovae, and the immediate followup of high-energy transients such as gamma-ray bursts (Castro-Tirado, 2008, 2010b; Castro-Tirado et al., 2010).

The number of Robotic Autonomous Observatories (RAOs) has rapidly grown. Figure 57 shows the location of more than 100 RAOs worldwide (Castro Cerón, 2011). They are providing excellent results which should be impossible to obtain with the larger telescopes subject to strict scheduling, and in any case not available for long term runs of observations.

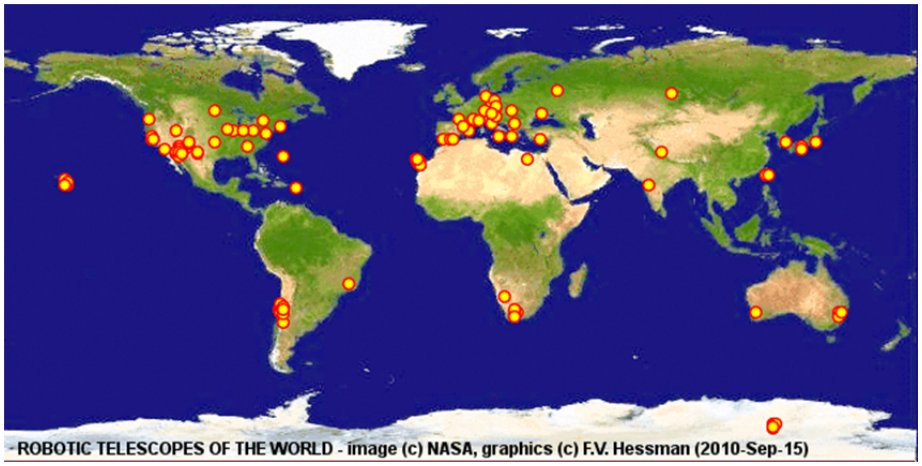

Figure 57: The Robotic Autonomous Observatories worldwide (adopted from Castro Cerón (2011) after Hessman (2001a,b).

The most important news about the many scientific results obtained with the RAOs can be found in the proceedings of the series of Workshops on Robotic Autonomous Observatories (Bloom, Castro-Tirado, Hanlon & Kotani, 2010; Guziy, Pandey, Tello & Castro-Tirado, 2012; Tello, Riva, Hiriart & Castro-Tirado, 2014; Caballero-García, Pandey, Hiriart & Castro-Tirado, 2016; Castro-Tirado, Pandey & Caballero-García, 2021).

Just for giving to the reader a short panorama about the many small ground- and space-based experiments, not necessarily autonomous, we list the following:

a) **MITSuME (Multicolor Imaging Telescope for Survey and Monstrous Explosions)** has been built to perform Multi-color photometry of NIR/
optical afterglow covering the wavebands from K_s to g' allowing the photometric redshift measurements up to z $\sim$ 10. Two 50 cm optical telescopes are built at Akeno, Yamanashi in eastern Japan, and at OAO, Okayama in western Japan. Each telescope has a Tricolor Camera, which allows us to take simultaneous images in g', R_c, and I_c bands. These telescopes respond automatically to GCN alerts and start taking series of tricolor images, which are immediately processed through the analysis pipeline on site. The pipeline consists of source finding, catalog matching, sky coordinates mapping to the image pixels, and photometry of the found sources. An automated search for an optical counterpart is performed. While waiting for GRBs, the MITSuME Telescopes automatically patrol pre-selected interesting objects such as AGNs and galactic transients for multiwavelength studies with Fermi (GLAST) and MAXI (Shimokawabe et al., 2009).

b) **The CHASE (CHilean Automatic Supernova sEarch)** project began in 2007 (Pignata et al.,

2009) with the goal to discover young, nearby southern supernovae in order to i) better understand the physics of exploding stars and their progenitors, and ii) refine the methods to derive extragalactic distances. During the first four years of operation, CHASE has produced more than 130 supernovae, being the most successful project of its type in the southern hemisphere (Hamuy et al., 2012).

c) **TSUBAME** is an interesting example of a micro-satellite developed by the students of Tokyo Institute of Technology (Arimoto et al., 2008). The name Tsubame means "swift" in Japanese, referring to the fast spacecraft attitude changes for event monitoring; it also connotes a certain relationship to NASA's gamma-ray mission, Swift. In addition, Tsubame happens to be the logo of Tokyo Tech, symbolized by a swallow. It was launched from Russia on Nov 6, 2014 for measuring hard X-ray polarization of GRBs in order to reveal the nature of their central engine (Kurita et al., 2015).

d) **SLATS: Super Low Altitude Test Satellite "TSUBAME"**. SLATS – launched on December 23, 2017, and ended on October 1, 2019 (JAXA http://
global.jaxa.jp/) – is the first Earth observation satellite to use a super low orbit. A "super low orbit" refers to an orbit with an altitude lower than 300 km. This orbit is an undeveloped region and it has yet to be fully utilized by satellites. Satellites in a super low orbit will bring benefits such as high resolution observations for optical imagers, low power transmissions for active sensors, and cost reductions for satellite manufacturing and launches. This is due to the closer range to the Earth. A satellite in a super low orbit like SLATS will be exposed to air resistance, which is approximately 1,000 times greater than that of most Earth observation satellites at an altitude of 600 to 800 km. Consequently, this type of satellite will require a greater amount of fuel than conventional satellites. In order to solve the atmospheric drag issue, JAXA has adopted an ion engine. The ion engine uses fuel 10 times more efficiently than gas jets. Furthermore, they are developing a compact satellite to minimize air resistance, and will verify that our technology can support orbiting at super low altitudes over an extended period of time. Then JAXA will take the first step toward practical application of a super low altitude satellite.

c) **The Russian global network of telescopes robot MASTER** (Lipunov et al., 2010). MASTER is very fast positioning alert, follow up and survey twin telecopes Global network with own real-time auto-detection software. MASTER goal is One Sky in One Night up to 20-21 mag. The network is spread along the whole world. In the following are reported the MASTER Net Sites: i) MASTER-Amur: Russia, near Blagoveschensk. Blagoveschensk State Pedagogic University. ii) MASTER-Tunka: Russia, near Irkutsk. Applied Physics Institute, Irkutsk State University. iii) MASTER-Ural: Russia, near Ekaterinburg, Since 2008. Kourovka Astronomical Observatory, Ural State University. iv) MASTER-Kislovodsk: Russia, Near Kislovodsk. Kislovodsk Solar Station of the Pulkovo Observatory, Sternberg Astronomical Institute, Lomonosov Moscow State University. v) MASTER-SAAO: South Africa, Sutherland, since 2014. South African Astonomical Observatory (SAAO). vi) MASTER-IAC: Spain, Canarias Islands, since 2015 The Instituto de Astrofísica de Canarias (IAC). vii) MASTER-OAFA: Argentina, since 2012 Observatorio Astronomico Felix Aguilar (OAFA) , Instituto de Ciencias Astronomicas de la Tierra y del Espacio (ICATE), National University of San Juan. viii) MASTER-Progenitor: Russia, Moscow, Alexander Krylov Observatory, Since 2002.

d) **Very small satellites for multifreqyency astrophysics** have been discussed by Hudec (2017). About the small satellites we can assist to a strong competition (typically for ESA missions, 60 proposals for 1 satellite), and moreover all the system is affected by funding problems.

The development of the Pico (Cube) and Nanosatellites is running at many Universities, mostly with involvement of students for evident goals of education.

The standard size for a CubeSat is 1 Liter Volume, i.e. 10 x 10 x 10 cm^3 and typically a weight of $\sim$ 1.3 kg. Multiple modules are possible, i.e. 3 Units = 3 modules/units, i.e. 10 x 10 x 30 cm^3, typically up to 12 Units.

The range of weight of Picosatellites is 0.1-1 kg, Femtosatellites 10-100 g, Nanosatellites 1-10 kg, Microsatellites 10-100 kg.

Recent technological progress allows their use in any field of astrophysics.

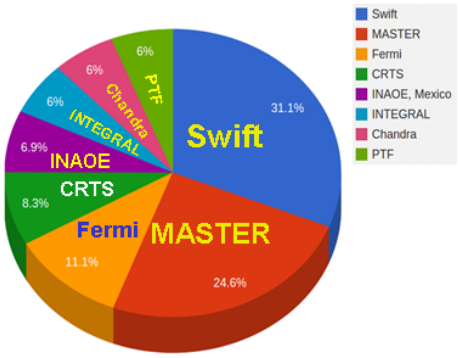

Figure 58: Contribution of different space- and ground-based experiments to the transient alerts in Astronomer's telegrams in the period 2013-2014 (after Buckley, 2015).

Undoubtedly MASTER contributions to transient alerts in Astronomer's telegrams is fundamental. For instance in the period 2013-2014, MASTER contribution is of order 25% of the total as shown in Fig. 58 (after Buckley, 2015).

Though we have not shown a complete list of small experiments both space- and ground-based, we are able to affirm that small telescopes are unreplaceable tools complementary to larger telescopes and to bigger ground- and space-based multifrequency experiments.

Undoubtedly the advent of new generation experiments ground– and space–based have given a strong impulse for verifying current theories, and for providing new experimental inputs for developing a new physics for going, probably, over the standard model (SM). Recent results coming from Active Physics Experiments (APEs) and Passive Physics Experiments (PPEs) have opened such a new path.

An extensive review on the situation about the knowledge of the physics of our Universe has been published by Giovannelli & Sabau-Graziati (2016c). The reader interested is invited to look at that paper. However, we are obliged to discuss a few topics that, in our opinion, could be useful for a better understanding of the open problems still existing in the modern astrophysics.

5.3 Active physics experiments

It is important to discuss briefly the most important active physics experiment: The Large

Hadron Collider (LHC).

5.3.1 The Large Hadron Collider (LHC)

The Large Hadron Collider (LHC) is the world's largest and most powerful particle accelerator (https://home.cern/topics/large-hadron-collider). It first started up on 10 September 2008, and remains the latest addition to CERN's accelerator complex. The LHC consists of a 27 km ring of superconducting magnets with a number of accelerating structures to boost the energy of the particles along the way. Figure 59 shows a partial view of the tunnel hosting the accelerator.

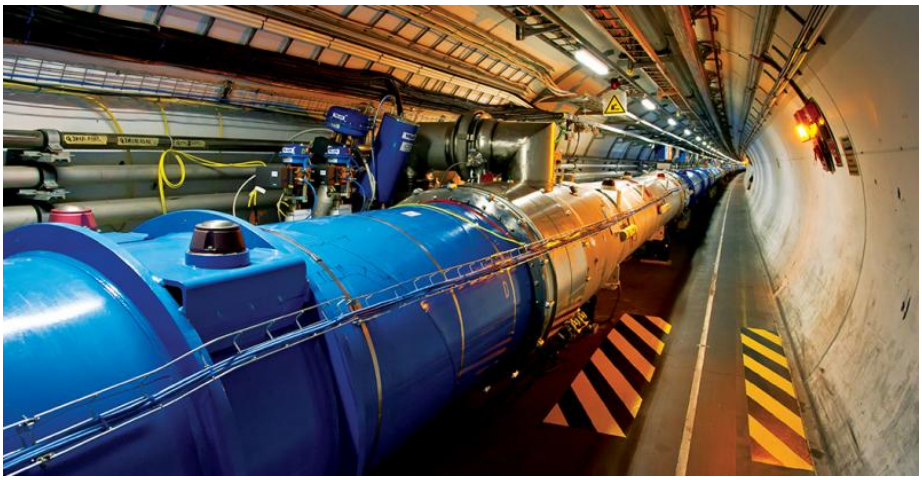

Figure 59: The Large Hadron Collider is the world's largest and most powerful particle accelerator (Image: CERN, at https://home.cern/topics/large-hadron-collider).

All the controls for the accelerator, its services and technical infrastructure are housed under one roof at the CERN Control Centre. From here, the beams inside the LHC are made to collide at four locations around the accelerator ring, corresponding to the positions of four particle detectors – ATLAS (A Toroidal LHC ApparatuS), CMS (Compact Muon Solenoid), ALICE (A large Ion Collider Experiment) and LHCb (Large Hadron Collider beauty). There are three more smaller experiments: LHCf (Large Hadron Collider forward), TOTEM (TOTal Elastic and diffractive cross section Measurement), and MoEDAL (Monopole and Exotics Detector at the LHC). TOTEM is installed close to the CMS interaction point, LHCf is installed near ATLAS, and MoEDAL is close to the LHCb detector. The position of the four main experiments are shown in Fig. 60 (https://home.cern/topics/large-hadron-collider).

The LHC will answer some of the fundamental open questions in physics, concerning the basic laws governing the interactions and forces among the elementary objects, the deep structure of space and time, and in particular the interrelation between quantum mechanics and general relativity. Data is also needed from high-energy particle experiments to suggest which versions of current scientific models are more likely to be correct – in particular to choose between the Standard Model and Higgs-less model and to validate their predictions and allow further theoretical development. Many theorists expect new physics beyond the Standard Model to emerge at the TeV energy level, as the Standard Model appears to be unsatisfactory. Issues explored by LHC collisions include i) the mass of elementary particles being generated by the Higgs mechanism; ii) supersymmetry, an

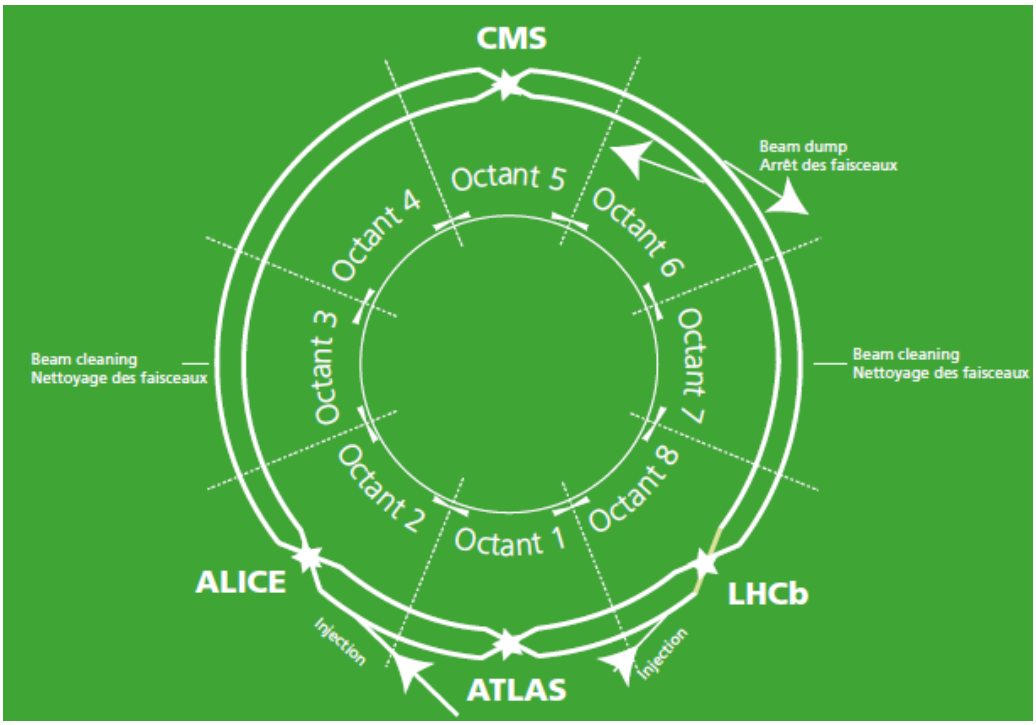

Figure 60: Localization of the four main experiments at LHC (CERN-Brossure-2017-002-Eng, p. 26).

extension of the Standard Model and Poincaré symmetry; iii) extra dimensions, as predicted by various models based on string theory; iv) the nature of the dark matter that appears to account for $\sim 27\%$ of the mass-energy of the universe; v) answer to the question if the electroweak force and the strong nuclear force are just different manifestations of one universal unified force, as predicted by various Grand Unification Theories; vi) why the fourth fundamental force (gravity) is so many orders of magnitude weaker than the other three fundamental forces; vii) are there additional sources of quark flavour mixing, beyond those already present within the Standard Model?; viii) why are there apparent violations of the symmetry between matter and antimatter?; ix) what are the nature and properties of quark-gluon plasma, thought to have existed in the early universe and in certain compact and strange astronomical objects today?

The Large Hadron Collider (LHC) can be considered as the eighth-wonder of the world. In this sense we can consider LHC as the vessel sailing the Dark Energy and Dark Matter unknown oceans. LHC is a complementary tool for HE observatories looking directly at the Universe. LHC is probably the highest and ultimately active-physics technological wonder, difficult to be outdated because of dimensions and costs. Probably in the next decades it will be cheaper to develop more sensitive passive-physics ground-based experiments, and even if space-based or Moon-based.

The Standard Model of particle physics takes quarks and leptons to be fundamental elementary particles, and describes the forces that govern their interactions as mediated through the exchange of further elementary particles. The exchanged particles are photons in the case of the electromagnetic interaction, W and Z bosons in the case of the weak interaction, and gluons in the case of the strong interaction. After the discovery of the W and Z bosons in the early 1980s, the elucida-

tion of the mechanism by which they acquire mass became an important goal for particle physics. Within the Standard Model the W and Z bosons have masses generated via the symmetry breaking Englert-Brout-Higgs-Guralnik-Hagen-Kibble mechanism, proposed in 1964 and giving rise to a massive scalar particle, the Standard Model Higgs boson (Jakobs & Seez, 2015).

The hunt to Higgs boson – often called "*the God particle*" because it's said to be what caused the "Big Bang" that created our Universe: matter obtains mass interacting with Higgs field – started a few years ago with the most powerful accelerators constructed in the world, in particular with the different experiments of the LHC. These experiments can provide information about the first moment of the life of the Universe. LHC is a complementary tool for HE observatories looking directly to the Universe.

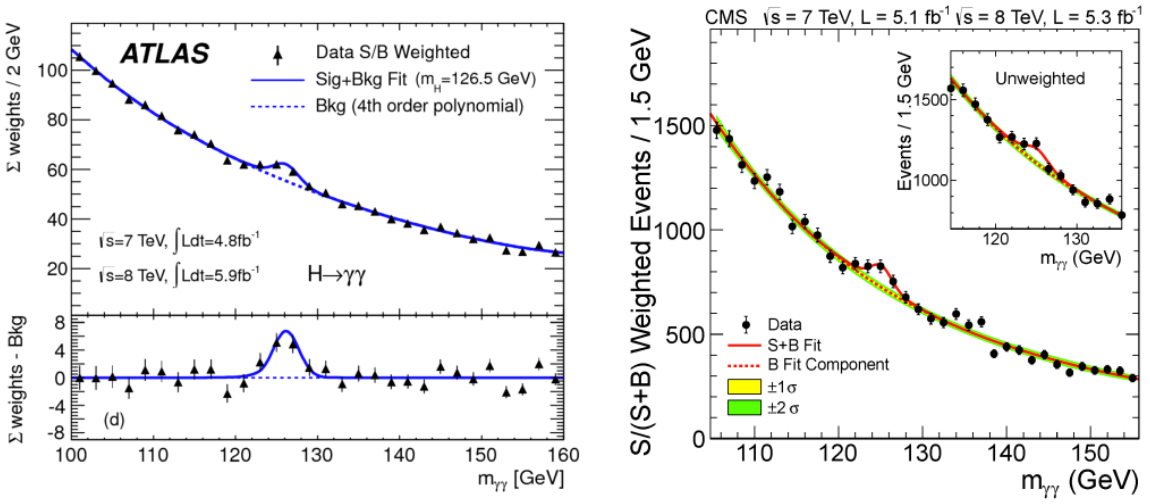

Figure 61: ATLAS and CMS results for the probable Higgs boson (adopted from Jakobs & Seez (2015), after The ATLAS Collaboration (2012), and The CMS Collaboration (2012b).

The Higgs boson discovery was announced by the ATLAS and CMS collaborations on 4th July 2012. Evidence for a new particle with the mass of about 125 GeV and the properties of the Standard Model Higgs boson.

From ATLAS results, a 5.0 σ excess at $\sim$ 126.5 GeV has been detected. This value is compatible with the expected mass of Higg's boson (Gianotti, 2012; Aad et al., 2012). The Compact Muon Solenoid (CMS) experiment at LHC detected a new boson at 125.3 ± 0.6 GeV with 4.9σ significance (Incandela, 2012; The CMS Collaboration, 2012a). This result, together with that from ATLAS, if confirmed, would complete the SM of physics. Figure 61 shows the results from ATLAS and CMS (Jakobs & Seez, 2015).

Thanks to collisions at 13 TeV the experiment Large Hadron Collider beauty (LHCb) at LHC detected a new particle: the Pentaquark. The existence of the pentaquark was theoretically suggested since 1960-ies (Gell-Mann, 1964). Pentaquark gives a new way for the combination of the quarks that are the fundamental constituents of neutrons and protons (Cardini, 2015; Aaij et al., 2015).

5.4 Passive physics experiments

Among the many problems to be solved for the cosmological knowledge of the structure of the young universe, dark energy and the standard λCDM model, which better reproduces the observations of cosmology following the Big Bang, the most energetic processes in the universe, the big telescopes ground- and space-based for examining every phase of cosmic history: from the first luminous glows after the Big Bang to the formation of galaxies, stars, and planets to the evolution of our own solar system, one of the most important question still open is the search for experimental proof of the inflation. The expansion is thought to have been triggered by the phase transition that marked the end of the preceding grand unification epoch at $\approx 10^{-36}$ s after the Big Bang. It is not known exactly when the inflationary epoch ended, but it is thought to have been between $\approx 10^{-33}$ and $\approx 10^{-32}$ s after the Big Bang. The experimental proof of the inflation could come from measurements of Cosmic Microwave Background (CMB) polarization. Winstein (2007, 2009) discussed the problem of CMB polarization in the following decade.

We know from the theory that linear polarization of the CMB photons is induced via Thomson scattering by quadrupole anisotropy at recombination that occurred at z $\sim$ 1100 corresponding to t $\sim 1.2 \times 10^{13}$ s after the Big Bang. In turn, quadrupole anisotropy is induced by: i) density perturbations (scalar relics of inflation) producing a curl–free polarization vector field (E–modes); ii) gravitational waves (tensor relics of inflation) producing both curl–free and curl–polarization fields (B–modes).

No other sources for a curl–polarization field on the CMB at large angular scales exist. Thus, B–modes are a clear signature of inflation (e.g. de Bernardis, 2014).

5.4.1 The Cherenkov Telescope Array

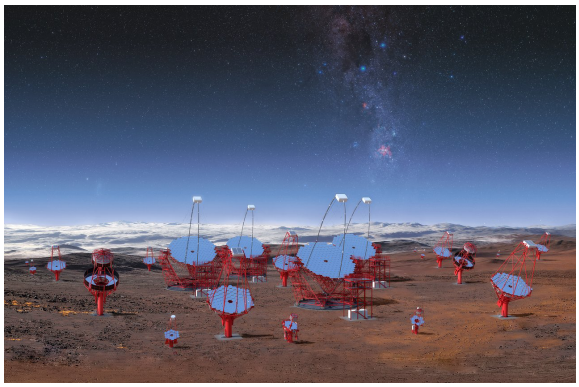

Figure 62: The CTA Telescopes in Southern Hemisphere (*http* : *//www.eso.org*; Credit: CTA/M-A. Besel/IAC (G.P. Diaz)/ESO).

The Cherenkov Telescope Array (CTA) will be a next-generation ground-based observatory for very high energy gamma-ray astronomy. It will consist of two arrays of dishes, a southern-hemisphere array at ESO's Paranal Observatory (e.g. Hofmann et al., 2017) and a northern array on the island of La Palma, Spain (e.g. Williams et al., 2019).

Figure 62 shows the CTA Telescopes in Southern Hemisphere (*http* : *//www.eso.org*; Credit: CTA/M-A. Besel/IAC (G.P. Diaz)/ESO). This image illustrates all three classes of

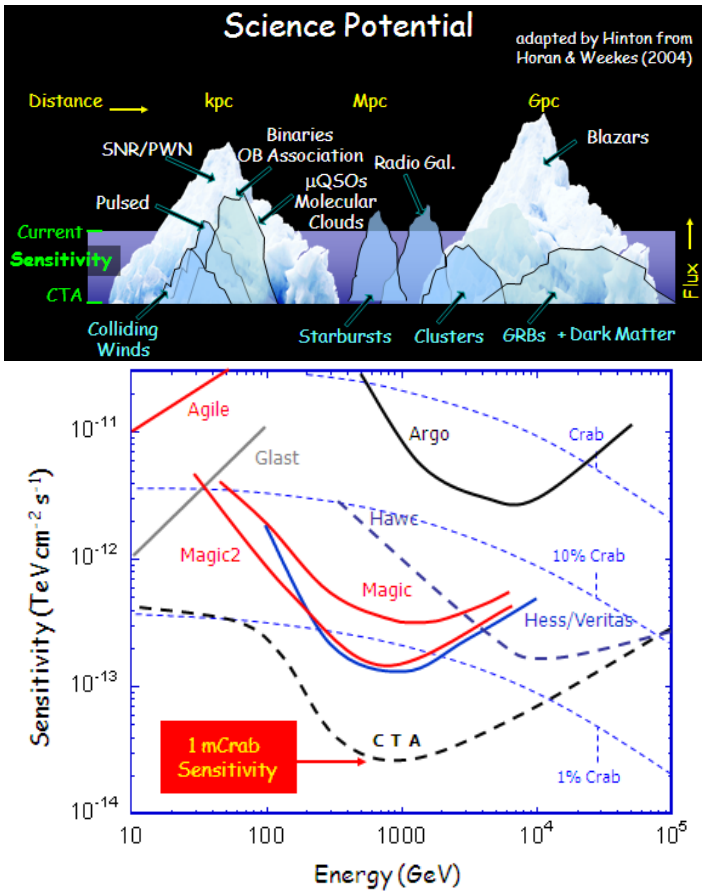

Figure 63: Upper panel: New horizons in VHE astrophysics with the advent of the CTA (Paredes & Persic, 2009); Lower panel: The sensitivity of most of the HE experiments versus energy (after http://www.cfar.ie/research-areas.html).

the telescopes planned for the southern hemisphere at ESO's Paranal Observatory, as viewed from the center of the array. This rendering is not an accurate representation of the final array layout, but it illustrates the enormous scale of the CTA telescopes and the array itself.

Figure 63 shows:(upper panel) a sketch of the science potential of the current experiments in comparison with the forthcoming CTA (Paredes & Persic, 2009); (lower panel) the sensitivity of most of the high energy experiments, including that of CTA. It is impressive to note that the sensitivity of the CTA at 1 TeV is 1 mCrab (after http://www.cfar.ie/research-areas.html).

A complete description of the Science that can be performed with the CTA has been published by Acharya et al. (2019).

5.4.2 ESO–Extremely Large Telescope

Astronomy is experiencing a golden era. The past decade alone has brought amazing discoveries that have excited people from all walks of life, from finding planets around Proxima Centauri, the nearest star to the Sun, to the first image of a black hole.

Extremely large telescopes are considered worldwide to be one of the highest priorities in ground-based astronomy. They will vastly advance astrophysical knowledge, allowing detailed

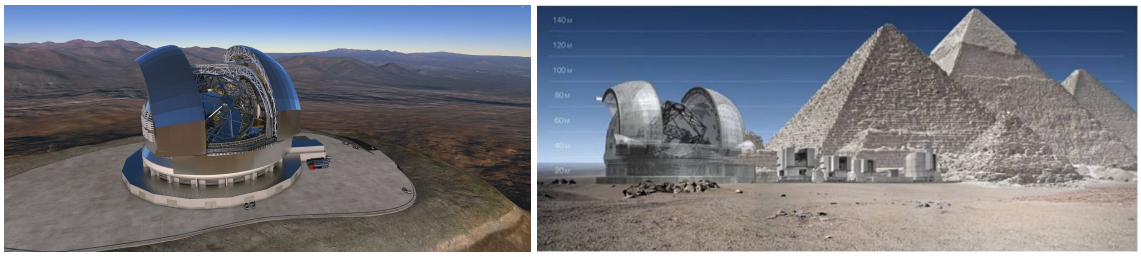

Figure 64: Left panel: the dome of the E-ELT in La Silla observatory (https://www.eso.org/public/teles-instr/elt/); Right panel: the grandeur of the telescope in comparison with the pyramids (Gilmozzi, 2013).

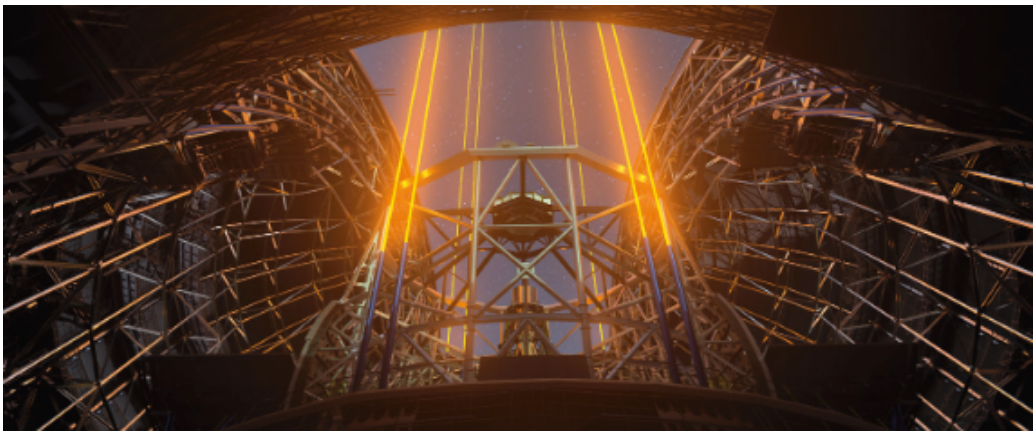

Figure 65: This artistic illustration depicts the laser guide stars of the future ELT. Like many other systems on the ELT, the multiple laser guide stars are vital to its operation, helping it adapt to the ever-changing atmospheric conditions above the telescope. This information is sent to the ELT's M4 mirror which will adjust its shape to compensate for the distortion caused by atmospheric turbulence, allowing astronomers to observe finer details of much fainter astronomical objects than would otherwise be possible from the ground (adopted from Kasper et al., 2021

.

studies of subjects including planets around other stars, the first objects in the Universe, supermassive black holes, and the nature and distribution of the dark matter and dark energy which dominate the Universe (https://www.eso.org/public/italy/teles-instr/elt/).

Since 2005 ESO has been working with its community and industry to develop an extremely large optical/infrared telescope, named the ELT (Extremely Large Telescope). This revolutionary new ground-based telescope concept will have a 39-meter main mirror and will be the largest optical/near-infrared telescope in the world: "the world's biggest eye on the sky" (Gilmozzi & Spyromilio, 2007, 2009; Gilmozzi, 2008, 2009; Gilmozzi & Kissler-Patig, 2011; McPherson et et al., 2012; Liske, Padovani & Kissler-Patig, 2012; Ramsay et al., 2016; Padovani, 2018).

The final approval of E-ELT occurred at ESO on December 3, 2014 (de Zeeuw, Tamai & Liske, 2014). On May 25, 2016 ESO Signs Largest Ever Ground-based Astronomy Contract for ELT Dome and Telescope Structure (eso1617 - Organisation Release).

An expanded view of the Universe (Science with the European Extremely Large Telescope) can be found in http://www.eso.org/sci/facilities/eelt/docs/.

Figure 64 shows the dome of the E-ELT in La Silla observatory (left panel) and the grandeur of the telescope in comparison with the pyramids (right panel) (https://www.eso.org/public/teles-instr/elt/; Gilmozzi, 2013, respectively).

Kasper et al. (2021) discuss *A Roadmap for Exoearth Imaging with the ELT* and show an impressive image of the laser guide stars of the future ELT, reported in Fig. 65.

The technical first light for the ELT remains targeted for the end of 2027. All major contracts placed as of mid-2018 (more than 30) are compatible with this deadline. This is however very challenging and there is a natural risk that difficulties along the way impact this target. This is unavoidable when building such a one-of-a-kind huge and complex machine (https://elt.eso.org/about/faq/). It is important to mention a white paper about ESO-Athena synergy (Padovani et al., 2017).

5.4.3 Canadian Hydrogen Intensity Mapping Experiment: CHIME

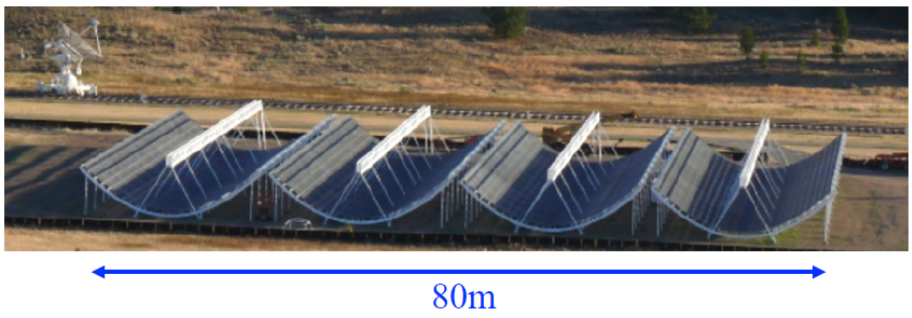

Figure 66: Canadian Hydrogen Intensity Mapping Experiment (Smith, 2019).

The Canadian Hydrogen Intensity Mapping Experiment (CHIME) (Fig. 66) is an interferometric radio telescope located at the Dominion Radio Astrophysical Observatory (DRAO) in British Columbia, Canada. It consists of four 100 x 20-meter semi-cylinders on which 1024 dual-polarization radio receivers sensitive to frequencies between 400-800 MHz are installed. The main aim of the project is to deepen the cosmological knowledge of the structure of the young universe, dark energy and the standard λCDM model, which better reproduces the observations of cosmology following the Big Bang (e.g. Bandura et al., 2014). The telescope was inaugurated on 7 September 2017 (Murray, 2018: http://www.astronomy.com/news/2018/03/chime-begins-its-cosmic-search).

CHIME is a digital telescope, which means all of its "imaging" is done digitally by software. CHIME has a 4 x 256 array of antennas and can form all 1024 independent beams in real time. Raw sensitivity is the same as the same 1024 single-feed radio telescopes (Smith, 2019).

A usual dish of a radio telescope is replaced by an array of antennas whose signals are digitized. by summing signals with appropriate delays, can simulate the dish in software, and focus on part of the sky. The telescope can be repointed by changing delays.

Starting from the preliminary detections of CO, [CII], Lyα and low-redshift 21cm, and a host of experiments set to go online in the next few years, the field is rapidly progressing on all fronts, with great anticipation for a flood of new exciting results, Kovetz et al. (2017) after reviewing the first detections reported to date, they survey the experimental landscape, presenting

the parameters and capabilities of relevant instruments such as COMAP, mmIMe, AIM-CO, CCAT-p, TIME, CONCERTO, CHIME, HIRAX, HERA, STARFIRE, MeerKAT/SKA and SPHEREx. Finally, they describe recent theoretical advances: different approaches to modeling line luminosity functions, several techniques to separate the desired signal from foregrounds, statistical methods to analyze the data, and frameworks to generate realistic intensity map simulations.

5.4.4 e-ASTROGAM Observatory

e-ASTROGAM (enhanced ASTROGAM) is a gamma-ray mission concept proposed as a response to the European Space Agency (ESA) Call for the fifth Medium-size mission (M5) of the Cosmic Vision Science Programme. The planned launch date is 2029.

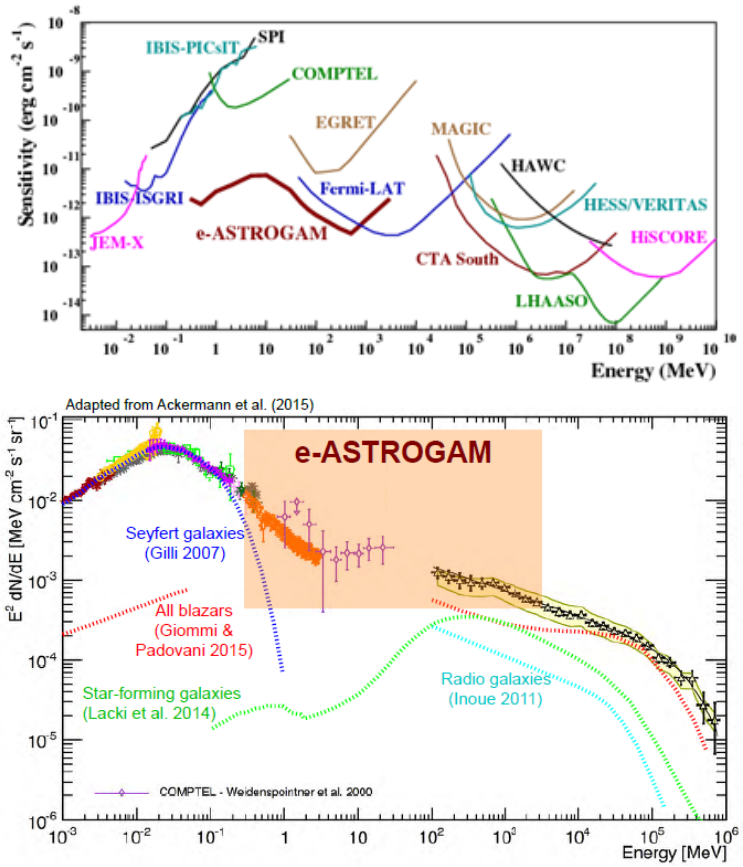

Figure 67: Upper panel: the sensitivity of e-ASTROGAM compared with those of the past, present and future experiments; lower panel: the compilation of measurements of extragalactic sources between 1 keV and 820 GeV, The semitransparent band indicates the energy region in which e-ASTROGAM will strongly improve on present knowledge (adopted from De Angelis, et al., 2017).

e-ASTROGAM is a breakthrough Observatory space mission, with a detector composed by a Silicon tracker, a calorimeter, and an anticoincidence system, dedicated to the study of the non-thermal Universe in the photon energy range from 0.3 MeV to 3 GeV - the lower energy limit can be pushed to energies as low as 150 keV, albeit with rapidly degrading angular resolution, for the tracker, and to 30 keV for calorimetric detection.

The mission is based on an advanced space-proven detector technology, with unprecedented sensitivity, angular and energy resolution, combined with polarimetric capability. Thanks to its performance in the MeV-GeV domain, substantially improving its predecessors, e-ASTROGAM will open a new window on the non-thermal Universe, making pioneering observations of the most powerful Galactic and extragalactic sources, elucidating the nature of their relativistic outflows and their effects on the surroundings (De Angelis, et al., 2017).

Figure 67 shows: in the upper panel the sensitivity of e-ASTROGAM compared with those of the past, present and future experiments; in the lower panel the compilation of measurements of extragalactic sources between 1 keV and 820 GeV, The semitransparent band indicates the energy region in which e-ASTROGAM will strongly improve on present knowledge (De Angelis, et al., 2017).

5.4.5 Imaging X-ray Polarimetry Explorer (IXPE)

The Imaging X-ray Polarimetry Explorer is the Instrument on board the SMEX mission IXPE. The IXPE mission, announced on 13 January 2017, is a NASA mission in partnership with the Italian space agency, Agenzia Spaziale Italiana (ASI). It has been launched at 1 a.m. EST on December 9, 2021.

The IXPE mission will fly three telescope systems capable of measuring the polarization of X-rays emitted by cosmic sources. ASI will contribute IXPE's three polarization-sensitive X-ray detectors which are designed, built and tested in Italy, and the use of its equatorial ground station located at Malindi, Kenya.

The focal plane Detector Units (DUs) and the Detector Service Unit (DSU) were developed by INAF-IAPS and INFN and were manufactured by OHB-IT.

NASA will supply the X-ray telescopes and use of its facilities to perform end-to-end X-ray calibration and science operations.

Ball Aerospace in Broomfield, Colorado, will provide the spacecraft and mission integration. Ball Aerospace will also operate the flight system with support from LASP (Laboratory for Atmospheric and Space Physics) at the University of Colorado at Boulder.

Other partners include Stanford University, Nagoya University and MIT (Massachusetts Institute of Technology) (http://ixpe.iaps.inaf.it/).

During the first two years of the mission, IXPE will open a new astrophysical 'window'. The main targets of the mission will be active galactic nuclei (AGN), microquasars, pulsars and pulsar wind nebulae, magnetars, X-ray binaries, supernova remnants and the galactic center. IXPE will provide contemporary polarization, variability, spectral and imaging measurements, thus allowing the study of the geometry and physical processes of radiation emission and particle acceleration, in environments with extreme magnetic and gravitational fields.

Many results have been obtained from the latter mentioned objects: e.g. Accreting Pulsars Cen X-3 (Tsygankov et al., 2022), GX 3012 (Suleimanov et al., 2023), EXO 2030+375 (Malacaria et al., 2023), 4U 1820-303 (Di Marco et al., 2023), 1A 0535+262 (Long et al., 2023), Vela X-1 (Forsblom et al., 2023), Black Hole Transient Swift J1727.8-1613 (Veledina et al., 2023), Seyfert galaxy NGC 4151 (Gianolli et al., 2023), Blazar Mrk 421 (Di Gesu et al., 2023), Stellar Mass Black Hole Cyg X-1 (Rodriguez-Cavero et al., 2023), Black Hole X-ray Binary 4U 1630-47 (Rodriguez-Cavero et al., 2023).

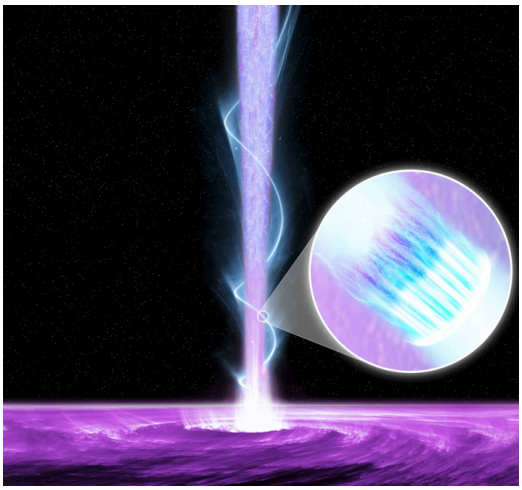

Figure 68: The structure of a black hole jet as inferred from recent observations of the Markarian 421 blazar with the IXPE (Di Gesu et al., 2023) (Credit: NASA/Pablo Garcia).

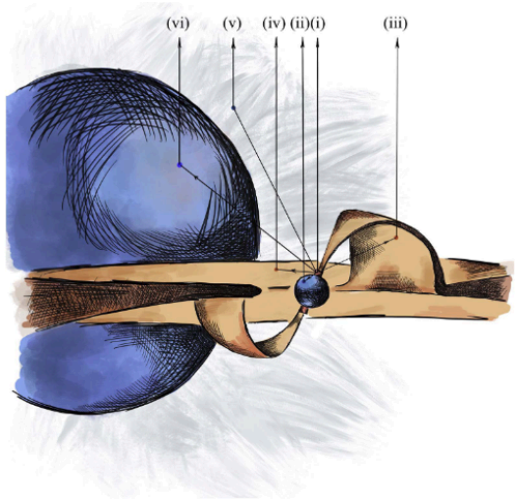

Figure 69: Schematic view of the system with the polarization mechanisms: (i) the intrinsic polarization from the hot spot, (ii) reflection from the NS surface, (iii) reflection from the accretion curtain, (iv) reflection from the accretion disk, (v) scattering by the stellar wind, and (vi) reflection by the optical companion (Tsygankov et al., 2022)

An artist's rendering (Fig. 68) shows the structure of a black hole jet as inferred from recent observations of the Markarian 421 blazar with the IXPE (Di Gesu et al., 2023). The jet is powered by the accretion disk shown at the bottom of the image, which is made up of material orbiting and falling into the black hole. The jet is pervaded by a helical magnetic field. Ixpe's observations showed that the X-rays must be generated in a shock found within material spiraling around the helical field lines. The inset shows the region that actively emits the light we observe. The X-rays are generated in the white region closest to the shock front, while the optical and radio emission must come from more turbulent regions further away from the shock.

Figure 69 shows schematically the geometry of the accreting pulsar Cen X-3, and the processes

occurring inside the system, thanks to the detection of polarization made by the IXPE (Tsygankov et al., 2022).

5.4.6 The James Webb Space Telescope (JWST)

The James Webb Space Telescope (JWST) will be a giant leap forward in our quest to understand the Universe and our origins. JWST will examine every phase of cosmic history: from the first luminous glows after the Big Bang to the formation of galaxies, stars, and planets to the evolution of our own solar system (https://jwst.nasa.gov/science.html).

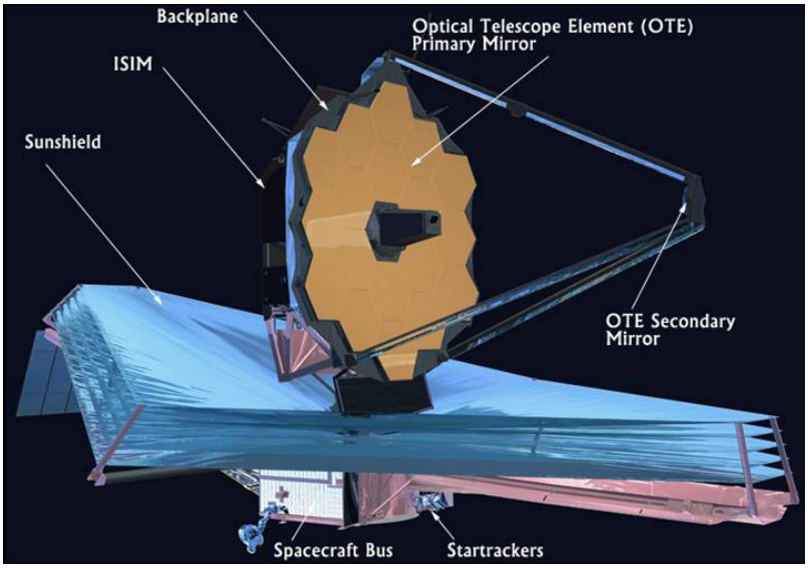

Figure 70: Sketch of the JWST (jwst.nasa.gov).

Webb often gets called the replacement for Hubble, but we prefer to call it a successor. After all, Webb is the scientific successor to Hubble; its science goals were motivated by results from Hubble. Hubble's science pushed us to look to longer wavelengths to "go beyond" what Hubble has already done. In particular, more distant objects are more highly redshifted, and their light is pushed from the UV and optical into the near-infrared. Thus observations of these distant objects (like the first galaxies formed in the Universe, for example) requires an infrared telescope.

This is the other reason that Webb is not a replacement for Hubble; its capabilities are not identical. Webb will primarily look at the Universe in the infrared, while Hubble studies it primarily at optical and ultraviolet wavelengths (though it has some infrared capability). Webb also has a much bigger mirror than Hubble. This larger light collecting area means that Webb can peer farther back into time than Hubble is capable of doing. Hubble is in a very close orbit around the earth, while Webb will be 1.5 x 10^6 km away at the second Lagrange (L2) point.

The backplane is the spine of the telescope and is the structure on which the mirrors and instruments will be mounted, as showed in Fig 70 (jwst.nasa.gov). The *Potential Science with JWST* can be found in a series of white papers at http://www.stsci.edu/jwst/about-jwst/history/white-papers.

A complete description of the JWST potential science is reported in the review paper by Gardner et al. (2006) A synthesis of the potential science that can be performed by the JWST is reported in the paper by Gardner (2009).

Figure 71: Upper left: The Hubble and Webb telescopes side by side comparisons visual gains of the Cluster of galaxies SMACS 0723 (Credit: NASA, ESA, CSA, STSc); Upper right: A portion of the "Cosmic Cliffs" of the Carina Nebula as captured by Hubble (top) and Webb (bottom). The infrared image from Webb allows us not only to see far greater detail, but to pierce through the nebula's clouds and see numerous objects beyond (Credit: Hubble Heritage/Space Telescope Science Institut/NASA, ESA, CSA, STScI, Webb ERO/Acknowledgement: N. Smith Et Al. (JHU)/STScI); Lower left: JWST has captured a new image of the famous Pillars of Creation — first imaged by the HST in 1995 — that reveals new details about the region(Credit: NASA, ESA, CSA, STScI; Joseph DePasquale (STScI), Anton M. Koekemoer (STScI), Alyssa Pagan (STScI); Lower right: Image of Saturn and some of its moons, captured by the JWST's NIRCam instrument on June 25, 2023. In this monochrome image, NIRCam filter F323N (3.23 microns) was color mapped with an orange hue [Credit: NASA, ESA, CSA, STScI, M. Tiscareno (SETI Institute), M. Hedman (University of Idaho), M. El Moutamid (Cornell University), M. Showalter (SETI Institute), L. Fletcher (University of Leicester), H. Hammel (AURA); image processing by J. DePasquale (STScI)].

After several delays, the JWST was scheduled for launch in 2021, based on recommendations by an Independent Review Board. Finally JWST was launched from the Guaiana Space Center, Korou, French Guaiana on December 25, 2021 at 1:20 PM CET.

Among the other extraordinary capabilities of JWST, a particular attention can be devoted to the infrared telescope: it will help us see almost every part of our universe in greater detail, including the most distant galaxies, allowing us a glimpse into the past.

Just to understand the enormous capabilities of the JWST, Fig. 71 reports several examples of images in comparison with those of the HST, and the splendid image of Saturn with several satellites.

5.4.7 The GAMMA-400 gamma-ray telescope

The GAMMA-400 gamma-ray telescope: the next absolutely necessary step in the development of extraterrestrial high-energy γ-ray astronomy is the improvement of the physical and technical characteristics of γ-ray telescopes, especially the angular and energy resolutions. Such a

new generation telescope will be GAMMA-400, which will be installed onboard the Russian space observatory (Cumani et al., 2015; Galper, Topchiev & Yurkin, 2018).

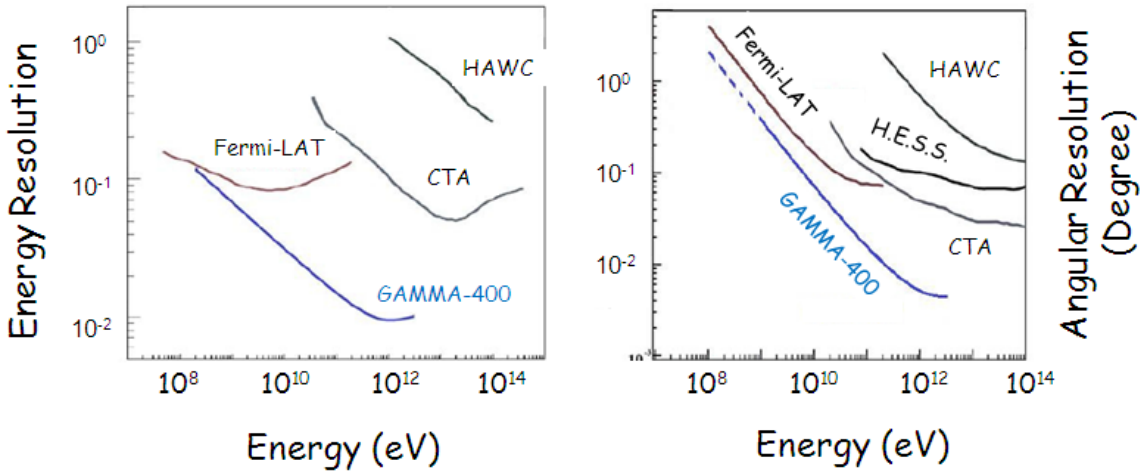

Figure 72: Energy and angular resolutions of GAMMA-400 versus other experiments (adapted from Topchiev et al., 2015).

The GAMMA-400 gamma-ray telescope is intended to measure the fluxes of gamma-rays and cosmic-ray electrons and positrons in the energy range from 100 MeV to several TeV. Such measurements concern the following scientific tasks: investigation of point sources of gamma-rays, studies of the energy spectra of Galactic and extragalactic diffuse emission, studies of gamma-ray bursts and gamma-ray emission from the Sun, as well as high precision measurements of spectra of high-energy electrons and positrons. Also the GAMMA- 400 instrument provides the possibility for protons and nuclei measurements up to knee. But the main goal for the GAMMA-400 mission is to perform a sensitive search for signatures of dark matter particles in high-energy gamma-ray emission (Topchiev et al., 2017a, 2019 and the references therein).

The GAMMA-400 will operate in the highly elliptic orbit continuously for a long time with the unprecedented angular ($\sim 0.01^\circ$ at $E_\gamma = 100$ GeV) and energy ($\sim 1\%$ at $E_\gamma = 100$ GeV) resolutions better than the Fermi-LAT, as well as ground γ-ray telescopes, by a factor of 5-10. GAMMA-400 will permit to resolve γ-rays from annihilation or decay of dark matter particles, identify many discrete sources (many of which are variable), to clarify the structure of extended sources, to specify the data on the diffuse emission (Topchiev et al., 2017b). Figure 72 shows the energy and angular resolutions of GAMMA-400 versus other experiments (Topchiev et al., 2015). In April 2020, Lavochkin Scientific development and production center Director General Vladimir Kolmykov announced that tha launch is planned for 2030.

5.4.8 The BICEP (Background Imaging of Cosmic Extragalactic Polarization) and the Keck Array

The BICEP (Background Imaging of Cosmic Extragalactic Polarization) and the Keck Array are a series of cosmic microwave background (CMB) experiments. They aim to measure the polarization of the CMB; in particular, measuring the B-mode of the CMB. The experiments have had four generations of instrumentation, consisting of BICEP1, BICEP2, the Keck Array, and BICEP3.

These experiments are observing from the South Pole, and their aims are to discover signatures of Inflation by actually detecting the Cosmic Gravitational Background (CGB) via its weak imprint as the unique B-mode polarization signature of the CMB, directly probing the Universe at an earlier time than ever before. Each generation represents a large increase in sensitivity to B-mode polarization. BICEP1 observed from 2006-2008 with 98 detectors, BICEP2 began observing in the beginning of 2010 with 512 detectors, and the first three of five Keck Array telescopes began observing in the beginning of 2011, each with 512 detectors. The final two Keck Array receivers were deployed during the summer season of 2012. BICEP3, with a total of 2,560 detectors, has been operational since May 2016.

Figure 73 shows the installation of the BICEP experiment at the South Pole which is near the middle of the Antarctic plateau, the driest environment on the planet.

The main goal of BICEP experiments is to test the validity of the theory of the Inflation (Keating et al., 2003a,b; Ogburn IV et al., 2010).

Figure 73: BICEP experiment at the South Pole (https://physicsforme.com/tag/bicep2/).

In particular, if Inflation happened immediately after the Big Bang, it would have produced turbulence in the structure of space-time itself-gravitational waves like the kind LIGO detected recently. While these waves would be too weak for LIGO to see, they would twist the orientation of the light, which is known as polarization.

A few years ago the collaboration of the BICEP2 experiment claimed the detection of E-mode (Crites et al., 2015) and B-mode polarization of the CMB at at 7.0 σ significance (Ade et al., 2015). If B-mode polarization could be confirmed, the inflationary model of the Universe would be definitively confirmed, also. However, big discoveries need big confirmations. For a robust detection of B-modes, independent measurements and precise measurements of polarized foregrounds are mandatory.

Indeed, a key element to the primordial interpretation advanced by the BICEP2 team was excluding an explanation based on polarized thermal dust emission from our galaxy (Bucher, 2015a,b). An independent analysis casted doubt on the BICEP2 claim (Flauger, Hill & Spergel, 2014). In September 2014 the Planck team published a paper on the level of polarized dust emission measured across the whole sky, and in particular in the BICEP2 field (Planck Collaboration,

2014). This work also extrapolated the polarized dust signal seen in the Planck 353 GHz map (a frequency in the Wien tail of the CMB blackbody where dust dominates) down to 150 GHz and reached the conclusion that the BICEP B mode signal could be entirely explained by polarized dust emission although a primordial B mode contribution could not be ruled out.

Indeed it is important to remark that the detection of the primordial B modes has not been achieved yet, not only because it is an extremely faint signal, but also because of contamination by foregrounds that emit at the same frequencies, most noticeably the galactic thermal dust emission.

However, the theory of inflation is criticized by Ijjas, Steinhardt & Loeb (2013) after Planck2013 results. They suggest that the origin of the Universe is not the Big Bang, but could be a "bouncing" Universe that does not need the inflation. Membrane-Universes that clashed endlessly could be a "plausible" alternative model for the Universe (Erickson et al., 2007; Steinhardt, Turok & Starkman, 2008). Cyclic models of the universe have the advantage of avoiding initial conditions problems related to postulating any sort of beginning in time (Ijjas, 2018; Ijjas & Steinhardt, 2018).

For all these reasons is even more important to find an experimental proof of the Inflation.

In order to find unequivocal experimental proof of the primordial polarization of the CMB, BICEP Array has been developed and described by Ade et al., (2021a). They report the performance of BICEP3, which has been observing CMB polarization from the South Pole since 2016. The three-year data set, from 2016-2018, reached a map depth of 2.8 K-arcmin (46 nK-deg) over an effective area of 584.9 square degrees, corresponding to a total sensitivity of T = 1.3 nK. A suite of jackknife shows possible sources of systematic false polarization are controlled below the level of statistical sensitivity in each test. Ade et al. (2021b) present results from an analysis of all data taken by the BICEP2, Keck Array and BICEP3 CMB polarization experiments up to and including the 2018 observing season. They add additional Keck Array observations at 220 GHz and BICEP3 observations at 95 GHz to the previous 95/150/220 GHz data set. They find the strongest constraints to date on primordial gravitational waves.

5.4.9 LSPE (Large Scale Polarization Explorer)

The Large Scale Polarization Explorer (LSPE) is designed to measure the polarization of the CMB at large angular scales, and in particular to constrain the curl component of CMB polarization (B-mode). This is produced by tensor perturbations generated during cosmic inflation in the very early Universe (Seljak & Zaldarriaga, 1997; Kamionkowski & Kovetz, 2016). The level of this signal is unknown: current inflation models are unable to provide a firm reference value. However, the detection of this signal would be of utmost importance, providing a way to measure the energy-scale of inflation and a window on the physics at extremely high energies. While the level of CMB temperature anisotropy is of the order of 100 μK r.m.s. and the level of the gradient component of CMB polarization (E-mode generated by scalar – density perturbations) is of the order of 3 μK, the current upper limits for the level of B-mode polarization are a fraction of μK, corresponding to a ratio between the amplitude of tensor perturbations and the amplitude of scalar perturbations (tensor-to-scalar ratio) $r < 0.044$ at 95% confidence level, combining data from the Planck satellite and the BICEP/Keck ground telescopes (Aghanim et al., 2020; Tristram et al., 2021; Ade et al., 2018). The B-mode of inflationary origin is observable at large angular scales, greater than 1.5 deg. The main scientific target of LSPE is to improve this limit.

Two instruments will be used:

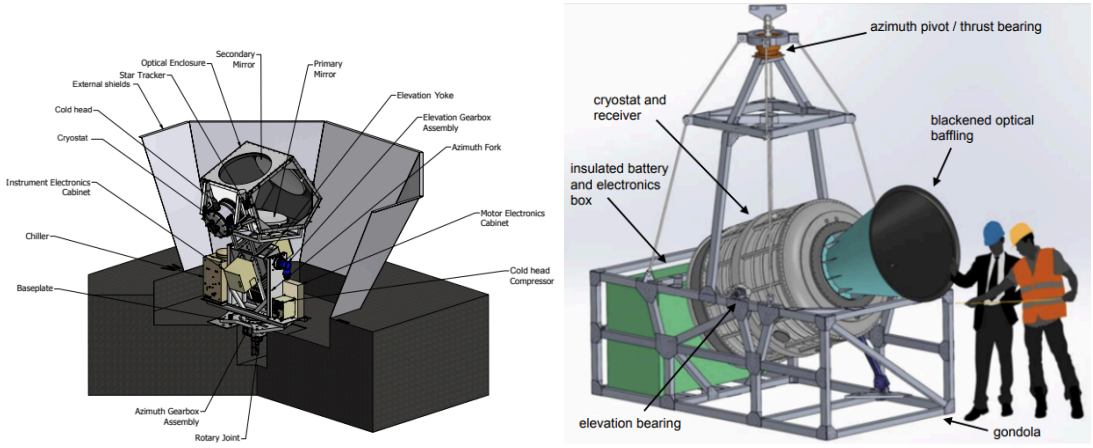

Figure 74: Left panel: LSPE-Strip optical system overview. The mirrors are held inside a co-moving optical enclosure. Right panel: LSPE-SWIPE overview. The instrument is contained in a large liquid Helium cryostat, which also contains the optical elements, including the HWP based Stokes polarimeter. The on-board electronics and the Lithium batteries based power system are contained in an Aerogel insulated box, to optimize thermal balance (adopted from Addamo et al., 2021).

- LSPE-Strip is a coherent polarimeter array that will observe the microwave sky from the Teide Observatory in Tenerife in two frequency bands centred at 43 GHz (Q-band, 49 receivers) and 95 GHz (W-band, 6 receivers) through a dual-reflector crossed-Dragone telescope of $\sim$ 1.5 m projected aperture.

- LSPE-SWIPE (Short-Wavelength Instrument for the Polarization Explorer) is a mm-wave polarimeter operated onboard a stratospheric balloon. The general idea of SWIPE is to use a cryogenic rotating Half-Wave Plate to modulate the incoming polarized radiation and to maximize the sensitivity to CMB polarization at large scales using a very wide focal plane populated with multi-moded bolometers.

Figure 74 shows: LSPE-Strip optical system overview (left panel) and LSPE-SWIPE overview (right panel) (Addamo et al., 2021).

5.4.10 QUBIC Experiment

QUBIC is an experiment based on the concept of bolometric interferometry and designed to constrain tightly the B-mode polarization anisotropies of the CMB (Mennella et al., 2018, 2019; Piat et al., 2019; Mele et al., 2020; Battistelli et al., 2020).

B-mode searches need multi-frequency sensitive instruments to control foreground contamination, and an unprecedented level of control of systematic effects that should be designed in-hardware, as much as possible.

QUBIC is designed to address all aspects of this challenge with a novel kind of instrument, a Bolometric Interferometer, combining the background-limited sensitivity of Transition-Edge-Sensors and the control of systematics allowed by the observation of interference fringe patterns, while operating at two frequencies to disentangle polarized foregrounds from primordial B mode

polarization. de Bernardis et al. (2018) made an accurate analysis of the scientific results that could be brought by the QUBIC experiment.

QUBIC is the only European ground based B-mode project with the scientific potential of discovering and measuring B-modes. It is the natural project for the European CMB community to continue at the edge cutting level it has reached with Planck (https://www.roma2.infn.it/node/588).

The first QUBIC module is operating since 2018 from the ground, observing the sky in two spectral bands centred at 150 and 220 GHz, and has been installed in Alto Chorrillos, province of Salta, Argentina (Scóccola et al., 2021).

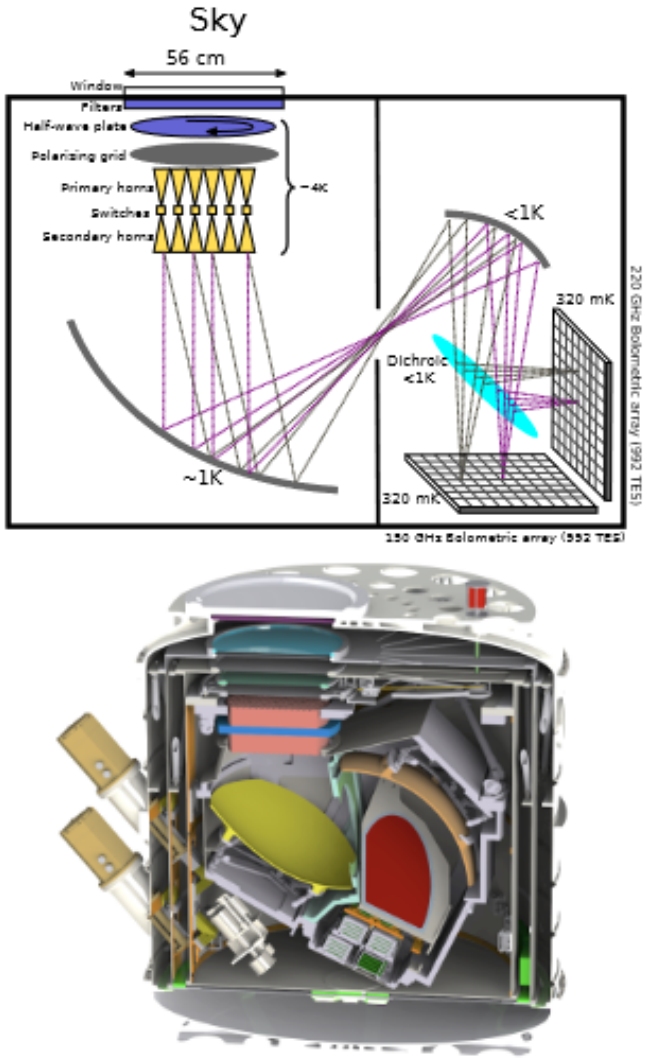

Figure 75: Schematic of the QUBIC instrument (top) and sectional cut of the cryostat (bottom) showing the same sub-systems in their real configuration (adopted from O'Sullivan et al., 2021).

Figure 75 shows the schematic of the QUBIC instrument (top) and sectional cut of the cryostat (bottom) showing the same sub-systems in their real configuration (O'Sullivan et al., 2021).

5.4.11 Square Kilometre Array

From the SKA Global Headquarters, Friday 19 December 2019 the good news has been reported: *An independent panel of external reviewers from major astronomy projects has given the SKA's overall design, costing & planning the nod, clearing the way for the preparation of the SKA construction proposal*.

Figure 76: Left panel: South Africa's MeerKAT radiotelescope is the prototype for the SKA. Credit: South African Radio Astronomy Observatory. Right panel: The stunning radio image obtained by MeerKAT shows the central portions of the Milky Way galaxy. Its plane, marked by a series of bright features, runs horizontally through the image, while the newly discovered radio bubbles extend vertically above and below. (Credit: SARAO. Adapted from results published in Heywood et al., 2019.)

The Square Kilometre Array (SKA) is a planned large radio interferometer designed to operate over a wide range of frequencies, and with an order of magnitude greater sensitivity and survey speed than any current radio telescope. The SKA will address many important topics in astronomy, ranging from planet formation to distant galaxies (Weltman et al., 2018). In their work, they consider the perspective of the SKA as a facility for studying physics. They review four areas in which the SKA is expected to make major contributions to our understanding of fundamental physics: cosmic dawn and reionisation; gravity and gravitational radiation; cosmology and dark energy; and dark matter and astroparticle physics. These discussions demonstrate that the SKA will be a spectacular physics machine, which will provide many new breakthroughs and novel insights on matter, energy and spacetime.

Figure 76 (left panel) shows the South Africa's MeerKAT radiotelescope which is the prototype for the SKA. Figure 76 (right panel) shows the impressive result coming from MeerKAT radiotelescope about the central portion of our Galaxy (Credit: SARAO – adapted from Heywood et al. (2019).

5.5 Cosmic Ray Physics Experiments

In two past experiments (Milagro and ARGO-YBJ) the limited capability to discriminate the background was mainly due to the small dimensions of the central detectors (pond and carpet). For this reason in the new experiments, like HAWC and LHAASO, the discrimination of the CR background is made studying shower characteristics far from the shower core (at distances R $>$ 40 m from the core, the dimension of the Milagro and ARGO-YBJ detectors). Milagro developed

analysis techniques for CR background discrimination only when the array of small tanks was added and the instrumented area enlarged.

5.5.1 HAWC (High-Altitude Water Cherenkov Gamma-ray Observatory)

The HAWC is a great example of collaboration among humans. In the following I report the Statement from the HAWC Leadership (March 24, 2021) (https://www.hawc-observatory.org/):

The HAWC Collaboration stands in solidarity with the Asian, Desi, and Pacific Islander community and against hate and racism. We are outraged by the recent horrific crime in Atlanta that we see as part of a larger pattern of discrimination and racism targeting Asian Americans. As in our message of June 8, 2020 (below), we reiterate our belief that scientific discoveries are made not by hardware, but by people and that we can only achieve the best scientific results when we include people of all ethnicities, races, gender identities, and backgrounds in the process. We also believe that it is our role to speak out against violence, discrimination and oppression wherever it occurs. We once again pledge to do more to bring change to our collaboration, our institutions, our countries and society as a whole.

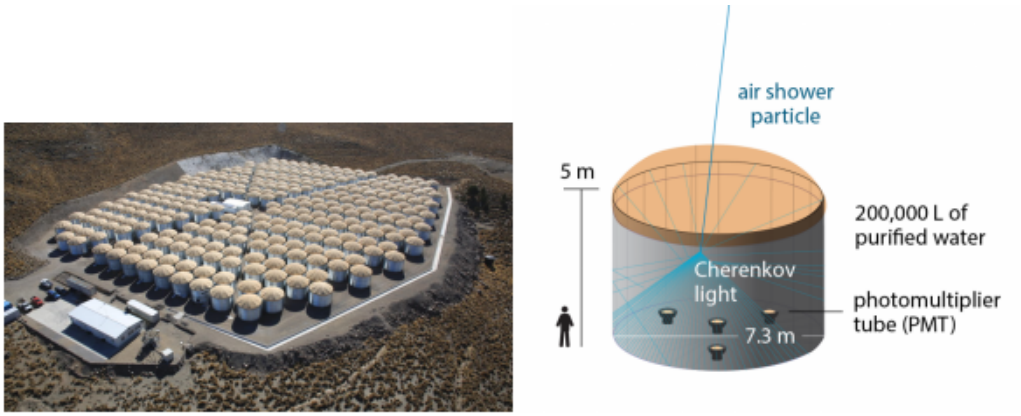

Figure 77: Layout of the HAWC experiment. The sketch of a water tank is shown on the right side (adopted from Di Sciascio, 2019).

HAWC is a highly competitive cosmic ray and gamma ray observatory installed in Mexico, within the Pico de Orizaba National Park, and therefore with the leading participation of a Mexican scientific community. HAWC is distinguished globally by its unique ability to monitor two-thirds of the sky deep enough to detect the emission of gamma rays with TeV energies from the Crab Nebula each sidereal day. Built based on the experience of MILAGRO, the first Cherenkov water observatory capable of efficiently discriminating atmospheric cascades produced by gamma rays from those caused by cosmic rays, and thus clearly detecting celestial sources of very high energy photons, HAWC benefits from a optimized layout and a high altitude site. After a year and a half of partial operation with a third of the array up and running, HAWC went into 100% operation on March 20, 2015. In addition to confirming with much greater scope the main results of MILAGRO, such as the Nebula detections of the Crab and the blazar Mrk 421, and the anisotropy in the distribution of cosmic rays, in two years of operation with the complete array HAWC has clearly detected some 40 sources in the Galactic Plane, several of them for the first time; has drawn

continuous light curves of the Crab, Mrk 421 and Mrk 501 (Abeysekara et al., 2017a); reported bursts from these active galaxies; and tracked episodic events in other bands of the electromagnetic or neutrino spectrum and gravitational waves. To date, HAWC has scanned two-thirds of the sky with a depth of 1/20 of the flow of the Crab Nebula, being the only detector with this capability in the world (https://www.hawc-observatory.org/support/redhawc.php).

HAWC consists of an array of 300 water Cherenkov detectors made from 5 m high, 7.32 m diameter, water storage thanks covering an instrumental area of $\sim$ 22,000 m^2 (the actual thank coverage is $\sim$ 12,550 m^2 with a coverage factor $<$ 60%). Figure 77 shows the layout of the HAWC experiment. The sketch of a water tank is shown on the right side (Di Sciascio, 2019).

The first HAWC catalog of TeV gamma-ray sources is reported in the paper by Abeysekara et al. (2017b).

5.5.2 LHAASO (Large High Altitude Air Shower Observatory)

The Large High Altitude Air Shower Observatory (LHAASO), thanks to the large area of the km^2 array and the high capability of background rejection, can reach sensitivities above 30 TeV range $\sim$ 100 times higher than that of current instruments, offering the possibility to monitor for the first time the γ-ray sky up to PeV energies. In addition, at sub-TeV and TeV energies LHAASO will continuously observe all the Northern flaring gamma-ray sky with a sensitivity of a few percent of the Crab Nebula flux.

LHAASO will enable studies in CR physics and γ-ray astronomy that are unattainable with the current suite of instruments (He, for Lhaaso Collaboration, 2015). LHAASO will perform an unbiased sky survey of the Northern sky with a detection threshold better than 10% Crab units at sub-TeV/TeV and 100 TeV energies in one year. This unique detector will be capable of continuously surveying the γ-ray sky for steady and transient sources from a few hundred GeV to the PeV energy domain. From its location LHAASO will observe at TeV energies and with high sensitivity about 30 of the sources catalogued by Fermi-LAT at lower energy, monitoring the variability of 15 AGNs (mainly blazars) at least (Di Sciascio et al., 2016; Di Sciascio, 2019).

Figure 78 shows the integral sensitivity of LHAASO as a function of the energy compared to HAWC, HESS, MAGIC II and CTA-South sensitivities (Di Sciascio, 2019).

The LHAASO plans to build a hybrid extensive air shower (EAS) array with an area of about 1 km^2 at an altitude of 4410 m a.s.l. in Sichuan province, China, aiming at very high energy γ-ray astronomy and cosmic ray physics around the spectrum knees. With an extensive air shower array covering an area of 1.3 km^2 equipped with $>$ 40,000 m^2 muon detectors and 78,000 m^2 water Cherenkov detector array, a sensitivity of about 1% Crab unit to gamma ray sources is achieved at $2\times$ 10^{12} eV and $5\times$ 10^{13} eV, thus the LHAASO will survey the entire northern sky for γ-ray sources with full duty cycle and high sensitivity. The spectra of all sources in its field of view will be measured simultaneously over a wide energy range from from 10^{11} eV to 10^{15} eV. This measurement will offer a great opportunity for identifying cosmic ray origins among the sources. The LHAASO is also equipped with 12 Cherenkov/fluorescence telescopes, so it will serve as an effective detector for energy spectrum measurement of different mass groups of cosmic rays over a wide energy range from 10^{14} eV to 10^{18} eV (He, 2019).

The status of the LHAASO Experiment is the following: civil construction started in the middle of 2016. One year later, a 35 kV power transmission line was ready, climbing 29 km from an

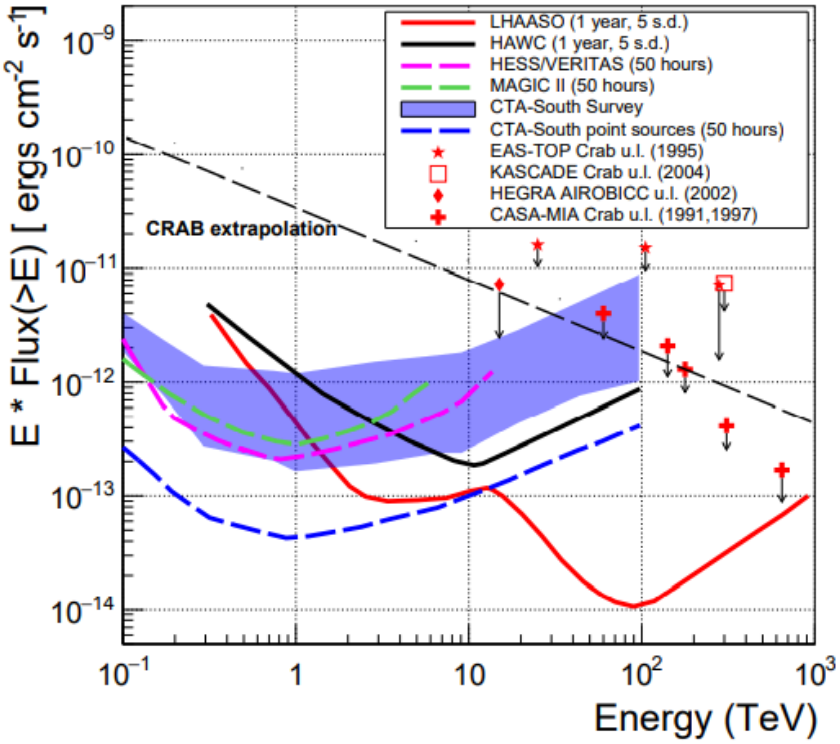

Figure 78: Integral sensitivity of LHAASO as a function of the energy compared to HAWC, HESS, MAGIC II and CTA-South sensitivities. The CTA-South sensitivity to sky survey is also shown. Upper limits to ultra high-energy γ-ray emission set by different experiments in the Northern hemisphere are also reported (adopted from Di Sciascio, 2019).

Figure 79: Photos of the LHAASO site in November 2017 (left) and in July 2019 (right) (Adopted from He, 2019).

altitude of 3,800 m up to 4,410 m a.s.l.. In November 2017, the site was ready for construction of the water pools, and roads with a total length of about 20 km were built to reach each MD (Muon Detector) as shown in Fig. 79 (left), and in July 2019 (right) (He, 2019).

5.5.3 TAIGA (Tunka Advanced Instrument for cosmic ray physics and Gamma Astronomy)

The study of energy spectrum and mass composition of cosmic rays (CR) in the range of $10^{15} - 10^{18}$ eV is of crucial importance for the understanding of origin and propagation of CR in

the Galaxy. For the energy range of gamma quanta above 30 TeV there are a number of fundamental questions which presently have no answers, and first of all this is the question on the sources of Galactic cosmic rays with $\sim$ PeV energies, the energy region proximately adjoining the classical knee in the all-particle energy spectrum. It should be noted that to date there was not detected a single photon with an energy more than 80 TeV (Tkachev et al., 2018).

The γ-ray observatory TAIGA is designed to study the flux of gamma rays and charged cosmic rays in the energy range of 10^{13}˘10^{18} eV (Budnev, et al., 2016). The installation will include a network of 500 wide field of view (FOV $\sim$ 0.6 sr) timing Cherenkov light detectors, named TAIGA-HiSCORE (High Sensitivity Cosmic Origin Explorer) (Tluczykont et al., 2014), and up to 16 imaging atmospheric Cherenkov telescopes (IACTs) with shower image analysis (FOV $\sim$ 10×10 degrees), covering an area of 5 km^2, and muon detectors with a total sensitive area of 2000 m^2, distributed over an area of 1 km^2. The observatory is placed in the Tunka valley (50 km from Lake Baikal) at the same place where the EAS Cherenkov array Tunka-133 is located (Berezhnev et al., 2012).

Thus there are three arrays to study charged CRs in operation at the Tunka site: Tunka-133 (Berezhnev et al, 2012), Tunka-Rex and Tunka-Grande (Prosin et al, 2016), as shown in Fig. 80 (Budnev et al., 2017). Their measurement of the energy spectrum and mass composition is important in order to understand the acceleration limit of the Galactic CR sources and the transition from Galactic to extragalactic CR.

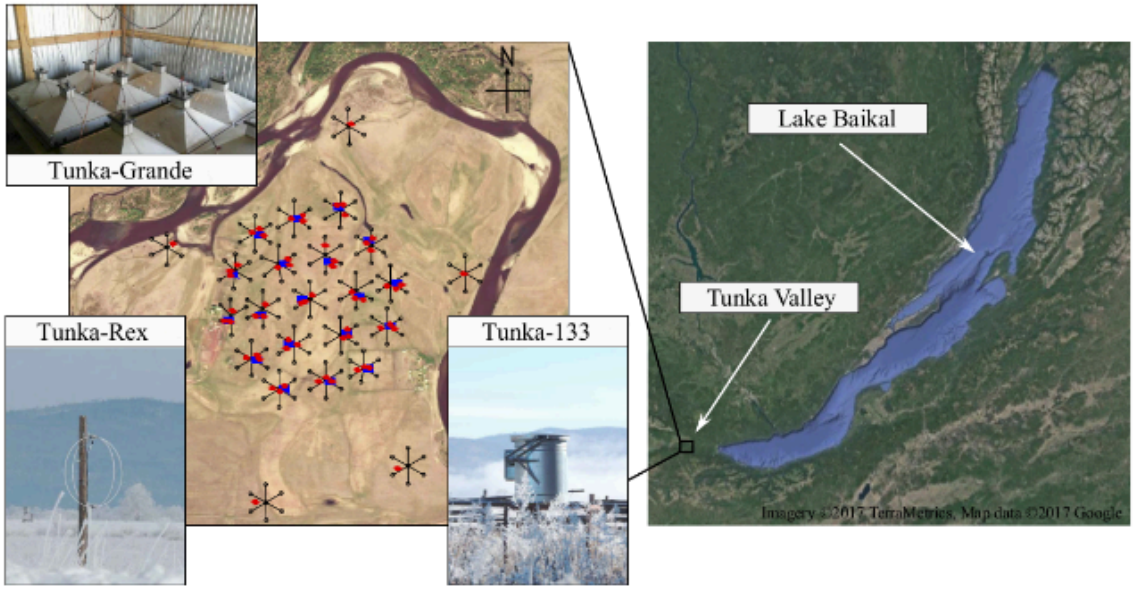

Figure 80: The EAS arrays for studying cosmic rays in Tunka Valley (adopted from Budnev et al., 2017).

The advantage of IACT telescopes combined with a wide-angle timing array is the possibility to use the information about the EAS characteristics (core position, direction, energy) for a separation of the CR events from the gamma rays, that can be better reconstructed by the timing array than by a single IACT. This allows, even for a distance between the IACTs of up to 600 m, to maintain a level of rejection $\sim$ 0.01 of showers induced by CRs at the energy of 100 TeV. So TAIGA is

a hybrid detector, combining the imaging with the non-imaging technique of the EAS Cherenkov radiation measurements (Tkachev et al., 2018).

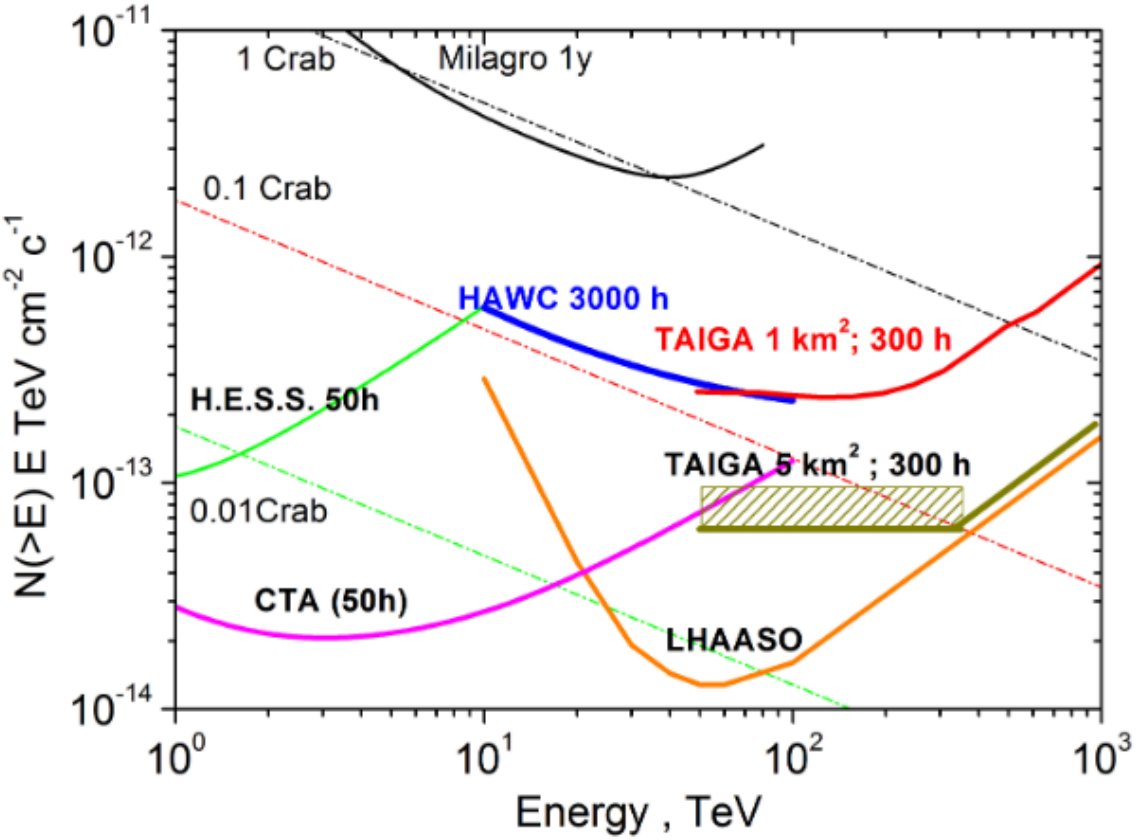

Figure 81: Integral sensitivity of TAIGA Experiment for detection of local sources in comparison with other experiments (adopted from Budnev et al., 2017).

The expected integral sensitivity of the 1 km^2 TAIGA setup for 300 hours source observation with at energy 100 TeV will be about 2.5×10^{13} TeV cm^2 sec^1 will surpass the sensitivity of operated and planned installations in the ultra-high energy range, as shown in Fig. 81 (Budnev et al., 2017). With such an array it would be possible to solve the following objectives:

- Study of the high-energy edge of the spectrum of the most bright galactic gamma-ray sources.
- Search for Galactic Pevatrons.
- Apply the new hybrid approach (common operation of IACTs, wide-angle timing array and muon detectors) for studying the cosmic rays mass composition in the "knee" region ($10^{14}10^{16}$ eV).
- Explore the high energy region of the energy spectrum of the brightest extragalactic source Mkr 421.
- Study of CR anisotropy in the energy region 1003000 TeV.

Important results from Tunka-133 have been reported in Fig. 82 (Budnev et al., 2021). The spectrum is compared to results from other experiments: KASCADE (Antoni et al., 2003), EAS-TOP (Aglietta et al., 1999), Tibet (Amenomori et al., 2008), IceTop (Aartsen et al., 2013). All the spectra are practically indistinguishable at the energy of the first (classical) knee.

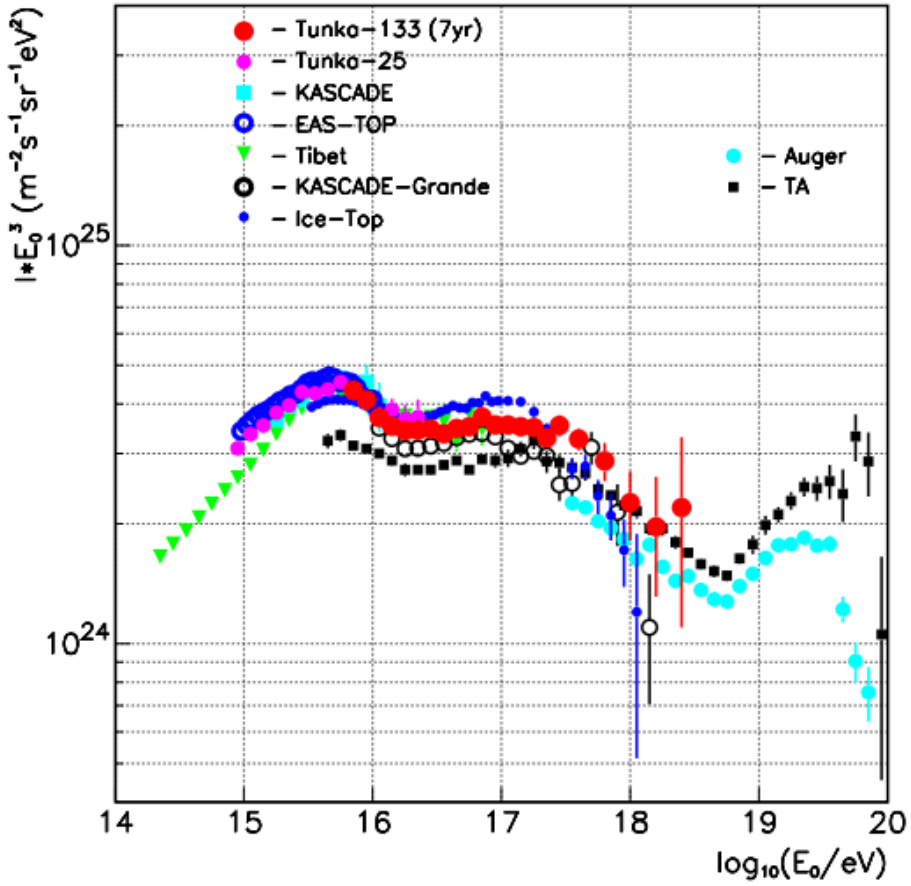

Figure 82: Comparison of energy spectra obtained at the Tunka site to other experimental results (adopted from Budnev et al., 2021).

The Tunka-133 spectrum can be described as follows:

- The primary CR energy spectrum in the range of $6 \times 10^{15} - 10^{18}$ eV has a number of features: the spectrum becomes harder (the index changes from $\gamma = 3.28 \pm 0.01$ to $\gamma = 2.99 \pm 0.01$) at $E_0 = 2 \times 10^{16}$ eV and steeper ($\gamma = 3.29 \pm 0.09$) at $E_0 = 3 \times 10^{17}$ eV.
- In the energy range of $10^{16} - 10^{17}$ eV, the observed spectrum is consistent with spectra of KASCADE-Grande (Apel et al., 2012) and IceTop (Aartsen et al., 2013).
- Beyond the energy of 10^{17} eV, the Tunka-133 spectrum is consistent with those from the Telescope Array (Abu-Zayyad et al., 2013) and the Pierre Auger Observatory (Schulz, 2013).

Moreover, the TAIGA experiment will be the northernmost γ-ray experiment, and its location provides advantages for observation of the sources with large declinations. So, γ-ray source in the

Tycho SNR, virtually inaccessible for HAWC (HAWC website: http://www.hawc-observatory.org/) and LHAASO (Di Sciascio, 2016) will be in the field of view of the TAIGA during 500 hours per year.

Of course the list of big experiments is far to be complete, but it is enough to show to the reader the efforts that the international scientific community are facing both for determining the frontier scientific tests to validate the current theories and for the difficulties in providing sufficient budgets for their realization.

6. Habitable Zone in the Milky Way and Exoplanets

The most important questions about the possible origin of life in our Universe became a real scientific question in the last couple decades when it appeared a near certainty that other planets must orbit other stars. And yet, it could not be proven, until the early 1990's. Then, radio and optical astronomers detected small changes in stellar emission which revealed the presence of first a few, and now many, planetary systems around other stars. We call these planets "exoplanets" to distinguish them from our own solar system neighbors (http://science.nasa.gov/astrophysics/focus-areas/exoplanet-exploration/).

Figure 83 shows the cumulative detection per year by using different techniques updated to 12th November 2021 (exoplanetarchive.ipac.caltech.edu).

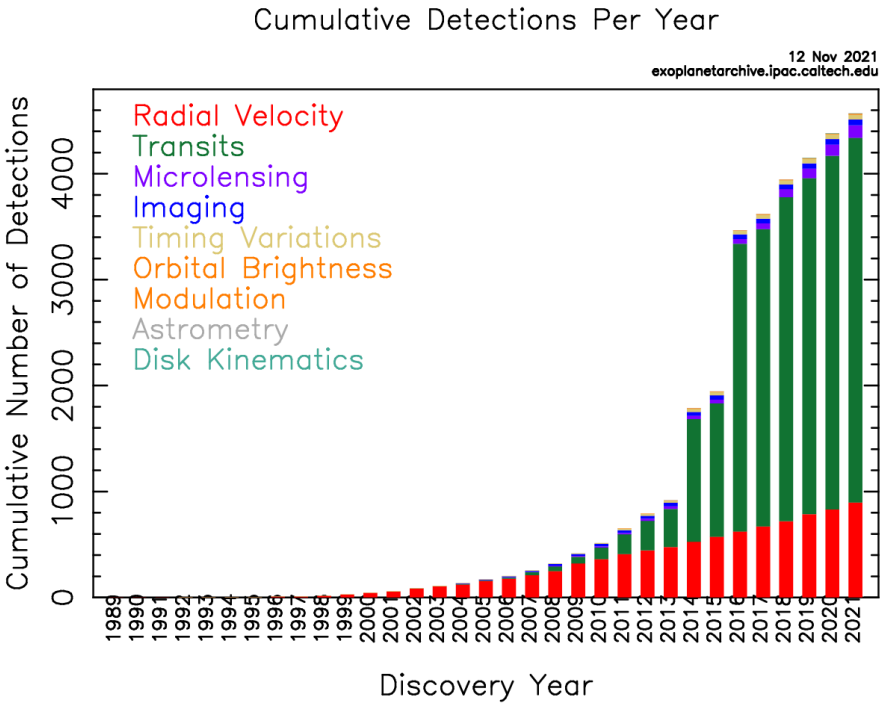

Figure 83: Cumulative number of detections of exoplanets per year, updated to 12th November 2021 (adopted from exoplanetarchive.ipac.caltech.edu)

From the *Open Exoplanet Catalog* updated to Sunday October 3 16:24:54 2021 (*), we know 4572 confirmed exoplanets, 4700 planets (including Solar System objects and unconfirmed exoplanets), 3493 planetary systems, 180 binary systems (http://www.openexoplanetcatalogue.com).

The number of discovered planets is growing very fast. Indeed on June 20, 2022 Kepler mission gives 8793 candidate exoplanets and a number of confirmed exoplanets equal to 5054, within these 3789 planetary systems solar-like.

(*) List of contributors: Andrew Tribick, Christian Sturm, Hanno Rein, Ryan Varley, Jaroslav Merc, Marc-Antoine Martinod, Knutover, Tobias Mueller, Landrok, Allen B. Davis, Sol-D, Daveshoszowski, Marc-Antoine, Kenneth J Cott, Christian Sturm, Ewan Douglas, Cadenarmstrong, Kevin Knittel, James Gregory, Miguel De Val-Borro, Darryl Hemsley, Paul A. Wilson, Florian Cabot, Everett Schlawin, Allen Davis, Paul Zwerger, Rajeev-Jeyaraj, Senger Hanno, Paul Anthony Wilson, Callum Rodwell, Diamondraph, Planetaryscience, Dave, Randomcoinforall, Orome, Claudionor Buzzo Raymundo, Dobb13, Allen Davis

We have gone from suspecting exoplanets existed to knowing that there are more exoplanets than stars in our galaxy.

Figure 84 shows the distribution of Kepler planet candidates by size as of July 23, 2015 (Image Credit: NASA Ames/W Stenzel). As we can see there are 955 Earth-like planets in the neighbourhood of solar system.

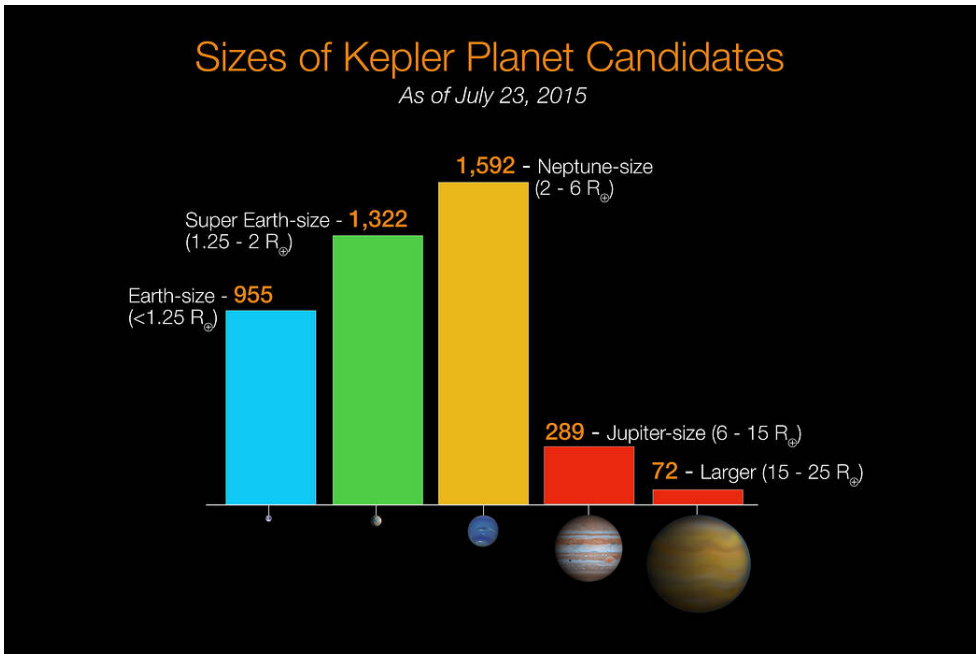

Figure 84: The distribution of Kepler planet candidates by size as of July 23, 2015 (Image Credit: NASA Ames/W Stenzel).

One of the most exiting result of Kepler mission was the discovery of the planets orbiting around Kepler-62 star (Borucki et al., 2013). They present the detection of five planets – Kepler-62b, c, d, e, and f – of size 1.31, 0.54, 1.95, 1.61 and 1.41 Earth radii ($R_\oplus$), orbiting a K2V star at periods of 5.7, 12.4, 18.2, 122.4 and 267.3 days, respectively. The outermost planets (Kepler-62e

& -62f) are super-Earth-size (1.25 $<$ planet radius $\leq$ 2.0 $R_{\oplus}$) planets in the habitable zone (HZ) of their host star, receiving 1.2 ± 0.2 and 0.41 ± 0.05 times the solar flux at Earth's orbit ($S_{\odot}$). Theoretical models of Kepler-62e and -62f for a stellar age of $\sim$ 7 Gyr suggest that both planets could be solid: either with a rocky composition or composed of mostly solid water in their bulk.

Figure 85 shows an artistic picture of the comparison of the planetary system around the star Kepler-62 with our own Solar System (https://www.nasa.gov /content/kepler-62-and-the-solar-system – Image credit: NASA Ames/JPL-Cal tech; Last Updated: Aug 7, 2017).

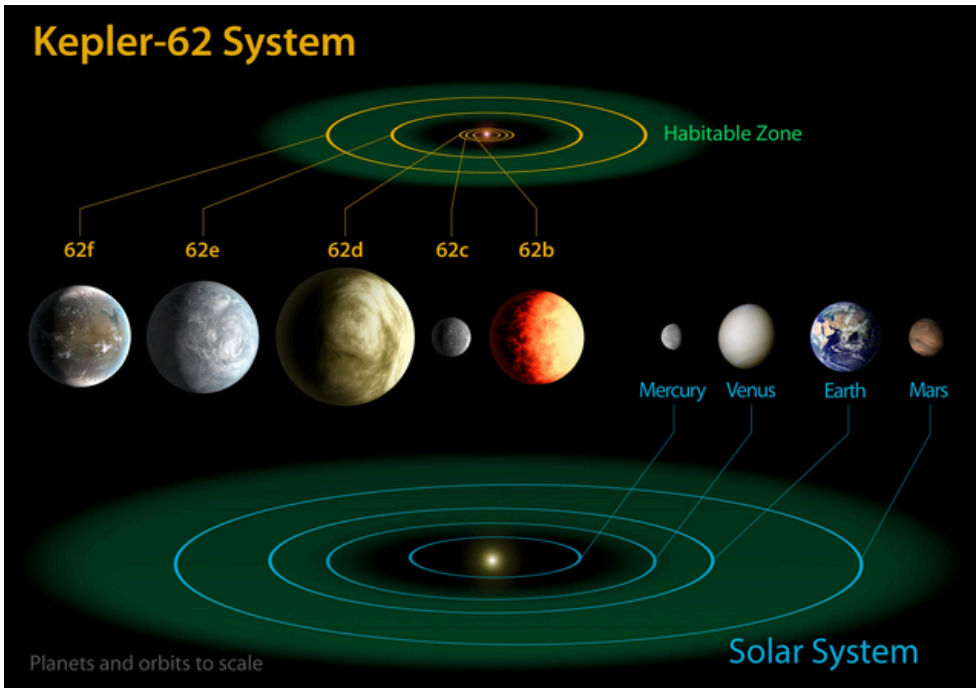

Figure 85: Comparison of the planetary system around the star Kepler-62 with our own Solar System. The relative size of the planetary orbits (top and bottom) is to scale. The planets (center) are also to scale, relative to each other. The habitable zone – the zone around the star that allows for liquid water on the surface of a planet orbiting at that distance – is shown in green. Kepler-62e and Kepler-62f are the best candidates yet for habitable planets: solid planets orbiting their host star in the habitable zone (credit: NASA Ames/JPL-Caltech; Last Updated: Aug 7, 2017).

Figure 86 shows the mass (left) and the radius (right) versus orbital period of the discovered exoplanets as of 2014 (Batalha, 2014).

The research of potential habitable exoplanets has been strongly supported during last two decades. Indeed, this field of astrophysics is now probably the most exciting since the discovery of planets Earth-like could open a serious debate about the possibility of life outside of solar system.

The list of the potential habitable exoplanets updated to 5th August 2021 (Planetary Habitable Laboratory - PHL - University of Puerto Rico at Arecibo, http://phl.upr.edu/projects/habitable-exoplanets-catalog) contains 60 objects: 1 subterran-size (Mars size) planet, 23 Earth–size planets, 36 super-Earth–size planets. Figure 87 artistically shows such potential habitable exoplanets (updated to 5th October 2020). This represents a list of the exoplanets that are more likely to have a

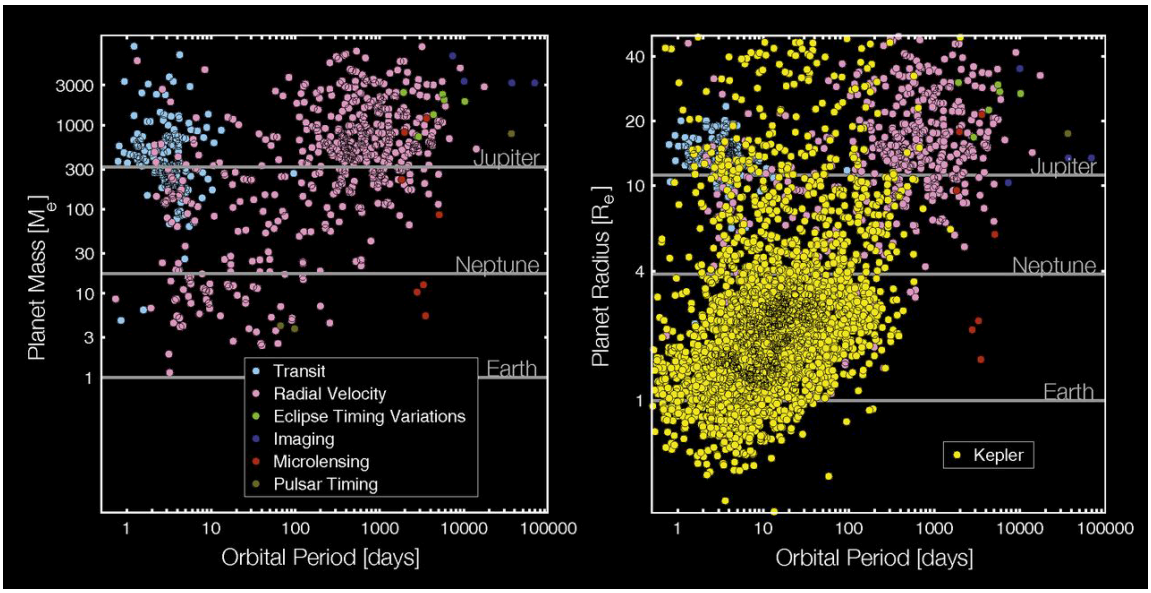

Figure 86: Non-Kepler exoplanet discoveries (Left) are plotted as mass versus orbital period, colored according to the detection technique. A simplified mass-radius relation is used to transform planetary mass to radius (Right), and the $>$ 3,500 Kepler discoveries (yellow) are added for comparison. Eighty-six percent of the non-Kepler discoveries are larger than Neptune, whereas the inverse is true of the Kepler discoveries: 85% are smaller than Neptune (adopted from Batalha, 2014).

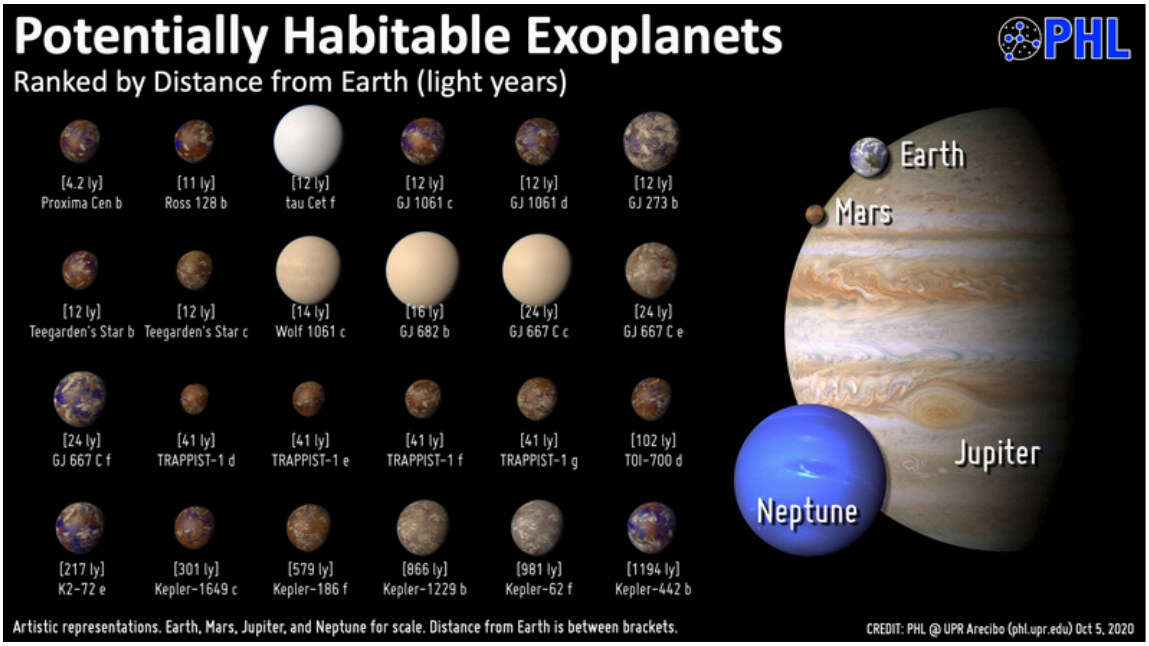

Figure 87: Current potential habitable exoplanets (2020, Credit: PHL@UPR Arecibo).

rocky composition and maintain surface liquid water (i.e. 0.5 < Planet Radius ≤ 1.5 Earth radii or 0.1 < Planet Minimum Mass ≤ 5 Earth masses,and the planet is orbiting within the conservative habitable zone) (Credit: PHL@UPR Arecibo).

This list is continuously updated and the number of such exoplanets is rapidly increasing.

The Exoplanet Data Explorer is an interactive table and plotter for exploring and displaying data from the Exoplanet Orbit Database. The Exoplanet Orbit Database is a carefully constructed compilation of quality, spectroscopic orbital parameters of exoplanets orbiting normal stars from the peer-reviewed literature, and updates the Catalog of nearby exoplanets. A detailed description of the Exoplanet Orbit Database and Explorers was published by Han et al. (2014). The latest list in CSV format was updated on 2021, August 5 and is available at http://phl.upr.edu/hec.

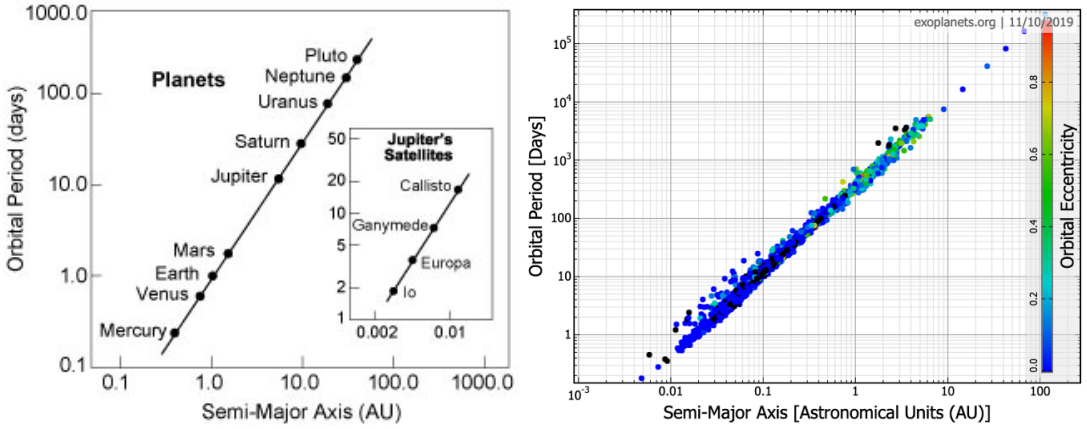

Figure 88: Left panel: the orbital periods of the planets versus their semi-major axes. The straight line has a slope of 3/2, thereby verifying Kepler's third law (NASA Cosmos). Right panel: the same for exoplanets discovered up to 11th October 2019 (Eklavya, 2019).

Figure 88 (left panel) shows the orbital periods of the solar system planets versus their semi-major axes (NASA Cosmos); Fig. 88 (right panel shows the same diagram for the exoplanets discovered up to 11th October 2019 (Eklavya, 2019). We can note how all exoplanets are similar in terms of obeying the same laws of gravity and motion, leading us to conclude that rules of physics apply to every element in the universe. However, the orbits become more elliptical as the eccentricity increases. At low orbital eccentricity, it is harder to determine the semi-major axis correctly. The blue points therefore have a larger margin of error than the other points. Hence we can assume that these planets are either not exactly following Kepler's law due to their low eccentricity and extreme closeness to their star, or else they are indeed following the law but marginal errors in the measurement of the orbital period have been done.

The presence of numerous exoplanets in the vicinity of solar system – within a distance of $\sim$ 0.9 kpc, which is the range accessible by the Kepler mission – plays an important role in speculating about the possible number of such exoplanets within the whole habitable zone of our galaxy. Such habitable zone has an internal radius of $\sim$ 4 kpc and an external radius of $\sim$ 11 kpc, as shown in Fig. 89 (after Lineweaver, Fenner & Gibson, 2004), where the habitable zone in a Milky Way-like galaxy is represented in green. The number of stars contained in this zone is $\approx$ 10% of the total number of stars in the Galaxy. Taking into account that the thickness of the disk is $\approx$ 1 kpc, as

evaluated by the differential rotation of the Galaxy, the habitable volume is ~ 330 kpc^3. Therefore, if in a volume of ≈ 3.36 kpc^3 there are 955 Earth-size planets detected, in the habitable zone of our Galaxy we could expect $\approx 9.4 \times 10^4$ Earth-size planets, as lower limit.

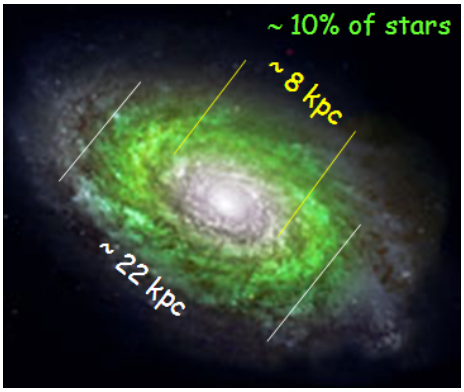

Figure 89: Habitable zone of a Milky Way-like galaxy (Giovannelli & Sabau-Graziati, 2016c, after Lineweaver, Fenner & Gibson, 2004; Image courtesy: Yeshe Fenner, Space Telescope Institute).

Planets around other stars are the rule rather than the exception, and there are likely hundreds of billions of exoplanets in the Milky Way alone (Maruyama, Ebisuzaki & Kurokawa, 2019). Therefore, it is evident that the probability of finding numerous habitable planets becomes very high. Next generation instruments ground– and space–based will provide valuable information about this intriguing problem.

Studies about exoplanet predictions around stars have been performed by Bovaird & Lineweaver (2013). They predict the existence of a low-radius ($R < 2.5\ R_{\odot}$) exoplanet within the habitable zone of KOI-812 and that the average number of planets in the habitable zone of a star is 1–2.

For life-forms like us, the most important feature of Earth is its habitability. Understanding habitability and using that knowledge to locate the nearest habitable planet may be crucial for our survival as a species. During the past decade, expectations that the universe could be filled with habitable planets have been bolstered by the increasingly large overlap between terrestrial environments known to harbor life and the variety of environments on newly detected rocky exoplanets. The inhabited and uninhabited regions on Earth tell us that temperature and the presence of water are the main constraints that can be used in a habitability classification scheme for rocky planets. Lineweaver & Chopra (2012) compiled and reviewed the recent exoplanet detections suggesting that the fraction of stars with planets is $\sim 100\%$, and that the fraction with rocky planets may be comparably large. They reviewed extensions to the circumstellar habitable zone (HZ), including an abiogenesis habitable zone and the galactic habitable zone.

Earth is located in a dangerous part of the universe. Threats to life on Earth are manifold and range from asteroid impacts to supernova explosions and from supervolcano eruptions to human-induced disasters. If the survival of the human species is to be ensured for the long term, then life on Earth has to spread to other planetary bodies. Mars is the most Earth-like planet we currently know and is the second closest planet; further it possesses a moderate surface gravity, an atmosphere, abundant water and carbon dioxide, together with a range of essential minerals. Thus, Mars is ideally suited to be a first colonization target. Here we argue that the most practical way that this

can be accomplished is via a series of initial one-way human missions (Schulze-Makuch & Davies, 2013).

However, we have interesting news about the presence of water in the universe. We knew that all the water found on Earth, has been transported by small bodies such as comets and asteroids. On the contrary, the work "*The ancient heritage of water ice in the solar system*" (Cleeves et al., 2014) has carried the knowledge one step further. It is understood that the water now present in Earth's oceans, and is present in other solar system bodies, has remained virtually unchanged with respect to that in the interstellar medium. This means that this water has not changed during the process of planet formation. This allows us to understand that the initial conditions that have favored the emergence of life are not unique, i.e. not dependent on the unique characteristics of our solar system. They can, however, be common in space.

Astrobiology is an interdisciplinary scientific field, recently born, not only focused on the search of extraterrestrial life, but also on deciphering the key environmental parameters that have enabled the emergence of life on Earth. Understanding these physical and chemical parameters is fundamental knowledge necessary not only for discovering life or signs of life on other planets, but also for understanding our own terrestrial environment. Recent papers by Cottin et al. (2017a,b) presented an interdisciplinary review of current research in astrobiology, covering the major advances and main outlooks in the field. They reviewed the most recent discoveries, the new understanding of planetary system formation including the specificity of the Earth among the diversity of planets, the origin of water on Earth and its unique combined properties among solvents for the emergence of life, the idea that the Earth could have been habitable during the Hadean Era, the inventory of endogenous and exogenous sources of organic matter and new concepts about how chemistry could evolve towards biological molecules and biological systems. In addition, many new findings show the remarkable potential life has for adaptation and survival in extreme environments. All those results from different fields of science are guiding our perspectives and strategies to look for life in other Solar System objects as well as beyond, in extrasolar worlds.

An intriguing question about the probability of finding a number of civilization in the Galaxy arises. It is now evident that Drake's formula (Drake, 1962) must be object of a robust revision.

For years, the search for manifestations of extraterrestrial civilizations has been one of humanity's most ambitious projects. Major efforts are now focused on the interception of messages from extraterrestrial civilizations, and the millimeter range is promising for these purposes (Dyson,1960). The Millimetron space observatory is aimed at conducting astronomical observations to probe a broad range of objects in the Universe in the wavelength range 20 μm to 20 mm, including the search for extraterrestrial life (Smirnov et al., 2012; Kardashev et al., 2014, and the references therein).

Important news have been published by Anglada-Escudé et al. (2016). They reported observations that reveal the presence of a small planet with a minimum mass of about 1.3 Earth masses orbiting Proxima Centauri (d = 1.295 pc) with a period of $\approx$ 11.2 days at a semi-major-axis distance of $\sim$ 0.05 AU. Its equilibrium temperature is within the range where water could be liquid on its surface.

By using the European Southern Observatory's HARPS – a high precision instrument fitted to the 3.6-m telescope at the La Silla Observatory in Chile – 102 red dwarf stars neighbouring the sun over a period of six years have been studied. Red dwarfs are smaller and cooler than the Sun,

however it's been found that 40% of red dwarf stars may have Earth-sized planets orbiting them that have the right conditions for life. New observations with Harps mean that about 40% of all red dwarf stars have a super-Earth orbiting in the habitable zone where liquid water can exist on the surface of the planet. Because red dwarfs are so common – there are about 160 billion of them in the Milky Way – this leads us to the astonishing result that there are tens of billions of these planets in our galaxy alone (Bonfils et al., 2013).

Therefore, planets around other stars are the rule rather than the exception, and there are likely hundreds of billions of exoplanets in the Milky Way alone. NASA's Kepler space telescope has found more than 2,400 alien worlds, including a new haul of 95 planets announced on Feb. 15, 2018.

A good help in finding and analyzing extrasolar planets can come from four recent "simple" programs:

- The TRAPPIST (TRAnsiting Planets and PlanetesImals Small Telescopes) consists in a network of two 60-cm robotic telescopes, one in Chile and one in Morocco, used by the Origins in Cosmology and Astrophysics (OrCA) researchers to contribute to the fields of astrobiology and planetology through two complementary approaches: the photometric detection and characterization of exoplanets transiting nearby stars (PI: Michael Gillon), and the photometric study of small bodies of our solar system (PI: Emmanuel Jehin) (Jehin et al., 2011).

- The Search for habitable Planets EClipsing ULtra-cOOl Stars (SPECULOOS) Southern Observatory (SSO), a new facility of four 1-meter robotic telescopes at Cerro Paranal. The exquisite astronomical conditions at Cerro Paranal will enable SPECULOOS to detect exoplanets as small as Mars. It will explore approximately 1000 of the smallest (≤ 0.15 $R_{\odot}$), brightest (≤ 12.5 K_{mag}, and nearest ($d \leq 40$ pc) very low mass stars and brown dwarfs. The ultimate goals of the project are to reveal the frequency of temperate terrestrial planets around the lowest-mass stars and brown dwarfs, to probe the diversity of their bulk compositions, atmospheres and surface conditions, and to assess their potential habitability (Delrez et al., 2018; Jehin et al., 2018).

  It is interesting to remark the importance of the book *SPECULOOS Exoplanet Search and Its Prototype on TRAPPIST* (Burdanov et al., 2018).

- ARIEL ESA mission (Pascale et al., 2018) – scheduled for launch in 2029 – was conceived to observe a large number (~ 1000) of transiting planets for a chemical survey of exoplanets, including gas giants, Neptunes, super-Earths and Earth-size planets around a range of host star types using transit spectroscopy in the 1.25-7.8 μm spectral range and multiple narrow-band photometry in the optical. ARIEL will thus provide a representative picture of the chemical nature of the exoplanets and relate this directly to the type and chemical environment of the host star (Tinetti et al., 2018).

- The Transiting Exoplanet Survey Satellite (TESS) is designed to discover thousands of exoplanets in orbit around the brightest dwarf stars in the sky. In its prime mission, a two-year survey of the solar neighborhood, TESS monitored the brightness of stars for periodic drops caused by planet transits. The prime mission ended on July 4, 2020 and TESS is now in

an extended mission. TESS is finding planets ranging from small, rocky worlds to giant planets, showcasing the diversity of planets in the galaxy. TESS finished its primary mission by imaging about 75% of the starry sky as part of a two-year-long survey. In capturing this giant mosaic, TESS found 66 new exoplanets, or worlds beyond our solar system, as well as nearly 2,100 candidates to be confirmed. TESS has discovered its first Earth-size world. The planet, HD 21749c, is about 89% Earth's diameter. It orbits HD 21749, a K-type star with about 70% of the Sun's mass located 53 light-years away in the southern constellation Reticulum, and is the second planet TESS has identified in the system. The new world is likely rocky and circles very close to its star, completing one orbit in just under eight days. The planet is likely very hot, with surface temperatures perhaps as high as 800 °F (427 °C). The star that HD 21749c orbits is bright and relatively nearby, and therefore well suited to more detailed follow-up studies, which could provide critical information about the planet's properties, including potentially the first mass measurement of an Earth-size planet found by TESS (Dragomir et al., 2019).

Following the NASA Exoplanet Exploration page (https://exoplanets.nasa.gov/the-search-for-life/life-signs/) we can say that our early planet finding missions, such as NASA's Kepler and its new incarnation, K2, or the recently-launched James Webb Space Telescope, could yield bare bones evidence of the potentially habitable worlds. Perhaps K2's examination of nearer, brighter stars will stumble across an Earth-sized planet in its star's habitable zone, close enough for follow ups by other instruments to reveal oceans, blue skies and continents. Or James Webb, designed in part to investigate gas giants and super Earths, might find an outsized version of our planet. With a possible launch in the mid 2020s, WFIRST (Wide-Field Infrared Survey Telescope), could zero in on a distant planet's reflected light to detect the signatures of oxygen, water vapor, or some other powerful indication of possible life.

But unless we get lucky, the search for signs of life could take decades. Discovering another blue-white marble hidden in the star field, like a sand grain on the beach, will probably require an even larger imaging telescope. Designs are already underway for that next-generation planet finder, to be sent aloft in the 2030s or 2040s.

However, we are going to study $\sim$ 50,000 Clusters of Galaxies (Boller, 2017), and we have millions more. We know the lower limit of the extrapolated number of Earth-size planets in the habitable zone of our Galaxy. Thus a natural extrapolation can be reasonably thought. Thus, we can dare to say that we are approaching to the philosophical results obtained by two great free thinkers:

- Siddhartha Gautama also known as Shakyamuni (the sage of Shaka – between the VI and V century B.C.) who exposes a grandiose vision of the universe: through the concept of "**major system of worlds**", a concept on huge scale that implies both the existence of countless galaxies and the possibility of sentient life on other planets other than our own (from the Lotus Sutra – the central text of Mahayana Buddhism).

- About 2000 years later, Giordano Bruno (Nola 1548 – Roma 17th February 1600) who was burned alive in Campo dei Fiori by the "Saint Inquisition" because of his thought – summarized in *De l'infinito, universo e mondi* (Giordano Bruno, 1584) (see Fig. 90) – that produced

the same conclusions of Siddharta: **The Universe is infinite and is populated by a myriad of worlds**. Moreover he was saying that "*Whether we like it or not, we are the cause of ourselves. Being born in this world, we fall into the illusion of the senses: we believe in what appears. We ignore that we are blind and deaf. Then the fear attacks us and we forget that we are "divine". We can change the course of events*".

These philosophical lucubrations were not exactly in agreement with the position of the Roman (Catholic) Church!

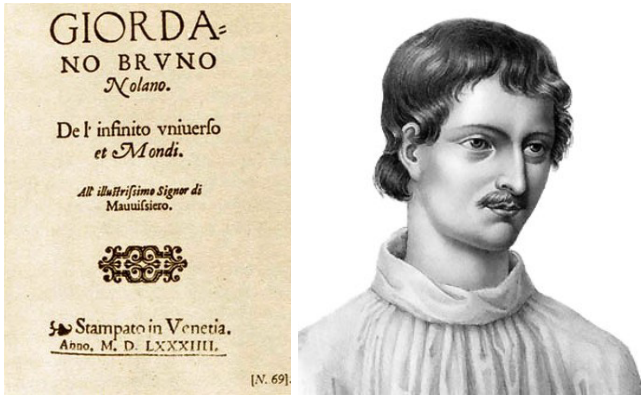

Figure 90: Left panel: Frontispiece of the original publication of *De l'infinito, universo et mondi* (Giordano Bruno, 1584). Right panel: Giordano Bruno (Rixner & Siber, 1824).

Of course we must wait scientific confirmation for the "alien life". We must wait even more for the discovery of "intelligent life". But, the number of discovered planets is growing very fast. Thus, I can reasonably affirm that the **Universe is full of life**, hoping to avoid to be burned alive like Giordano Bruno.

A very important news, which could save me to be burned alive, is coming from the detection of a planet in an external galaxy M51 (Di Stefano et al., 2021). Indeed, many lines of reasoning suggest that external galaxies should host planetary systems, but detecting them by methods typically used in our own Galaxy is not possible. An alternative approach is to study the temporal behaviour of X-rays emitted by bright extragalactic X-ray sources, where an orbiting planet would temporarily block the X-rays and cause a brief eclipse. They report on such a potential event in the X-ray binary M51-ULS-1 in the galaxy M51. They examined a range of explanations for the observed X-ray dip, including a variety of transiting objects and enhancements in the density of gas and dust. The latter are ruled out by the absence of changes in X-ray colours, save any with sharp density gradients that cannot be probed with their data. Instead, the data are well fit by a planet transit model in which the eclipser is most likely to be the size of Saturn. They also find that the locations of possible orbits are consistent with the survival of a planet bound to a mass-transfer binary. With this fundamental paper, the search for **extroplanets**, planets in orbits located outside our galaxy, has now become a realistic and practical enterprise.

In my opinion we are witnessing a revolution similar to that of the discovery of a planet orbiting the star 51 Pegasi by Mayor & Queloz (1995). Until then, no planets were known rotating around a star outside the solar system, but the two planets orbiting the pulsar PSR 1257+12 announced by Wolszczan & Frail (1992).

Sir Arthur C. Clarke (December 16, 1917 Minehead, UK - March 19, 2008 Colombo, Sri Lanka) – very famous professional fiction writer – said about the intelligent life in the Universe: "*Two possibilities exist: either we are alone in the Universe or we are not. Both are equally terrifying*".

It is important for me to close this section with the beautiful words full of hope of William Borucki – principal investigator for NASA's Kepler mission: *If we find lots of planets like ours... we'll know it's likely that we aren't alone, and that someday we might be able to join other intelligent life in the universe*.

7. Origin of terrestrial life

The origin of life on Earth is one of the most intriguing fields of research because it stimulates the curiosity of the entire human race. To tackle such research, the skills of a multitude of scientists who are experts in the various fields of research are necessary: from geology, to paleontology, to biology, to chemistry, to physics, and to the new born astrobiology.

A multitude of articles and reviews have been published in the last twenty years. They discuss in depth the theme of the origin of life on Earth (e.g. Woese, 1998, 2000, 2002; Luisi, 2006; Arndt & Nisbet, 2012; Koonin, 2014; Martin & Sousa, 2016; Knoll, Bergmann & Strauss, 2016 ; Kaiser, 2017; Cappellini et al., 2018; Martin, Bryant & Beatty, 2018; de Vries & Archibald, 2018).

It is our desire to venture into a short journey that gives the reader a chance to deepen the theme of the origin of life on the planet Earth and the further developments marked in a preponderant way by the presence of homo sapiens.

The Earth is 4.6 billion years old and microbial life is thought to have first appeared between 3.8 and 3.9 billion years ago; in fact, 80% of Earth's history was exclusively microbial life. Microbial life is still the dominant life form on Earth. It has been estimated that the total number of microbial cells on Earth on the order of 2.5 $\times 10^{30}$ cells, making it the major fraction of biomass on the planet.

Phylogeny refers to the evolutionary relationships between organisms. The Three Domain System, proposed by Woese (1998), is an evolutionary model of phylogeny based on differences in the sequences of nucleotides in the cell's ribosomal RNAs (rRNA), as well as the cell's membrane lipid structure and its sensitivity to antibiotics. Comparing rRNA structure is especially useful. Because rRNA molecules throughout nature carry out the same function, their structure changes very little over time. Therefore similarities and dissimilarities in rRNA nucleotide sequences are a good indication of how related or unrelated different cells and organisms are.

There are various hypotheses as to the origin of prokaryotic and eukaryotic cells. Because all cells are similar in nature, it is generally thought that all cells came from a common ancestor cell termed the **L**ast **U**niversal **C**ommon **A**ncestor (LUCA). These LUCAs eventually evolved into three different cell types, each representing a domain. The three domains are the Archaea, the Bacteria, and the Eukarya (Kaiser, 2017).

Figure 91 shows the phylogenetic tree of life (Woese, 2000; Koonin, 2014; Kaiser, 2017).

The universal phylogenetic tree not only spans all extant life, but its root and earliest branchings represent stages in the evolutionary process before modern cell types had come into being. The evolution of the cell is an interplay between vertically derived and horizontally acquired variation.

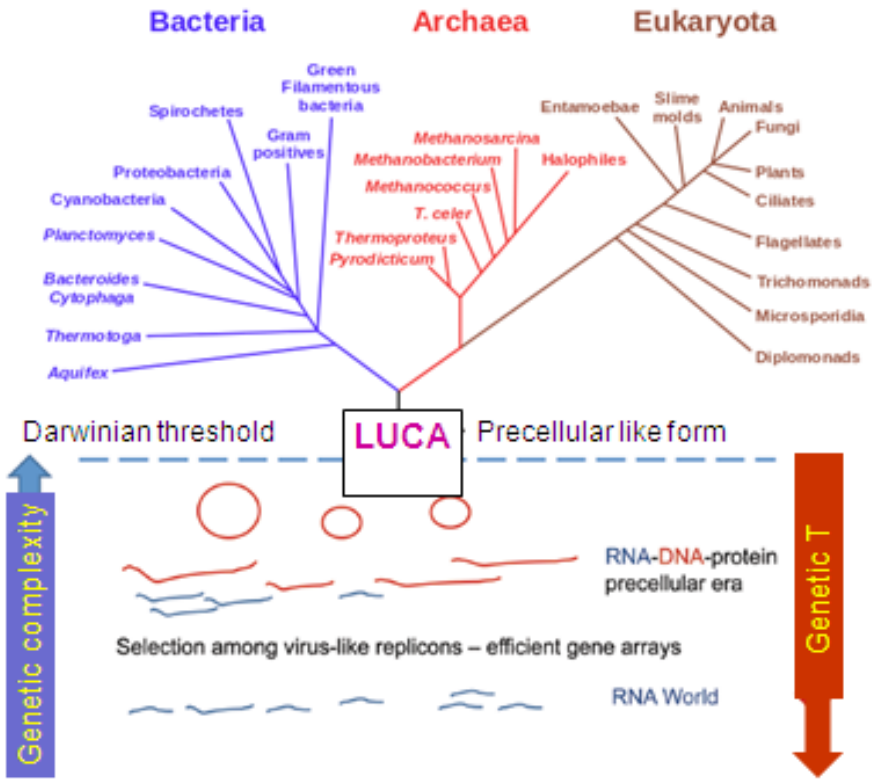

Figure 91: The phylogenetic tree of life (adapted from Kaiser, 2017, after Woese, 2000 and Koonin, 2014).

Primitive cellular entities were necessarily simpler and more modular in design than are modern cells. Consequently, horizontal gene transfer early on was pervasive, dominating the evolutionary dynamic. The root of the universal phylogenetic tree represents the first stage in cellular evolution when the evolving cell became sufficiently integrated and stable to the erosive effects of horizontal gene transfer that true organismal lineages could exist (Woese, 2000).

Woese (2002) discussed a theory for the evolution of cellular organization. As a cell design becomes more complex and interconnected a critical point is reached where a more integrated cellular organization emerges, and vertically generated novelty can and does assume greater importance. This critical point is called the "Darwinian Threshold".

Phylogenomics and metagenomics have revealed enormous genetic and molecular diversity and extremely high abundance of viruses and related selfish genetic elements that come across as the dominant biological entities on earth. Furthermore, the perennial arms race between viruses and their cellular hosts is one of the defining factors of evolution. Microbial phylogenomics adds new dimensions to the fundamental picture of evolution, demonstrating that the traditional concepts based on the study of the evolution of multicellular animals and plants represent only the proverbial tip of the enormous iceberg of life's history. The scientist that made a greater contribution to this new era of evolutionary biology was Carl Woese (1928-2012) (Koonin, 2014).

Following the very interesting history of the "Early Life on Earth" (Four Peaks Technologies, 2012a), we can take a short excursion on the evolution of life on our planet.

There is a general agreement that the first life on earth appeared sometime before 3.9 Gyr ago. The origins of life are known to have come after the presence of liquid water on Earth. But other than that, there is no solid evidence to pin down a more precise date. However, once large pools of water had formed, it was possible for life to exist. There is carbon isotope evidence for life in the world's oldest known sedimentary rocks from the Isua Greenstone Belt of West Greenland estimated to be 3.85 Gyr old. These carbon rich rock layers probably accumulated as plankton bacteria on the surface, died and settled to the ocean floor. These early life forms were not only alive, but capable of photosynthesis, that is inhaling carbon dioxide and exhaling oxygen. The earliest life form was very simple. It was almost certainly cyanobacteria (mistakenly called blue-green algae at times). We know it existed 3.9 Gyr at the latest because the first life also left behind the first fossils. Assuming it took about 100 million years for life to progress to the point of photosynthesis (which is pretty sophisticated), life began at least 4.0 billion years ago. Indeed, Bell & Harrison (2013 and the references therein) found evidence that life likely existed on earth at least 4.1 Gyr ago. The researchers, led by Bell, studied more than 10,000 zircons searching for carbon, the key component for life. Zircons are heavy, durable minerals originally formed from molten rocks in Western Australia. They capture and preserve their immediate environment, which means they serve as time capsules. The carbon contained in zircon has a characteristic signature, a specific ratio of ^{12}C to ^{13}C, that indicates the presence of photo-synthetic life. They identified 656 zircons containing dark specks and closely analyzed 79 of them using a technique that shows the molecular and chemical structure of ancient micro-organisms in three dimensions. One of the 79 zircons contained graphite, which is pure carbon, in two locations. The graphite is older than the zircon containing it. They know the zircon is 4.1 Gyr old based on its ratio of uranium to lead. They do not know how much older the graphite is (Bell et al., 2015).

Much life on earth belongs to the eukaryote family, all the way from blue-green algae to human beings. All multicellular organisms are eukaryotes, including animals, plants and fungi. On a numerical count basis, eukaryotes represent a tiny minority of all living things. Even in the human body, there are 10 times more microbe prokaryotes than human cells. It is believed that certain cyanobacteria evolved into blue-green algae eukaryotes about 2.5 Gyr ago much, much later than when cyanobacteria first appeared. The origin of the eukaryotic cell is considered a milestone in the evolution of life since they include all complex cells and almost all multicellular organisms. It was the development of the nucleus, which allowed highly complex forms of life to eventually evolve.

Stromatolites are the longest living form of life on the planet. They can be traced back at least 3.5 Gyr. Current marine stromatolites are only several thousand years old and can be found in waters in Western Australia and the Bahamas. Stromatolites are rock-like objects formed in shallow waters by living single celled micro-organisms, cyanobacteria, bound together in successive layers of carbonate sediment grains. Cyanobacteria come in population densities of over 3 billion organisms per square meter. Each cyanobacteria cell secretes a sticky film of mucus that traps local sediment grains. The sediment grains are bound together by the mucus and the cyanobacteria then grows over the grains. The bacteria are mobile and they photosynthesize, so they move towards light from the sun. Because the cyanobacteria need sunlight to photosynthesize, the stromatolites are generally found in water less than 200 cm deep where there is considerable sunlight. Their mobility also allows them to keep up with the growing sediment layers. The first records

of stromatolites began about 3.5 Gyr ago. Their presence indicates that even at such an early age, advanced prokaryotes were present, indicating that life on earth could have began much earlier, maybe as early as 4.0 Gyr. Stromatolites peaked about 1.25 Gyr and then began to decline. Today marine stromatolites can be found only in isolated areas like Shark Bay, Australia and the Bahamas. As an example of their decline, at Lake Clifton in Western Australia, scientists are witnessing algae (eukaryotes) out competing cyanobacteria, caused by an increase in nutrient levels in the water (Moore & Burne, 1994; Couradeau et al., 2011).

The first multicelled organisms are believed to have been red algae, which appeared sometime between 1.4 and 1.2 Gyr ago. This was about two billion years after stromatolites first appeared. Thus, more than one-half the time life has been present on Earth, it was occupied by only single cell organisms.

Ancient micro-fossils of red algae were preserved and have been found on Somerset Island in northern arctic Canada. These fossils are as old as 1.2 Gyr. The first multicellular organisms had certain characteristics that have defined all complex life forms since. Red algae invented sex and reproduced sexually. The male red algae releases sperm into the water which floats nearby coming into contact with the female's reproductive organ and fertilization occurs. Upon contact, the barriers dissolve inside of the female's reproductive organs. The male nucleus divides and one-half merges with the female nucleus. The female develops a large bulb which eventually buds off from the rest of the algae. This bulb is essentially a juvenile red algae which needs only time and nutrients to grow to an adult.

Sexual reproduction using egg and sperm cells is characteristic of multicelled organisms and first appeared in red algae. This development allowed much more complex life forms (including humans) to eventually evolve. So if you go back far enough, we all have red algae to thank for our existence.

7.1 The Cambrian explosion

In the book "*The Cambrian Explosion: The Construction of Animal Biodiversity*", Erwin & Valentine (2013) describe the Cambrian Period, which records one of the most extraordinary transitions in the history of life. In this book the authors synthesize research from many fields to explain why there was such remarkable novelty of animal forms. This book is an integrative work of the highest quality, covering one of the most fascinating and transformative periods in life's history.

The Cambrian Period (541-485 Myr ago) witnessed a wild explosion of new life forms. Along with new burrowing lifestyles came hard body parts like shells and spines. Hard body parts allowed animals to more drastically engineer their environments, such as digging burrows. A shift also occurred towards more active animals, with defined heads and tails for directional movement to chase prey. Active feeding by well-armored animals like trilobites may have further disrupted the sea floor that the soft Ediacaran creatures had lived on.

Trilobites were the dominant species during this period. Trilobites are extinct arthropods, animals with a hard skin shell and jointed legs. Trilobites were distant relatives of modern lobsters and horseshoe crabs. Trilobites had three (tri-lobe) segmented, rather flat, top plated bodies. They could curl up into balls for protection in seas that were increasingly filled with predators. **Trilobites were the first animals to develop eyes**. Trilobites came in many varieties and sizes. Their length was $\approx 10-70$ cm. Trilobites proved to be among the most successful and enduring of all prehistoric

animals. More than 17,000 species are known to have existed and they survived for approximately 300 Myr and then perished. A dramatic lowering of sea levels at the time probably contributed to their demise.

A dominant animal of the Cambrian Period was the giant anomalocaris, which trapped its prey with two claw-tipped appendages lined with hooks in the front of its mouth. Anomalocaris, which means abnormal shrimp, had true compound eyes. For the time in which it lived, the anomalocaris was a gigantic creature reaching lengths of up to $\approx$ 200 cm. Anomalocaris was a free-swimming animal that undulated through the water by flexing its body like a modern dolphin. They fed on trilobites and other arthropods, worms and mollusks. Anomalocaris was the largest and most fearsome predator of the Cambrian Period. Sponges also grew in the Cambrian seas. These animals belong to the phylum "porifera" because of all the tiny pores in their bodies. One species of sponge from this period had many branches that made it look like a tree. Another type of sponge looked like an ice cream cone without the ice cream. Many of the sponges became extinct when water temperatures dropped at the end of the Cambrian period. The Cambrian Period ended with a mass extinction. The leading theory is that a period of continental glaciation occurred when the climate of the Earth cooled at the end of the Cambrian. It was suggested that the cold conditions wiped out much of the warm water organisms because they were cold intolerant. Advancing glaciers would have lowered the temperature and the levels of the shallow seas where so many marine species lived. Changes in the temperature and also the reduction of the amount of oxygen in the water would have meant the end for many species that could not readily adapt. The loss of their habitat and the increased competition among the remaining displaced species led to the demise of many of them – a truly mass extinction.

The diversification of animals that occurred over a geologically short period (the Cambrian explosion) is commonly believed that was triggered by an increase of atmospheric oxygen. However, a causal relationship between the Cambrian explosion and increasing atmospheric oxygen lacks convincing evidence.

Indeed, Hammarlund, von Stedingk & Påhlman (2018) challenge that view. They start with the fact that hypoxia ($<$ 1-3% O_2) maintains cellular immaturity (stemness), whereas adult stem cells continuously – and paradoxically – regenerate animal tissue in oxygenated settings. Novel insights from tumour biology illuminate how cell stemness nevertheless can be achieved through the action of oxygen-sensing transcription factors in oxygenated, regenerating tissue. They suggest that these hypoxia-inducible transcription factors provided animals with unprecedented control over cell stemness that allowed them to cope with fluctuating oxygen concentrations. Thus, a refinement of the cellular hypoxia-response machinery enabled cell stemness at oxic conditions and, then, animals to evolve into the oxic realm. This view on the onset of animal diversification is consistent with geological evidence and provides a new perspective on the challenges and evolution of multicellular life.

7.2 Plant life

About 450 Myr ago , soon after the Cambrian Period, plants began to make their way onto land. The first plants needed a source of water for photosynthesis, so they were found on marsh land where they could easily obtain water from the damp soil. Because they did not have any tissue that conducted water very well, they had to stay close to a supply in order to obtain the water they

needed for photosynthesis. One of the major steps in plant evolution was the widespread evolution of spores as a form of plant reproduction. Spores are unicell organisms that are mobile and can reproduce forming new plants. Because spores could migrate by wind from place to place, they allowed plants to spread across the land. Spores eventually evolved into seeds, which are the multi-cell reproduction organisms of most of our current day plants. Another major development about 430 Myr was the first appearance of vascular systems within plants. These are plant veins that circulate water, chemicals, and minerals within the plant. About 375 Myr, plants that had root systems and leaves appeared for the first time. These advancements allowed plants of this era to become much larger and to function internally like plants of today. As more time passed, about 300 Myr, conifers appeared and thrived. Some of the trees of this family are pines, cedars, cypress, and massive redwoods. Conifers are cone bearing seed plants, mostly trees. The conifer family rapidly spread until massive conifer forests covered most of the planet. Ferns were also quite abundant as they grew well in the undergrowth of the large conifer forests (Four Peaks Technologies, 2012a).

7.3 Animal life

For at least 1.4 Gyr after the beginning of life, no animal ever trod on land. One reason was it takes a long time for creatures to evolve from one species to another. Going from living in water to living on land was a major step and would have taken a major amount of time. Another reason might have been ultraviolet rays. For a long time, the Earth did not have an ozone layer. Any creature that ventured on to land for any length of time would have been destroyed by the deadly radiation. After an oxygenated atmosphere developed, an ozone layer formed and land was safer to tread. However, the first large animals to walk the Earth were probably walking fish who still lived in water. Initially there was no food on the land so there was no pressing reason for them to live there permanently.

Trace fossils are the evidence of life preserved in sediments as a result of the living activities of organisms. They include surface tracks, trails, subsurface burrows, as well as fecal material and the marks produced by dying animals. They are evidence left behind by living things, but not direct evidence of the creatures themselves. There is fossil evidence of animal tracks on land from about 530 Myr. These tracks were probably made by tiny arthropods, animals with no spinal column (invertebrates), but have an external skeleton, a segmented body, and jointed appendages. Arthropods include flies, insects, worms, crabs, scorpions, starfish and octopus. The overwhelming majority of animal species are invertebrates. Only about 4% of all animal species have a spinal column.

It is believed that tetrapods, four limbed animals having a spinal column (vertebrates), walked on land about 400 Myr according to fossil evidence. Tetrap-ods were aquatic creatures that lived in swamps and shallow ponds but ventured onto land occasionally, perhaps to mate or to hide from enemies (e.g. Clack, 2009). On land there were no enemies while in the sea there were plenty of them. Tetrapods probably also walked on the floors of their shallow swamps and ponds. Eventually tetrapods took up permanent residence on land and survived on small insects and small plants most likely plant mats related to the green algae family. Tetrapods include amphibians, reptiles, birds, dinosaurs and mammals. The development of the vertebrate structure paved the way for more advanced animals and eventually humans (e.g. the book edited by Barrett & Milner, 2012, in which articles about studies on the earliest four-legged vertebrates, lizards, marine reptiles, turtles,

dinosaurs, birds and mammals, ranging in age from just after the origin of tetrapods to the origins of modern bird families, with an emphasis on Palaeozoic and Mesozoic faunas are presented; George & Blieck, 2011; and Pardo et al., 2017 and references therein).

Recently, Gess & Ahlberg (2018) found that the first tetrapods of Africa lived within the Devonian Antarctic Circle 360 Myr ago. Therefore, fossils of four-legged vertebrates also evolved in polar regions, and not just in the tropics as previously believed. The evolution of tetrapods from fishes during the Devonian period was a key event in our distant ancestry. New-found fossils are coming from the latest Devonian Waterloo Farm locality near Grahamstown in the Eastern Cape, South Africa.

At this point of the evolution, when the vertebrates appeared, the way for more advanced animals and eventually humans was opened.

7.4 The evolution of humans

Following the very interesting history of the "Early Humans" (Four Peaks Technologies, 2012b), we can take a short excursion on the evolution of humans on our planet.

While hunting for fossils in the Afar Triangle in Ethiopia, in November 1974, paleo-anthropologist Donald Johanson and graduate student Tom Gray stumbled upon the partial remains of a previously unknown species of an ape-like hominid.

The mysterious skeleton (nicknamed **Lucy**) was eventually classified as a 3.2 Myr old "Australopithecus afarensis" – one of humankind's earliest ancestors. The headline grabbing find filled in crucial gaps in the human family tree.

Her large pelvic opening suggested she was female, and wear on her wisdom teeth hinted she was probably around 20 years old when she died. She would have appeared more ape-like than human, with long arms and a protruding belly. Unlike knuckle dragging apes, however, the structure of her bones showed that she yet walked erect (Lieberman, 2012), and her brain was tiny (Johanson & Maitland, 1981).

A very interesting revolutionary discovery demonstrated that "Lucy" was not alone (Haile-Selassie et al., 2012).

Indeed, until 1995, the fossil record suggested there was only one pre-human species at any given time before 3 Myr ago. It was thought each species gave rise to another new species through time in a linear manner. But the discovery of Australopithecus bahrelghazali from Chad in 1995 and Kenyanthropus platyops from Kenya in 2001 challenged this idea. These two species were not widely accepted, and instead considered as geographic variants of Lucy's species, Australopithecus afarensis.

The discovery of a 3.4 Myr old Burtele partial foot from the Woranso-Mille announced by Haile-Selassie in 2012 was the first conclusive evidence that another early human ancestor species lived alongside Australopithecus afarensis.

The Woranso-Mille paleontological study area in Ethiopia's Afar region reveals that there were at least two, if not three, early human species living at the same time and in close geographic proximity.

This key research site has yielded new and unexpected evidence indicating that there were multiple species with different locomotor and dietary adaptations.

How did multiple closely related species manage to co-exist in a relatively small area? How did they partition the available resources? These new discoveries keep expanding our knowledge and, at the same time, raise more questions about human origins.

The fourth species was identified as Australopithecus deyiremeda, a 3.5 to 3.3 Myr old human ancestor species from Ethiopia (Haile-Selassie et al., 2015). Beall (2016) reports in his article a summary of the evolution of the primates:

- 55 Myr ago – First primitive primates evolve;
- 15 Myr ago – Hominidae (great apes) evolve from the ancestors of the gibbon;
- 8 Myr ago – First gorillas evolve. Later, chimp and human lineages diverge;
- 5.5 Myr ago – Ardipithecus, early "proto-human" shares traits with chimps and gorillas;
- 4 Myr ago – Ape like early humans, the Australopithecines appeared. They had brains no larger than a chimpanzee's but other more human like features;
- 3.9-2.9 Myr ago – Australoipithecus afarensis lived in Africa;
- 2.7 Myr ago – Paranthropus, lived in woods and had massive jaws for chewing;
- 2.3 Myr ago – Homo habilis first thought to have appeared in Africa
- 1.85 Myr ago – First "modern" hand emerges;
- 1.8 Myr ago – Homo ergaster begins to appear in fossil record;
- 1.6 Myr ago – Hand axes become the first major technological innovation;
- 0.8 Myr ago – Early humans control fire and create hearths. Brain size increases rapidly;
- 0.4 Myr ago – Neanderthals first begin to appear and spread across Europe and Asia;
- 0.2 Myr ago – Homo sapiens – modern humans – appear in Africa;
- 0.04 Myr ago – Modern humans reach Europe.

Figure 92 shows a sketch of the human evolution (Four Peaks Technologies, 2012b).

A recent paper by Du et al. (2018) demonstrates that pattern and process in hominin brain size evolution are scale-dependent. Their findings provide a quantitative basis for developing and testing scale-explicit hypotheses about the factors that led brain size to increase during hominin evolution.

Cappellini et al. (2018) in their review conclude that studies of ancient biomolecules have come a long way-from retrieval of short sequences of mitochondrial DNA from late Holocene materials to the assembly of full nuclear genome sequences and characterization of proteins and lipids dating back millions of years. These studies have profoundly deepened our understanding of the origin of early life forms, adaptation and extinction processes, and past migrations and admixtures that gave rise to present-day biological diversity, including in our own species. Today, ancient biomolecules can provide direct insights into both the deep and recent evolutionary past, at a scale and level of detail that few would have predicted less than a decade ago.

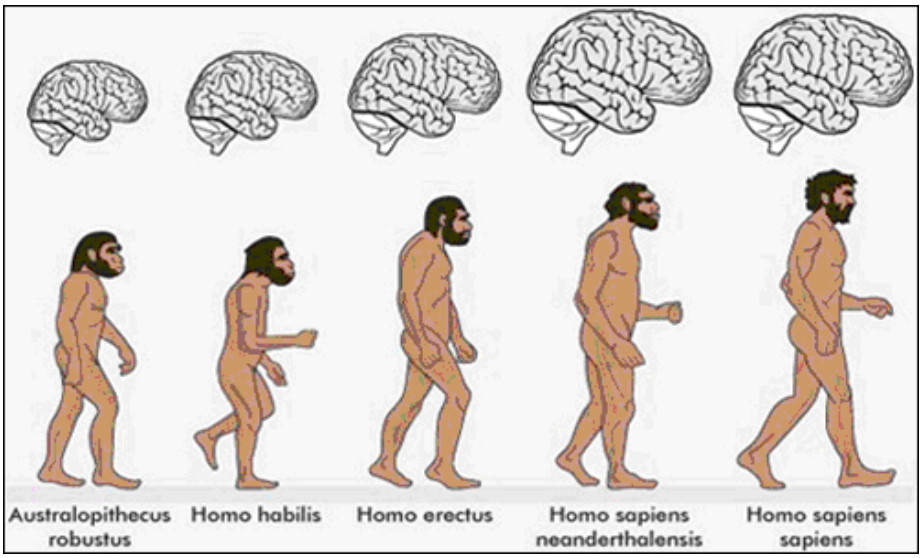

Figure 92: The complex evolution of humans (adopted from Four Peaks Technologies, 2012b).

7.5 What *intelligent* humanity is doing?

A short but important paper about *The Future of Human Longevity: A Demographer's Perspective* appeared in Science many years ago (Wilmoth, 1998). One of the greatest achievements of modern civilization has been the enormous reduction in human mortality. Life expectancy at birth, among early humans, was likely about 20 to 30 years (Preston, 1995). By 1900, the average length of life in industrialized nations had doubled relative to this historical extreme. Around the year 2000, life expectancy at birth was around 80 years in Japan and a few other countries, and its rise continues unabated. In recent decades, the populations of developed countries have grown considerably older, because of increasing survival to older ages as well as smaller numbers of births. Consequently, both legislators and the general public have begun to consider society's role in the support of this ever-expanding elderly population. In this new demographic context, questions about the future of human longevity have acquired a special significance for public policy and fiscal planning. Wilmoth (1998) discussed such a problem that is now extremely important for the future of the humanity.

It is important to remind a talk made by Wilmoth (2009) about the *Increase of Human Longevity: Past, Present and Future*, where he clearly discussed the following items:

- Historical increase of longevity
- Age patterns of mortality
- Medical causes of death
- Social and historical causes
- Limits to the human life span?
- Future prospects

An important book about *Life Span: Evolutionary, Ecological, and Demographic Perspectives* (Carey & Tuljapurkar, 2003) is based on a series of papers presented at the workshop held on 14-18 May 2001 at the Petros M. Nomikos Conference Centre on the Greek island of Santorini.

The volume is concerned with the biodemography of life span, a subject that has recently emerged at the confluence of demography and biology. Over the twentieth century, human life span measured as period life expectancy has increased by more than 50% in most industrialized countries, driving concern about the benefits and costs of longer life and raising keen interest in whether we can maintain the past rate of increase in life span. Biodemography brings together methods, materials, theories, and analyses from both biology and demography with the aim of understanding the past and anticipating the future of life span.

Without any doubt, life expectancy has grown considerably from prehistory to today. Figure 93 shows this evolution (Finch, 2012).

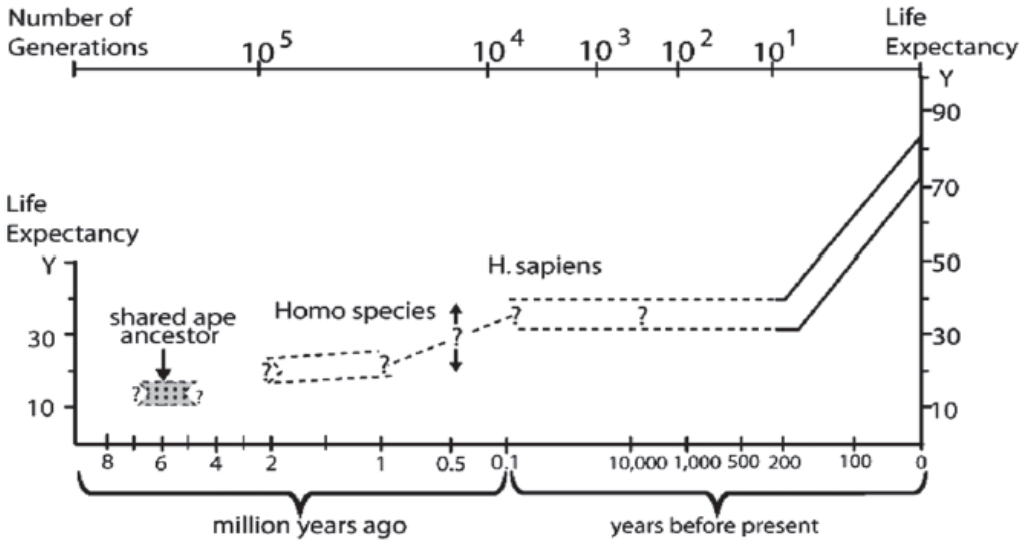

Figure 93: The evolution of the human life expectancy (Adopted from Finch, 2012).

However, the differences in the current world are at shameful levels. In fact, as shown in Fig. 94, there is a direct correlation between the life expectancy at birth and the amount of energy available per capita (Pielke Jr., 2013).

The life expectancy at birth and the amount of energy available per capita is dramatically enforced by the effective average life of populations of different continents as shown in Fig. 95. The difference between Africa and Europe-North America-Japan are dramatically evident. Our responsibility for this state of affairs is evident and a great effort by the most fortunate countries is required to heal it.

A relationship between the life expectancy and the national income in current purchasing-power parity dollars shows how dramatic is the situation in the world about the "*Income Inequality and Health*, as pointed out by Deaton (2003).

Figure 96 shows a recent version of the Preston (1975) curve, the international relationship between life expectancy and national income in current purchasing-power parity dollars (after adjusting for inflation and cross-country price differences). Among the poorest countries, increases

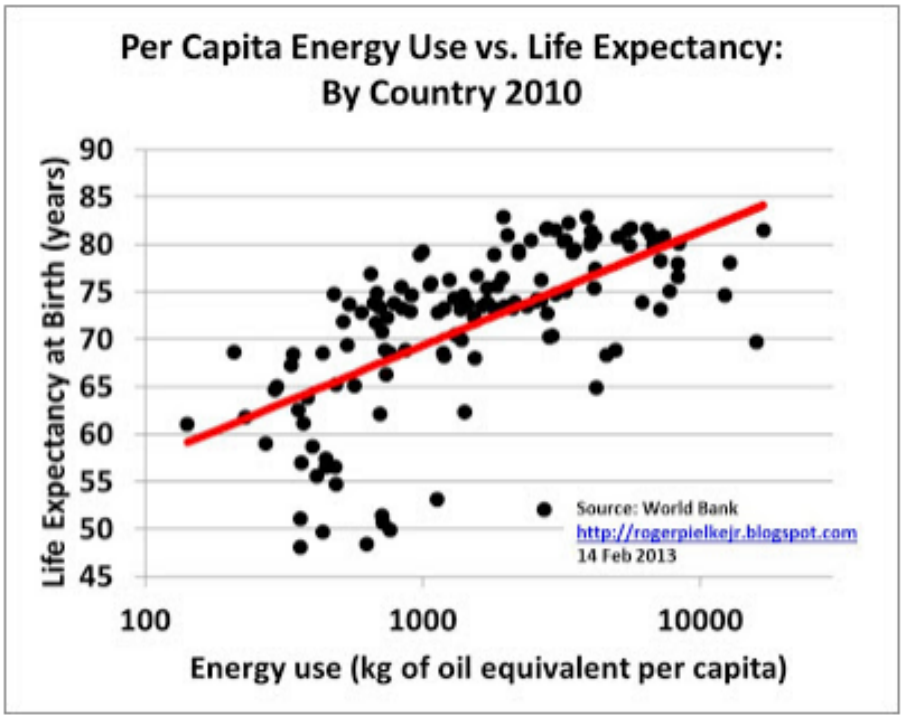

Figure 94: The energy use (expressed as kilograms of oil equivalent per capita) versus life expectancy at birth (expressed in years) for 151 countries in the "World Bank Development indicators database" that had data for both variables in 2010 (adopted from Pielke Jr., 2013).

in average income are strongly associated with increases in life expectancy, but as income per head rises, the relationship flattens out, and is weaker or even absent among the richest countries.

These data carry a powerful message: "*Energy poverty is not the only factor which contributes to below the average life expectancies, but it is clearly a very important factor*". Indeed, the countries having less energy available are the poorest ones and a relationship between the quality of life index (QL) – defined in a scale from 0 to 10 – versus the available energy per capita (ECR) (see Fig. 97: Pasten & Santamarina, 2012) enforce the former conclusion.

Moreover, the quality of life index is strictly correlated to the five-year population growth rate PG_5 (see Fig. 98: Pasten & Santamarina, 2012). The poorer the countries the higher the birth rate is.

This increase in population closely correlated with the quality of life in different continents makes it possible to make fairly accurate predictions on the world population in the coming decades, as shown in Fig. 99 (United Nations, 2017).

Then, the crucial problem is associated with the overpopulation of the planet, which under optimal conditions could accommodate 2 billions people, as many as in 1950. The solution is anything but simple. In fact, it is not enough just to act well in everyday life. It is absolutely necessary to reduce the number of inhabitants or think seriously about colonizing the solar system.

An important review about the global population projections has been published by Lutz & Samir (2010). These projections crossed with those reported in other many papers and in the world population previsions to 2300 reported by the United Nations (2004) allow to estimate that around

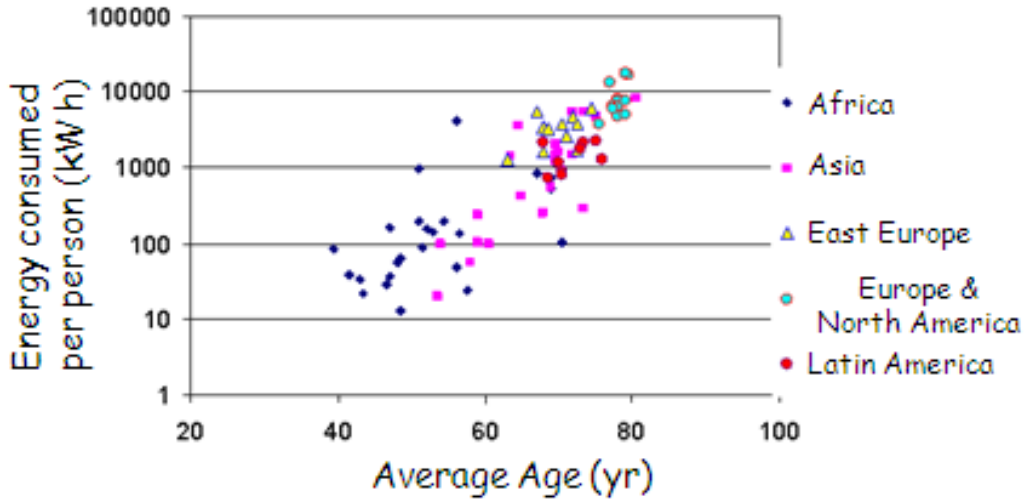

Figure 95: The average-life in years of populations belong to different continents versus the energy consumed pro capita in kWh (Adapted from Saraceno, 2009).

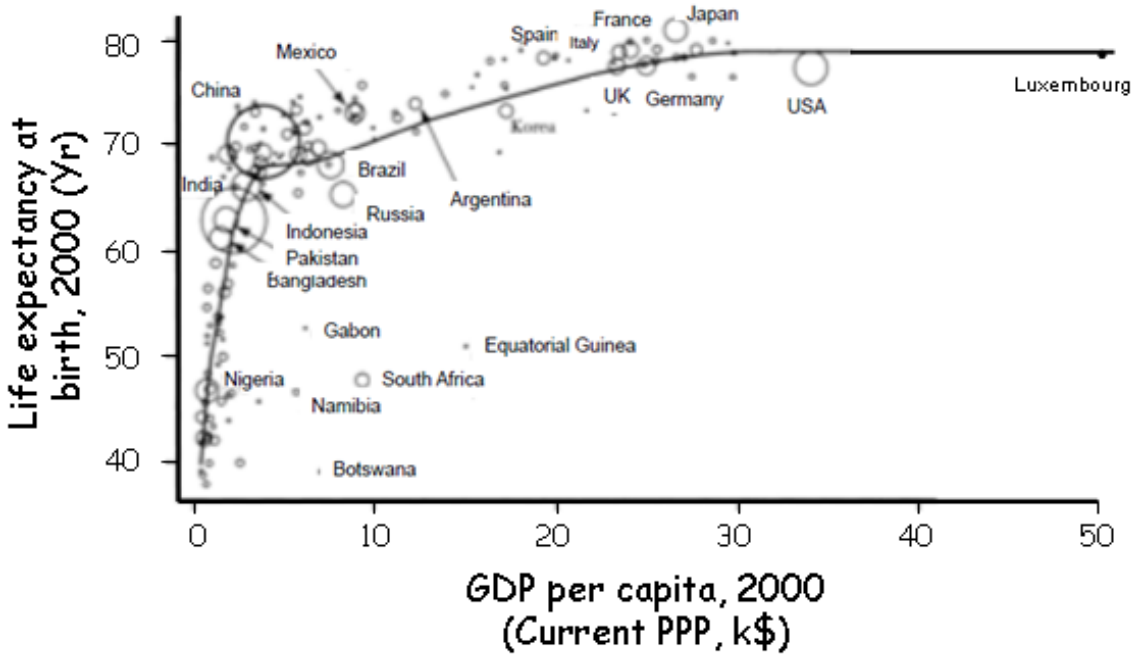

Figure 96: The Preston Curve updated: Life Expectancy versus Gross Domestic Product (GDP) per capita expressed in Current Purchasing-Power Parity (PPP) in kilo dollars) (updated from Deaton, 2003).

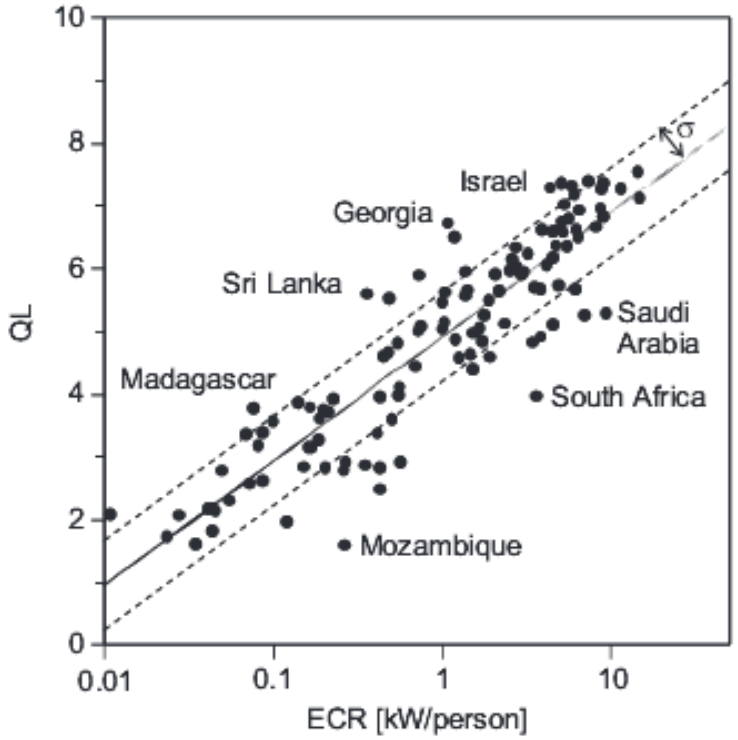

Figure 97: Quality of life index (QL) versus energy consumption rate per capita (ECR). Data for 118 countries with populations larger than four million in 2005. The continuous line is the mean trend; dashed lines show the plus and minus one standard deviation trends (adopted from Pasten & Santamarina, 2012).

2075 the peoples of the Earth will have reached a good wellbeing and the population will begin to decrease because the children are:

- a wealth in poor and agricultural societies;
- a high cost in the rich and urbanized ones.

Figure 111 (upper panel) shows these estimates for the total world population, and for the populations belong to rich and poor countries, respectively (Saraceno, 2009). Figure 100 (lower panel) shows the historic reversal populations: the number of children between 0-14 years will become less than the number of people of age over 65 years (Chamie, 2016).

Estimates of the world population extended up to 2300 bring a wave of optimism to the future of humanity. In fact, in the hypothesis that humanity does not self-destruct, we could reach a decrease in the world population, for the benefit of the health of the planet, but only if we arrive at a more equitable distribution of wealth. **This is the crucial point!**

But unfortunately, the alarms of an imminent disaster are there for all to see. The temperature of the planet is increasing dramatically, as shown in Fig. 101 (Saraceno, 2012), and this can cause irreparable damage to the survival of the human species and beyond.

Indeed, for instance, *the 2017 Hurricane Season Really Is More Intense Than Normal*, like shown in Fig. 102. There have been 13 named storms in 2017. Only four other seasons since 1995 have had that many by Sept. 18. Just two more by the end of the year would put 2017 in the top 15 since 1851, when reliable records begin (Astor, 2017).

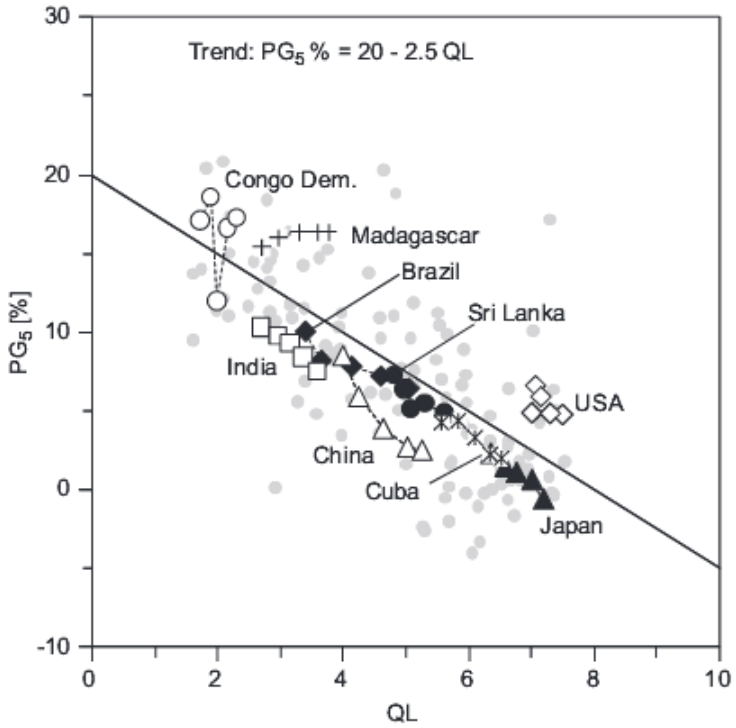

Figure 98: Five-year population growth rate PG_5 and quality of life index QL. The evolution of selected countries from 1980 to 2010 is shown in five-year intervals. The corresponding QL is the one at the beginning of the period. Dots represent 119 countries with populations larger than four million in the period 2005-2010. The line captures the global trend in the 30-year period from 1980 to 2010 (adopted from Pasten & Santamarina, 2012).

TABLE 1. POPULATION OF THE WORLD AND REGIONS, 2017, 2030, 2050 AND 2100, ACCORDING TO THE MEDIUM-VARIANT PROJECTION

Region	*Population (millions)*			
	2017	*2030*	*2050*	*2100*
World	7 550	8 551	9 772	11 184
Africa	1 256	1 704	2 528	4 468
Asia	4 504	4 947	5 257	4 780
Europe	742	739	716	653
Latin America and the Caribbean	646	718	780	712
Northern America	361	395	435	499
Oceania	41	48	57	72

Source: United Nations, Department of Economic and Social Affairs, Population Division (2017). *World Population Prospects: The 2017 Revision*. New York: United Nations.

Figure 99: Population of the world and regions 2017, 2030, 2050, 2100 according to the medium-variant projection (United Nations, 2017).

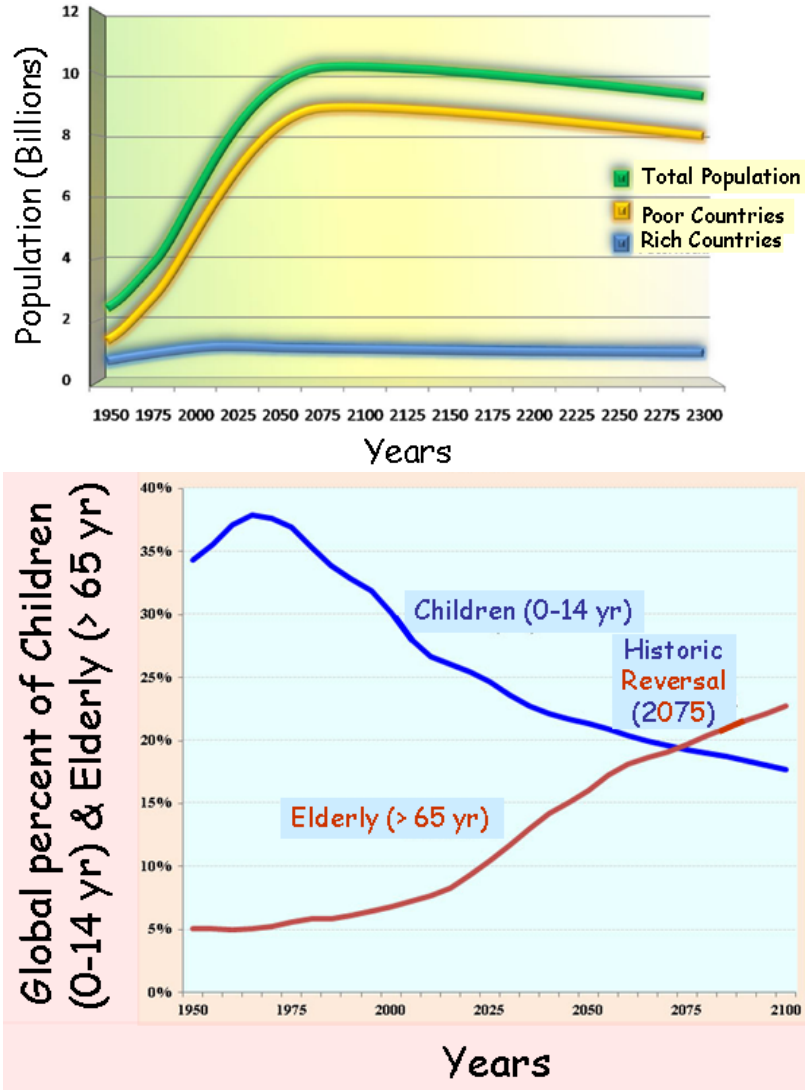

Figure 100: (Upper panel: World population estimate up to 2300 (adapted from Saraceno, 2009). Lower panel: Global percent of children (0-14 yr) and elderly (> 65 yr) from 1950 to 2100 (adapted from Chamie, 2016).

The winds of such hurricanes are extremely high, e.g.: Harvey (v_{max} = 215 km/h), Irma (v_{max} = 285 km/h), Jose (v_{max} = 250 km/h), Maria (v_{max} = 280 km/h), and the tropical storm Katia (v_{max} = 120 km/h) (Wikipedia, 2017). It is superfluous to remind that the energy is proportional to v^2_{max}!!! **And the most important effects are evaluated in the provoked "damage" in U.S. dollars, without admitting that the effects of such hurricanes are son of the "stupidity" of humans!!!**

In this regard, see the article by Shaviv (2016). He discusses the phenomenon called *Global Warming* or in the new name *Climate Change* that refers to the behavior of the 'Temperature of the Earth' as a function of time. The 'temperature of the Earth' is a complicated term as it is measured in different locations and one has to define at what location and how to average the temperature over

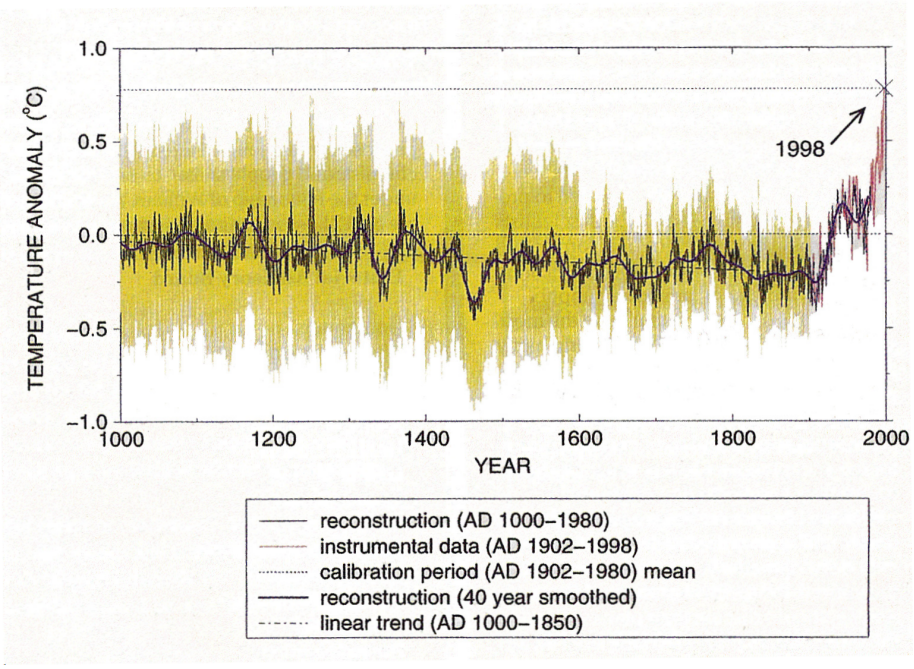

Figure 101: The temperature of the Earth from the year 1000 A.C. (adopted from Saraceno, 2012).

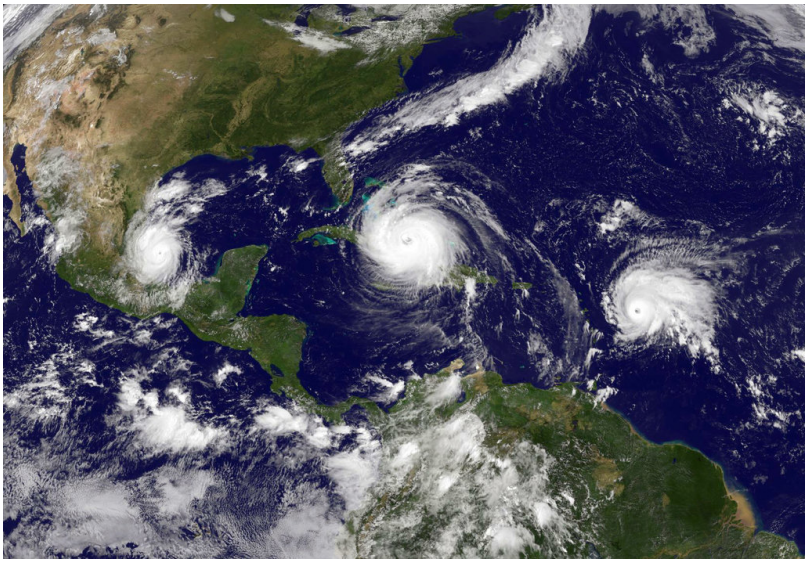

Figure 102: On September 8, 2017 three storms threatened land: from left, Tropical Storm Katia, Hurricane Irma and Tropical Storm Jose, which would intensify into a hurricane (Adopted from Astor, 2017 - Credit: NOAA/NASA GOES Project).

the complicated surface of the Earth so as to obtain a single number. The atmosphere, or better said the troposphere, can be considered as a boundary layer. However, this layer is not isothermal and shows large temporal and location temperature variations. The conclusions are not given because the problem is so complicated that the numerous theoretical models lead to significantly different results from each other.

The risk is that someone in the future will look at our species as we look at that of the dinosaurs!

Then, if we look for "Intelligent Lives" in the universe .... Why we should look for those like ours? (Giovannelli, 2001b).

I would like to suggest renaming *homo sapiens* to *homo stultus*.

8. Great examples of synergy between Astrophysics and History

- Bernd Aschenbach modified Sedov's relation for determining the age of SNRs (Aschenbach, 2016). He used as test the SNR Vela Jr (RX 0852.0-3946) – discovered during the ROSAT All-Sky-Survey in X-rays (Aschenbach, 1998) – and he gave an age of $T_{Aschenbach} \sim 725$ yr – contrary to $T_{Sedov} \sim 1714$ yr – and a distance of ~ 386 pc.

  Historical document (Tatsunokuchi Persecution of Nichiren Daishonin "the Buddha of the last day of the law") supports this result with an exceptional precision: The date of the explosion was 12 September 1271 (1 ± 2 a.m. - between the hours of the rat and the ox) (Soka Gakkai, 1999). How is it possible to affirm that the explosion of the SN Vela Jr happened in that date with a strong precision?

  The answer, indeed, can be found in the writings of Nichiren Daishonin. This buddhist monk presented to the public authority the "Risho Ankoku Ron" (Establishing the Correct Teaching for the peace in the country) three times: a strong and clear critic to the behaviour of authority. For this reason he was persecuted and sentenced to death.

  At that moment Nichiren was about to be beheaded, a luminous object (full Moon) shot across the sky, brightly illuminating the surroundings. The executioner fell on his face, his eyes blinded. The soldiers were filled with panic. Terrified, the soldiers called off the execution. This happened on the twelfth day of the ninth month of 1271, between the hours of the rat and the ox (11:00 p.m. to 3:00 a.m.). The event culminated 10° above the horizon, celestial declination -46° (position of Vela Jr).

- One of the best-located novae of antiquity, recorded by Korean royal astronomers, erupted on 11 March 1437 A.D (Clark, & Stephenson, 1977). It lay within the asterism Wei (the tail of the modern constellation Scorpius), within ≈ 1 degree of one of the two stars ζ Sco or η Sco. It was seen for 14 days before vanishing, consistent with a fast-declining classical nova while ruling out a supernova. The central star of the nebula is not a cataclysmic variable. However, a star about 15" from the shell center is both the strong emission-line cataclysmic variable 2MASS J17012815-4306123 and the variable X-ray source IGR J17014-4306 (Masetti et al., 2013). The measured proper motion of the 17th magnitude cataclysmic variable, listed in multiple catalogues, displays large scatter.

Shara et al. (2017), reconsidering the proper motion of the cataclysmic variable, found that its position in the year 1437 A.D. was in fact that of the nova of 1437 A.D.

9. The use of wisdom in physics

And now some examples of problems resolved with the help of multifrequency observations and good small quantities of wisdom in physics.

9.1 The classical T Tauri star RU Lupi

The usefulness of the relationship between the X-ray luminosity and rotational velocity (Pallavicini et al., 1981) has been demonstrated by e.g. Giovannelli (1994).

Indeed, a long-term (1982-1988) multifrequency program on Classical T Tauri Stars (CTTSs) was developed by the international group leaded by Franco Giovannelli. The facilities used for such a campaign were the International Ultraviolet Explorer (IUE), the ASTRON X-ray/UV Soviet satellite, and the ESO 0.6-m UBVRI telescope, 1-m IR telescope, 1.5-m telescope for low resolution optical spectroscopy, and 3.6-m telescope for Echelle high resolution spectroscopy.

The results were published in two main papers, the first with the experimental results (Giovannelli et al., 1995), the second with the interpretation of data and modeling (Lamzin et al., 1996). A review paper about RU Lupi was published by Giovannelli (1994).

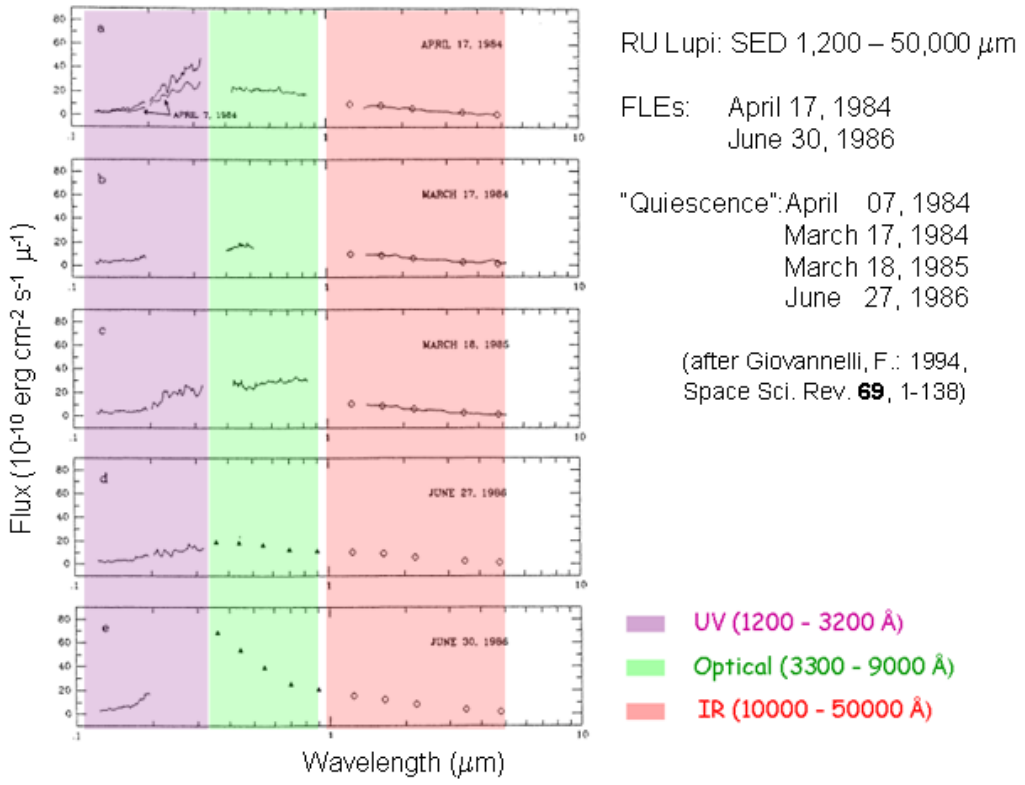

Figure 103: SED (1,200-50,000 μm) of RU Lupi in different epochs (after Giovannelli, 1994).

One of the main results obtained during the long-term multifrequency program was the simultaneous detection of emissions in different energy bands that allowed to construct the Spectral Energy Distribution (SED) of RU Lupi, as shown in Fig. 103.

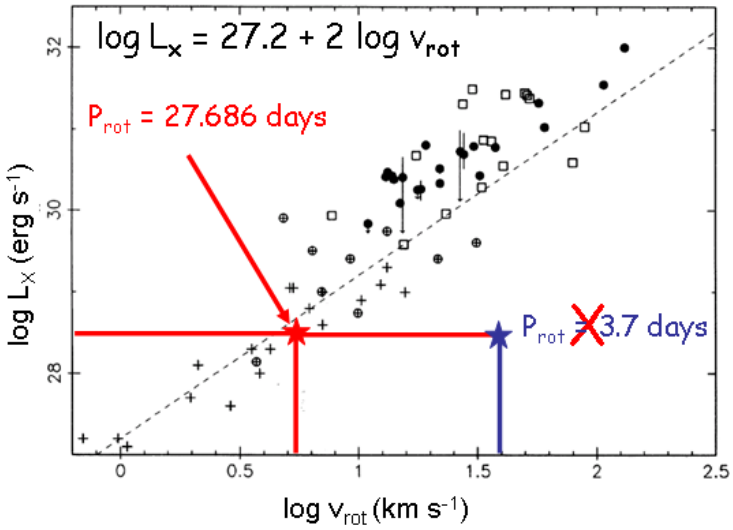

Figure 104: X-ray luminosity vs stellar equatorial velocity for TTS (•), late-type dwarfs (+), dKe-dMe stars (⊕), and RS CVn systems (□). The right position of RU Lupi is marked with a red cross, and the wrong position is marked with a blue cross (Giovannelli, 1994 after Bouvier, 1990).

In two occasions, RU Lupi showed a strong activity (Flare-Like Events: FLEs), much higher than that in "quiescence". Together with the FLEs reported in the literature, these two FLEs allowed to determine their periodicity: $P_{FLEs} = 27.686 \pm 0.002$ days (Giovannelli, 1994). This could be the rotational period of RU Lupi. Indeed, if we use the relationship between the X-ray luminosity (L_X) versus the rotational velocity (v_{rot}) for T Tauri stars, late-type dwarfs, dKe-dMe stars, and RS CVn systems (Bouvier, 1990) – directly derived from the Fig. 24 (Rosner, Golub & Vaiana, 1985, after Pallavicini et al., 1981) – the position of RU Lupi fits the relationship log L_X = 27.2 + 2 log v_{rot} if $P_{FLEs} = 27.686 \pm 0.002$ days is used, instead of using the "wrong" value reported in the literature of 3.7 days – that simply does not exist (Giovannelli et al., 1991) – whose wrong origin is largely commented in the paper by Giovannelli (1994). Figure 104 shows the diagram of the X-ray luminosity (L_X) versus the rotational velocity (v_{rot}) where the "correct" location of RU Lupi is marked with a red cross, and the "wrong" position with a blue cross.

9.2 The Cataclysmic Variable SS Cygni

A clear example of the use of wisdom in physics is coming from the history of the CV SS Cygni. In spite that it is the most observed CV since the end of the 19th century (Parkhurst & Zaccheus, 1900; Zuckerman, 1961), there is still a controversy about its nature. An extensive review about SS Cyg was published by Giovannelli & Martinez-Pais (1991).

Probably, the "mistake" about the nature of SS Cyg born after the publication of a paper in Nature by Bath & van Paradijs (1983) where SS Cyg was classified as dwarf nova (DN) on the basis of optical behaviour, typical of DNe. This paper originated a bandwagon effect in the literature (see

Michael Friedjung's comment (1985) in the first historical Frascati Workshop 1984: Giovannelli, 1985) that "obliged" almost all the subsequent authors to start the papers saying that SS Cyg is a DN (NMCVs), without paying attention to other possibilities well documented in the so-called second class literature.

Therefore, my suggestion is to reconsider the problem about the nature of SS Cyg without any a priori bias.

A paper by Hill et al. (2017) suggested to me to tell the history of the determination of the parameters of SS Cygni, and more, especially for the benefit of younger colleagues. Indeed, Fig. 105 shows the system parameters of SS Cyg, and in the last line, marked with a light red rectangle, the parameters derived by Giovannelli et al. (1983) are reported. These parameters, in spite of their origin from several measurements coming from different wavelength regions, are still valid if compared to "more accurate" experimental sources.

Table 2. System parameters of SS Cyg, with columns 1–7 listing the authors, the systemic velocity, the inclination, the radial-velocity semi-amplitude of the secondary star, the primary mass, the secondary mass and the mass ratio.

Author	γ (km s^{-1})	i (degrees)	K_2	M_1 ($M_\odot$)	M_2 ($M_\odot$)	$q = \frac{M_2}{M_1}$
This work	-15.2	45	163.9	0.94	0.59	0.628
Hessman et al. (1984)	-15.1 ± 1	–	155 ± 2	–	–	0.595
North et al. (2002)	-13.09 ± 2.88	–	165 ± 1	–	–	0.68 ± 0.02
Bitner et al. (2007)	-13.1 ± 2.9	45–56	162.5 ± 1	0.81 ± 0.19	0.55 ± 0.13	0.685 ± 0.015
Martinez-Pais et al. (1994)	–	–	162.5 ± 3	–	–	–
Giovannelli et al. (1983)	–	40^{+1}_{-2}	–	$0.97^{+0.14}_{-0.05}$	$0.56^{+0.08}_{-0.03}$	$0.58^{+0.12}_{-0.10}$

Figure 105: System parameters of SS Cyg (adapted from Hill et al., 2017).

As discussed by Smak (1985), emission lines are the most prominent features in the optical and ultraviolet spectra of CVs. Typically these are lines of H, neutral and ionized He, and ionized Ca. Their intensities are different in different systems. In the case of CVs with accretion disk around the white dwarf, the emission lines are often double peaked.

Indeed, the behaviour of the emission lines demonstrates that the transferred material does in fact produce a true disk rather than an amorphous cloud. Smak (1969) and Huang (1972) calculated the emission line profiles expected from gas disks of CVs and found that they should be double peaked and should have extensive wings.

The double component comes from the disk and originates from the surface of a flat, Keplerian disk (Smak, 1981), like shows in Fig. 106. Almost regardless of the radial distribution of the emitting atoms, the half-separation of the two peaks gives, to within $\sim 15\%$ (Smak, 1969; Huang, 1972), the rotational velocity of the outer edge of the disk, V_d sin i (where i is the orbital inclination). For V_d we have:

$$V_d^2 = \frac{GM_{WD}}{R_d} \tag{9.1}$$

and for the observed velocity V_{obs}, we have:

$$\frac{1}{2}\frac{\Delta\lambda}{\lambda} = \frac{V_{obs}}{c} \tag{9.2}$$

$$V_{\rm obs} = V_{\rm d} \sin i \tag{9.3}$$

where:

R_d = outer radius of the disk; $\Delta\lambda$ = separation of the peaks; c = light velocity; V_{obs} = observed velocity; G = gravitational constant; M_{WD} = mass of the white dwarf; i = orbital inclination angle.

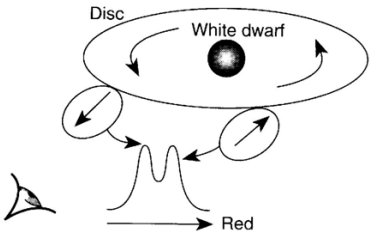

Figure 106: Sketch of the production of doubling in the emission lines from a flat, Keplerian accretion disk around the white dwarf in NMCVs (Smak, 1981, 1985).

Giovannelli et al. (1983), with an hazardous operation for that time, started to collect all information coming from different wavelength regions for determining the parameters of SS Cyg, namely:

- Their V_{obs} = 192 $\pm$ 10 km s^{-1} from the doubling observed in the Balmer emission lines in spectra taken during a quiescent phase of the system, as supported by the AAVSO measurements.
- The optical pulsations measured during different states of SS Cygni and ranging from 7.3 s (Hildebrand, Spillar & Stiening, 1981) to 10.9 s (Horne & Gomer, 1980; Patterson, 1979, 1981; Giovannelli, 1981).
- The X-ray pulsation of 9.735 $\pm$ 0.002 s measured by Patterson, Robinson & Kiplinger (1978)
- The available orbital data and the ratio between the external radius of the disk R_d and the separation, a, between the two components of the system, determined by Stover et al. (1980), Kiplinger (1979a,b), and Joy (1956).
- The mass-radius relationship for the white dwarf by Hartle & Thorne (1968).
- The mass-radius relationship for the secondary star by Plavec (1968).

By using Hartle & Thorne (1968) mass-radius relationship for the white dwarf and the minimum and maximum values of the optical pulsations, they limited the values of the orbital inclination angle between 38° and 41° (see Fig. 107, left panel). Then, if the X-ray pulsation of 9.7 s gives an upper limit to the Keplerian period at dwarf nova surface (Cordova et al., 1980), the lower limit of the mass of the white dwarf is 0.9 $M_\odot$. Thus, they constructed a table in which are reported all the

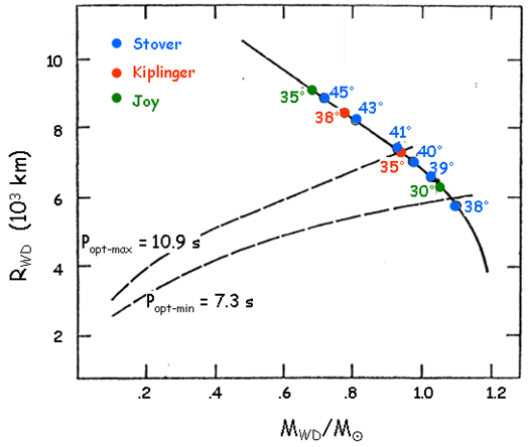

	i (deg)	50	45	44	43	42	41	40	39	38	35
	S	12.0	13.0	13.2	13.5	13.7	14.0	14.3	14.6	14.9	16.0
$(a/10^{10})$ cm	K	9.9	10.7	10.9	11.1	11.4	11.6	11.8	12.1	12.3	13.3
	J	11.8	12.7	13.0	13.2	13.5	13.7	14.0	14.3	14.6	15.7
	S	0.33	0.42	0.45	0.47	0.50	0.53	0.56	0.60	0.64	0.79
$M_R/M_\odot$	K	0.22	0.27	0.29	0.31	0.32	0.34	0.36	0.39	0.42	0.52
	J	0.44	0.57	0.60	0.63	0.67	0.71	0.75	0.80	0.86	1.06
	S	0.57	0.73	0.78	0.81	0.86	0.93	0.97	1.04	1.11	1.37
$M_{wd}/M_\odot$	K	0.29	0.37	0.39	0.42	0.43	0.46	0.49	0.52	0.56	0.69
	J	0.40	0.51	0.54	0.57	0.60	0.64	0.68	0.72	0.77	0.95
	S	0.57	0.62	0.63	0.64	0.66	0.67	0.68	0.70	0.71	0.77
$R_R/R_\odot$	K	0.50	0.54	0.56	0.57	0.58	0.59	0.60	0.62	0.63	0.67
	J	0.66	0.71	0.72	0.74	0.75	0.77	0.78	0.80	0.82	0.88
	S	2.40	2.60	2.65	2.70	2.75	2.80	2.86	2.92	2.99	3.20
$R_d/R_\odot$	K	2.58	2.78	2.84	2.89	2.96	3.02	3.07	3.14	3.21	3.43
	J	11.20	12.10	12.30	12.50	12.80	13.00	13.30	13.60	13.90	14.90

Figure 107: Left panel: mass-radius relationship for the WD and possible orbital inclination angles delimited by the values of optical pulsations (Adapted from Giovannelli et al., 1983). Right panel: table with orbital parameters for different values of orbital inclination angles. Light-red horizontal rectangles show the most probable values, coming from Stover et al. (1980), and the light-red vertical rectangle shows the orbital parameters of SS Cyg (adapted from Giovannelli et al., 1983).

parameters for different values of the orbital inclination angle (Fig. 107, right panel). Therefore, the orbital parameters of SS Cyg can be derived from the column marked with a light-red rectangle.

Thus, the orbital parameters of SS Cyg are:

$i = 40^{\circ}{}^{+1^{\circ}}_{-2^{\circ}}$; $a = 14.3^{+0.6}_{-0.3} \times 10^{10}$ cm; $M_R = 0.56^{+0.08}_{-0.03}$ $M_\odot$; $M_{WD} = 0.97^{+0.14}_{-0.05}$ $M_\odot$; $R_R = 0.68^{+0.03}_{-0.01}$ $R_\odot$; $R_d = 2.86^{+0.13}_{-0.06} \times 10^{10}$ cm.

From the H_β in emission, Giovannelli et al. (1983) determined the width at the level of continuum as ≈ 2500 km s^{-1}. This imply a value of the innermost part of the accretion disk of $R_{in} \approx 3.6 \times 10^9$ cm. This value is consistent with the radius of the WD ($R_{WD} = 5 \times 10^8$ cm) derived by Martinez-Pais et al. (1994). Bisikalo et al. (2008) by using Doppler tomography for SS Cyg in quiescence found $R_{in} = (2.6 - 3.3) \times 10^9$ cm, in agreement with the value derived, with less elaborate mode, by Giovannelli et al. (1983).

From the goodness of Giovannelli et al. (1983) parameters several other results are coming out, like the position of SS Cyg in the plot of the Keplerian period at the surface of the WD, contrary to the position plotted by Patterson (1981), who used the Chandrasekhar limit for the WD mass of SS Cyg (see Fig. 119, left panel). Another interesting results is reported in Fig. 119 (right panel). Indeed, if we use the diagram $\dot{M}_{tr}$ vs R_d (the mean mass-transfer rate vs. radius of the accretion disk) and the critical accretion rate marked with red line in the right panel of Fig. 119 (Schreiber & Lasota, 2007):

$$\dot{M}_{crit} = 9.5 \times 10^{15} \text{ g s}^{-1} \times R_{10}^{2.68} \times M_{WD}\ (M_\odot)$$

(being R_{10} the accretion disk radius in unit of 10^{10} cm),

and the critical accretion rate for SS Cyg derived with the Giovannelli et al. (1983) parameters is:

$\dot{M}_{crit}$(SS Cyg) = 1.6 $\times 10^{17}$ g s^{-1}

Thus, the position of SS Cyg is marked with the light-red rectangle, according to experimental error bars, in the right panel of Fig. 108.

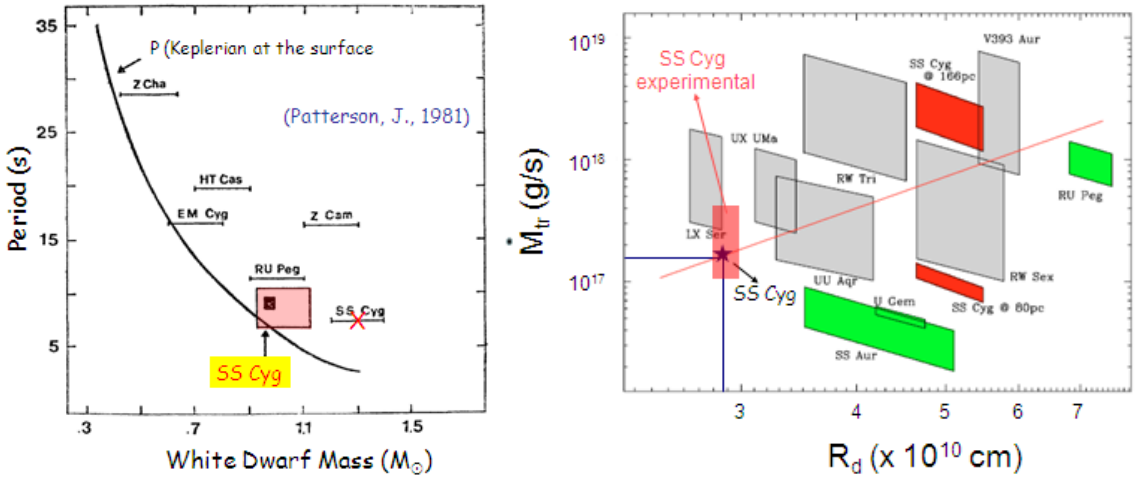

Figure 108: Left panel: Keplerian period at the WD surface versus WD mass (Giovannelli et al., 1983 after Patterson, 1981). Right panel: (adapted from Schreiber & Lasota, 2007).

In my opinion, another open question is that about the nature of SS Cyg: NMCV or MCV (IP). There are many papers that discuss such a problem, like those by Giovannelli (1985, 1996), Lombardi, Giovannelli & Gaudenzi (1987), Giovannelli, Martinez-Pais & Sabau-Graziati (1992), Gaudenzi et al. (2002), Giovannelli & Sabau-Graziati (1999, 2012a,b). In particular in the latter two papers by Giovannelli & Sabau-Graziati (2012a,b) a deep discussion of the pro and contra about the IP nature of SS Cyg is reported.

Name[a]	α, δ[b] (IBIS position)	type[c]	offset[d] (°)	Map code[e]	Count rate[f] (ct s^{-1})	Exposure (ks)	Flux[g] 20-100 keV	P_{orb} (min)	P_{spin} (s)	Distance[h] (pc)	Refs
1RXS J002258.3+614311	5.739,61.714	IP	1.7	B4(8.7)	0.15 ± 0.01	3707	0.81	241.98	503.53	510	[1,2,3,4]
V709 Cas	7.207,59.303	IP	0.8	B5(54.3)	1.03 ± 0.01	3562	5.53	320.4	312.77	300	[1,2,5]
XY Ari•	44.047,19.457	IP	1.1	B5(5.5)	0.53 ± 0.12	119	2.85	363.884	206.298	610	[1,2,6]
GK Per	52.777,43.928	IP/DN	1.7	B5(4.7)	0.26 ± 0.07	277	1.4	2875.4	351.34	-	[1,2]
TV Col•	82.357,-32.819	IP	0.1	B4(11.6)	0.68 ± 0.08	248	0.37	329.181	1911	330	[1,2,7,8]
TW Pic•	83.795,-57.908	IP?/VY Scl?••	2.5	B1(5.8)	0.3 ± 0.07	303	1.61	-	-	-	[1,2,9,10,11]
BY Cam	85.728,60.842	AP	1.2	B5(5.1)	0.69 ± 0.11	162	3.7	201.298	11846.4	140	[1,2]
MU Cam	96.316,73.567	IP	0.6	B4(5.4)	0.24 ± 0.06	548	1.29	283.104	1187.24	440	[1,2,12]
SWIFT J0732.5−1331•	113.13,-13.513	IP	1.6	B3(6.1)	0.39 ± 0.06	409	2.09	336.24	513.42	-	[1,2,13]
V834 Cen	212.268,-45.290	P	0.9	B1(5.4)	0.16 ± 0.03	1675	0.86	101.51712	6091.9272	70	[1,2]
IGR J14536−5522	223.421,-55.394	P	2.0	B4 (11.9)	0.27 ± 0.03	2658	1.45	189.36	11361.6	140	[1,2,14]
NY Lup	237.052,-45.481	IP	0.5	B5(49.1)	1.17 ± 0.03	3141	6.28	591.84	693.01	-	[1,2,15]
V2400 Oph	258.173,-24.279	IP	2.2	B3(33.4)	0.68 ± 0.02	4453	3.65	204.48	927.6	180	[1,2,16]
1H 1726−058	262.606,-5.984	IP	0.7	B5(22.8)	0.85 ± 0.04	1449	4.56	925.27	128	-	[1,2,17]
V2487 Oph	262.968,-19.244	IP/Nova	2.3	B3(9.1)	0.18 ± 0.02	4562	0.97	-	-	-	[1,2,18]
AX J1832.3−0840•	278.083,-8.721	?	3.1	B4(5.5)	0.07 ± 0.03	3000	0.38	-	-	-	[1,2,19,20]
V1223 Sgr	283.753,-31.153	IP	0.8	B5(52.2)	1.45 ± 0.03	2358	7.79	201.951	746	150	[1,2]
V1432 Aql	295.052,-10.421	AP	0.2	B5(30.8)	0.69 ± 0.07	429	3.7	201.938	12150.4	240	[1,2,21,22]
V2069 Cyg	320.906,42.279	IP•	1.8	B5(6.2)	0.21 ± 0.03	1648	1.13	448.824	743.2	-	[1,2,23,24]
1RXS J213344.1+510725	323.446,51.122	IP	0.3	B5(25.8)	0.65 ± 0.03	2207	3.49	431.568	570.82	-	[1,2,25]
SS Cyg	325.698,43.582	DN	0.6	B5(23.0)	0.7 ± 0.03	1674	3.76	396.3872	-	-	[1,2,26]
FO Aqr	334.514,-8.354	IP	1.7	B4(6.1)	0.65 ± 0.2	54	3.49	290.966	1254.45	250	[1,2,27]
AO Psc•	343.815,-3.194	IP	1.3	B4(4.8)	0.43 ± 0.11	108	2.31	215.461	805.2	200	[1,2,28,29]

Figure 109: List of CVs measured by the INTEGRAL observatory in the hard X-ray range (adapted by Scaringi et al. (2010).

However, since I would like to convince a reader that it is always appropriate to use wisdom in every event of life and in particular in science, I ask a question below to which each one will be able to answer as best he can, however trying to avoid prejudices.

INTEGRAL observatory measured hard X-ray emission from 23 MCVs, with the exception of SS Cyg, classified as NMCV, as shown in Fig. 109 (Scaringi et al., 2010). Thus, my question is: why all the CVs measured by the INTEGRAL are MCVs, but SS Cyg? And, if SS Cyg is NMCV, why INTEGRAL did not measure any other NMCV?

9.3 X-ray/Be systems

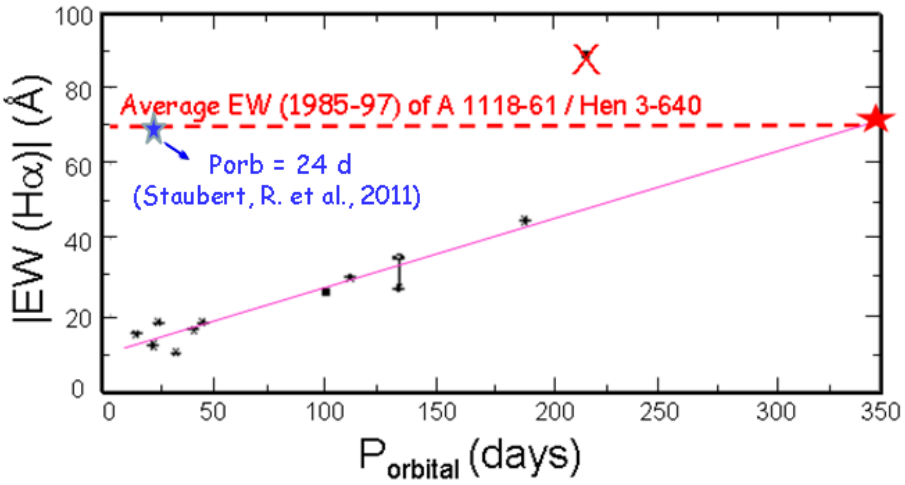

Figure 110: The relationship between H_α-EW and P_{orb} in X-ray/Be systems (after Reig, Fabregat & Coe, 1997; Villada et al., 1999).

Another example of the use of wisdom is that referred to the X-ray/Be system A 1118-61/Hen 3-640, for which Reig, Fabregat & Coe (1997) used one single measurement of the equivalent width (EW) of H_α (89 Å) in their interesting diagram in which a relationship between the H_α-EWs and the orbital period (P_{orb}) of Be/X-ray binaries has been found. The point relative to A 1118-61/Hen 3-640 system (red cross in Fig. 110) is clearly outside of the line best fitting the other data. However, if we use the average value (from 1985 to 1997) of H_α-EW = 70 Å, like reported in Villada et al. (1999), also the position of the A 1118-61/Hen 3-640 system is well on the line best fitting the data (red star in Fig. 110). Moreover an indication of the possible value of the orbital period ($\sim$ 350 days), not yet known, is coming from that diagram. This can help the search for the orbital period of the system around the value of 350 days. However, a value of orbital period of 24 days was reported by Staubert et al. (2011). In my opinion this value is wrong. Indeed if we put such a value in the diagram of Fig. 110 (blue cross) in correspondence with the average value of H_α-EW = 70 Å, it appears completely outside the line best fitting the data.

10. Conclusions and perspectives

In this review paper I have discussed several arguments that in my opinion are fundamental for the comprehension of the physics of our Universe. I have emphasized with some examples the use of wisdom in physics.

It is important the *Great examples of synergy between Astrophysics and History*, that I discussed for demonstrating that Sedov's formula for determining the age of SNRs can be revisited,

thanks to the recalibration of the age of the SNR Vela Jr (Aschenbach, 2016) experimentally supported by a historical document. The second example is the one that allowed the recognition of a cataclysmic variable – now not in the center of the nebula – as responsible of the explosion of the nova of 1437 A.D.

I discussed about the small and big space- and ground-based experiments that provide measurements necessary for the advancement of the knowledge of the physics of our Universe. Thanks to these results I discussed the present situation about the problems resolved and those still open, far from the completeness due to my limited knowledge.

As I discussed in the introduction, I can state that the Universe is interconnected in all its components: from cosmic network, to clusters of galaxies, to galaxies, to stars, to planets, to living beings, up to the simple bacterium. Therefore even every manifestation of life on our planet is subject to interconnection with all the surrounding environment. I can affirm that the whole Universe is a vital whole interconnected with more or less strong links between the various components, but that certainly exist.

It appears evident the role of the magnetic field intensity at the surface of the white dwarf in CVs. It was also remarked the importance of studying the evolutionary path of CVs that very probably is a continuous path connecting the so-called NMCVs with MCVs.

Indeed, the detection of several SW Sex systems having orbital periods inside the so-called 'period gap' opens a new interesting problem about the continuity in the evolution of CVs. Are the IPCVs and PCVs smoothly connected via the SW Sex-like systems placed just in between?

In order to fully understand the emission properties and evolution of CVs, the mass–transfer process needs to be clearly understood, especially magnetic mass transfer, as well as the properties of magnetic viscosity in the accretion disks around compact objects. Consequently, the investigation on the magnetic field intensities in WDs appears crucial in understanding the evolution of CVs systems, by which it is possible to generate classical novae (e.g., Isern et al., 1997) and type-Ia supernovae (e.g., Isern et al., 1993).

In those catastrophic processes the production of light and heavy elements, and then the knowledge of their abundances provides strong direct inputs for cosmological models and cosmic ray generation problems.

I want to conclude with a general warning, apparently underestimated, like discussed in Subsection 1.1: if we have not experimental information about the cross sections of nuclear reactions occurring in the stars it is hard to describe the correct star evolution.

The LUNA (Laboratory for Underground Nuclear Astrophysics) is devoted to measure nuclear cross sections relevant in astrophysics and astroparticle physics. It is the most valuable experiment running underground in the Gran Sasso Laboratory of the INFN. LUNA experiment provided the measures of the cross-sections of many nuclear reactions occurring in the stars for a better knowledge of stellar evolution.

I have discussed about:

- GRBs giving a general panorama on the models best fitting the data.
- The confirmation of the theory of General Relativity with the detection of Gravitational Waves and Gravitational Lenses.

- The Big Bang Nucleosynthesis theory that has been proved.
- The flatness of the Universe.
- An exhaustive excursion on the determination of the Hubble constant.
- The reionization epoch.
- The history of star formation.
- The background radiation in the universe.
- The unified model for compact sources.
- Jets in astrophysics.
- The tidal disruption of stars by massive Black Holes.
- Some points on neutrinos

An interesting part has been devoted to the "habitable zone in the Milky Way and exoplanets" with the description of several experiments for hunting exoplanets.

I wanted to underline the behaviour of mankind, which behaves as a declared enemy of Gaia, forgetting to be a guest of the planet and not a master.

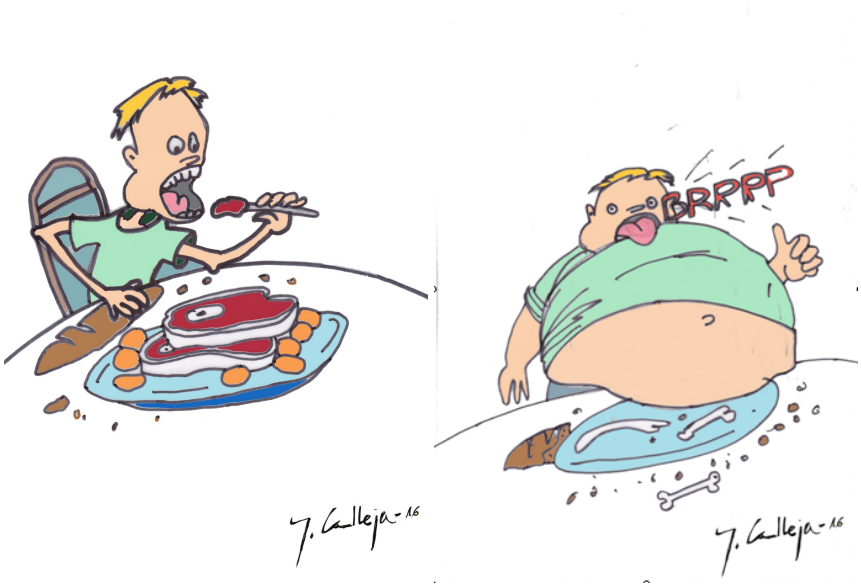

Figure 111: Left panel: Mass accretion onto a thin guy. Right panel: The fat guy after the accretion process (Jaime Sanchez Calleja, 2016).

I have discussed about the accretion processes in cosmic sources of different nature. We have learned that the accretion is universal even into the oceans and in the space.... and at the table, as clearly shown in the cartoon of Fig. 111 (Jaime Sanchez Calleja, 2016).

In order to give some scientific perspectives for the next decade it is worth mentioning a few sentences of the preface, summary and the scientific opportunities of the book *Pathways to Discovery in Astronomy and Astrophysics for the 2020s* (National Academies of Sciences, Engineering, and Medicine, 2021). The great efforts in developing science in the most astounding field of modern physics (astrophysics) are evident. Indeed, we live in an extraordinary period of discovery in astronomy and astrophysics. Six Nobel Prizes have been awarded over the past decade alone for discoveries based on astronomical data (dark energy, gravitational waves, neutrino oscillations, the discovery of exoplanets, cosmology, supermassive black holes). Many of the ambitious scientific visions of the *2010 New Worlds New Horizons (NWNH)* (National Research Council, 2010). NWNH decadal survey are being fulfilled, but momentum has only grown. We stand on the threshold of new endeavors that will transform not only our understanding of the universe and the processes and physical paradigms that govern it, but also humanity's place in it.

The National Academies of Sciences, Engineering, and Medicine shall convene an ad hoc survey committee and supporting study panels to carry out a decadal survey in astronomy and astrophysics. The study will generate consensus recommendations to implement a comprehensive strategy and vision for a decade of transformative science at the frontiers of astronomy and astrophysics.

The report of such a Committee for a *Decadal Survey on Astronomy and Astrophysics 2020 (Astro2020)* proposes a broad, integrated plan for space- and ground-based astronomy and astrophysics for the decade 2023-2032 (Fiona Harrison & Robert Kennicutt, Co-Chairs, 2021).

The survey's scientific vision is framed around three broad themes that embrace some of the most exciting new discoveries and progress since the start of the millennium, and that promise to address some of the most fundamental and profound questions in our exploration of the cosmos. The first theme, Worlds and Suns in Context builds on revolutionary advances in our observations of exoplanets and stars and aims to understand their formation, evolution, and interconnected nature, and to characterize other solar-like systems, including potentially habitable analogs to our own. New Messengers and New Physics will exploit the new observational tools of gravitational waves and particles, along with temporal monitoring of the sky across the electromagnetic spectrum and wide-area surveys from the ultraviolet and visible to microwave and radio to probe some of the most energetic processes in the universe and also address the nature of dark matter, dark energy, and cosmological inflation. Research in the third theme, Cosmic Ecosystems, will link observations and modeling of the stars, galaxies, and the gas and energetic processes that couple their formation, evolution, and destinies. Within each of these broad and rich scientific themes, three priority areas motivate recommended investments over the coming decade. "Pathways to Habitable Worlds" is a step-by-step program to identify and characterize Earth-like extrasolar planets, with the ultimate goal of obtaining imaging and spectroscopy of potentially habitable worlds. "New Windows on the Dynamic Universe" is aimed at combining time-resolved multi-wavelength electromagnetic observations from space and the ground with non-electromagnetic signals to probe the nature of black holes, neutron stars, the explosive events and mergers that give rise to them, and to use signatures imprinted by gravitational waves to understand what happened in the earliest moments in the birth of the universe. "Unveiling the Drivers of Galaxy Growth" is aimed at revolutionizing our understanding of the origins and evolution of galaxies, from the nature of the tenuous cosmic webs of gas that feed them, to the nature of how this gas condenses and drives the formation of

stars.

A very important news, I discussed, is the detection of a planet in an external galaxy M51 (Di Stefano et al., 2021). With this fundamental paper, the search for **extroplanets**, planets in orbits located outside our galaxy, has now become a realistic and practical enterprise.

In my opinion we are witnessing a revolution similar to that of the discovery of a planet orbiting the star 51 Pegasi by Mayor & Queloz (1995). Until then, no planets were known rotating around a star outside the solar system, but the two planets orbiting the pulsar PSR 1257+12 announced by Wolszczan & Frail (1992).

Finally I can conclude with Fig. 112 that clearly explain all the mysteries of our Universe (Giovannelli, 2000), or if you prefer the same attempt written in another language as shown in Fig. 113 (Giovannelli, 2021). People who are able to read these sentences can understand that "**The truth is written in the book of the Nature. We must learn to read this book**".

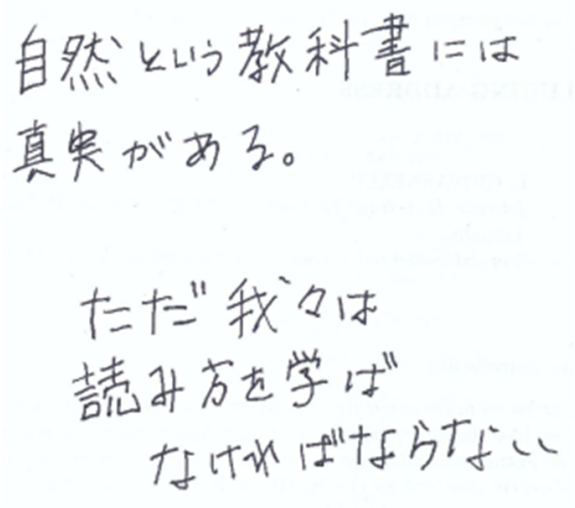

Figure 112: Understanding our Universe (Giovannelli, 2000).

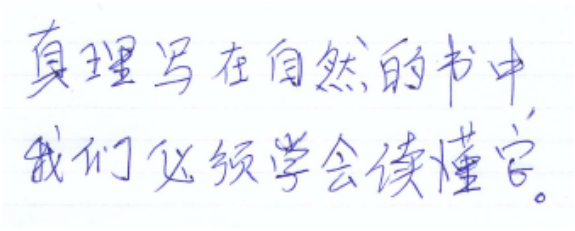

Figure 113: Understanding our Universe (Adopted from Giovannelli, 2021).

The experiments provide the basic alphabet, immersed in an apparently chaotic soup, but necessary to understand the nature. From that soup we must extract words and phrases to compose the book of the nature. In other words, the data coming from the experiments constitute the basic alphabet that we use for constructing models that attempt to describe the nature. But we have a lot of models for interpreting the experimental data by the light of science. Depending on the hypotheses the results could run against the experiments. Then, in order to be acceptable, models can take into account and justify **ALL the available data**.

The same concept was expressed in much more incisive terms by Richard Phillips Feynman – Nobel laureate in Physics in 1965 – also known as *The Great Explainer*: **It doesn't matter how beautiful your theory is, it doesn't matter how smart you are. If it doesn't agree with experiment, it's wrong**.

Acknowledgments This research has made use of:

- The NASA's Astrophysics Data System;
- the NASA Exoplanet Archive, which is operated by the California Institute of Technology, under contract with the National Aeronautics and Space Administration under the Exoplanet Exploration Program;
- the Exoplanet Orbit Database and the Exoplanet Data Explorer at exoplanets.org.

References

[1] Aad, G. (The ATLAS Collaboration): 2012, PhL B 718, 369-390.

[2] Aaij, R. et al.: 2015, arXiv:1507.03414v2 [hep-ex] 25 Jul.

[3] Aartsen, M.G., Abbasi, R., Abdou, Y., Ackermann, M., Adams, J. et al.: 2013, PhRv D 88, Issue 4, id. 042004.

[4] Abazajian, K.N. et al.: 2012, arXiv:1204.5379v1 [hep-ph] 18 Apr 2012

[5] Abbott, B.P. et al.: 2016a, PhRvL 116, 061102.

[6] Abbott, B.P. et al.: 2016b, PhRvL 116,1103.

[7] Abbott, B.P. et al.: 2016c, Living Rev. Relativity 19, Issue 1, article id. 1, 39 pp.

[8] Abbott, B.P. et al.: 2017a, PhRvL 119, Issue 16, id.161101, 18 pp.

[9] Abbott, B.P. et al.: 2017b, ApJL 848, Issue 2, article id. L12, 59 pp.

[10] Abbott, B.P. et al. (The LIGO Scientific Collaboration and The Virgo Collaboration, The 1M2H Collaboration, The Dark Energy Camera GW-EM Collaboration and the DES Collaboration, The DLT40 Collaboration, The Las Cumbres Observatory Collaboration, The VINROUGE Collaboration & The MASTER Collaboration): 2017c, Nature 551, 85-88.

[11] Abbott, B.P. et al. (LIGO Scientific Collaboration and Virgo Collaboration): 2019, PhRv X 9, Issue 3, id.031040.

[12] Abbott, B.P. et al.: 2017a, PhRvL 119, Issue 16, id.161101, 18 pp.

[13] Abbott, B.P. et al.: 2017b, ApJL 848, Issue 2, article id. L12, 59 pp.

[14] Abdo, A.A., Ackermann, M., Ajello, M., Allafort, A., Atwood, W.B. et al.: 2010, ApJ, 723, Issue 2, 1082-1096.

[15] Abe, K., Abgrall, N., Aihara, H., Ajima, Y., Albert, J.B. et al.: 2011, Nucl. Instr. & Meth. in Phys. Res. A, 659, Issue 1, 106-135.

[16] Abe, K., J. Adam, J., Aihara, H., Akiri, T., Andreopoulos, C. et al.: 2015, arXiv:1409.7469v2 [hep-ex] 10 Feb 2015.

[17] Abeysekara, A.U., Albert, A., Alfaro, R., Alvarez, C., Álvarez, J.D. et al.: 2017a, ApJ 841, Issue 2, article id. 100, 13 pp.

[18] Abeysekara, A.U., Albert, A., Alfaro, R., Alvarez, C., Álvarez, J.D. et al.: 2017b, ApJ 843, Issue 1, article id. 40, 21 pp.

[19] Abramowicz, M.A., Fragile, P.C.: 2013, Living Rev. in Relativity 16, Issue 1, article id. 1, 88 pp.

[20] Abu-Zayyad, T., Aida, R., Allen, M., Anderson, R., Azuma, R. et al.: 2013, ApJL 768, Issue 1, article id. L1, 5 pp.

[21] Acharya, B.F., Agudo, I., Al Samaral, I., Alfaro, R., Alfaro, J. et al. (The CTA Consortium): 2019, *Science with the Cherenkov Telescope Array*. Edited by CTA Consortium. Published by World Scientific Publishing Co. Pte. Ltd. – Also in arXiv:1709.07997v2.

[22] Acquafredda, R., Adam, T., Agafonova, N., Alvarez Sanchez, P., Ambrosio, M. et al.: 2009, J. Instr. 04, Issue 04, 04018.

[23] Adams, F.C., Shu, F.H.: 1986, ApJ 308. 836.

[24] Adams, F.C., Lada, C.J., Shu, F.H.: 1988, ApJ 326, 865-883.

[25] Adams, F.C., Emerson, J.P., Fuller, G.A.: 1990, ApJ 357, 606-620.

[26] Addamo, G., Ade, P.A.R., Baccigalupi, C., Baldini, A.M., Battaglia, P.M. et al.: 2021, JCAP 2021, Issue 08, id. 008, 69 pp.

[27] Ade, P.A.R. et al. (BICEP2/Keck Collaboration; Planck Collaboration): 2015, PhRvL 114, Issue 10, id. 101301.

[28] Ade, P.A.R. et al. (BICEP2 Collaboration; Keck Array Collaboration): 2018, PhRvL 121, Issue 22, id. 221301.

[29] Adelberger, E.G., Austin, S.M., Bahcall, J.N., Balantekin, A.B., Bogaert, G. et al.: 1998, Rev. Mod. Phys., 70, 1265-1291.

[30] Adelberger, E.G., García, A., Robertson, R.G. Hamish, Snover, K.A., Balantekin, A.B. et al.: 2011, Rev. Mod. Phys., 83, Issue 1, 195-246.

[31] Agafonova, N. et al., OPERA Collaboration: 2018, PhRvL 120, Issue 21, id. 211801.

[32] Aghanim, N., Akrami, Y., Arroja, F., Ashdown, M., Aumont, J. et al. (Planck Collaboration): 2020, A&A 641, id. A1, 56 pp.

[33] Aglietta, M., Alessandro, B., Antonioli, P., Arneodo, F., Bergamasco, L. et al.: 1999, Nucl. Phys. B Proc. Suppl. 75, Issue 1-2, 251-255.

[34] Albert, J. & Magic Collaboration: 2008, Science 320, Issue 5884, 1752-1754.

[35] Alcalá, J.M., Antoniucci, S., Biazzo, K., Bacciotti, F., Bianchi, E. et al.: 2015, *Jets, Disks and the Dawn of Planets*, Proc. of the 2nd JEDI meeting (JEts and Disk at INAF), S. Antoniucci, J. Alcalá, C. Codella, B. Nisini (Eds.), arXiv:1506.07073.

[36] Aldering, G.: 2005, NewAR 49, 346-353.

[37] ALMA Partnership; Brogan, C.L., Pérez, L.M., Hunter, T.R., Dent, W.R.F., Hales, A.S. et al.: 2015, ApJL 808, Issue 1, article id. L3, 10 pp.

[38] Amaro-Seoane, P., Audley, H., Babak, S., Baker, J., Barausse, E. et al.: 2017, arXiv:1702.00786.

[39] Amenomori, M., Bi, X.J., Chen, D., Cui, S.W., Danzengluobu, Ding, L.K. et al.: 2008, ApJ 678, Issue 2, 1165-1179.

[40] An, F., An, G., , An, Q., Antonelli, V., Baussan, E. et al.: 2015, arXiv:1507.05613v2 [physics.ins-det] 18 Oct 2015, 224 pp.

[41] Anders, M., Trezzi, D., Bellini, A., Aliotta, M., Bemmerer, D. et al.: 2013, EPJA, 49, id.28.

[42] Anders, M., Trezzi, D., Menegazzo, R., Aliotta, M., Bellini, A. et al. (LUNA Collaboration): 2014, Phys. Rev. Lett. 113, Issue 4, id.042501.

[43] André, P., 1994: in *The Cold Universe*, Montmerle Th., Lada C.J., Mirabel, I.F. & Trân Thanh Vân, J. (Eds), Editions Frontières, Paris, p. 179.

[44] Andrews, S.: 2016, in *Resolving planet formation in the era of ALMA and extreme AO*, Proc. of the conference held 16-20 May, 2016 in Santiago, Chile, id. 13.

[45] Andrews, S.M., Wilner, D.J., Zhu, Z., Birnstiel, T., Carpenter, J.M. et al.: 2016, ApJL 820, Issue 2, article id. L40, 5 pp.

[46] Andrews, S.M., Huang, J., Pérez, L.M., Isella, A., Dullemond, C.P. et al.: 2018, The Messenger 174, 19-23.

[47] Ansdell, M., Williams, J.P., van der Marel, N., Carpenter, J.M., Guidi, G. et al.: 2016, ApJ 828, Issue 1, article id. 46, 15 pp.

[48] Antoni, T., Apel, W.D., Badea, A.F., Bekk, K., Bercuci, A. et al. (KASCADE Collaboration): 2003, Astropart. Phys. 19, Issue 6, 703-714.

[49] Antoniucci, S.: 2018, talk at the *Accretion Processes in Cosmic Sources - II*, and Online at https://pos.sissa.it/cgi-bin/reader/conf.cgi?confid=342, id.14.

[50] Apel, W.D., Arteaga-Velázquez, J.C., Bekk, K., Bertaina, M., Blümer, J. et al.: 2012, Astrop. Phys. 36, Issue 1, 183-194.

[51] Arimoto, M., Tsubuku, Y., Toizumi, T., Kobayashi, M., Yatsu, Y. et al.: 2008, *Gamma-Ray Bursts 2007*, AIP Conf. Proc. 1000, 607-610.

[52] Arndt, N.T., Nisbet, E.G.: 2012, Annu. Rev. Earth Planet. Sci. 40, 521-549.

[53] Arquilla, R., Goldsmith, P.F.: 1986, ApJ 303, 356-374.

[54] Aschenbach, B.: 1998, Nature 396, Issue 6707, 141-142.

[55] Aschenbach, B.: 2016, in *Frontier Research in Astrophysics II*. Online at https://pos.sissa.it/cgi-bin/reader/conf.cgi?confid=269, id.36.

[56] Aso, Y., Ohashi, N., Saigo, K., Koyamatsu, S., Aikawa, Y. et al.: 2015, ApJ 812, Issue 1, article id. 27, 20 pp.

[57] Astor, M.: 2017, online at https://www.nytimes.com/2017/09/19/us/hurricanes-irma-harvey-maria.html

[58] Baade, W., Zwicky, F.: 1934, Phys. Rev. 45, 138.

[59] Bambi, C. (Ed.): 2016, *Astrophysics of Black Holes: From Fundamental Aspects to Latest Developments*, Astrophysics and Space Science Library, Volume 440, 207 pp.

[60] Bambi, C.: 2017, *Black Holes: A Laboratory for Testing Strong Gravity*, Springer Nature Singapore Pte Ltd., ISBN 978-981-10-4523-3, 340 pp.

[61] Bañados, E., Novak, M., Neeleman, M., Walter, F., Decarli, R. et al.: 2019, ApJ 881, Issue 1, article id. L23, 6 pp.

[62] Barone, F., Di Fiore, L., Milano, L., Russo, G.: 1992, General Relativity and Gravitation, 24, No. 3, 323-341.

[63] Barrett, P.M, Milner, A.R. (Eds.): 2012, *Special Papers in Palaeontology, Number 86, Studies on Fossil Tetrapods*, Wiley-Blackwell, ISBN: 978-1-444-36189-6, 280 pp.

[64] Bartelmann, M.: 2008, Rev. Mod. Astron. 20, Cosmic Matter, edited by Siegfried Röser. ISBN: 978-3-527-40820-7 (HB). Wiley, p. 92.

[65] Batalha, N.M.: 2014, Proc. of the National Academy of Sciences 111, Issue 35, 12647-12654.

[66] Bath, G.T.: 1969, ApJ 158, 571-587.

[67] Bath, G.T.: 1975, MNRAS 171, 311-328.

[68] Bath, G.T.: 1976, in *Structure and Evolution of Close Binary Systems*, IAU Symp. 73), 173-192.

[69] Bath, G.T.: 1978, Q. Jl R. astr. Soc. 19, 442-455.

[70] Bath, G.T.: 1980, in *Close binary stars: Observations and interpretation*, IAU Symp., M.J. Plavec, D.M. Popper & R.K. Ulrich (Eds.) p. 155-160.

[71] Bath, G.T.: 1984, Phys. Scr. 1984, 101.

[72] Bath, G.T., Evans, W.D., Papaloizou, J., Pringle, J.E.: 1974, MNRAS 169, 447-470.

[73] Bath, G.T., van Paradijs, J.: 1983, Nature, 305, 33.

[74] Battistelli, E.S., Ade, P., Alberro, J.G., Almela, A., Amico, G. et al.: 2020, J. Low Temp. Phys. 199, Issue 1-2, 482-490.

[75] Beall, A.: 2016, Article For Mailonline, Published: 15:03 BST, 7 June 2016 - Updated: 16:22 BST, 7 June 2016.

[76] Beall, J.H., Knight, F.K., Smith, H.A., Wood, K.S., Lebofsky, M., Rieke, G.: 1984, ApJ 284, 745-750.

[77] Beall, J.H., Guillory, J., Rose, D.V.: 1999, in *Multifrequency Behaviour of High Energy Cosmic Sources*, F. Giovannelli & L. Sabau-Graziati (Eds.), Mem. SAIt. 70, 1235-1248.

[78] Beall, J.H.: 2002, in *Multifrequency Behaviour of High Energy Cosmic Sources*, F. Giovannelli & L. Sabau-Graziati (Eds.) Mem. SAIt. 73, 379-386.

[79] Beall, J.H.: 2003, ChJA&A Suppl. 3, 373-382.

[80] Beall, J.H.: 2014, in *Multifrequency Behaviour of High Energy Cosmic Sources - X*, F. Giovannelli & L. Sabau-Graziati (Eds.), Acta Polyt. CTU Proc. 1(1), 259-264.

[81] Beall, J.H., Guillory, J., Rose, D.V., Schindler, S., Colafrancesco, S.: 2006, ChJA&A Suppl. 6, Issue S1, 283-291.

[82] Beall, J.H., Guillory, J., Rose, D.V., Schindler, S., Colafrancesco, S.: 2007, in *Frontier Objects in Astrophysics and Particle Physics*, F. Giovannelli & G. Mannocchi (Eds.), Italian Physical Society, Editrice Compositori, Bologna, Vol. 93, 315.

[83] Beckwith, S.V.W.: 1998, talk at the *The Physics of Star Formation & Early Stellar Evolution*, NATO/ASI, Crete II, 3 June.

[84] Beckwith, S.V.W.: 1999, in *The Origin of Stars and Planetary Systems*, Charles J. Lada & Nikolaos D. Kylafis (Eds.), Kluwer Academic Publishers, p. 579.

[85] Beckwith, S.V.W., Sargent, A.I., Chini, R.S., Guesten, R.: 1990, AJ 99, 924-945.

[86] Beckwith, S.V.W., Sargent, A.I.: 1991, ApJ 381, 250-258.

[87] Beckwith, S.V.W., Sargent, A.I.: 1996, Nature 383, 139-144.

[88] Bednarek, W., Giovannelli, F., Karakula, S., Tkaczyk, W.: 1990 A&A 236, 268-274.

[89] Begelman, M.C., Blandford, R.D., Rees, M.J.; 1984, Rev. Mod. Phys. 56, Issue 2, 255-351.

[90] Belczynski, K., Ziółkowski, J.: 2009, ApJ 707, 870.

[91] Belczynski, K., Dominik, M., Bulik, T., O'Shaughnessy, R., Fryer, C., Holz, D.E.: 2010, ApJL 715, L138.

[92] Bell, E.A., Harrison, T.M.: 2013, Earth and Planetary Science Letters, Vol. 364, 1-11.

[93] Bell, E.A., Boehnke, P., Hopkins-Wielicki, M.D., Harrison, T.M.: 2015, LITHOS, Vol. 234, 15-26.

[94] Bennett, C.L., Larson, D., Weiland, J.L., Jarosik, N., Hinshaw, G.: 2013, ApJS 208, Issue 2, article id. 20, 54 pp.

[95] Bennett, C.L., Larson, D., Weiland, J.L., Hinshaw, G.: 2014, ApJ 794, Issue 2, article id. 135, 8 pp.

[96] Berezhnev, S.F., Besson, D., Budnev, N.M., Chiavassa, A., Chvalaev, O.A et al.: 2012, NI&M in Phys. Res. A, 692, 98-105.

[97] Berger, E., Fong, W., Chornock, R.: 2013, ApJL 774, Issue 2, article id. L23, 4 pp.

[98] Bernardini, M.G.: 2015, J.HE Astrophys. 7, 64-72.

[99] Bernardini, F., de Martino, D., Mukai, K., Israel, G., Falanga, M. et al.: 2015, MNRAS 453, Issue 3, 3100-3106.

[100] de Bernardis, P., Ade, P.A.R., Bock, J.J., Bond, J.R., Borrill, J. et al.: 2000, Nature 404, Issue 6781, 955-959.

[101] de Bernardis, P.: 2014, talk at the Mondello Workshop *Frontier Research in Astrophysics - I*.

[102] de Bernardis, P., Ade, P., Amico, G., Auguste, D., Aumont, J. et al.: 2018, Boletín de la Asociación Argentina de Astronomía 60, 107-114.

[103] Beskin, V.S., Balogh, A., Falanga, M., Lyutikov, M., Mereghetti, S., Piran, T., Treumann, R.A. (Eds.): 2015, *The Strongest Magnetic Fields in the Universe*, Space Sciences Series of ISSI, Vol. 54, Springer Science+Business Media New York, ISBN 978-1-4939-3549-9, 579 pp.

[104] Beskin, V.S., Balogh, A., Falanga, M., Treumann, R.A.: 2016a, in The Strongest Magnetic Fields in the Universe: Spa. Sci. Ser. of ISSI, Vol. 54. p. 3.

[105] Beskin, V.S., Balogh, A., Falanga, M., Lyutikov, M., Mereghetti, S. et al.: 2016b, in The Strongest Magnetic Fields in the Universe: Spa. Sci. Ser. of ISSI, Vol. 54. ISBN 978-1-4939-3549-9. Springer.

[106] Bianchini, A.: 1990, in *Physics of Classical Novae*, A. Cassatella & R. Viotti (eds.), Springer-Verlag, Lecture Notes in Physics, 369, 13.

[107] Bianco, F.B., Howell, D.A., Sullivan, M., Conley, A., Kasen, D., et al.: 2011, ApJ, 741, Issue 1, article id. 20, 12 pp.

[108] Bignami, G.F., Fichtel, C.E., Kniffen, D.A., Thompson, D.J.: 1975, ApJ 199, 54-60.

[109] Birnstiel, T.: 2010, The Evolution of Gas and Dust in Protoplanetary Accretion Disks, PhD Thesis, Heidelberg University, Germany.

[110] Bisikalo, D.V., Kononov, D.A., Kaigorodov, P.V., Zhilkin, A.G., Boyarchuk, A.A.: 2008, ARep 52, 318-326.

[111] Bisikalo, D.V., Zhilkin, A.G.: 2012, in *From Interacting Binaries to Exoplanets: Essential Modeling Tools*, M.T. Richards & I. Hubeny (Eds.), IAU Symp. 282, 509-516.

[112] Bisikalo, D.V., Zhilkin, A.G.: 2015, Acta Polyt. CTU Proc. 2, 60-65.

[113] Bisikalo, D.V., Kurbatov, E.P., Pavlyuchenkov, Ya.N., Zhilkin, A.G., Kaygorodov, P.V.: 2016, MNRAS 458, 3892-3903.

[114] Bisnovatyi-Kogan, G.S.: 2011, *Stellar Physics 2: Stellar Evolution and Stability*, Berlin-Heidelberg: Springer-Verlag.

[115] Bisnovatyi-Kogan, G.S., Giovannelli, G.: 2017, A&A 599, A55, 7 pp. (BKG17).

[116] Blanch Bigas, O., Lopez, R., Carmona, E., MAGIC Collaboration; Pérez-Torres, M.A.: 2015, arXiv:1501.06405.

[117] Blandford, R.D., Kochanek, C.S.: 2004, in *Dark Matter in the Universe (Second Edition)*, J. Bahcall et al. (Eds.), World Scientific Publishing Co. Pte. Ltd., ISBN 9789812567185, pp. 103-158.

[118] Blaes, O.: 2014, SSRv 183, 21-41.

[119] Bloom, J., Castro-Tirado, A.J., Hanlon, L., Kotani, T. (Eds.): 2010, *I Workshop on Robotic Autonomous Observatories*, Advances in Astronomy, Vol. 2010.

[120] Blumenthal, G.R., Tucker, W.H.: 1974, Ann. Rev. A&A 12, 23-46.

[121] Bode, M.F.: 2011a, J. British Astron. Association 121, no.1, p. 47.

[122] Bode, M.F.: 2011b, arXiv:1111.4941.

[123] Bode, M.F., Evans, A. (eds.): 2008, *Classical Novae*, Cambridge Astrophys. Ser., No. 43, Cambridge University Press.

bibitem Boller, T.: 2017, talk at the Frascati Workshop 2017 *Multifrequency Behaviour of High Energy Cosmic Source - XII*.

[124] Boneva, D., Kaigorodov, P.V., Bisikalo, D.V., Kononov, D.A.: 2009, ARep 53, 1004-1012.

[125] Bonfils, X., Delfosse, X., Udry, S., Forveille, T., Mayor, M. et al.: 2013, A&A 549, id. A109, 75 pp.

[126] Botts, C.: 2015, in *Handbook of Cosmic Hazards and Planetary Defense*, Joseph, N. Pelton & Firooz Allahdadi (Eds.), Springer Reference, © Springer International Publishing Switzerland 2015, pp. 891-918.

[127] Bouvier, J.: 1990, AJ 99, 946-964.

[128] Bovaird, T., Lineweaver, C.H.: 2013, MNRAS 435, Issue 2, 1126-1138.

[129] Bucher, M. (on behalf of the PLANCK Collaboration): 2015a, Nucl and Part. Phys. Proc. 267-269, p. 245-253.

[130] Bucher, M. (on behalf of the PLANCK Collaboration): 2015b, Int. J. Mod. Phys. D, Volume 24, Issue 2, id. 1530004-303.

[131] Brinkworth, C.S., Hoard, D.W., Wachter, S., Howell, S.B., Ciardi, D.R., et al: 2007, in *15th European Workshop on WDs*, R. Napiwotzki & M. R. Burleigh (eds.), ASP Conf. Ser. 372, 333-336.

[132] Brogan, C.L., Pérez, L.M., Hunter, T.R., Dent, W.R.F., Hales, A.S. et al. (ALMA Partnership): 2015, ApJL 808, Issue 1, article id. L3, 10 pp.

[133] Broggini, C., Bemmerer, D., Guglielmetti, A., Menegazzo, R.: 2010, Annu. Rev. Nucl. Part. Sci. 60, 53-73.

[134] Broggini, C., Bemmerer, D., Caciolli, A., Trezzi, D.: 2018, Progr. in Part. and Nucl. Phys. 98, 55-84.

[135] Bromm, V., Loeb, A.: 2002, ApJ 575, Issue 1, 111-116.

[136] Brown, W.R., Kilic, M., Allende Prieto, C.A., Kenyon, S.J.: 2011, MNRAS, 411, Issue 1, L31-L35.

[137] Bruno, C.G., Scott, D.A., Aliotta, M., Formicola, A., Best, A. et al. (LUNA Collaboration): 2016, Phys. Rev. Lett. 117, Issue 14, id.142502.

[138] Bruno Giordano Nolano: 1584, *De l'infinito, universo et mondi*, Stampato in Venezia, Anno MDLXXXIV, in *Dialoghi filosofici italiani*, a cura di Michele Ciliberto, Mondadori, Milano (2000).

[139] Buckley, D., 2015, talk at the Palermo Workshop on "*The Golden Age of Cataclysmic Variables and Related Objects - III*".

[140] Buckley, D.A.H., Meintjes, P.J., Potter, S.B., Marsh, T.R., Gänsicke, B.T.: 2017, Nat. As. 1, id. 0029.

[141] Budnev, N., Astapov, I., Bezyazeekov, P., Bogdanov, A., Boreyko, V. et al.: 2016, J. Phys. Conf. Ser. 718, Issue 5, article id. 052006.

[142] Budnev, N., Kuzmichev, L.A., Mirzoyan, R., Astapov, I., Bezyazeekov, P. et al.: 2017, 35th ICRC, Proc. of Science 301. Online at https://pos.sissa.it/cgi-bin/reader/conf.cgi?confid=301, id. 768.

[143] Budnev, N.N., Chiavassa, A., Gress, O.A., Gress, T.I., Dyachok, A.N. et al.: 2021, arXiv:2104.03599v1 [astro-ph.HE] 8 Apr 2021.

[144] Burbidge, E.Margaret, Burbidge, G.R., Fowler, W.A., Hoyle, F.: 1957, Rev. Mod. Phys. 29, 547-655.

[145] Burger, M., van Dessel, E.L., Giovannelli, F., Sabau-Graziati, L., Bartolini, C. et al.: 1996, in *Multifrequency Behaviour of High Energy Cosmic Sources*, F. Giovannelli & L. Sabau-Graziati (eds.), Mem. SAIt. 67, 365.

[146] Burles, S., Nollett, K.M., Turner, M.S.: 2001, ApJ 552, Issue 1, L1-L5.

[147] Burrows, C.J., Stapelfeldt, K.R., Watson, A.M., Krist, J.E., Ballester, G.E. et al.: 1996, ApJ 473, 437-451.

[148] Buson, S. (Fermi-LAT Collaboration): 2014, in *Frobtier Research in Astrophysics*, Franco Giovannelli & Lola Sabau-Graziati (Eds.), http://pos.sissa.it/cgi-bin/reader/conf.cgi?confid=237, id. 7.

[149] Caballero-García, M.D., Pandey, S.B., Hiriart, D. & Castro-Tirado, A.J. (Eds.): 2016, *IV Workshop on Robotic Autonomous Observatories*, RMxAC, Vol. 48.

[150] Calvet, N., Hartmann, L., Strom, S.E.: 2000, in *Protostars and Planets IV*, (Book - Tucson: University of Arizona Press; Mannings, V., Boss, A.P., Russell, S.S. - Eds.), p. 377-398. Also arXiv:astro-ph/9902335.

[151] Cameron, A.G.W.: 1958, Ann. Rev. Nucl. Part. Sci. 8, 299-326.

[152] Cami, J., Bernard-Salas, J., Peeters, E., Malek, S.E.: 2010, Sci., 329, Issue 5996, 1180-1182.

[153] Camilo, F., Ransom, S.M., Halpern, J.P., Reynolds, J., Helfand, D.J. et al.: 2006, Nature, 442, Issue 7105, 892-895.

[154] Cappellini, E., Prohaska, A. Racimo, F., Welker, F., Winther Pedersen, M. et al.: 2018, Annu. Rev. Biochem. 87, 1029-1060. Online at https://doi.org/10.1146/annurev-biochem-062917-012002.

[155] Cardini, A.: 2015, *Interview of Alessandro Cardini, P.I. of LHCb*, 14th July 2015.

[156] Carey, James R., Tuljapurkar, Shripad (Eds.): 2003, *Life Span: Evolutionary, Ecological, and Demographic Perspectives*, Population and Development Review, A Supplement to Volume 29, 308 pp., Population Council, New York.

[157] Carpenter, J.M., Bouwman, J., Mamajek, E.E., Meyer, M.R., Hillenbrand, L.A. et al.: 2009, ApJ Suppl. Ser. 181, 197-226.

[158] Carpenter, J. et al.: 2018, *The ALMA Development Roadmap*, https://www.eso.org/sci/facilities/alma/developmentstudies/ALMA¬Deve lopment¬Roadmap¬public.pdf

[159] Carpenter, J., Iono, D., Testi, L., Whyborn, N., Wootten, A., Evans, N.: 2019, arXiv:1902.02856.

[160] Casares, J.: 2015, ApJ 808, Issue 1, article id. 80, 11 pp.

[161] Casares, J., Jonker, P.G.: 2014, SSRv 183, 223-252.

[162] Casares, J., Negueruela, I., Ribó, M., Ribas, I., Paredes, J.M. et al.: 2014, Nature 505, Issue 7483, 378-381.

[163] Caselli, P.: 2002, P&SS 50, Issue 12-13, 1133-1144.

[164] Caselli, P.: 2003, Ap&SS 285, Issue 3, 619-631.

[165] Cassatella, A., Viotti, R. (eds.): 1990, *Physics of Classical Novae*, Springer-Verlag, Lecture Notes in Physics, 369.

[166] Castro Cerón, J.M.: 2011, talk at the Frascati Workshop 2011 on "*Multifrequency Behaviour of High Energy Cosmic Sources*".

[167] Castro-Tirado, A.J.: 2008, in *3rd Symposium of the Astrophysics Group of the Spanish Royal Physical Society (RSEF)*, A. Ulla & M. Manteiga (Eds.), Lecture Notes and Essays in Astrophysics 3, 131.

[168] Castro-Tirado, A.J.: 2010a, Adv. Astron. Vol. 2010, Article ID 570489, 8 pp.

[169] Castro-Tirado, A.J.: 2010b, Adv. Astron. Vol. 2010, Article ID 824731, 1 p.

[170] Castro-Tirado, A.J., Brandt, S., Lund, N., Lapshov, I., Sunyaev, R.A.: 1994, ApJ Suppl. Ser. 92, 469-472.

[171] Castro-Tirado, A.J., Möller, P., García-Segura, G., Gorosabel, J., Pérez, E. et al.: 2010, A&A 517, id. A61, 9 pp.

[172] Castro-Tirado, A.J., Pandey, S.B., Caballero-García, M.D (Eds.): 2021, *VI Workshop on Robotic Autonomous Observatories* Rev. Mex. A&A Conf. Ser. 53,

[173] Catanese, M., Akerlof, C.W., Badran, H.M., Biller, S.D., Bond, I.H. et al.: 1998, ApJ 501, Issue 2, 616-623.

[174] Cautun, M., Benitez-Llambay, A., Deason, A.J., Frenk, C.S., Fattahi, A. et al.: 2020, MNRAS 494, Issue 3, 4291-4313.

[175] Cavanna, F. (on behalf of the LUNA collaboration): 2018, in International Symposium on ´*Capture Gamma-Ray Spectroscopy and Related Topics (CGS16)*, Sun, Yang (Ed.), EPJ Web of Conferences, Volume 178, id.01007.

[176] Cavanna, F., Depalo, R., Aliotta, M., Anders, M., Bemmerer, D. et al. (LUNA Collaboration): 2015, Phys. Rev. Lett. 115, Issue 25, id.252501.

[177] Chadwick, P.M., Lyons, K., McComb, T.J.L., Orford, K.J., Osborne, J.L. et al.: 1999, ApJ 521, Issue 2, 547-551.

[178] Chamie, J.: 2016, *The Historic Reversal of Population*, Online at http://www.ipsnews.net/2016/08/the-historic-reversal-of-populations/

[179] Chatterjee, J.: 2013, *Legal Aspects of Space Debris Remediation: Active Removal of Debris and On-Orbit satellite Servicing*, Master of Law Degree Thesis, McGill University, Montreal, Canada. Online at http://digitool.library.mcgill.ca/webclient/StreamGate?folder$_id = 0\&dvs = 1552495872672{\sim}456$

[180] Chatterjee, J., Pelton, J.N., Allahdadi, F.: 2015, in *Handbook of Cosmic Hazards and Planetary Defense*, Joseph, N. Pelton & Firooz Allahdadi (Eds.), Springer Reference, © Springer International Publishing Switzerland 2015, pp. 921-940.

[181] Chaty, S.: 1998, *Multi-wavelength study of the microquasar GRS 1915+105 and of high-energy binary sources in the Galaxy*, PhD Thesis, Paris XI University (France).

[182] Chaty, S.: 2011, in *Evolution of compact binaries*, Linda Schmidtobreick, Matthias R. Schreiber & Claus Tappert (Eds.). ASP Conf. Proc. 447. 29-43.

[183] Chiang, E.I., Goldreich, P.: 1997, ApJ 490, 368-376.

[184] Chiosi, E., Chiosi, C., Trevisan, P., Piovan, L., Orio, M.: 2015, MNRAS 448, Issue 3, 2100-2125.

[185] Christenson, J.H., Cronin, J.W., Fitch, V.L., Turlay, R.: 1964, PhRvL, 13, Issue 4, 138-140.

[186] Churazov, E., Sunyaev, R., Isern, J., Knödlseder, J., Jean, P. et al.: 2014, Nature 512, Issue 7515, 406-408.

[187] Churazov, E., Sunyaev, R., Isern, J., Bikmaev, I., Bravo, E. et al.: 2015, ApJ 812, Issue 1, article id. 62, 17 pp.

[188] Ciardi, B., Loeb, A.: 2000, ApJ 540, Issue 2, 687-696.

[189] Cieza, L.A.: 2016, in Young Stars & Planets Near the Sun, IAU Symp. 314, 128-134.

[190] Cieza, L.A., Prieto, J.L., Zhu, Z., Tobin, J.J., Williams, J.P. et al.: 2016, AAS Meeting 227, id. 343.05.

[191] Clack, J.A: 2009, Evo Edu Outreach 2, 213-223.

[192] Clark, D.H., Stephenson, F.R.: 1977, *The Galactic Supernovae*, New York: Pergamon Press, 1st ed.

[193] Clarke, F.J., Gosling, A.J., Doolin, S., Goodall, P. Perez, S. et al.: 2008, in *Ground-based and Airborne Instrumentation for Astronomy II*, McLean, Ian S., Casali, Mark M. (Eds.), Proc. of the SPIE 7014, article id. 70145A, 8 pp.

[194] Clay, J.: 1927, Proc. Nederlandsche Akad. v. Wet. 30, 1115.

bibitem Cleeves, L. I., Bergin, E.A., Alexander, C.M.O.'D., Du, F., Graninger, D. Öberg, K.I. Harries, T.J: 2014, Science, 345, Issue 6204, 1590-1593.

[195] Coburn, W., Heindl, W.A., Rothschild, R.E., Gruber, D.E., Kreykenbohm, I. et al.: 2002, ApJ 580, Issue 1, 394-412.

[196] Coe, M.J., Carpenter, G.F., Engel, A.R., Quenby, J.J.: 1975, Nature 256, 630.

[197] Coe, M.J., Reig, P., McBride, V.A., Galache, J.L., Fabregat, J.: 2006, MNRAS 368, 447.

[198] Coe, M.J., Bird, A.J., Buckley, D.A.H., Corbet, R.H.D., Dean, A.J. et al.: 2010, MNRAS 406, Issue 4, 2533-2539.

[199] Cohen, M.: 1983, ApJ 270, L69.

[200] Coleiro, A., Chaty, S.: 2013, ApJ 764, 185.

[201] Contopoulos, I., Gabuzda, D., Kylafis, N. (Eds.): 2015, *The Formation and Disruption of Black Hole Jets*, Astrophysics and Space Science Library, Volume 414. ISBN 978-3-319-10355-6. Springer International Publishing Switzerland, 273 pp.

[202] Cooley, J.W., Tukey, J.W.: 1965, *An algorithm for the machine calculation of complex Fourier series*, Math. Comput. 19, 297-301.

[203] Cooray, A.: 2016, Royal Society Open Science 3: 150555. http://dx.doi.org/10.1098/rsos.150555.

[204] Coppi, P.S., Aharonian, F.A.: 1997, ApJ, 487, Issue 1, L9-L12.

[205] Corbet, R.H.D.: 1984, A&A 141, 91.

[206] Corbet, R.H.D.: 1986, MNRAS 220, 1047.

[207] Cordova, F.A., Chester, T.J., Tuohy, I.R., Garmire, G.P.: 1980, ApJ 235, 163-176.

[208] Costamante, L.: 2012, in *Multifrequency Behaviour of High Energy Cosmic Sources*, F. Giovannelli & L. Sabau-Graziati (Eds.), Mem. SAIt., 83, 138-145.

[209] Cottin, H., Kotler, J.M., Bartik, K., Cleaves, H.J., Cockell, C.S. et al.: 2017a, SSRv 209, Issue 1-4, 1-42.

[210] Cottin, H., Kotler, J.M., Billi, D., Cockell, C., Demets, R. et al.: 2017b, SSRv 209, Issue 1-4, pp. 83-181.

[211] Couradeau, E., Benzerara, K., Moreira, D., Gérard, E., Kaźmierczak, J., Tavera, R., López-García, P.: 2011, PLoS ONE, Vol. 6, Issue 12, e28767, pp. 1-16.

[212] Crites, A.T., Henning, J.W., Ade, P.A.R., Aird, K.A., Austermann, J.E. et al.: 2015, ApJ 805, 36, 18 pp.

[213] Cucchiara, A., Levan, A.J., Fox, D.B., Tanvir, N.R., Ukwatta, T.N. et al.: 2011, ApJ, 736, Issue 1, article id. 7, 12 pp

[214] Cumani, P., Galper, A.M., Bonvicini, V., Topchiev, N.P., Adriani, O. et al.: 2015, arXiv:1502.02976.

[215] Dado, S., Dar, A., De Rújula, A.: 2009, ApJ 696, Issue 1, 994-1020.

[216] Dado, S., Dar, A.: 2013a, ApJ 775, Issue 1, article id. 16, 7 pp.

[217] Dado, S., Dar, A.: 2013b, A&A 558, id.A115, 7 pp.

[218] Dado, S., Dar, A.: 2016, PhRvD 94, Issue 6, id.063007.

[219] Dai, X., Kochanek, C.S.: 2005, ApJ 625, Issue 2, 633-642.

[220] Damon, E., Eisler, D., Rasolt, D., Shaw, A., Story, K. et al.: 2004, Proc. of the Fall 2004 Astronomy 233 Symposium on *Measurements of the Hubble Constant*, D.B. Campbell & J. Deneva (Eds), offered by the Cornell University Astronomy Department and the College of Arts and Sciences under the John S. Knight Institute Sophomore Seminar Program, 61 pp.

[221] Dar, A.: 1997, in *Very High Energy Phenomena in the Universe* Morion Workshop. ISBN 2-86332-217-6 Editions Frontieres, Y. Giraud-Heraud & J. Tran Thanh Van (Eds.), p.69. (arXiv:astro-ph/9704187v2).

[222] Dar, A.: 2003, in *Frontier Objects in Astrophysics and Particle Physics*, F. Giovannelli & G. Mannocchi (Eds.), Italian Physical Society 85, 253-265.

[223] Dar, A.: 2006, ChJA&A Supp. 6, Issue S1, 323-329.

[224] Dar, A.: 2017, talk at the Frascati Workshop 2017 *Multifrequency Behaviour of High Energy Cosmic Sources - XIII*.

[225] Dar, A., De Rújula, A.: 2000, arXiv:astro-ph/0008474.

[226] Darnley, M.J., Ribeiro, V.A.R.M., Bode, M.F., Hounsell, R.A., Williams, R.P.: 2012, ApJ 746, Issue 1, article id. 61, 10 pp.

[227] Darnley, M.J., Bode, M.F., Harman, D.J., Hounsell, R.A., Munari, U. et al.: 2014, in *Stella Novae: Past and Future Decades*, P.A. Woudt & V.A.R.M. Ribeiro (Eds.). ASP Conf. Ser. Vol. 490, 49-55.

[228] De Angelis, A., Tatischeff, V., Tavani, M., Oberlack, U., Grenier, I. et al.: 2017, Exp. Astron. 44, Issue 1, 25-82.

[229] De Angelis, A., Mallamaci, M: 2018, The European Physical Journal Plus, Volume 133, Issue 8, article id. 324, 18 pp.

[230] Deaton, A.: 2003, Journal of Economic Literature, Vol. 41, No. 1, 113-158. Published online at https://www.jstor.org/stable/3217389

[231] Delrez, L., Gillon, M., Queloz, D., Demory, B.-O., Almleaky, Y. et al.: 2018, Proc. of the SPIE 10700, id. 107001I, 21 pp.

[232] De Pasquale, M., Page, M.J., Kann, D.A., Oates, S.R., Schulze, S. et al.: 2016, MNRAS 462, Issue 1, 1111-1122.

[233] Dent, W.R.F., Wyatt, M.C., Roberge, A., Augereau, J.-C., Casassus, S. et al.: 2014, Scieence 343, Issue 6178, 1490-1492.

[234] Depalo, R., Cavanna, F., Aliotta, M., Anders, M., Bemmerer, D. et al. (LUNA Collaboration): 2016, Phys. Rev. C. 94, 055804.

[235] Di Gesu, L., Marshall, H.L., Ehlert, S.R., Kim, D.E., Donnarumma, I. et al.: 2023, Nature Astronomy, Advanced Online Publication, 10.1038/s41550-023-02032-7.

[236] Di Leva, A., Scott, D.A., Caciolli, A., Formicola, A., Strieder, F. et al. (LUNA Collaboration): 2014, Phys. Rev. C, 89, Issue 1, id.015803 and erratum Phys. Rev C, 90, Issue 1, id.019902.

[237] Di Marco, A., La Monaca, F., Poutanen, J., Russell, T.D., Anitra, A. et al.: 2023, ApJL 953, Issue 2, id.L22, 13 pp.

[238] Di Sciascio, G.: 2019, JPhCS 1263, Issue 1, article id. 012003.

[239] Di Sciascio, G. on behalf of the Lhaaso Collaboration: 2016, Nucl. Part. Phys. Proc. 279-281, 166-173.

[240] Di Stefano, R., Berndtsson, J., Urquhart, R., Roberto Soria, R., Kashyap, V.L., Theron W. Carmichael, T.W., Imara, N.: 2021, Nat Astron. https://doi.org/10.1038/s41550-021-01495-w

[241] Dong, R., Zhu, Z., Whitney, B.: 2015, ApJ 809, Issue 1, article id. 93, 18 pp.

[242] Dopita, M.A., Krauss, L.M., Sutherland, R.S., Kobayashi, C., Lineweaver, C.H.: 2011, Astrophys. Space Sci., 335, Issue 2, 345-352.

[243] Dragomir, D., Teske, J., Günther, M.N., Ségransan, D., Burt, J.A. et al.: 2019, ApJL 875, Issue 2, article id. L7, 10 pp.

[244] Drake, F.D.: 1962, *Intelligent Life in Space*, New York: Macmillan, 128 pp.

[245] Drouart, A., Dubrulle, B., Gautier, D., Robert, F.: 1999, Icarus 140, Issue 1, 129-155.

[246] Du, A., Zipkin, A.M., Hatala, K.G., Renner, E., Baker, J.L. et al.: 2018, in *Hominin brain size evolution are scale-dependent*, Proc. R. Soc. B 285: 20172738. http://dx.doi.org/10.1098/rspb.2017.2738

[247] Dullemond, C.P., Hollenbach, D., Kamp, I., D'Alessio, P.: 2007, in Protostars and Planets, V,B. Reipurth, D. Jewitt & K. Keil (Eds.), University of Arizona Press, Tucson, 951 pp., p.555-572.

[248] Dullemond, C.P., Monnier, J.D.: 2010, ARA&A 48, 205-239.

[249] Duncan, R.C., Thompson, C., 1992, ApJ 392, L9-L13.

[250] Durrer, R.: 2015, Classical and Quantum Gravity, 32, Issue 12, article id. 124007.

[251] Dutrey, A.: 2007, Comptes Rendus Geosciences 339, issue 14-15, 862-871.

[252] Dutrey, A., Guilloteau, S., Duvert, G., Prato, L., Simon, M. et al.: 1996, A&A 309, 493-504.

[253] Dyson, F.: 1960, Science, 131, Issue 3414, 1667-1668.

[254] Eklavya: 2019, *Understanding Exoplanets with Data Science – Exoplanets II: Interpretation of Data*, https://towardsdatascience.com

[255] Elsasser, H., Staude, H.J.: 1978, A&A 70, L3.

[256] Enoch, M.L., Corder, S., Dunham, M.M., Duchêne, G.: 2009, ApJ 707, Issue 1, 103-113.

[257] Enoto, T.: 2018, in *Quarks and Compact Stars 2017 (QCS2017)*, JPS Conf. Proc., id.011046, 7 pp.

[258] Erickson, J.K., Gratton, S., Steinhardt, P.J., Turok, N.: 2007, PhRvD 75, Issue 12, id. 123507.

[259] Erwin, D., Valentine, J.: 2013, *The Cambrian Explosion: The Construction of Animal Biodiversity*, Published January 18th by W.H. Freeman.

[260] Evans, A.: 2011, in *Asymmetric Planetary Nebulae 5 Conference*, A.A. Zijlstra, F. Lykou, I. McDonald, & E. Lagadec (eds.), Jodrell Bank Centre for Astrophysics, p. 305.

[261] Evans, A., Bode, M.F., O'Brien, T.J., Darnley, M.J. (eds.): 2008, *RS Ophiuchi (2006) and the Recurrent Nova Phenomenon*, ASP Conf. Ser., Vol. 401.

[262] Evans, P.A., Beardmore, A.P., Page, K.L., Osborne, J.P., O'Brien, P.T. et al.: 2009, MNRAS 397, 1177-1201.

[263] Fabbiano, G., Hartmann, L., Raymond, J., Steiner, J., Branduardi-Raymont, G., Matilsky, T.!981, ApJ 243, 911-925.

[264] Falanga, M., Belloni, T., Casella, P., Gilfanov, M., Jonker, P., King, A. (Eds.): 2015, *The Physics of Accretion onto Black Holes*, Springer, Space Sciences Series of ISSI, Vol. 49, 483 pp.

[265] Fan, X., Strauss, M.A., Schneider, D.P., Becker, R.H., White, R.L. et al.: 2003, AJ 125, Issue 4, 1649-1659.

[266] Fang, M., Pascucci, I., Edwards, S., Gorti, U., Banzatti, A. et al.: 2018, ApJ 868, Issue 1, article id. 28, 35 pp.

[267] Feigelson, E.D., Montmerle, T.: 1999, *High-energy processes in young stellar objects*, Annu. Rev. Astron. Astrophys. 37, 363-408.

[268] Ferrario, L., Wickramasinghe, D.T.: 2005, MNRAS 356, 615-620.

[269] Ferrario, L., Wickramasinghe, D.T.: 2007, ASP Conf. Ser. 372, 163-168.

[270] Ferrario, L., de Martino, D., Gänsicke, B.T.: 2015, SSRv 191, 111-169.

[271] Ferrario, L., Melatos, A., Zrake, J.: 2015, SSRv 191, 77-109.

[272] Finch, C,E,: 2012, Proc of the American Philosophical Soc. 156, 9-44.

[273] Finger, M.H., Wilson, R.B., Harmon, B.A.: 1996, ApJ 459, 288.

[274] Finger, M.H., Camero-Arranz, A., Kretschmar, P., Wilson, C., and Patel, S.: 2006, BAAS 38, 359.

[275] Fishbach, M., Gray, R., Magaña Hernandez, I., Qi, H., Sur, A. et al.: 2019, ApJ 871, Issue 1, article id. L13, 10 pp.

[276] Fischer A., Beuermann K.: 2001, A&A 373, 211.

[277] Fisher-Quann, R.: 2017, *Is Space Junk a problem?*, Quark Magazine.
Online at https://quarkmag.co
m/is-space-junk-a-problem-67e865f702a9.

[278] Flauger, R., Hill, J.C., Spergel, D.N.: 2014, JCAP Issue 08, article id. 039. (arXiv:1405.7351).

[279] Fogli, G.L., Lisi, E., Marrone, A., Palazzo, A., Rotunno, A.M.: 2008, Ph. Rev. Letter, 101, Issue 14, id. 141801.

[280] Fogli, G.L., Lisi, E., Marrone, A., Palazzo, A., Rotunno, A.M.: 2011, Phys. Rev. D, 84, Issue 5, id. 053007.

[281] Fogli, G.L., Lisi, E., Marrone, A., Montanino, D., Palazzo, A., Rotunno, A.M: 2012, Phys. Rev. D, 86, Issue 1, id. 013012.

[282] Forman, W., Jones, C., Cominsky, L., Julien, P., Murray, S. et al.: 1978, ApJ Suppl. Ser. 38, 357.

[283] Forsblom, S.V., Poutanen, J., Tsygankov, S.S., Bachetti, M., Di Marco, A. et al.: 2023, ApJL 947, Issue 2, id.L20, 10 pp.

[284] Four Peaks Technologies, Scottsdale, AZ: 2012a, http://www.earlyearth
central.com/early_life_page.html

[285] Four Peaks Technologies, Scottsdale, AZ: 2012b, http://www.earlyearth
central.com/human_page.html

[286] Frank, J., King, A.R., Raine, D.J.: 2002, *Accretion power in astrophysics: Third Edition*, Cambridge and New York, Cambridge University Press, 398 pp.

[287] Freedman, W.L., Madore, B.F.: 2010, ARA&A 48, 673-710.

[288] Friedjung, M.: 1985, in *Multifrequency Behaviour of Galactic Accreting Sources*, F. Giovannelli (Ed.), Editrice SIDEREA, Roma, Italy, p. 370-371.

[289] Fryer, C.L., Belczynski, K., Wiktorowicz, G., Dominik, M., Kalogera, V., Holz, D.E.: 2012, ApJ 749, 91.

[290] Fumagalli, M., Patel, S.G., Franx, M., Brammer, G., van Dokkum, P. et al.: 2012, APJL, 757, Issue 2, article id. L22, 6 pp.

[291] Galper, A.M., Topchiev, N.P., Yurkin, Yu.T.: 2018, ARep 62, Issue 12, 882-889.

[292] Gänsicke, B.T.: 2005, in *The Astrophysics of Cataclysmic Variables and Related Objects*, J.-M. Hameury & J.-P. Lasota (Eds.), ASP Conf. Ser. Vol. 330, 3.

[293] Gardner, J.P.: 2009, in *AKARI, a Light to Illuminate the Misty Universe*, Takashi Onaka, Glenn J. White, Takao Nakagawa & Issei Yamamura (Eds.), ASP Conf. Ser. 418, 365-373.

[294] Gardner, J.P., Mather, J.C., Clampin, M., Doyon, R., Greenhouse, M.A. et al.: 2006, SSRv 123, Issue 4, 485-606.

[295] Gaudenzi, S., Giovannelli, F., Lombardi, R., Claudi, R.: 1986, in *New Insights in Astrophysics : 8 Years of UV Astronomy with IUE*, Compiled by E.J. Rolfe. ESA SP-263. 455-458.

[296] Gaudenzi, S., Giovannelli, F., Lombardi, R., Claudi, R.: 1990, AcA, 40, 105-115.

[297] Gaudenzi, S., Claudi, R.U., Giovannelli, F., Lombardi, R., Pelosi, M., Strappolini, M.: 2002, Mem. SAIt 73, 213-222.

[298] Gaudenzi S., Giovannelli, F., Mandalari, M., Corradini, M., Lombardi, R.: 2011, A&A 525, id. A147, 11 pp.

[299] Gehrels, N., Spergel, D. (WFIRST SDT Project): 2015, J. Phys. Conf. Ser. 610 012007.

[300] Gehrels, N., Cannizzo, J.K.: 2015, J. HE Astrophys. 7, 2-11.

[301] Gell-Mann, M.: 1964, PhL, 8, 214.

[302] George, D., Blieck, A.: 2011, PLoS ONE, Vol. 6, Issue 7, e22136, pp. 1-7.

[303] Gess, R., Ahlberg, P.E.: 2018, Science 360, 1120-1124.

[304] Geyer, R., Jambeck, J.R., Law, K.L.: 2017, Sci. Adv. 3, e1700782, 5 pp.

[305] Ghirlanda, G., Bernardini, M.G., Calderone, G., D'Avanzo, P.: 2015, J. HE Astrophys. 7, 81-89.

[306] Ghosh, P.: 1994, in *The Evolution of X-Ray Binaries*, S.S. Holt & C.S. Day (Eds.), AIP Conf. Proc. 308, 439.

[307] Ghosh, S.K.: 2009, in *Frontier Objects in Astrophysics and Particle Physics*, F. Giovannelli & G. Mannocchi, (Eds.), SIF, Bologna, Italy, 98, 243-254.

[308] Giacconi, R., Gursky, H., Paolini, F.R., Rossi, B.: 1962, Phys. Rev. Lett. 9, 439.

[309] Giacconi, R., Gursky, H., Kellog, E., Schreier, E., Tananbaum, H.: 1971, Astrophys. J. Lett. 167, L67.

[310] Giacconi, R., Branduardi, G., Briel, U., Epstein, A., Fabricant, D.: 1979, ApJ 230, 540.

[311] Giallongo, E., D'Odorico, S., Fontana, A., McMahon, R.G., Savaglio, S. et al.: 1994, ApJ, 425, no. 1, L1-L4.

[312] Gianolli, V.E., Kim, D.E., Bianchi, S., Agís-González, B., Madejski, G. et al.: 2023, MNRAS 523, Issue 3, 4468-4476.

[313] Gianotti, F., 2012, 4th July–talk at CERN

[314] Gilmozzi, R.: 2008, *Extremely Large Telescopes: Which Wavelengths?*, Retirement Symposium for Arne Ardeberg. Edited by Andersen, Torben E. Proceedings of the SPIE, Volume 6986, article id. 698604, 8 pp.

[315] Gilmozzi, R.: 2009, The Messenger 136, 2-7.

[316] Gilmozzi, R.: 2013, talk at the Palermo Workshop 2013 on *The Golden Age of Cataclysmic Variables and Related Objects - II*.

[317] Gilmozzi, R., Spyromilio, J.: 2007, The Messenger 127, 11-19.

[318] Gilmozzi, R., Spyromilio, J.: 2009, in *Science with the VLT in the ELT Era*, Ap&SS Proc. Springer Netherlands, pp. 217-223.

[319] Gilmozzi, R., Kissler-Patig, M.: 2011, The Messenger 143, 25-25.

[320] Giovannelli, F.: 1981, Space Sci. Rev. 30, Issue 1-4, 213-219.

[321] Giovannelli, F. (Ed.): 1985, *Multifrequency Behaviour of Galactic Accreting Sources*, Editrice SIDEREA, Roma, Italy, 371 pp.

[322] Giovannelli, F.: 1994, SSRv 69, 1-138.

[323] Giovannelli, F.: 1996, in *Multifrequency Behaviour of High Energy Cosmic Sources*, F. Giovannelli & L. Sabau-Graziati (Eds.), Mem. S.A.It., 67, 401-413.

[324] Giovannelli, F. (Ed.): 2001a, *The bridge between the big bang and biology: stars, planetary systems, atmospheres, volcanoes: their link to life*, Franco Giovannelli (Ed.), Consiglio Nazionale delle Ricerche (CNR): President's Bureau of the CNR, Mario Apice (General Coordinator), pp. 1-440.

[325] Giovannelli, F.: 2001b, in *The Bridge between the Big Bang and Biology (Stars, Planetary Systems, Atmospheres, Volcanoes: Their Link to Life)*, F. Giovannelli (ed.), President Bureau of the CNR, Roma, Italy, p. 439.

[326] Giovannelli, F.: 2008, Ch. J. A&A Suppl. 8, 237-258.

[327] Giovannelli, F.: 2016, in *Proceedings of the 4th Ann. Conf. on High Energy Astrophysics in Southern Africa (HEASA 2016)*. Online at http://pos.sissa.it/cgi-bin/reader/conf.cgi?confid=275, id. 31.

[328] Giovannelli, F.: 2017, *The Golden Age of Cataclysmic Variables and Related Objects - IV*, Online at https://pos.sissa.it/cgi-bin/reader/conf.cgi?confid=315, id. 1.

[329] Giovannelli, F.: 2018, in *Accretion Processes in Cosmic Sources II*, Online at https://pos.sissa.it/cgi-bin/reader/conf.cgi?confid=342, id. 1.

[330] Giovannelli, F.: 2021, *The Golden Age of Cataclysmic Variables and Related Objects - V*, Online at https://pos.sissa.it/cgi-bin/reader/conf.cgi?confid=368, id. 1.

[331] Giovannelli, F., Karakuła, S., Tkaczyk, W.: 1981, in *Origin of Cosmic Rays*, Setti, G., Spada, G. & Wolfendale, A.W. (Eds.), IAU Symp. 94, 335-336.

[332] Giovannelli, F., Karakuła, S., Tkaczyk, W.: 1982, AcA 32, 121-130.

[333] Giovannelli, F., Gaudenzi, S., Rossi, C., Piccioni, A.: 1983, AcA 33, 319-330.

[334] Giovannelli, F., Polcaro, V.F.: 1986, MNRAS 222, 619-627.

[335] Giovannelli, F., Ziółkowski, J.: 1990, AcA 40, 95-103.

[336] Giovannelli, F., Errico, L., Vittone, A.A., Rossi, C.: 1991, A&AS 87, 89-95.

[337] Giovannelli, F., Martinez-Pais, I.G.: 1991, Space Sci. Rev. 56, 313-372.

[338] Giovannelli, F., Sabau-Graziati, L.: 1992, SSRv 59, 1-81.

[339] Giovannelli, F., Martinez-Pals, I.G., Sabau-Graziati, L.: 1992, in *Viña del Mar Workshop on Cataclysmic Variable Stars*, Nikolaus Vogt (Ed.), ASP Conf. Ser. 29, 119-124.

[340] Giovannelli, F., Vittone, A.A., Rossi, C., Errico, L., Bisnovatyi-Kogan, G.S., Kurt, V.G., Lamzin, S.A. et al.: 1995, A&AS 114, 341.

[341] Giovannelli, F., Sabau-Graziati, L. (Eds.): 1996, *Multifrequency Behaviour of High Energy Cosmic Sources*, SAIt Vol. 67.

[342] Giovannelli, F., Sabau-Graziati, L.: 1998, in *Ultraviolet Astrophysics Beyond the IUE Final Archive*, W. Wamstecker & R.Gonzalez-Riestra (eds.), ESA SP-413, 419-424.

[343] Giovannelli, F., Sabau-Graziati, L. (Eds.): 1999, *Multifrequency Behaviour of High Energy Cosmic Sources*, SAIt Vol. 70.

[344] Giovannelli, F., Sabau-Graziati, L.: 2000, in *The Evolution of the Milky Way: stars versus clusters*, Francesca Matteucci & Franco Giovannelli (Eds.), Published by Kluwer Academic Publishers, P. O. Box 17, 3300 AA Dordrecht, ISBN 0-7923-6679-4, p. 151.

[345] Giovannelli, F., Sabau-Graziati, L.: 2001, Ap&SS, 276, 67-80.

[346] Giovannelli, F., Sabau-Graziati, L. (Eds.): 2002, *Multifrequency Behaviour of High Energy Cosmic Sources*, SAIt Vol. 73.

[347] Giovannelli, F., Sabau-Graziati, L.: 2004, SSR, 112, 1-443 (GSG2004).

[348] Giovannelli, F., Sabau-Graziati, L.: 2006, Chinese J. A&A Suppl. 6, Issue S1, p. 1-28.

[349] Giovannelli, F., Bernabei, S., Rossi, C., Sabau-Graziati, L.: 2007, A&A, 475, 651.

[350] Giovannelli, F., Sabau-Graziati, L. (Eds.): 2010, *Multifrequency Behaviour of High Energy Cosmic Sources*, SAIt Vol. 81.

[351] Giovannelli, F., Sabau-Graziati, L.: 2011, Acta Polytechnica Vol. 51, No. 2., p. 21.

[352] Giovannelli, F., Sabau-Graziati, L.: 2012a, in *The Golden Age of Cataclysmic Variables and Related Objects*, F. Giovannelli & L. Sabau-Graziati (eds.), Mem. S.A.It., 83 N. 2, 698.

[353] Giovannelli, F., Sabau-Graziati, L.: 2012b, *Multifrequency Behaviour of High Energy Cosmic Sources*, F. Giovannelli & L. Sabau-Graziati (Eds.), SAIt Vol. 83.

[354] Giovannelli, F., Sabau-Graziati, L. (Eds.): 2012c, in *The Golden Age of Cataclysmic Variables and Related Objects*, Mem. S.A.It., 83 N. 2, 433 pp.

[355] Giovannelli, F., Bisnovatyi-Kogan, G.S., Klepnev, A.S.: 2013, A&A 560, id.A1, 11 pp (GBK13).

[356] Giovannelli, F., Sabau-Graziati, L.: 2014, in *Multifrequency Behaviour of High Energy Cosmic Sources - X*, Acta Polytechnica CTU Proceedings 1(1), p. 1-12.

[357] Giovannelli, F., Sabau-Graziati, L.: 2015a, in *The Golden Age of Cataclysmic Variables and Related Objects - II*, F. Giovannelli & L. Sabau-Graziati (Eds.), Acta Polytechnica, CTU Proc. ISSN 2336-5382, Vol. 2 No. 1, 3-20.

[358] Giovannelli, F., Sabau-Graziati, L.: 2015b, in *The Golden Age of Cataclysmic Variables and Related Objects - III*, Online at http://pos.sissa.it/cgi-bin/reader/conf.cgi?confid=255, id. 1.

[359] Giovannelli, F., Sabau-Graziati, L. (Eds.): 2015c, *Multifrequency Behaviour of High Energy Cosmic Sources - XI*, PoS-SISSA - http://pos.sissa.it/cgi-bin/reader/conf.cgi?confid=246.

[360] Giovannelli, F., Sabau-Graziati, L. (Eds.): 2015d, *The Golden Age of Cataclysmic Variables and Related Objects - II*, Acta Polytechnica, CTU Proc. ISSN 2336-5382, Vol. 2 No. 1, 333 pp.

[361] Giovannelli, F., Bisnovatyi-Kogan, G.S., Bruni, I., Corfini, G., Martinelli, F., Rossi, C.: 2015a, AcA 65, 107-116.

[362] Giovannelli, F., Rossi, C., Bisnovatyi-Kogan, G., Bruni, I., Fasano, A., Salas Procas, J.: 2015b, in *Multifrequency Behaviour of High Energy Cosmic Sources XI*, Online at http://pos.sissa.it/cgi-bin/reader/conf.cgi?confid=246, id.39

[363] Giovannelli, F., Sabau-Graziati, L.: 2016a, in *Accretion Processes in Cosmic Sources*, Online at http://pos.sissa.it/cgi-bin/reader/conf.cgi?confid=288, id.1.

[364] Giovannelli, F., Sabau-Graziati, L. (Eds.): 2016b, *Accretion Processes in Cosmic Sources: Young Stellar Objects, Cataclysmic Variables and Related Objects, X-ray Binary Systems, Active Galactic Nuclei - I*, Online at http://pos.sissa.it/cgi-bin/reader/conf.cgi?confid=288.

[365] Giovannelli, F., Sabau-Graziati, L.: 2016c, in *Frontier Research in Astrophysics II*, Online at https://pos.sissa.it/cgi-bin/reader/conf.cgi?confid=269, id. 1.

[366] Giovannelli, F., Sabau-Graziati, L.: 2017, in *Multifrequency Behaviour of High Energy Cosmic Sources - XII*, On line at https://pos.sissa.it/cgi-bin/reader/conf.cgi?confid=306, id. 1.

[367] Giovannelli, F., Sabau-Graziati, L.: 2019, in *Frontier Research in Astrophysics III*, Online at https://pos.sissa.it/cgi-bin/reader/conf.cgi?confid=331, id. 1.

[368] Giovannelli, F., Sabau-Graziati, L.: 2020, in *Multifrequency Behaviour of High Energy Cosmic Sources - XIII*, Online at https://pos.sissa.it/cgi-bin/reader/conf.cgi?confid=362, id. 3.

[369] Girichidis, P., Offner, S.S.R., Kritsuk, A.G., Klessen, R.S., Hennebelle, P. et al.: 2020, SSRv 216, Issue 4, article id. 68.

[370] Gnedin, N.Y.: 2000, ApJ, 535, 530-554.

[371] Gnedin, N.Y., Glover, S.G.O., Klessen, R.S., Springel, V. (Eds.): 2015, *Star Formation in Galaxy Evolution: Connecting Numerical Models to Reality*, Springer, ISBN 978-3-662-47889-9.

[372] Godon, P., Sion, E.M.: 2002, ApJ, 566, Issue 2, 1084-1090.

[373] Goliasch, J., Nelson, L.: 2015, ApJ 809, Issue 1, article id. 80, 19 pp.

[374] González-Casanova, D.F., Lazarian, A., Santos-Lima, R: 2016, ApJ 819, Issue 2, article id. 96, 11 pp.

[375] Goodman, J.: 1993, ApJ 406, 596-613.

[376] Gorti, U., Liseau, R., Sándor, Z., Clarke, C.: 2016, SSRv 205, Issue 1-4, 125-152.

[377] de Gouveia Dal Pino, E.M.: 2005, Brazilian Journal of Physics 35, Issue 4B, 1163-1166.

[378] de Gouveia Dal Pino, E.M., Piovezan, P.P., Kadowaki, L.H.S.: 2010, A&A 518, id. A5, 9 pp.

[379] Greggio, L., Renzini, A., Daddi, E.: 2008, MNRAS 388, Issue 2, 829-837.

[380] Grimm, H.-J.: 2003, PhD Thesis, Ludwig-Maximilians-Universitat, München, Germany.

[381] Grudzinska, M., Belczynski, K., Casares, J., de Mink, S.E., Ziolkowski, J.: 2015, MNRAS, 452, 2773-2787.

[382] Gustavino, C.: 2007, in *Frontier Objects in Astrophysics and Particle Physics*, F. Giovannelli & G. Mannocchi (Eds.), Italian Physical Society, Ed. Compositori, Bologna, Italy, 93, 191-204.

[383] Gustavino, C.: , in *Frontier Objects in Astrophysics and Particle Physics*, F. Giovannelli & G. Mannocchi (Eds.), Italian Physical Society, Ed. Compositori, Bologna, Italy, 98, 77-90.

[384] Gustavino, C.: 2011, in *Frontier Objects in Astrophysics and Particle Physics*, F. Giovannelli & G. Mannocchi (Eds.), Italian Physical Society, Ed. Compositori, Bologna, Italy, 103, 657.

[385] Gustavino, C.: 2012, in *Nuclei in the Cosmos (NIC XII)*, Online at http://pos.sissa.it/cgi-bin/reader/conf.cgi?confid=146, id. 74.

[386] Gustavino, C.: 2013, AcPol 53, 534-537.

[387] Gustavino, C. (on behalf of the LUNA collaboration): 2019, in *RICAP18, 7th Roma International Conference on Astroparticle Physics*, Edited De Vincenzi, M., Capone, A. & Morselli, A. (Eds.), EPJ Web of Conferences, Volume 209, id. 01043.

[388] Guy, J., Sullivan, M., Conley, A., Regnault, N., Astier, P., et al.: 2010, A&A, 523, id. A7, 34 pp.

[389] Guziy, S., Pandey, S.B., Tello, J.C. & Castro-Tirado, A.J. (Eds.): 2012, *II Workshop on Robotic Autonomous Observatories*, Astron. Soc. of India Conf. Ser., Vol. 7.

[390] Hack, M., La Dous, C. (Eds.): 1993, *Cataclysmic Variables and Related Objects*, NASA SP-507.

[391] Haile-Selassie, Y., Saylor, B.Z., Deino, A., Levin, N.E., Alene, M., Latimer, B.M.: 2012, Nature 483, 565-600.

[392] Haile-Selassie, Y., Gibert, L., Melillo, S.M., Ryan, T.M., Alene, M. et al.: 2015, Nature 521, 483-498.

[393] Hammarlund, E.U., von Stedingk, K., Påhlman, S.: 2018, Nature Ecology & Evolution Vol. 2, 220-228. DOI: 10.1038/s41559-017-0410-5.

[394] Hamuy, M. et al., 2012, in *Multifrequency Behaviour of High Energy Cosmic Sources*, Franco Giovannelli & Lola Sabau-Graziati (eds.), Mem. SAIt., 83, 388.

[395] Han, E., Wang, S.X., Wright, J.T., Feng, Y.K., Zhao, M.: 2014, PASP 126, Issue 943, 827-837.

[396] Harding, A.K.: 2013, Front. Phys., 8, Issue 6, 679-692.

[397] Haridasu, B.S., Lukovic, V.V., D'Agostino, R., Vittorio, N.: 2017, A&A 600, id. L1, 5 pp.

[398] Harrison, T.E., McNamara, B.J., Szkody, P., McArthur, B.E., Benedict, G.F. et al.: 1999, ApJ 515, Issue 2, L93-L96.

[399] Harrison, Fiona, & Kennicutt, Robert, Co-Chairs: 2021, *Committee for a Decadal Survey on Astronomy and Astrophysics 2020*, in *Pathways to Discovery in Astronomy and Astrophysics for the 2020s*, Washington, DC: The National Academies Press. https://doi.org/10.17226/26141.

[400] Hartle, J.B., Thorne, K.S.: 1968, ApJ 153, 807-834.

[401] Hartmann, L.: 1998, *Accretion Processes in Star Formation*, Cambridge, UK; New York: Cambridge University Press, (Cambridge astrophysics series; 32). ISBN 0521435072.

[402] Hartmann, L., Herczeg, G., Calvet, N.: 2016, ARA&A 54, 135-180.

[403] Hartmann, L., Kenyon, S.J.: 1987a, ApJ 312, 243-253.

[404] Hartmann, L., Kenyon, S.J.: 1987b, ApJ 322, 393-398.

[405] Hartman, R.C., Bertsch. D.L., Bloom, S.D., Chen, A.W., Deines-Jones, P. et al.: 1999, ApJ Suppl. Ser. 123, 79.

[406] Hartwig, T., Volonteri, M., Bromm, V., Klessen, R.S., Barausse, E. et al.: 2016, MNRAS Lett. 460, Issue 1, L74-L78.

[407] Hasinger, G., Miyaji, T., Schmidt, J.H.M.M.: 2000, MPE-Report 1999, 273, p. 83.

[408] Hayakawa, S.: 1952, Prog. Theor. Phys. 8, 571.

[409] He, H.H. for the LHAASO collaboration; 2015, Proc. of the ICRC2015. Online at http://pos.sissa.it/cgi-bin/reader/conf.cgi?confid=236, id.1010.

[410] He, H.H.: 2019, Proc. of the ICRC2019. Online at https://pos.sissa.it/cgi-bin/reader/conf.cgi?confid=358, id. 693.

[411] Hellier, C.: 2001, *Cataclysmic Variable Stars*, Springer.

[412] Henning, Th., Michel, B., Stognienko, R.: 1995, P&SS 43, 1333-1343.

[413] Henry, R.C.: 1999, ApJL 516, L49-L52.

[414] Henry, R.C.: 2002, in *Multifrequency Behaviour of High Energy Cosmic Sources*, F. Giovannelli & L. Sabau-Graziati (Eds,), Mem. S.A.It. 73 N. 1, 67-75.

[415] Henry, R.C., Murthy, J., Overduin, J., Tyler, J.: 2015, ApJ 798, Issue 1, article id. 14, 25 pp.

[416] Hertzfeld, H.R., Schieb, P.-A.: 2015, in *Handbook of Cosmic Hazards and Planetary Defense*, Joseph, N. Pelton & Firooz Allahdadi (Eds.), Springer Reference, © Springer International Publishing Switzerland 2015, pp. 993-1006.

[417] Hessman, F.V.: 2001a, *Small Telescope Astronomy on Global Scales*, Wen-Ping Chen, Claudia Lemme & Bohdan Paczynski(Eds.), IAU Colloquium 183, ASP Conf. Ser. 246, 13-21.

[418] Hessman, F.V.: 2001b, *Small Telescope Astronomy on Global Scales*, Wen-Ping Chen, Claudia Lemme & Bohdan Paczynski(Eds.), IAU Colloquium 183, ASP Conf. Ser. 246, 357-360.

[419] Hess, V.F.: 1912, Physik Zh. 13, 1084.

[420] van den Heuvel, E.P.J.: 2009, in *Physics of Relativistic Objects in Compact Binaries: From Birth to Coalescence*, Ap&SS Library 359. 125-198.

[421] van den Heuvel, E.P.J., Rappaport, S.: 1987, in *Physics of Be Stars*, A. Slettebak & T.P. Snow (Eds.), Cambridge and New York, Cambridge University Press, Proc. of the IAU Coll. N. 92, p. 291.

[422] Heywood, I., Camilo, F., Cotton, W.D., Yusef-Zadeh, F., Abbott, T.D. et al.: 2019, Nature 573, Issue 7773, 235-237.

[423] Hill, C.A., Smith, R.C., Hebb, L., Szkody, P.: 2017, MNRAS 472, 2937-2944.

[424] Hildebrand, R.H., Spillar, E.J., Stiening, R.F.: 1981, ApJ 243, 223-227.

[425] Hofmann, W. (for the CTA Consortium): 2017, The Messenger 168, 21-25.

[426] Hopkins, A,M., Beacom, J.F., 2006, ApJ, 651, 142-154 – Erratum: 2008, ApJ 682, 1486.

[427] Horne, K.: 1985, MNRAS 213, 129-141.

[428] Horne, K., Gomer, R.: 1980, ApJ 237, 845-849.

[429] Howell, S.B., Cash, J., Mason, K.O., Herzog, A.E.: 1999, AJ 117, 1014.

[430] Howell, S.B., Brinkworth, C., Hoard, D.W., Wachter, S., Harrison, T., et al.: 2006, ApJL 646, Issue 1, L65-L68.

[431] Howell, D.A., Conley, A., Della Valle, M., Nugent, P., Perlmutter, S., et al.: 2009, arXiv0903, 1086H.

[432] Hoyle, F., Fowler, W.A.: 1960, ApJ, 132, 565-590.

[433] Huang, S.-S.: 1972, ApJ 171, 549-564.

[434] Huchra, J.: 2008, https://www.cfa.harvard.edu/∼dfabricant/huchra/hubble/

[435] Huchra, J.: 2010, https://www.cfa.harvard.edu/∼dfabricant/huchra/hubble.plot.dat

[436] Hudec, R.: 2017, in *Multifrequency Behaviour of High Energy Cosmic Sources - XII*, Online at https://pos.sissa.it/cgi-bin/reader/conf.cgi?confid=306, id. 83

[437] Hudec, R., Hudec, L., Klíma, M.: 2012, Acta Polytechnica, 52, No. 1, 27.

[438] Hudec, R., Hudec, L.: 2013, Acta Polytechnica, 53, No. 3, 23.

[439] Hulleman, F., van Kerkwijk, M.H., Kulkarni, S.R.: 2000, Nature 408, Issue 6813, 689-692.

[440] Hurley, K.: 2007, talk at the Frascati Workshop 2007 on *Multifrequency Behaviour of High Energy Cosmic Sorces - VII*.

[441] Hurley, K.: 2008, ChJA&A Suppl. 8, 202-212.

[442] Iben, I., Jr., Tutukov, A.V.: 1984, ApJS, 54, 335-372.

[443] Ibrahim, A.I., Markwardt, C.B., Swank, J.H., Ransom, S., Roberts, M. et al.: 2004, ApJ 609, Issue 1, L21-L24.

[444] Isern, J., Hernanz, M., García-Berro, E.: 1993, in *White Dwarfs: Advances in Observation and Theory*, M.A. Barstow (ed.), Kluwer Academic Publ., Dordrecht, Holland, NATO ASI Ser., C403, 139.

[445] Isern, J., Hernanz, M., Abia, C., José, J.: 1997, in *Frontier Objects in Astrophysics and Particle Physics*, F. Giovannelli & G. Mannocchi (eds.), Italian Physical Society, Editrice Compositori, Bologna, Italy, 57, 113.

[446] Ijjas, A.: 2018, Classical and Quantum Gravity Vol. 35, Issue 7, article id. 075010.

[447] Ijjas, A., Steinhardt, P.J., Loeb, A.: 2013, PhLB 723, Issue 4-5, 261-266.

[448] Ijjas, A., Steinhardt, P.J.: 2018, Classical and Quantum Gravity, Vol. 35, Issue 13, article id. 135004.

[449] Illarionov, A.F., Sunyaev, R.A.: 1975, A&A 39, 185.

[450] Incandela, J.: 2012, UCSB/CERN, Talk on July 4, 2012.

[451] Isella, A.: 2006, PhD at the Universita' degli Studi di Milano, Milano, Italy

[452] Isella, A.: 2016, in *From Interstellar Clouds to Star-Forming Galaxies: Universal Processes?*, IAU Symp. 315, 107-113.

[453] Isella, A., Carpenter, J.M., Sargent, A.I.: 2009, ApJ 701, Issue 1, 260-282.

[454] Isella, A., Turner, N.: 2016, arXiv:1608.05123.

[455] Jakhu, R.S.: 2015, in *Handbook of Cosmic Hazards and Planetary Defense*, Joseph, N. Pelton & Firooz Allahdadi (Eds.), Springer Reference, © Springer International Publishing Switzerland 2015, pp. 1069-1084.

[456] Jakobs, K., Seez, C.: 2015, Scholarpedia 10(9):32413.

[457] Jeffers, S.V., Min, M., Canovas, H., Rodenhuis, M., Keller, C.U.: 2014, A&A 561, id. A23, 9 pp.

[458] Jehin, E., Gillon, M., Queloz, D., Magain, P., Manfroid, J. et al.: 2011, The Messenger 145, 2-6.

[459] Jehin, E., Gillon, M., Queloz, D., Delrez, L., Burdanov, A et al.: 2018, The Messenger 174, 2-7.

[460] Jiang, L., Egami, E., Kashikawa, N., Walth, G., Matsuda, Y. et al.: 2011, ApJ 743, Issue 1, article id. 65, 10 pp.

[461] Johanson, D.. Maitland E.: 1981, *Lucy: The Beginnings of Humankind*, ISBN 0-671-25036-1, New York: Simon and Schuster.

[462] Johnstone, Wm. R.: 2004, http://www.johnstonsarchive.net/relativity/bh ctable.html

[463] Jonas, F.M.: 2015, in *Handbook of Cosmic Hazards and Planetary Defense*, Joseph, N. Pelton & Firooz Allahdadi (Eds.), Springer Reference, © Springer International Publishing Switzerland 2015, pp. 835-849.

[464] Jonas, F.M., Allahdadi, F.:: 2015, in *Handbook of Cosmic Hazards and Planetary Defense*, Joseph, N. Pelton & Firooz Allahdadi (Eds.), Springer Reference, © Springer International Publishing Switzerland 2015, pp. 875-889.

[465] Joy, A.H.: 1956, ApJ 124, 317-320.

[466] Kaiser, G,: 2017, in *1.3: Classification - The Three Domain System*, https://bio.libretexts.org/.

[467] Kamionkowski, M., Kovetz, E.D.: 2016, ARA&A 54, 227-269.

[468] Kaplinghat, M., Chu, M., Haiman, Z., Holder, Gilbert P. et al.: 2003, ApJ 583, Issue 1, 24-32.

[469] Kardashev, N.S., Novikov, I.D., Lukash, V.N., Pilipenko, S.V., Mikheeva, E.V. et al.: 2014, Physics-Uspekhi Vol. 57, Issue 12, article id. 1199-1228.

[470] Kashikawa, N., Shimasaku, K., Malkan, M.A., Doi, M., Matsuda, Y. et al.: 2006, ApJ 648, Issue 1, 7-22.

[471] Kashikawa, N.: 2007, in *At the Edge of the Universe: Latest Results from the Deepest Astronomical Surveys*, J. Afonso, H.C. Ferguson, B. Mobasher & R. Norris (Eds.), ASP Conf. Series 380, 11-16.

[472] Kasper, M., Cerpa Urra, N., Pathak, P., Bonse, M., Jalo Nousiainen, J. et al.: 2021, The Messenger 182, 38-43.

[473] Kaspi, V.M.: 2010, PNAS 107, Issue 16, 7147-7152.

[474] Kaspi, V.M., Beloborodov, A.M.: 2017, ARA&A 55, issue 1, 261-301.

[475] Kastner, J.H., Qi, C., Dickson-Vandervelde, D.A., Hily-Blant, P., Forveille, T. et al.: 2018, ApJ 863, Issue 1, article id. 106, 14 pp.

[476] Kataoka, A., Tsukagoshi, T., Momose, M., Nagai, H. Muto, T. et al.: 2016a, ApJL 831, Issue 2, article id. L12, 6 pp.

[477] Keating, B.G., Ade, P.A.R., Bock, J.J., Hivon, E., Holzapfel, W.L. et al.: 2003a, SPIE 4843, 284-295.

[478] Keating, B.G., O'Dell, C.W., Gundersen, J.O., Piccirillo, L., Stebor, N.C., Timbie, P.T.: 2003b, ApJS 144, Issue 1, 1-20.

[479] Kataoka, A., Muto, T., Momose, M., Tsukagoshi, T. Dullemond, C.P.: 2016b, ApJ 820, Issue 1, article id. 54, 8 pp.

[480] Kennicutt, R.C., Jr.: 1998, ARA&A, 36, 189-232.

[481] Kennicutt, R.C., Evans, N.J.: 2012, ARA&A, 50, 531-608.

[482] Kepler, S.O., Pelisoli, I., Jordan, S., Kleinman, S.J., Koester, D. et al.: 2013, MNRAS 429, Issue 4, 2934-2944.

[483] Kepler, S.O., Pelisoli, I., Koester, D., Ourique, G., Kleinman, S.J. et al.: 2015, MNRAS 446, Issue 4, 4078-4087.

[484] Kilic, M., Brown, W.R., Allende Prieto, C., Agüeros, M.A.; Heinke, C., Kenyon, S.J.: 2011, ApJ 727, Issue 1, article id. 3, 12 pp.

[485] King, A.: 2019, in *Black Hole Formation and Growth*, Saas-Fee Advanced Course, Volume 48. ISBN 978-3-662-59798-9. Springer-Verlag GmbH Germany, part of Springer Nature, p. 95-157.

[486] Kiplinger, A.L.: 1979a, ApJ 234, 997-1015.

[487] Kiplinger, A.L.: 1979b, AJ 84, 655-660.

[488] Kistler, M.D., Stanek, K.Z., Kochanek, C.S., Prieto, J.L., Thompson, T.A.: 2013, ApJ 770, Issue 2, article id. 88, 8 pp.

[489] Kitamoto, S., Enoto, T., Safi-Harb, S., Pottschmidt, K., Ferrigno, C. et al.: 2014, arXiv:1412.1165.

[490] Klinkrad, H.: 2015, in *Handbook of Cosmic Hazards and Planetary Defense*, Joseph, N. Pelton & Firooz Allahdadi (Eds.), Springer Reference, © Springer International Publishing Switzerland 2015, pp. 807-834.

[491] Knoll, A.H., Bergmann, K.D., Strauss, J.V.: 2016, Phil. Trans. R. Soc. B 371, 20150493. Online at http://dx.doi.org/10.1098/rstb.2015.0493

[492] Knox, L.: 2003, New Astr. Rev. 47, Issue 11-12, 883-886.

[493] Kochanek, C.S.: 2003, in *Hubble's Science Legacy: Future Optical/Ultraviolet Astronomy from Space*, Kenneth R. Sembach, J. Chris Blades, Garth D. Illingworth and Robert C. Kennicutt, Jr. (Eds), ASPC 291, 245-252.

[494] Kogut, A., Spergel, D.N., Barnes, C., Bennett, C.L., Halpern, M. et al.: 2003, ApJS 148, Issue 1, pp. 161-173.

[495] Komatsu, E., Smith, K.M., Dunkley, J., Bennett, C.L., Gold, B. et al.: 2011, ApJS, 192, Issue 2, article id. 18, 47 pp.

[496] Komossa, S.: 2015, JHEAp 7, 148-157.

[497] Kononov, D.A., Giovannelli, F., Bruni, I., Bisikalo, D.V.: 2012, A&A 538, id. A94, 7 pp.

[498] Koonin, E.V.: 2014, in *Carl Woese special issue*, www.landesbioscience.com, rNa Biology 11:3, 197-204.

[499] Körding, E., Rupen, M., Knigge, C., Fender, R., Dhawan, V. et al.: 2008, Science 320, Issue 5881, 1318-1320.

[500] Kormendy, J., Ho, L.C.: 2013, ARA&A 51, 511-653.

[501] Kotze, E.J., Potter, S.B., McBride, V.A.: 2015, A&A 579, id. A77, 9 pp.

[502] Kotze, E.J., Potter, S.B., McBride, V.A.: 2016, A&A 595, id. A47, 12 pp.

[503] Kovetz, E.D., Viero, M.P., Lidz, A., Newburgh, L., Rahman, M. et al.: 2017, arXiv:1709.09066.

[504] Kowalski, M., Rubin, D., Aldering, G, Agostinho, R.J., Amadon, A., et al.: 2008, ApJ, 686, Issue 2, 749-778.

[505] Kraft, R.P.: 1967, ApJ 150, 551-570.

[506] Kratter, K., Lodato, G.: 2016, ARA&A 54, 271-311.

[507] Kumar, P., Zhang, B.: 2015, PhR 561, 1-109.

[508] Kurita, S., Ohuchi, H., Arimoto, M., Yatsu, Y., Kawai, N. et al.: 2015, arXiv:1503.01975.

[509] Lamb, D.Q., Reichart, D.E.: 2000, ApJ 536, Issue 1, 1-18.

[510] Lamzin, S.A., Bisnovatyi-Kogan, G.S., Errico, L., Giovannelli, F., Katysheva, N.A., Rossi, C., Vittone, A.A.: 1996, A&A 306, 877.

[511] Landi, R., Bassani, L., Dean, A.J., Bird, A.J., Fiocchi, M. et al.: 2009, MNRAS 392, Issue 2, 630-640.

[512] Lasota, J.-P.: 2001, New Astron. Rev. 45, Issue 7, 449-508.

[513] Lasota, J.-P.: 2016, in *Astrophysics of Black Holes*, Cosimo Bambi (Ed.), Astrophysics and Space Science Library, Volume 440. ISBN 978-3-662-52857-0. Springer-Verlag Berlin Heidelberg, p. 1.

[514] Lebreton, L., Slat, B., Ferrari, F., Sainte-Rose, B., Aitken, J. et al.: 2018, Scientific Reports, 8:4666, DOI:10.1038/s41598-018-22939-w, www.nature.com/scientificreports, pp. 1-15.

[515] Levitan, D.: 2013, *Finding Needles in the Haystack: A Search for AM CVn Systems using the Palomar Transient Factory*, Ph.D. Thesis, California Institute of Technology, U.S.A.

[516] Liang, E-W., Zhang, B-B., Zhang, B.: 2007, ApJ 670, Issue 1, 565-583.

bibitem Lieberman, D.E.: 2012, Nature 483, 550-551.

[517] Lineweaver, C.H., Fenner, Y. & Gibson, B.K., 2004, Nature, 303, 59.

[518] Lineweaver, C.H. & Chopra, A., 2012, Ann. Rev. of Earth and Planetary Sci., 40 (issue 1), 597

[519] Linsky, J.L., Schöller, M.: 2015, SSRv 191, Issue 1-4, 27-76.

[520] Lipunov, V.M.: 1987, Ap&SS 132, no. 1, 1-51.

[521] Lipunov, V.M.: 1995, in *Frontier Objects in Astrophysics and Particle Physics*, F. Giovannelli & G. Mannocchi (Eds.), SIF, Bologna, Italy, 47, 61-76.

[522] Lipunov, V.M.: 2018, talk at the Mondello Workshop 2018 in *Frontier Research in Astrophysics - III*.

[523] Lipunov, V.M., Postnov, K.A.: 1988, Ap&SS 145, no. 1, 1-45.

[524] Lipunov, V., Kornilov, V., Gorbovskoy, E., Shatskij, N., Kuvshinov, D. et al.: 2010, Advances in Astronomy, 2010, article id. 349171.

[525] Lipunov, V., Grinshpun, V., Vlasenko, D.: 2021, New Astrn. Rev. 93, 101631.

[526] Lira, P.: 1995, Masters thesis, Univ. Chile.

[527] Liske, J., Padovani, P., Kissler-Patig, M.: 2012, in *Ground-based and Airborne Telescopes IV*, Proc. SPIE 8444, article id. 84441I, 8 pp.

[528] Liu, Q.Z., van Paradijs, J., van den Heuvel, E.P.J.: 2006, A&A 455, 1165.

[529] Liu, Q.Z., van Paradijs, J., van den Heuvel, E.P.J.: 2007, A&A 469, 807.

[530] Loeb, A., Barkana, R.: 2001, ARA&A 39, 19-66.

[531] Lombardi, R., Giovannelli, F., Gaudenzi, S.: 1987, Astroph. Space Sci. 130, Issue 1-2, 275-278.

[532] Long, K., White, R.L.: 1980, ApJ 239, L65-L68.

[533] Long, X., Feng, H., Li, H., Kong, L-D., Heyl, J.: 2023, ApJ 950, Issue 2, id. 76, 4 pp.

[534] Lubin, P, Hughes, G.B.: 2015, in *Handbook of Cosmic Hazards and Planetary Defense*, Joseph, N. Pelton & Firooz Allahdadi (Eds.), Springer Reference, © Springer International Publishing Switzerland 2015, pp. 941-991.

[535] Luisi, P.L.: 2006, The Emergence of Life. From Chemical Origin to Synthetic Biology, Cambridge Univeristy Press.

[536] Luisi, P.L., Capra, F.: 2014, *The systems View of Life*, Cambridge Univ. Press, 510 pp.

[537] Lutz, W., Samir, K.C.: 2010, Phil. Trans. R. Soc. B 365, 2779-2791.

[538] Lynden-Bell, D., Pringle, J.E.: 1974, MNRAS 168, 603-637.

[539] Machida, M.N., Inutsuka, S., Matsumoto, T.: 2010, ApJ 724, Issue 2, 1006-1020.

[540] Madau, P., Dickinson, M.: 2014, ARA&A, 52, 415-486.

[541] Magorrian, J., Tremaine, S.: 1999, MNRAS 309, 447-460.

[542] Maguire, K., Sullivan, M., Ellis, R.S., Nugent, P.E., Howell, D.A. et al.: 2012, MNRAS, 426, 2359.

[543] Maier, D. – VERITAS Collaboration: 2015, Proc. of the 34th ICRC, Online at http://pos.sissa.it/cgi-bin/reader/conf.cgi?confid=236, id. 754.

[544] Malacaria, C., Heyl, J., Doroshenko, V., Tsygankov, S.S., Poutanen, J. et al.: 2023, A&A 675, id. A29, 10 pp.

[545] Manara, C.F., Rosotti, G., Testi, L., Natta, A., Alcalá, J.M. et al.: 2016, A&A 591, id. L3, 6 pp.

[546] Mannucci, F., Della Valle, M., Panagia, N.: 2006, MNRAS, 370, Issue 2, 773-783.

[547] Mantle, V.J., Bath, G.T.: 1983, MNRAS 202, 151-157.

[548] Marscher, A.P.: 2005, *Future Directions in High Resolution Astronomy*, J. Romney & M. Reid (Eds.), ASP Conf. Proc. 340, 25-29.

[549] Marsh, T.R.: 2001, in *Astrotomography, Indirect Imaging Methods in Observational Astronomy*, H.M.J. Boffin, D. Steeghs & J. Cuypers (Eds.), Lecture Notes in Physics 573, 1-27.

[550] Marsh, T.R., Horne, K.: 1988, MNRAS 235, 269-286.

[551] Marsh, T.R., Gänsicke, B.T., Hümmerich, S., Hambsch, F.-J., Bernhard, K., et al.: 2016, Nature 537, Issue 7620, 374-377.

[552] Martin, J., Rea, N., Torres, D.F., Papitto, A.: 2014, MNRAS 444, Issue 3, 2910-2924.

[553] Martin, W.F., Sousa, F.L.: 2016, Cold Spring Harb Perspect Biol 8, a018127 – Online at http://cshperspectives.cshlp.org/

[554] Martin, W.F., Bryant, D.A., Beatty, J.T.: 2018, FEMS Microbiology Reviews, fux056, 42, 205-231. Online at http://creativecommons.org/licenses/by/4.0/.

[555] Martinez-Pais, I.G., Giovannelli, F., Rossi, C.; Gaudenzi, S.: 1994, A&A 291, 455-467.

[556] Martinez-Pais, I.G., Giovannelli, F., Gaudenzi, S, Rossi, C.: 1996, A&A, 308, 833-846.

[557] de Martino, D.: 2016, in *The Universe of Digital Sky Surveys*, Ap&SS Proc. 42, 257.

[558] de Martino, D., Sala, G., Balman, S., Bernardini, F., Bianchini, A. et al.: 2015, arXiv150102767.

[559] Maruyama, S., Ebisuzaki, T., Kurokawa, K.: 2019, in *Frontier Research in Astrophysics - III*. Online at https://pos.sissa.it/cgi-bin/reader/conf.cgi?confid=331, id.71

[560] Maselli, A., Melandri, A., Nava, L., Mundell, C.G., Kawai, N. et al.: 2014, Science 343, Issue 6166, 48-51.

[561] Masetti, N., Parisi, P., Palazzi, E., Jiménez-Bailón, E. et al.: 2013, A&A 556, id. A120, 21 pp.

[562] Mather, J.C., Cheng, E.S., Eplee, R.E. Jr., Isaacman, R.B., Meyer, S.S. et al.: 1990, ApJL 354, L37-L40.

[563] Matsuoka, Y., Onoue, M., Kashikawa, N., Iwasawa, K., Strauss, M.A. et al.: 2016, ApJ 828, Issue 1, article id. 26, 14 pp.

[564] Mayor, M., Queloz, D.: 1995, Nature 378, Issue 6555, 355-359.

[565] McCaughrean, M.J., O'dell, C.R.: 1996, AJ 111, 1977-1987.

[566] McClintock, J.E., Narayan, R., Rybicki, G.B.: 2004, ApJ 615, 402-415.

[567] McConnell, NJ., Ma, C-P., Gebhardt, K., Wright, S.A., Murphy, J.D. et al.: 2011, Nature 480, Issue 7376, 215-218.

[568] McKee, C.F., Ostriker, E.C.: 2007, ARA&A, 45, Issue 1, 565-687.

[569] McLaughlin, M.A., Stairs, I.H., Kaspi, V.M., Lorimer, D.R., Kramer, M.: 2003, ApJ 591, Issue 2, L135-L138.

[570] McPherson, A., Gilmozzi, R., Spyromilio, J., Kissler-Patig, M., Ramsay, S.: 2012, The Messenger 148, 2-8.

[571] Mele, L., Ade, P., Alberro, J.G., Almela, A., Amico, G. et al.: 2020, J. Phys. Conf. Ser. 1548, Issue 1, article id. 012016.

[572] Mennella, A., Ade, P.A.R., Aumont, J., Banfi, S., Battaglia, P. et al.: 2018a, arXiv:1801.03730.

[573] Mennella, A., Ade, P., Amico, G., Auguste, D., Aumont, J. et al.: 2018b, arXiv:1812.00785.

[574] Meyer, M.R., Beckwith, S.V.W.: 2000, in *ISO Surveys of a Dusty Universe*, D. Lemke, M. Stickel & K. Wilke (Eds.), Lecture Notes in Physics 548, 341.

[575] Meyer, M.R. Backman, D., Beckwith, S.V.W., Brooke, T.Y., Carpenter, J.M. et al.: 2002, in *The Origin of Stars and Planets: The VLT View*. Proc. of the ESO Workshop Held in Garching, Germany, 24-27 April 2001, ESO ASTROPHYSICS SYMPOSIA. ISBN 3-540-43541-7. Edited by. J.F. Alves and M.J. McCaughrean. Springer-Verlag, 463-472.

[576] Meyer, Michael R., Hillenbrand, L.A., Backman, D., Beckwith, S., Bouwman, J. et al.: 2006, PASP 118, Issue 850, 1690-1710.

[577] Meyer, M.R., Backman, D.E., Weinberger, A.J., Wyatt, M.C.: 2007, in *Protostars and Planets*, V.B. Reipurth, D. Jewitt & K. Keil (Eds.), University of Arizona Press, Tucson, 951 pp., p. 573-588.

[578] Meylan, G., Jetzer, P., North, P., Schneider, P., Kochanek, C.S., Wambsganss, J.: 2006, *Gravitational lensing: strong, weak and micro*, G. Meylan, P. Jetzer & P. North (Eds.), Berlin: Springer, ISBN 3-540-30309-X, ISBN 978-3-540-30309-1, XIII + 552 pp. (Kochanek, C.S.: 2004, arXiv:astro-ph/0407232).

[579] Mezzetto, M.: 2011, in *Symposium on Prospects in the Physics of Discrete Symmetries*, Journal of Physics: Conference Series 335, 012005.

[580] Mineo, S., Gilfanov, M., Lehmer, B.D., Morrison, G.E., Sunyaev, R.: 2014, MNRAS 437, Issue 2, 1698-1707.

[581] Miotello, A., van Dishoeck, E.F., Kama, M., Bruderer, S.: 2016, A&A 594, id. A85, 19 pp.

[582] Mirabel, I.F., Rodriguez, L.F., Cordier, B., Paul, J., Lebrun, F.: 1992, Nature 358, Issue 6383, 215-217.

[583] Mirabel, I.F., Rodriguez, L.F.: 1994, Nature 371, Issue 6492, 46-48.

[584] Mirabel, I.F., Dijkstra, M., Laurent, P., Loeb, A., Pritchard, J.R.: 2011, A&A 528, id. A149, 6 pp.

[585] Mirabel, I.F., Chaty, S., Rodríguez, L.F., Sauvage, M.: 2015, *Extragalactic jets from every angle*, IAU Symp. 313, 370-373.

[586] Miszalski, B., Mikołajewska, J., Udalski, A.: 2013, MNRAS 432, Issue 4, 3186-3217.

[587] Mitrofanov, I.G.: 1978, Sov. Astron. Lett., 4, 119-122.

[588] Michel, F.C.: 1972, Ap&SS 15, 153.

[589] Mitrofanov, I.G.: 1980, in *Close Binary Stars: Observations and Interpretations*, D.M. Popper & R.K. Ulrich (eds.), D. Reidel Publ. Co., Dordrecht, Holland, p. 431-436.

[590] Moore, L.S., Burne, R.V.: 1994, in *Phanerozoic Stromatolites II*, J. Bertrand-Safati & C. Monty (Eds.), Crown Copyright, Printed in the Netherlands, pp. 3-29.

[591] Mudd, D., Martini, P., Zu, Y., Kochanek, C., Peterson, B.M. et al.: 2018, ApJ 862, Issue 2, article id. 123, 13 pp.

[592] Mundt, R., Fried, J.W.: 1983, ApJ 274, L83-L86.

[593] Nakar, E.: 2007, Phys. Rep. 442, 166-236.

[594] Nagase, F.: 1989, PASJ 41, no. 1, 1-79.

[595] National Research Council: 2010, *New Worlds, New Horizons in Astronomy and Astrophysics*, The National Academies Press, Washington, D.C., https://doi.org/10.17226/12951.

[596] National Academies of Sciences, Engineering, and Medicine: 2021, *Pathways to Discovery in Astronomy and Astrophysics for the 2020s*, Washington, DC: The National Academies Press. https://doi.org/10.17226/26141.

[597] Natta, A., Grinin, V., Mannings, V.: 2000, in *Protostars and Planets IV*, (Book - Tucson: University of Arizona Press), p. 559-588.

[598] Nelson, L.: 2012, J. Phys.: Conf. Ser. Volume 341, Issue 1, id. 012008.

[599] Neshpor, Yu.I., Stepanyan, A.A., Kalekin, O.P., Fomin, V.P., Chalenko, N.N., Shitov, V.G.: 1998, Astr. Lett. 24, Issue 2, 134-138.

[600] Nielsen, J.T., Guffanti, A., Sarkar, S. 2016, NatSR 6, id. 35596.

[601] O'dell, C.R., Wen, Z.: 1994, ApJ 436, 194-202.

[602] Ogburn, R.W., IV, Ade, P.A.R., Aikin, R.W., Amiri, M., Benton, S.J., et al.: 2010, SPIE 7741, id. 77411G.

[603] Olausen, S.A., Kaspi, V.M.: 2014a, ApJS 212, Issue 1, article id. 6, 22 pp.

[604] Olausen, S.A., Kaspi, V.M.: 2014b, Online Data Catalog: The McGill magnetar catalog http://www.physics.mcgill.ca/∼pulsar/magnetar/table1apj.html

[605] Ono, Y., Ouchi, M., Mobasher, B., Dickinson, M., Penner, K. et al.: 2012, ApJ 744, Issue 2, article id. 83, 13 pp.

[606] Orosz, J.A., Remillard, R.A., Bailyn, C.D., McClintock, J.E.: 1997, ApJL 478, L83.

[607] O'Sullivan, C., De Petris, M., Amico, G., Battistelli, E.S., de Bernardis, P. et al.: 2021, arXiv:2008.10119v2 [astro-ph.IM] 25 Aug 2021.

[608] Ota, K., Iye, M., Kashikawa, N., Shimasaku, K., Kobayashi, M. et al.: 2008, ApJ 677, Issue 1, 12-26.

[609] Otulakowska-Hypka, M., Olech, A., Patterson, J.: 2016, MNRAS 460, Issue 3, 2526-2541.

[610] Ouchi, M., Mobasher, B., Shimasaku, K., Ferguson, H.C., Fall, S.M. et al.: 2009a, ApJ 706, Issue 2, 1136-1151.

[611] Ouchi, M., Ono, Y., Egami, E., Saito, T., Oguri, M. et al.: 2009b, ApJ 696, Issue 2, 1164-1175.

[612] Ouchi, M., Shimasaku, K., Furusawa, H., Saito, T., Yoshida, M. et al.: 2010, ApJ 723, Issue 1, 869-894.

[613] Paczyński, B.: 1965, AcA 15, 197-210.

[614] Paczyński, B.: 1977, ApJ 216, 822-826.

[615] Padovani, P.: 2018, in *Protoplanetary disks seen through the eyes of new-generation high-resolution instruments*.
Online at https://indico.ict.inaf.it/event/631/, jedi2018, id. 6.

[616] Padovani, P., Combes, F., Diaz Trigo, M., Ettori, S., Hatziminaoglou, E. et al.: 2017, arXiv:1705.06064.

[617] Pallavicini, R.P., Golub, L., Rosner, R., Vaiana, G.S., Ayres, T., Linsky, J.L.: 1981, ApJ 248, 279-290.

[618] Pallavicini, R.P., Golub, L., Rosner, R., Vaiana, G.S.: 1982, in *Cool Stars, Stellar Systems, and the Sun*, M.S. Giampapa & L. Golub (eds.), SAO Rep. N. SP-392, Washington DC, USA, p. 77-85.

[619] Panagia, N., Fall, S.M., Mobasher, B., Dickinson, M., Ferguson, H.C. et al.: 2005, ApJ, 633, Issue 1, L1-L4.

[620] Paredes, J.M., Persic, M.: 2009, talk at the Frascati Workshop 2009 on *Multifrequency Behaviour of High Energy Cosmic Sources - VIII*.

[621] Pardo, J.D., Szostakiwskyj, M., Ahlberg, P.E., Anderson, J.S.: 2017, Nature 546, 642-653.

[622] Park, N.: 2017, Proc. of the 35th ICRC, PoS 301. Online at https://pos.sissa.it/cgi-bin/reader/conf.cgi?confid=301, id. 1116.

[623] Parkhurst, J.A., Zaccheus, D.: 1900, ApJ 12, 259-273.

[624] Pascale, E., Bezawada, N., Barstow, J., Beaulieu, J.-P., Bowles, N. et al.: 2018, Proc. of the SPIE 10698, id. 106980H, 10 pp.

[625] Pasten, C., Santamarina, J.C.: 2012, Energy Policy 49, 468-476.

[626] Patat, F., Chandra, P., Chevalier, R., Justham, S., Podsiadlowski, Ph., et al.: 2008, The Messenger, 131, 30-34.

[627] Patterson, J.: 1979, Ph.D. Thesis, The University of Texas at Austin (USA).

[628] Patterson, J.: 1981, APJ Suppl Ser. 45, 517-539.

[629] Patterson, J.: 1984, ApJ Suppl. Ser. 54, 443-493.

[630] Patterson, J.: 1992, ApJ 384, 234-248.

[631] Patterson, J.: 1994, PASP 106, 209-238.

[632] Patterson, J.: 2014, in *33rd Annual Symposium on Telescope Science*, Society for Astron. Sci., 33, 17-22.

[633] Patterson, J., Robinson, E.L., Kiplinger, A.L.: 1978, ApJ 226, L137-L139.

[634] Patterson, J., Uthas, H., Kemp, J., de Miguel, E., Krajci, Th.: 2013, MNRAS, 434, 1902.

[635] Plavec, M.: 1968, Astroph. Space Sci. 1, Issue 2, 239-263.

[636] Pekurovsky, D.: 2012, Siam J. Sci. Comput. Vol. 34, No. 4, pp. C192–C209, Society for Industrial and Applied Mathematics.

[637] Pelton, J.N.: 2015a, *New Solutions for the Space Debris Problem*, Springer Cham Heidelberg New York. Dordrecht London.

[638] Pelton, J.N.: 2015b, in *Handbook of Cosmic Hazards and Planetary Defense*, Joseph, N. Pelton & Firooz Allahdadi (Eds.), Springer Reference, © Springer International Publishing Switzerland 2015, pp. 851-874.

[639] Pelton, J.N.: 2015c, in *Handbook of Cosmic Hazards and Planetary Defense*, Joseph, N. Pelton & Firooz Allahdadi (Eds.), Springer Reference, © Springer International Publishing Switzerland 2015, pp. 1007-1025.

[640] Pelton, J.N., Allahdadi, F. (Eds.): 2015, *Handbook of Cosmic Hazards and Planetary Defense*, Springer Reference, © Springer International Publishing Switzerland 2015, 1127 pp.

[641] Perlmutter, S., Aldering, G., Goldhaber, G., Knop, R.A., Nugent, P. et al.: 1999, ApJ 517, Issue 2, 565-586.

[642] Pérez, L.M.: 2016, in *Resolving planet formation in the era of ALMA and extreme AO*, Proc. of the conference held 16-20 May, 2016 in Santiago, Chile, id. 51.

[643] Pérez, L.M., Carpenter, J.M., Andrews, S.M., Ricci, L., Isella, A. et al.: 2016, Science 353, Issue 6307, 1519-1521.

[644] Peterson, L., Winckler, J.R.: 1958, Phys. Rev. Lett. 1, Issue 6, 205-206.

[645] Phillips, M.M.: 2005, in *1604-2004: Supernovae as Cosmological Lighthouses*, M. Turatto, S. Benetti, L. Zampieri, and W. Shea (Eds.), ASPC, 342, 211-216.

[646] Phillips, M.M.: 2012, Publ. Astron. Soc. Australia 29, Issue 4, 434-446. (2011, arXiv: 11.4463v1).

[647] Phillips, M.M., Lira, P., Hamuy, M., Maza, J.: 1999, AJ, 118, Issue 4, 1766-1776.

[648] Piat, M., Bélier, B., Bergé, L., Bleurvacq, N., Chapron, C. et al.: 2019, arXiv:1911.12418.

[649] Piccioni, A., Bartolini, C., Bernabei, S., Guarnieri, A., Tarozzi, F., Valentini, G.: 1999, in *Frontier Objects in Astrophysics and Particle Physics*, F. Giovannelli & G. Mannocchi (Eds.), SIF, Bologna, Italy, 65, 195.

[650] Pielke Jr., R.: 2013, at http://rogerpielkejr.blogspot.com/2013/02/graph-of-day-life-expectancy-vs-energy.html

[651] Pignata, G., Maza, J., Hamuy, M., Antezana, R., Gonzales, L.: 2009, *XII Latin American IAU Regional Meeting*, G. Magris, G. Bruzual, & L. Carigi (Eds.), Rev. Mex. A&A Conf. Ser. 35, 317. (http://www.astroscu.unam.mx/ rmaa/).

[652] Piran, T.: 1999, Phys. Rep. 314, Issue 6, 575-667.

[653] Piron, F.: 2016, C. R. Physique 17, 617-631.

[654] Planck Collaboration: 2014, A&A 571, id. A11, 37 pp.

[655] Poggiani, R.: 2017a, in *Multifrequency Behaviour of High Energy Cosmic Sources - XII*. Online at https://pos.sissa.it/cgi-bin/reader/conf.cgi?confid=306, id.53.

[656] Poggiani, R.: 2017b, in *The Golden Age of Cataclysmic Variables and Related Objects - IV*. Online at https://pos.sissa.it/cgi-bin/reader/conf.cgi?confid=315, id. 8.

[657] Poggiani, R.: 2018, in *Frontier Researc in Astrophysics - III*. Online at https://pos.sissa.it/cgi-bin/chairman/chlist.cgi?confid=331, id. 013.

[658] Postnov, K.A., Yungelson, L.R.: 2014, Living Rev. in Relativity 17, Issue 1, article id. 3, 166 pp.

[659] Potter, M: 2015, in *Handbook of Cosmic Hazards and Planetary Defense*, Joseph, N. Pelton & Firooz Allahdadi (Eds.), Springer Reference, © Springer International Publishing Switzerland 2015, pp. 1045-1053.

[660] Prati, C. (on behalf of the LUNA collaboration): 2017, talk at the XV International Conference on *Astroparticle and Underground Physics*, 24-28 July, Subdury, ON, Canada.

[661] Preston, S.H.: 1975, Population Studies: A Journal of Demography, Vol. 29, Issue 2, 231-248. Published online 8th November 2011 at https://doi.org/10.1080/00324728.1975.10410201

[662] Preston, S.H.: 1995, in *The State of Humanity*, J. L. Simon (Ed.), Blackwell, Cambridge, pp. 30-36.

[663] Priedhorsky, W.C., Terrell, J.: 1983, Nature 303, 681.

[664] Pringle, J.E.: 1981, Ann. Rev. A&A 19, 137-162.

[665] Prosin, V.V., Berezhnev, S.F., Budnev, N.M., Brückner, M., Chiavassa, A et al.: 2016, in *Roma International Conference on Astroparticle Physics 2014 (RICAP-14)*, P. Piattelli, A. Capone, R. Coniglione, G. De Bonis, M. De Vincenzi, C. Distefano, A. Morselli, P. (Eds.), EPJ Web of Conferences 121, id. 03004.

[666] Prusti, T., de Bruijne, J.H.J., Brown, A.G.A., Vallenari, A., Babusiaux, C. et al. (Gaia Collaboration): 2016, A&A 595, id.A1, 36 pp.

[667] Punch, M., Akerlof, C.W., Cawley, M.F., Chantell, M., Fegan, D.J. et al.: 1992, Nature 358, Issue 6386, 477-478.

[668] Qi, C., Öberg, K.I., Wilner, D.J., D'Alessio, P., Bergin, E. et al.: 2013, Science 341, Issue 6146, 630-632.

[669] Quinn, J., Akerlof, C.W., Biller, S., Buckley, J., Carter-Lewis, D.A. et al.: 1996, ApJL 456, L83-L86.

[670] Raguzova, N.V., Lipunov, V.M.: 1999, A&A 349, 505.

[671] Rajoelimanana, A.F., Charles, P.A.: 2012, African Skies 16, 126-128.

[672] Ramaty, R., Lingenfelter, R.E.: 1982, Ann. Rev. Nucl. Part. Sci. 32, 235-269.

[673] Ramsay, S., Casali, M., Cirasuolo, M., Egner, S., Gray, P. et al.: 2016, Proc. SPIE 9908, id. 99081T, 12 pp.

[674] Rappaport, S., Joss, P.C.: 1981, in *X-Ray Astronomy with the Einstein Satellite*, R. Giacconi (ed.), D. Reidel Publ. Co., Dordrecht, Holland, p. 123.

[675] Rappoldi, A., Lucarelli, F., Pittori, C., Longo, F., Cattaneo, P.W. et al.: 2016, A&A 587, id. A93, 15 pp.

[676] Rees, M.J.: 1988a, in *Origins*, A.C. Fabian (ed.), Cambridge University Press, 1.

[677] Rees, M.J.: 2015, in *Handbook of Cosmic Hazards and Planetary Defense*, Joseph, N. Pelton & Firooz Allahdadi (Eds.), Springer Reference, © Springer International Publishing Switzerland 2015, p. vii.

[678] Rees, M.J.: 1988b, Nature, 333, 523-528.

[679] Reig, P., Fabregat, J., Coe, M.J.: 1997, A&A 322, 193-196.

[680] Renn, J., Sauer, T., Stachel, J.: 1997, Science 275, No. 5297, 184-186.

[681] Ressell, M.T., Turner, M.S.: 1990, Comm. Astrophys. 14, No. 6, 323-356.

[682] Ricci, L., Carpenter, J., Fu, B., Hughes, M. Corder, S., Andrea Isella, A.: 2015, in *Revolution in Astronomy with ALMA: THE THIRD YEAR*, Daisuke Iono, Ken'ichi Tatematsu, Al Wootten, Leonardo Testi (Eds.), ASP Conference Series, Vol. 499, 269-272.

[683] Riess, A.G., Filippenko, A.V., Challis, P., Clocchiatti, A., Diercks, A. et al.: 1998, AJ 116, Issue 3, 1009-1038.

[684] Riess, A.G., Strolger, L.-G., Tonry, J., Casertano, S., Ferguson, H.C. et al.: 2004, ApJ, 607, Issue 2, 665-687.

[685] Riess, A.G., Macri, L., Casertano, S., Lampeitl, H., Ferguson, H.C. et al.: 2011, ApJ, 730, Issue 2, article id. 119, 18 pp. – Erratum: 2011, ApJ, 732, 129.

[686] Rieger, F.M., de Oña-Wilhelmi, E., Aharonian, F.A.: 2013, Frontiers of Physics 8, Issue 6, 714-747.

[687] Ritter, H.: 1990, A&AS 85, 1179-1256.

[688] Ritter, H., Kolb, U.: 2003, A&A 404, 301.

[689] Rixner, T.A., Siber, T.: 1824, *Leben und Lehrmeinungen berühmter Physiker*, Sulzbach, Heft 5.

[690] Roberts, L.D.: 1992, *Addressing the Problem of Orbital Space Debris: Combining International Regulatory and Liability Regimes*, Boston College International & Comparative Law Review, Vol. XV, No.1, 51-73. Online at http://lawdigitalcommons.bc.edu/iclr/vol15/iss1/4.

[691] Robinson, E.L.: 1976, ARA&A 14, 119-142.

[692] Rodriguez Cavero, N., Krawczynski, H., Muleri, F., Dovčiak, M., Veledina, A. et al.: 2023, Bulletin of the American Astronomical Society, Vol. 55, No. 4 e-id 2023n4i109p06.

[693] Rodriguez Cavero, N., Marra, L., Krawczynski, H., Dovčiak, M., Bianchi, S. et al.: 2023, arXiv:2305.10630.

[694] Rodriguez-Gil, P.: 2003, Ph.D. Thesis, La Laguna University, Spain.

[695] Rosner, R., Golub, L., Vaiana, G.S.: 1985, ARA&A 23, 413-452.

[696] Ross, S.: 2015, in *Handbook of Cosmic Hazards and Planetary Defense*, Joseph, N. Pelton & Firooz Allahdadi (Eds.), Springer Reference, © Springer International Publishing Switzerland 2015, pp. 1085-1107.

[697] Rucinski, S.M.: 1985, AJ 90, 2321-2330.

[698] Sakai, N., Sakai, T., Hirota, T., Watanabe, Y., Ceccarelli, C. et al.: 2014, Nature 507, Issue 7490, 78-80.

[699] Sakharov, A.D.: 1991a, Soviet Physics Uspekhi 34, Issue 5, 392-393.

[700] Sakharov, A.D.: 1991b, Soviet Physics Uspekhi 34, Issue 5, 417-421

[701] Salewski, M., Geiger, B., Heidbrink, W.W., Jacobsen, A.S., S B Korsholm, S.B., et al. (the ASDEX Upgrade Team): 2015, Plasma Phys. Control. Fusion 57, 014021, 10 pp.

[702] Sanchez Calleja, J.: 2016, *Very funny cartoons* produced in occasion of the 2016 Saint Petersburg Workshop on *Accretion Processes in Cosmic Sources*, Saint Petersburg (Russian Federation, 5-10 September.

[703] Santangelo, A.: 2006, talk at the Vulcano Workshop on *Frontier Objects in Astrophysics and Particle Physics*

[704] Santangelo, A., Segreto, A., Giarrusso, S., Dal Fiume, D., Orlandini, M. et al.: 1999, ApJ 523, Issue 1, L85-L88.

[705] Santangelo, A., Picozza, P., Ebsizaki, T.: 2015, in *The 34th International Cosmic Ray Conference*, Online at http://pos.sissa.it/cgi-bin/reader/conf.cgi?confid=236, id. 618.

[706] Saraceno, P.: 2009, talk at Physics Dpt, La Sapienza University, Roma, Italy *Energia e Ambiente: i numeri che contano*.

[707] Saraceno, P.: 2012, *Beyond the Stars: Our Origins and the Search for Life in the Universe*, World Scientific Publishing Co. Pte. Ltd.

[708] Sargent, A.I., Beckwith, S.V.W.: 1987, ApJ 323, 294-305.

[709] Sargent, A.I., Beckwith, S.V.W.: 1989, in *Structure and Dynamics of the Interstellar Medium*, G. Tenorio-Tagle, M. Moles & J. Melnick (Eds.), IAU Coll. 120, Lecture Notes in Physics, volume 350, 215-220.

[710] Scalzo, R.A., Ruiter, A.J., Sim, S.A.: 2014, MNRAS, 445, Issue 3, 2535-2544.

[711] Scaringi, S.: 2015, talk at the Palermo Workshop on *The Golden Age of CVs and Related Objects - III*.

[712] Scaringi, S., Bird, A.J., Norton, A.J., Knigge, C., Hill, A.B. et al.: 2010, MNRAS 401, Issue 4, 2207-2218.

[713] Schaefer, B.E.: 2010, ApJS 187, 275-373.

[714] Schaefer, B.E.: 2011, ApJ 742, Issue 2, article id. 112, 28 pp.

[715] Schmidtobreick, L., Tappert, C.: 2014, in *Stella Novae: Past and Future Decades*, P.A. Woudt & V.A.R.M. Ribeiro(Eds.), ASP Conf. Ser. 490, 29-33.

[716] Schmidtobreick, L., Tappert, C.: 2015, Acta Polyt. CTU Proc. 2, 188-191.

[717] Schreiber, M.R., Lasota, J.-P.: 2007, A&A 473, Issue 3, 897-901.

[718] Schuecker, P.: 2005, Rev. Mod.Astron. 18, 76-105.

[719] Schuecker, P., Caldwell, R.R., Böhringer, H., Collins, C.A., Guzzo, L., Weinberg, N.N.: 2003, A&A 402, 53-63.

[720] Schulz, A.: 2013, Proc. of the 33rd ICRC, Alberto Saa (Ed.). ISBN: 978-1-5108-1008-2, p. 380-383.

[721] Schulze-Makuch, D., Davies, P.: 2013, J. British Interpl. Soc. 66, 11-14.

[722] Schutz, B.F.: 1986, Nature 323, 310-311.

[723] Scóccola, C.G., Ade, P., Alberro, J.G., Almela, A., Amico, G. et al.: 2021, Boletín de la Asociación Argentina de Astronomía 62, 177-179.

[724] Scott, D.A., Caciolli, A., Di Leva, A., Formicola, A., Aliotta, M. et al.: 2012, Phys. Rev. Lett, 109, Issue 20, id. 202501.

[725] Seitter, W.C..: 1990, in *Physics of Classical Novae*, A. Cassatella & R. Viotti (eds.), Springer-Verlag, Lecture Notes in Physics, 369, 79.

[726] Seljak, U., Zaldarriaga, M.: 2017, PhRvL 78, Issue 11, 2054-2057.

[727] Shahbaz, T., Bandyopadhyay, R.M., Charles, P.A., Wagner, R.M., Muhli, P., et al.: 1998, MNRAS 300, 1035.

[728] Shafter, A.W., Curtin, C., Pritchet, C.J., Bode, M.F., Darnley, M.J.: 2014, in *Stella Novae: Past and Future Decades*, P.A. Woudt & V.A.R.M. Ribeiro (eds.), ASP Conf. Ser., 490, 77.

[729] Shafter, A.W., Henze, M., Rector, T.A., Schweizer, F., Hornoch, K. et al.: 2015, ApJS, 216, 34.

[730] Shakura, N.I.: 1972, Astron. Zh. 49, 921.

[731] Shakura, N.I., Sunyaev, R.A.: 1973, A&A 24, 337.

[732] Shandarin, S., Habib, S., Heitmann, K.: 2010, PhRv D, 81, Issue 10, id. 103006.

[733] Shara, M.M., Iłkiewicz, K., Mikołajewska, J., Pagnotta, A., Bode, M.F. et al.: 2017, Nature 548, Issue 7669, 558-560.

[734] Shaviv, G.: 2016, in *Accretion Processes in Cosmic Sources*. Online at http://pos.sissa.it/cgi-bin/reader/conf.cgi?confid=288, id.60.

[735] Shaviv, N.J., Dar, A.: 1995, MNRAS 277, Issue 1, 287-296.

[736] Shimokawabe, T., Kawai, N., Mori, Y.A., Kudo, Y., Nakajima, H. et al.: 2009, AIPC 1133, 79-81.

[737] Simpson, M.K.: 2015, in *Handbook of Cosmic Hazards and Planetary Defense*, Joseph, N. Pelton & Firooz Allahdadi (Eds.), Springer Reference, © Springer International Publishing Switzerland 2015, pp. 1055-1067.

[738] Skinner, G.K.,, Bedford, D.K., Elsner, R.F., Leahy, D., Weisskopf, M.C., Grindlay, J.: 1982, Nature, 297, 568-570.

[739] Smak, J.: 1962, AcA 12, 28-54.

[740] Smak, J.: 1967, AcA, 17, 255-270.

[741] Smak, J.: 1969, AcA 119, 155-164.

[742] Smak, J.: 1972, AcA 22, 1-9.

[743] Smak, J.: 1981, AcA 31, 395-408.

[744] Smak, J.: 1984, PASP 96, 5-18.

[745] Smak, J.: 1985, in *Multifrequency) Behaviour of Galactic Accreting Sources*, F. Giovannelli (Ed.), SIDEREA, p. 3-16.

[746] Smirnov, A.V., Baryshev, A.M., Pilipenko, S.V., Myshonkova, N.V., Bulanov, V.B. et al.: 2012, SPIE 8442, article id. 84424C, 9 pp.

[747] Smith, K.: 2019, talk at LBNL, February.

[748] Smoot, G.F., Bennett, C.L., Kogut, A., Wright, E.L., Aymon, J. et al.: 1992, ApJL 396, L1-L5.

[749] Smoot, G.F.: 2007, *Nobel Lecture: Cosmic microwave background radiation anisotropies: Their discovery and utilization*, Rev. Mod. Phys. 79, Issue 4, 1349-1379.

[750] Soares-Santos, M., Palmese, A., Hartley, W., Annis, J., Garcia-Bellido, J et al.: 2019, ApJ 876, Issue 1, article id. L7, 15 pp.

[751] Soka Gakkai (Ed.): 1999, *The writings of Nichiren Daishonin*, Vol. I, p. 196.

[752] Spergel, D.N., Verde, L., Peiris, H.V., Komatsu, E., Nolta, M.R. et al.: 2003, ApJS, 148, Issue 1, 175-194.

[753] Srianand, R., Petitjean, P., Ledoux, C.: 2000, Nature 408, Issue 6815, 931-935.

[754] Stanev, T.: 2002, private communication.

[755] Staubert, R., Pottschmidt, K., Doroshenko, V., Wilms, J., Suchy, S. et al.: 2011, A&A 527, id. A7, 5 pp.

[756] Steinhardt, P.J., Turok, N., Starkman, G.D.: 2008, PhT 61, Issue 1, 59.

[757] Stoiko, M.: 1970, *Soviet Rocketry: Past. Present, and Future*, 272 pp., Publisher: Holt, Rinehart and Winston; 1st edition.

[758] Stover, R.J., Robinson, E.L., Nather, R.E., Montemayor, T.J.: 1980, ApJ 240, 597-607.

[759] Straniero, O., Imbriani, G., Strieder, F., Bemmerer, D., Broggini, C. et al.: 2013, ApJ, 763, id. 100, 10 pp.

[760] Straniero, O., Bruno, C.G., Aliotta, M., Best, A., Boeltzig, A. et al.: 2017, A&A 598, A128.

[761] Strieder, F., Limata, B., Formicola, A., Imbriani, G., Junker, M. et al.: 2012, PhL B, 707, Issue 1, 60-65.

[762] Stril, A., Cahn, R.N., Linder, E.V.: 2010, MNRAS 404, Issue 1, 239-246.

[763] Strom, K.M., Strom, S.E., Edwards, S., Cabrit, S., Skrutskie, M.F.: 1989a, AJ 97, 1451-1470.

[764] Strom, K.M., Margulis, M., Strom, S.E.: 1989b, ApJL 345, L79.

[765] Strong, A.W., Wolfendale, A.W., Worral, D.M.: 1976, MNRAS 175, 23.

[766] Suleimanov, V,F., Forsblom, S.V., Tsygankov, S.S., Poutanen, J., Doroshenko, V. et al.: 2023, arXiv:2305.15309.

[767] Sunyaev, R.A., Zeldovich, Ia.B.: 1980, ARA&A 18, 537-560.

[768] Surina, F., Bode, M.F., Darnley, M.J: 2011, arXiv:1111.5524.

[769] Surina, F., Bode, M.F., Darnley, M.J: 2015, Publ. Korean Astr. Soc. 30, 237-240.

[770] Swanenburg, B.N., Hermsen, W., Bennett, K., Bignami, G.F., Caraveo, P. et al.: 1978, Nature 275, 298.

[771] Swanenburg, B.N., Bennet, K., Bignami, G.F., Buccheri, R. Caraveo, P. et al.: 1981, ApJL 243, L69.

[772] Szkody, P., Gänsicke, B.T.: 2012, JAAVSO 40, no. 1, 563-571.

[773] Tanaka, Y.: 2001, in *The Century of Space Science*, J.A. Bleeker, J. Geiss & M. Huber (Eds.), Kluwer Academic Publishers, pp. 839-856.

[774] Tang, C-H., Huang, Y-F., Geng, J-J, Zhang, Z-B.: 2019, ApJS 245, Issue 1, article id. 1, 18 pp.

[775] Tanvir, N.R., Levan, A.J., Fruchter, A.S., Hjorth, J., Hounsell, R.A. et al.: 2013, Nature, 500, 547-549.

[776] Tazzari, M., Testi, L., Ercolano, B., Natta, A., Isella, A. et al.: 2016, A&A 588, id. A53, 19 pp.

[777] Tello, J.C., Riva, A., Hiriart, D. & Castro-Tirado, A.J. (Eds.): 2014, *III Workshop on Robotic Autonomous Observatories*, RMxAC, Vol. 45.

[778] Teymourian, A.: 2004, in Proc. of the Fall 2004 Astronomy 233 Symposium on *Measurements of the Hubble Constant*, D.B. Campbell & J. Deneva (Eds), offered by the Cornell University Astronomy Department and the College of Arts and Sciences under the John S. Knight Institute Sophomore Seminar Program, p. 55-61.

[779] The ATLAS Collaboration: 2012, PhLB, 716, 1-29

[780] The CMS Collaboration: 2012a, Science, 338 (6114), 1569-1575.

[781] The CMS Collaboration: 2012b, PhLB, 716, 30-61

[782] Thompson, C., Duncan, R.C., 1995, MNRAS, 275, 255-300.

[783] Thompson, C., Duncan, R.C., 1996, ApJ, 473, 322-342.

[784] Tinetti, G., Drossart, P., Eccleston, P., Hartogh, P., Heske, A. et al.: 2018, Exp. Astr. 46, Issue 1, 135-209.

[785] Tkachev, L., Astapov, I., Bezyazeekov, P., Borodin, A., Brueckner, M. et al.: 2018, Proc. of 2016 Int. Conf. on Ultra-High Energy Cosmic Rays (UHECR2016), id. 011027, 8 pp.

[786] Tluczykont, M. et al. (Taiga Collaboration): 2014, 40th COSPAR Scientific Assembly. Abstract id. E1.6-91-14.

[787] Tolstoy, E., Hill, V., Tosi, M.: 2009, ARA&A 47, Issue 1, 371-425.

[788] Topchiev, N.P., Galper, A.M., Bonvicini, V., Adriani, O., Aptekar, R.L. et al.: 2015, Proc. 34th ICRC. Online at http://pos.sissa.it/cgi-bin/reader/conf.cgi?confid=236, id. 1026.

[789] Topchiev, N.P., Galper, A., Bonvicini, V., Arkhangelskaja, I., Arkhangelskiy, A. et al.: 2017a, Proc. 35th ICRC. Online at https://pos.sissa.it/cgi-bin/reader/conf.cgi?confid=301, id. 802.

[790] Topchiev, N.P., Galper, A.M., Bonvicini, V., Adriani, O., Arkhangelskaja, I.V. et al: 2017b, in *SVHECRI 2016 - XIX International Symposium on Very High Energy Cosmic Ray Interactions*, Pattison, B. (Ed.), EPJ Web of Conferences, Volume 145, id. 06001.

[791] Topchiev, N.P., Galper, A.M., Arkhangelskaja, I.V., Arkhangelskiy, A.I., Bakaldin, A.V. et al.: 2019, in *International Symposium on Very High Energy Cosmic Ray Interactions (ISVHECRI 2018)*, Pattison, B., Itow, Y., Sako, T. & Menjo, H. (Eds.), EPJ Web of Conferences, Volume 208, id. 14004.

[792] Tonry, J.L., Schmidt, B.P., Barris, B., Candia, P., Challis, P. et al.: 2003, ApJ, 594, 1-24.

[793] Topka, K., Golub, L., Gorenstein, P., Harnden, F.R.,Jr.; Vaiana, G.S. et al.: 1982, ApJ 259, 677-692.

[794] Toshikawa, J., Kashikawa, N., Ota, K., Morokuma, T., Shibuya, T. et al.: 2012, ApJ, 750, Issue 2, article id. 137, 12 pp.

[795] Townsley, D.M., Bildsten, L.: 2005, ApJ, 628, Issue 1, 395-400.

[796] Treu, T., Marshall, P.J., Clowe, D.: 2012, Am. J. Phys. 80, N. 9, 753-763.

[797] Trezzi, D., Anders, M., Aliotta, M., Bellini, A., Bemmerer, D. et al. (LUNA Collaboration): 2017, Astrop. Phys. 89, 57-65.

[798] Tristram, M., Banday, A.J., Górski, K.M., Keskitalo, R., Lawrence, C.R. et al.: 2021, A&A 647, id. A128, 18 pp.

[799] Tronchetti, F.: 2015, in *Handbook of Cosmic Hazards and Planetary Defense*, Joseph, N. Pelton & Firooz Allahdadi (Eds.), Springer Reference, © Springer International Publishing Switzerland 2015, pp. 1027-1043.

[800] Trümper, J., Pietsch, W., Reppin, C., Voges, W., Staubert, R., Kendziorra, E.: 1978, ApJL 219, L105-L110.

[801] Tsebrenko, D., Soker, N.: 2015, EAS Publ. Ser. 71-72, 101-102.

[802] Tsygankov, S.S., Doroshenko, V., Poutanen, J., Heyl, J., Mushtukov, A.A. et al.: 2022, ApJL 941, Issue 1, id.L14, 16 pp.

[803] Tu, Z.L., Hu, J., Wang, F.Y.: 2019, MNRAS 484, Issue 3, 4337-4346.

[804] Turner, M.S., Riess, A.G.: 2002, ApJ 569, 18-22.

[805] Tyson, J.A.: 2000, Encyclopedia of Astronomy and Astrophysics, Edited by Paul Murdin, article 2144.

[806] Tyson, J.A., Kochanski, G.P., Dell'Antonio, I.P.: 1998, ApJL 498, Issue 2, L107-L110.

[807] United Nations, Dpt of Social and Economics Affairs, Population Division: 2004, *World Population to 2300*, ST/ESA/SER.A/236, New York, United Nations.

[808] United Nations, Dpt of Social and Economics Affairs, Population Division: 2017, in *World Population Prospects: The 2017 Revision*, New York, United Nations.

[809] Vaiana, G.S., Cassinelli, J.P., Fabbiano, G., Giacconi, R., Golub, R. et al.: 1981, ApJ 245, 163-182.

[810] Veledina, A., Muleri, F., Dovciak, M., Poutanen, J., Ratheesh, A. et al.: 2023, arXiv:2309.15928.

[811] Villada, M., Rossi, C., Polcaro, V.F., Giovannelli, F: 1999, A&A 344, 277-281.

[812] Villard, P.: 1900, Compt. Rend. Acad. Sci. Paris 130, 1010.

[813] Vink, J., Kuiper, L.: 2006, MNRAS 370, Issue 1, L14-L18.

[814] Voss, R., Nelemans, G.: 2008, Nature, 451, Issue 7180, 802-804.

[815] de Vries, J., Archibald, J.M.: 2018, New Phytologist 217, 1428-1434.

[816] Walsh, C., Juhász, A., Meeus, G., Dent, W.R.F., Maud, L.T. et al.: 2016, ApJ 831, Issue 2, article id. 200, 15 pp.

[817] Walter, F.M., Cash, W., Charles, P.A., Bowyer, C.S.: 1980, ApJ 236, 212-218.

[818] Walter, F.M., Bowyer, C.S.: 1981, ApJ 245, 671-676.

[819] Walter, R., Lutovinov, A.A., Bozzo, E., Tsygankov, S.S.: 2015, A&ARv 23, article id. 2, 99 pp.

[820] Wang, F.Y., Dai, Z.G., Liang, E.W.: 2015, New Astr. Rev. 67, 1-17.

[821] Wang, F., Fan, X., Yang, J., Wu, X-B., Yang, Q. et al.: 2017, ApJ, 839, Issue 1, article id. 27, 8 pp.

[822] Wang, F., Yang, J., Fan, X., Yue, M., Wu, X-B. et al.: 2018, ApJ 869, Issue 1, article id. L9, 6 pp.

[823] Wang, F., Yang, J., Fan, X., Wu, X-B., Yue, M. et al.: 2019a, ApJ 884, Issue 1, article id. 30, 20 pp.

[824] Wang, F., Zou, Y-C., Liu, F., Liao, B., Liu, Y. et al.: 2019b, arXiv:1902.05489.

[825] Wang, W., Han, J., Cautun, M., Li, Z., Ishigaki, M.N.: 2019, arXiv:1912.02599.

[826] Wang, W., Han, J., Cautun, M., Li, Z., Ishigaki, M.N.: 2020, Science China Physics, Mechanics & Astronomy 63, Issue 10, article id. 109801.

[827] Warner, B.: 1995, *Cataclysmic Variable Stars*, Camb. Astrophys. Ser., Vol. 28.

[828] Warner, B.: 2002, in *Classical Nova Explosions*, AIP Conf. Proc., 637, 3.

[829] Watson, D.M., Bohac, C.J., Hull, C., Forrest, W.J., Furlan, E. et al.: 2007, Nature 448, Issue 7157, 1026-1028.

[830] Webbink, R.F.: 1984, ApJ, 277, 355-360.

[831] Weltman, A., Bull, P., Camera, S., Kelley, K., Padmanabhan, H., Pritchard, J. et al.: 2018, arXiv:1810.02680.

[832] Whelan, J., Iben, I. Jr.: 1973, ApJ, 186, 1007-1014.

[833] Wheatley, P.J., Mauche, C.W., Mattei, J.A.: 2003, MNRAS 345, 49.

[834] White, R.J., Greene, T.P., Doppmann, G.W., Covey, K.R., Hillenbrand, L.A.; 2007, in *Protostars and Planet*, V,B. Reipurth, D. Jewitt & K. Keil (Eds.), University of Arizona Press, Tucson, 951 pp., p. 117-132. Also arXiv:astro-ph/0604081.

[835] Wickramasinghe, D.T., Ferrario, L.: 2000, PASP 112, Issue 773, 873-924.

[836] Wikipedia: 2017, Online at https://en.wikipedia.org/wiki/Timeline_of_the_2017_Atlantic_hurricane_season

[837] Wiktorowicz,G., Belczynski, K, Maccarone, T.J.: 2014, in *Binary Systems, their Evolution and Environments*, arXiv:1312.5924v2.

[838] Williams, D.A., Balmaverde, B., Benbow, W., Bucciantini, N., Buckley, J. et al. (for the CTA Consortium): 2019, *Astro2020: Decadal Survey on Astronomy and Astrophysics*, APC white papers, no. 291; Bulletin of the American Astronomical Society, Vol. 51, Issue 7, id. 291.

[839] Williams, L.L.R., Schechter, P.L.: 1997, arXiv:astro-ph/9709059, and Astron.& Geophys. 38, Issue 5, 10.

[840] Williams, S.C., Darnley, M.J., Bode, M.F., Shafter, A.W.: 2014, in *Stella Novae: Past and Future Decades*, P.A. Woudt & V.A.R.M. Ribeiro (eds.), ASP Conf. Ser., 490, 85-90.

[841] Williams, S.C., Darnley, M.J., Bode, M.F., Shafter, A.W.: 2016, ApJ. 817, Issue 2, article id. 143, 14 pp.

[842] Wilmoth, J.R.: 1998, Science 280, Issue 5362, pp. 395-397.

[843] Wilmoth, J.R.: 2009, talk on 22 December at the *Institute for Population and Social Security Research*, Tokyo, Japan

[844] Wilson, C.T.R.: 1900, Proc. Cambridge Phil. Soc. 11, 32.

[845] Winn, J.N., Rusin, D., Kochanek, C.S.: 2004, Nature 427, Issue 6975, 613-615.

[846] Winstein, B.: 2007, Int. J. Mod. Phy. D 16, Issue 12b, 2563.

[847] Winstein, B.: 2009, in *From Quantum to Cosmos: Fundamental Physics Research in Space*, Turyshev, Slava G. (Ed.), Published by World Scientific Publishing Co. Pte. Ltd., ISBN 9789814261210, pp. 697-705.

[848] Wise, J.H.: 2019, arXiv:1907.06653.

[849] Wittman, D.M., Tyson, J.A., Kirkman, D., Dell'Antonio, I., Bernstein, G.: 2000, Nature 405, Issue 6783, 143-148.

[850] Woese, C.R.: 1998, Proc. Natl. Acad. Sci. USA, Vol. 95, pp. 6854-6859.

[851] Woese, C.R.: 2000, Proc. Natl. Acad. Sci. USA, Vol. 97, no. 15, 8392-8396.

[852] Woese, C.R.: 2002, Proc. Natl. Acad. Sci. USA, Vol. 99, no. 13, 8742-8747.

[853] Wolf, S., Malbet, F., Alexander, R., Berger, J.-P., Creech-Eakman, M. et al.: 2012, A&ARv 20, id. 52, 83 pp.

[854] Wolschin, G.: 2003, in *Time, Quantum and Information*, L. Castell & O. Ischebeck (Eds.), Springer, Berlin, Germany, p. 115.

[855] Wolszczan, A., Frail, D.A.: 1992, Nature 355, 145-147.

[856] Wood, K.S., Meekins, J.F., Yentis, D.J., Smathers, H.W., Menutt, D.P.: 1984, Astrophys. J. Suppl. Ser. 56, 507.

[857] Wu, K.: 2009, Res.A&A 9, Issue 7, 725-744.

[858] Wu, K., Ramsay, G., Willes, A.: 2008, ChJA&A Suppl. 8, 169-174.

[859] Wu, Q., Czerny, B., Grzedzielski, M., Janiuk, A., Gu, W-M. et al.; 2016, ApJ 833, Issue 1, article id. 79, 6 pp.

[860] Wu, Xiangping: 2008, Talk at the Summer School on *Cosmic Reionization* at the KIAA- PKU, Beijing, China, July 1-11.

[861] Yan, H., Ma, Z., Ling, C., Cheng, C., Huang, J-S: 2023, ApJ 942, Issue 1, id. L9, 20 pp.

[862] Yang, J., Wang, F., Fan, X., Yue, M., Wu, X-B. et al.: 2019, AJ 157, Issue 6, article id. 236, 7 pp.

[863] Yaron, O., Prialnik, D., Shara, M.M., Kovetz, A.: 2005, ApJ, 623, 398.

[864] Yoon, S.-C., Podsiadlowski, Ph., Rosswog, S.: 2007, MNRAS, 380, Issue 3, 933-948.

[865] Yuan, F.: 2016, in *Astrophysics of Black Holes*, C. Bambi (Ed.), ApSSLibrary 440, 152-168.

[866] Zaldarriaga, M., Spergel, D.N., Seljak, U.: 1997, ApJ 488, Issue 1, 1-13.

[867] Zaroubi, S.: 2013, in *The First Galaxies*, ASSL, 396, 45-104.

[868] de Zeeuw, T., Tamai, R., Liske, J.: 2014, The Messenger 158, 3-6.

[869] Zel'dovich, Ya.B., Guseinov, O.Kh.: 1965, Sov. Phys. Doklady 10, 524.

[870] Zhang, B.: 2013a talk at the "*Multi-Messenger Transient Workshop*, KIAA, China.

[871] Zhang, B.: 2013b, in *Gamma-ray Bursts: 15 Years of GRB Afterglows*, A.J. Castro-Tirado, J.Gorosabel and I.H. Park (Eds.), EAS Publications Series 61, 285-293.

[872] Zhao, L., Zhang, B., Gao, H., Lan, L., Lü, H., Zhang, B.: 2019, ApJ 883, Issue 1, article id. 97, 22 pp.

[873] Zhilkin, A.G., Bisikalo, D.V.: 2009, in *Numerical Modeling of Space Plasma Flows: ASTRONUM-2008*, Nikolai V. Pogorelov, Edouard Audit, Phillip Colella & Gary P. Zank (Eds.), ASP Conf. Ser. 406, 118-123.

[874] Zhilkin, A.G., Bisikalo, D.V.: 2010, ARep 54, Issue 12, 1063-1077.

[875] Zhilkin, A.G., Bisikalo, D.V.: 2011, in *5th international conference of numerical modeling of space plasma flows (astronum 2010)*, Nikolai V. Pogorelov, Edouard Audit & Gary P. Zank, (Eds.), ASP Conf. Ser. 444, 91-96.

[876] Zhilkin, A.G., Bisikalo, D.V., Mason, P.A.: 2012, ARep 56, 257-274.

[877] Zinnecker, H., Yorke, H.W., 2007, ARA&A 45, 481-563.

[878] Ziółkowski, J.: 2013, Acta Polytechnica Vol 53, Suppl., 665.

[879] Zuckerman, M.-C. 1961, Annales d'Astrophysique 24, 431.

[880] Zwicky, F.: 1939, Phys. Rev. 55, 726.

DISCUSSION

DHEERAJ PASHAM: Can you apply your model for optical-X-ray lags to supermassive black holes? In stellar tidal disruption events we see several systems where the optical outburst leads the X-ray flare. Could this X-ray-optical time lag be explained with your model?

FRANCO GIOVANNELLI: The model developed by Bisnovatyi-Kogan and Giovannelli (2017, A&A 599, A55, 7 pp.) works very well for close binaries with accretion disks. In this case, the time lag is connected with effects of viscosity that define a radial motion of matter in the accretion disk. In the case of flashes in AGNs the latter model does not work. We considered the disruption of a star that is in the evolution phase of a giant which enters the radius of strong tidal forces. The matter with a low angular momentum that is released by the star falls into the SMBH in the form of a quasi-spherical flow with a velocity that is close to the free-fall velocity. An X-ray flash occurs when the falling matter reaches the hot inner regions. The time lag observed in these sources is identified with the time of the matter falling from the tidal radius onto the central region. The values of the tidal radius that we calculated in this model were compared with the theoretical radii of a tidal disruption that depends on the masses of the SMBH and of the star, and on the radius of the star. Knowing the SMBH masses from observations, and making a reasonable suggestion for the stellar mass that is on the order of one solar mass, we obtained that the radii of the disrupted star are between a few tens and a few hundreds of $R_{\odot}$. Table 6 of this review reports the time delay between the optical and X-ray flashes experimentally determined for several systems, and the radii of the disrupted star, as well as the radius at which the optical flash occurs.